THESIS ON CIVIL ENGINEERING F66

Renovation Need and Performance of Envelopes of Concrete Apartment Buildings in Estonia

SIMO ILOMETS

TTÜ PRESS

TALLINN UNIVERSITY OF TECHNOLOGY
School of Engineering
Department of Civil Engineering and Architecture
Nearly Zero Energy Buildings Research Group

The thesis was accepted for the commencement of the degree of Doctor of Philosophy in Engineering on 09.05.2017.

Supervisor: Professor Targo Kalamees, Nearly Zero Energy Buildings Research Group, Department of Civil Engineering and Architecture, School of Engineering, Tallinn University of Technology

Reviewers and opponents: Professor Jari Puttonen, Department of Civil Engineering, Aalto University, Finland;

Dr. Karolis Banionis, Head of Laboratory of Building Physics, Institute of Architecture and Civil Engineering, Kaunas University of Technology, Lithuania

Commencement: 28.06.2017 at 10:00 a.m. in a room NRG-131 in Tallinn University of Technology

Declaration: Hereby I declare that this doctoral thesis, my original investigation and achievement, submitted for the doctoral degree at Tallinn University of Technology has not been submitted for a doctoral or any equivalent academic degree elsewhere.

Deklaratsioon: deklareerin, et see doktoritöö, mis on minu iseseisva töö tulemus, on esitatud Tallinna Tehnikaülikooli doktorikraadi taotlemiseks ja selle alusel ei ole varem taotletud doktori- või sellega võrdsustatud teaduskraadi.

Simo Ilomets /

ISSN 1406-4766
ISBN 978-9949-83-106-7 (publication)
ISBN 978-9949-83-107-4 (PDF)

EHITUS F66

Eesti raudbetoon-suurpaneelelamute piirdetarindite renoveerimisvajadus ja toimivus

SIMO ILOMETS

TTÜ KIRJASTUS

To Sven and Andra

Ilomets, S. (2017) **Renovation need and performance of envelopes of concrete apartment buildings in Estonia.** Doctoral thesis, Tallinn University of Technology.

ABSTRACT

The future of ageing concrete apartment buildings is widely debated in Estonia as well as in neighbouring countries. Studies about the current technical condition of concrete apartment buildings from the 1960s show that in Estonia structures are in a satisfactory condition (except facades, balconies, awnings etc.). Shortcomings are related to poor indoor climate, energy efficiency and the hygrothermal performance of buildings, which increase the hygrothermal load on the building envelope from inside. Climate loads affect reinforcement corrosion from outside. Hence, the knowledge-based and detailed need for renovation and hygrothermal performance of the applied renovation scenario has to be studied.

Indoor hygrothermal loads were studied in order to have proper boundary conditions for deterministic and stochastic analysis. Based on the measurements, temperature models for central and stove heating systems as well as three humidity models are proposed. Moisture excess and moisture production in bedrooms for cold periods depends on the occupancy and was on average 2.8 g/m^3 and 72 g/h, respectively. Average air change rate 0.6 h^{-1} for bedroom and 0.32 h^{-1} for the entire dwelling unit, meaning an insufficient rate, was found for roughly 2/3 of the dwelling units.

Measured thermal bridges showed unacceptably low interior surface temperatures for several junctions. These combined with high indoor hygrothermal loads due to high moisture production and insufficient ventilation cause distressful 54% risk for calculated mould growth, confirmed by 46% as visually detected. Calculated risk for surface condensation is 51%. When it comes to energy efficiency, current walls have unacceptably high thermal transmittance and thermal bridges constitute 10–34% of the transmission heat loss of buildings, depending on whether the windows are replaced and positioned into the same plane as the additional external thermal insulation and whether balconies are rebuilt or not.

A method that combines existing corrosion propagation models and a hygrothermal simulation tool was proposed and validated in order to evaluate the need for renovation from outside. Results show that after carbonation has reached the reinforcement, corrosion propagation might take only three to six years. Applying additional external thermal insulation does not cause extensive corrosion while concrete dries out. In addition to insulating, also improving ventilation is advised to eliminate critical thermal bridges and stop degradation mechanisms. Also, new insulated facade improves the indoor thermal comfort and aesthetics. Renovation can be done only within a limited time-frame due to ongoing degradation and the huge construction volume of the existing housing stock.

Keywords: renovation, durability, thermal bridge, corrosion, humidity load

Ilomets, S. (2017) **Eesti raudbetoon-suurpaneelelamute piirdetarindite renoveerimisvajadus ja toimivus.** Doktoritöö, Tallinna Tehnikaülikool.

KOKKUVÕTE

Vananevate raudbetoonist korterelamute tuleviku üle diskuteeritakse ühiskonnas nii Eestis kui ka naaberriikides. Viimatised uuringud korterelamute tehnilise seisukorra kohta osutavad, et konstruktsioonid on üldiselt rahuldavas seisus (v.a. teatud fassaadid, rõdud ja varikatused). Peamised puudused on seotud sisekliima, energiatõhususe ning hoone ehitusfüüsikalise toimivusega, mis suurendavad sisekeskkonnast tulenevat ehitusfüüsikalist koormust hoone piirdetarinditele. Välised kliimakoormused mõjutavad betooni terasarmatuuri korrosiooni. Seega on vajalik teadmistepõhiselt ning süvitsi uurida piirdetarindite renoveerimisvajadust ning renoveerimislahenduse ehitusfüüsikalist toimivust.

Piirdetarinditele mõjuvat seesmist soojus- ja niiskuskoormust analüüsiti saamaks ääretingimused edasisteks määratud ja juhuslikeks arvutusteks. Välja on pakutud mõõtetulemustel baseeruvad ruumitemperatuuri mudelid keskküttega ning ahiküttega korteritele/eramutele ning kolm ruumiõhu niiskuskoormuse mudelit piirdetarindite ehitusfüüsikalisteks arvutusteks. Keskmine magamistubade niiskuslisa külmal perioodil oli 2,8 g/m^3 ja niiskustootlus 72 g/h (sõltub asustustihedusest). Õhuvahetuskordsus oli 0,6 h^{-1} magamistoas ehk 0,32 h^{-1} kogu korteri ulatuses. Ebapiisav ventilatisoon tuvastati 2/3 korterites.

Külmasildade mõõtetulemused osutavad mitme välispiirete liitekoha lubamatult madalatele sisepinnatemperatuuridele. Need, kombinatsioonis suure niiskustootluse ja ebapiisava ventilatsiooniga, annavad murettekitava arvutusliku hallituse tekke riski 54%. Visuaalselt tuvastatud hallitust esines vähemal või rohkemal määral 46% uuritud korterite välispiirete sisepinnal. Arvutuslik kondensaadi risk tarindi pinnal on 51%. Ehitusaegsete raudbetoonist välisseinte soojusläbivus on lubamatult suur. Külmasillad moodustavad piirdetarindite soojuskadudest 10–34% olenevalt sellest, et kuidas lahendatakse rõdude külmasillad ning kas aknad vahetatakse ja tõstetakse lisasoojustuse tasapinda või mitte.

Raudbetoonist seinapaneeli väliskoorikus toimuva korrosiooni hindamiseks on töös välja pakutud ja valideeritud meetod, mis kombineerib praegused korrosiooni mudelid soojus- ja niiskustehnilise tarkvaraga. Tulemused osutavad, et suure kaldvihma koormusega fassaadi pragunemine võib toimuda juba kolm kuni kuus aastat peale karboniseerumise jõudmist armatuurini.

Töö tulemusena on soovituslik parandada ventilatsiooni ning välispiirded lisasoojustada. Lisasoojustamine likvideerib lubamatud külmasillad ning peatab fassaadi lagunemise protsessid. Lisasoojustus ei põhjusta intensiivset armatuuri korrosiooni väliskooriku niiskuse välja kuivamise ajal. Lisaks tõuseb viimistletud lisasoojustusega soojusliku mugavuse tase hoones ning paraneb hoone väljanägemine. Renoveerimine on võimalik vaid piiratud aja jooksul jätkuvate lagunemisprotsesside ning elamufondi suure mahu tõttu.

Märksõnad: renoveerimine, kestvus, külmasild, korrosioon, niiskuskoormus

ACKNOWLEDGEMENTS

The thesis would not have been completed without the social support provided to me. My sincere gratitude to all these persons and institutions.

First, I thank my supervisor Prof. Targo Kalamees for introducing the possibility of starting doctoral studies on the given subject numerous years ago. I appreciate the opportunity to attend conferences, working meetings and doctoral schools in various countries. I am grateful for the time and continuous support within all these years and for being a personal example on diligence and punctuality in working that should be followed.

I thank DSc Jukka Lahdensivu for the teaching and help during my two autumns in Tampere and also for the constructive comments on our publications written in cooperation. I appreciate the whole research team with Arto and Toni first of all for the elaborative discussions held in Tampere.

I am grateful to Prof. Emer. Karl Õiger, Prof. Emer. Lembi-Merike Raado, Prof. Emer. Kaido Hääl and Prof. Jarek Kurnitski for their skilful guidance and help contributed to my professional competence. I also thank Professor Jari Puttonen for his constructive remarks and suggestions during the peer-review process. Ms Tiia Kaare edited the language of the thesis.

I thank every single member of our research team at Tallinn University of Technology with whom I have stepped this journey. Together, we have developed our joint events to something more than professional discussions. I hope that these have enriched and offered joy for everybody. I have followed the example of those who started earlier and wish ongoing strength of will to those still working on their thesis. In my opinion, it has always been more about the diverse, enriching journey as such than about the goal.

Last but not least, I express my gratitude to my dear family for their encouragement and back-up. Also close friends and relatives are acknowledged for their support.

Simo Ilomets

May, 2017

FINANCIAL SUPPORT

The thesis would not have been completed without the financial support provided to me. My sincere gratitude to all these persons and institutions.

The research work on which this thesis is based has been carried out at the Nearly Zero Energy Buildings Research Group, Department of Civil Engineering and Architecture, School of Engineering (former Chair of Building Physics and Energy Efficiency, Department of Structural Design, Faculty of Civil Engineering) at Tallinn University of Technology.

This research was supported by the Estonian Centre of Excellence in Zero Energy and Resource Efficient Smart Buildings and Districts, ZEBE, grant TK146 funded by the European Regional Development Fund, and by the Estonian Research Council, with Institutional research funding grant IUT1-15 ('Nearly-zero energy solutions and their implementation on the full-scale renovation of buildings'), Archimedes Foundation (by Research ESF measure 1.2.4, 'Reducing the environmental impact of buildings through improvements of energy performance' (3.2.0801.11-0035), and development of cooperation and innovation of universities, the sub-measure 'Doctoral Schools'. Research conducted for the thesis was supported by European Social Fund's Doctoral Studies and Internationalisation Programme DoRa. Also Horizon 2020 project 'VFP692 Development and advanced prefabrication of innovative, multifunctional building envelope elements for MOdular REtrofitting and CONNECTions (7.11.2014−6.11.2018)' is also acknowledged.

The studies were also financially supported by the scholarship of Karl Õiger Foundation, Scholarship of Olaf Herman and scholarships of the city of Tallinn. This work would not have been possible without this financial support. Partners from the International Energy Agency's cooperative project Annex 55 'Reliability of Energy Efficient Building Retrofitting - Probability Assessment of Performance and Cost (RAP-RETRO)' are acknowledged for their useful remarks and discussions.

I also thank colleagues from Tampere University of Technology for supporting my accommodation during the Tampere visit in autumn 2012.

Simo Ilomets

May, 2017

CONTENTS

LIST OF PUBLICATIONS

The thesis is predominantly based on the publications in the following peer-reviewed journals:

I **Ilomets, S.**, Kalamees, T. Indoor hygrothermal loads for the deterministic and stochastic design of the building envelope for dwellings in cold climates. (Submitted to Journal of Building Physics, 06.05.2016 and resubmitted after reviewing 17.04.2017)

II **Ilomets, S.**, Kalamees, T. Evaluation of the criticality of thermal bridges. Journal of Building Pathology and Rehabilitation (2016) 1:11

III **Ilomets, S.**, Kuusk, K., Paap, L., Arumägi, E., Kalamees, T. Impact of linear thermal bridges on thermal transmittance of renovated apartment buildings. Journal of Civil Engineering and Management (2017) 23:1, 96–104

and on publications in the following peer-reviewed conference proceedings:

IV **Ilomets, S.**, Kalamees, T. Case-study analysis on hygrothermal performance of ETICS on concrete wall after low-budget energy renovation. In: Proceedings of XII International Conference on Performance of Exterior Envelopes of Whole Buildings, Florida, USA, 01−05.12.2013, ASHRAE

V **Ilomets, S.**, Kalamees, T., Lahdensivu, J. Validation of the method to evaluate the corrosion propagation stage by hygrothermal simulation. In: Proceedings of Central Europe towards Sustainable Building 2016; Innovations for Sustainable Future, 22−24.06.2016, Prague

VI **Ilomets, S.**, Kalamees, T., Lahdensivu, J., Klõšeiko, P. Impact of ETICS on corrosion propagation of concrete facade. In: SBE16 Tallinn and Helsinki Conference. Build Green and Renovate Deep 5–7 October 2016, Tallinn and Helsinki / Energy Procedia 96 (2016) 67–76

These publications are referred to in the thesis by their Roman numbers.

AUTHOR'S CONTRIBUTION TO THE PUBLICATIONS

The author of the thesis is the principal author of all publications I−VI.

In publication I, the measured data were collected by the Building Physics research group of Tallinn University of Technology, the author of the thesis among others, in 2008−2012. Data analysis was performed by the author (except a fraction made by A. Mikola, acknowledged at the end of the publication) guided by the supervisor. The proposed models were developed and the publication itself written and improved in cooperation with the supervisor T. Kalamees.

In publication II, the thermography field measurements were mostly carried out by the author, helped by a few co-members of the research group. Data analysis was done by the author and looked over by the supervisor. The proposed method was developed as well as the paper written in cooperation with the supervisor T. Kalamees.

Calculations for publication III were mostly made by the author, helped by co-authors (calculations and field measurements) and supervised by T. Kalamees.

In publication IV, the case-study measurements were set up in situ, monitored, data collected and further analysed by the author. Thermography measurements were carried out and analysed by the author. A hygrothermal simulation model was created and applied by the author and improved in cooperation with the supervisor. The publication was written by the author and commented by supervisor T. Kalamees.

The field survey for publication V was done in Tampere University of Technology under the guidance of J. Lahdensivu. Simulations in order to validate the model were carried out by the author. The publication was written by the author and improved in cooperation with the co-authors and T. Kalamees and J. Lahdensivu.

In publication VI, simulations and the analysis of the results were carried out by the author. A model used for simulations was looked over by co-author P. Klõšeiko. A draft of the publication was written by the author, then improved by all authors and completed by the author of this thesis.

NOTATIONS

Abbreviations

ASHRAE	American Society of Heating, Refrigerating and Air-Conditioning Engineers
AVG	Average
CV	Coefficient of Variation
CPR	Construction Products Regulation
EN	European standard
EPS	Expanded Polystyrene
ETICS	External Thermal Insulation Composite System
EU	European Union
GOST	Gosudarstvennyy Standart (national standard)
HAM	Heat, Air and Moisture
ISO	International Organization for Standardization
MET	Metabolic Rate
MW	Mineral Wool
RC	Reinforced Concrete
REV	Reference Volume
PIR	Polyisocyanurate
SD	Standard Deviation
SNiP	Stroitel'nye Normy i Pravila (Construction Codes and Regulations)
WDR	Wind-Driven Rain

Symbols

A	area, m^2
C	CO_2 concentration, g/m^3
c	specific heat capacity, J/(kg·K)
d	diameter, mm
d	depth or thickness, mm
d_c	cover depth, mm
d_{carb}	carbonation depth, mm
F	Faraday's constant, F = 96487 A·s/mol
f_{Rsi}	temperature factor, -
G	moisture production, g/h
H	specific heat transfer, W/K
h_v	specific enthalpy of water vapour, J/kg
I_{cor}	corrosion current, A/m^2; $\mu A/cm^2$
j	flux, $kg/(m^2 \cdot s)$
j	rain intensity, $kg/(m^2 \cdot s)$; mm/h
K_g	air permeability, kg/(m·s·Pa)
k	carbonation coefficient, mm/√years
k_{wind}	wind coefficient, -
k_l	liquid water conductivity; kg/(m·s·Pa)
L_{2D}	thermal coupling coefficient from 2D calculations, W/(m·K)

l	length, m
M	mass, kg
M_{loss}	mass of steel dissolved at the anode during the overall time, kg/m^2
m	CO_2 production, g/h
N	number of elements, -
n	air change rate, h^{-1}
n	exponent of time (carbonation), -
O	occupancy, m^2/person
p	air pressure, Pa
Q	thermal energy, J
q	heat flux, W/m^2
R	thermal resistance, m^2·K/W
RH	relative humidity, %
t	temperature, °C
U	thermal transmittance, W/(m^2·K)
u	specific internal energy, J/kg
V	volume, m^3
v	velocity, m/s
w	width, mm
w	water content, kg/m^3
x	cross-section loss, μm
z	valence of corroding metal, -

Greek letters

β	wind angle, degrees
δ	water vapour permeability, kg/(m·s·Pa)
ε	emissivity, -
η	catch ratio, -
θ	porosity, m^3/m^3
λ	thermal conductivity, W/(m·K)
μ	water vapour diffusion resistance, -
ν	vapour content, g/m^3
ρ	density, kg/m^3
σ	energy or moisture source; energy or moisture sink
τ	time, s; h; years
χ	point thermal transmittance, W/K
Ψ	linear thermal transmittance, W/(m·K)

Subscripts

1D	one dimensional
2D	two dimensional
3D	three dimensional
c	cover
calc	calculated
carb	carbonation

cond	condensation
conv	convection
cor	corrosion
crit	critical
diff	diffusion
e	exterior, external, outdoor
f	failure
g	gas
hor	horizontal
0	initial
i	interior, internal, indoor
i	initiation
i	1D component in calculations of point thermal transmittance
j	1D component in calculations of linear thermal transmittance
meas	measured
p	propagation
r	real
red	reduced
res	resistance
s	surface
T	total
o	overall
v	vapour
w	water

1 INTRODUCTION

1.1 Background

Approximately two thirds of the population in Estonia live in apartment buildings (Statistics Estonia, 2016). The majority of these apartment buildings (blocks of flats) were constructed during the 1960s, 1970s, and 1980s (Statistics Estonia, 2016). By today, these buildings have been in service for approximately 30−50 years and due to their natural ageing combined with poor maintenance a growing need for renovation has emerged. The main causes of damage to facades together with indoor and outdoor hygrothermal loads affecting the building envelope are shown in Figure 1.1. A typical three-layer prefabricated reinforced concrete (RC) wall at the junction of an inserted floor slab is presented. Note that there is a zone without thermal insulation in the junction, causing a thermal bridge (high thermal transmittance and low interior surface temperature). Reinforcement corrosion takes place in carbonated, moist exterior concrete.

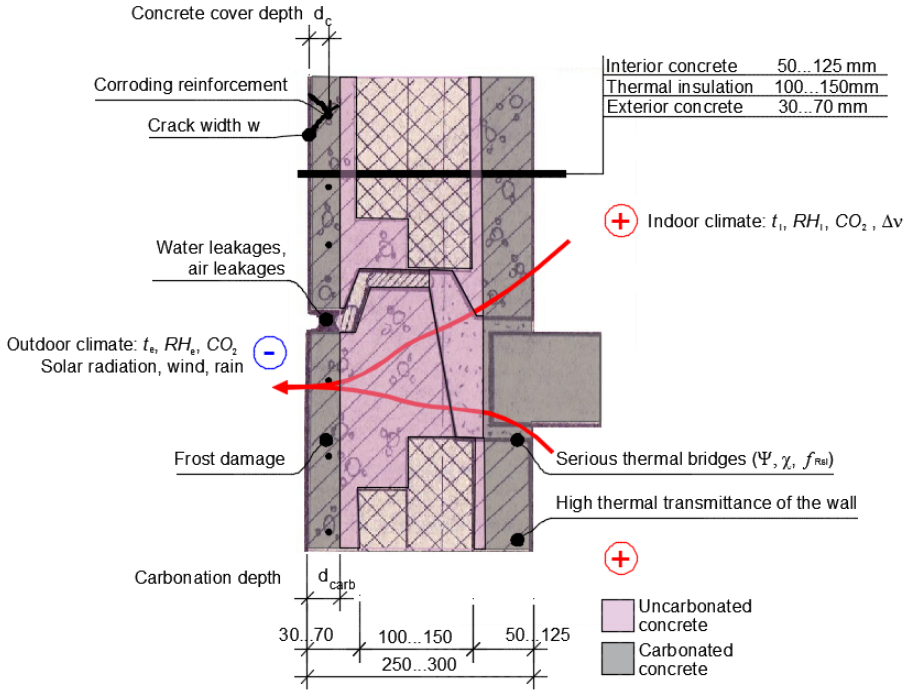

Figure 1.1. Vertical cross-section of a junction of two external wall large-panels and inserted floor slab of RC apartment building with the main damage and indoor and outdoor hygrothermal loads. In the pink areas the pH of the concrete is alkaline; grey shows areas where carbon dioxide has penetrated into the concrete causing carbonation.

In recent years the future of the ageing housing stock has become a subject of wide discussion in Estonia (Terk and Keskpaik, 2015) as well as in neighbouring

countries. Mostly renovation versus demolishing and rebuilding districts with apartment buildings composed of prefabricated reinforced concrete (RC) large panels is being discussed. Demolition in Estonia, however, is complicated because (i) 82% of the apartments are in private ownership (Statistics Estonia, 2016), and (ii) at least four times higher cost of rebuilding compared to major renovation (Kuusk et al., 2014). Studies of the current technical condition have pointed out that building structures in Estonia are predominantly in a satisfactory technical condition, but building components such as RC facades, balconies and loggias, overhangs, cornices and eaves often are not (EKK, 2012; Kalamees et al., 2009; Õiger, 2006; Technical Regulatory Authority, 2013). In 2012, a RC balcony barrier fell down from the fourth storey in Tallinn. In 2016, two accidents have taken place – a concrete awning collapsed in Keila, Estonia, and a concrete balcony in Riga, injuring two people. These examples prove the risks to which the referred sources point and indicate the urgent need for renovation due to safety reasons. In addition, shortcomings related to poor indoor climate, energy efficiency and hygrothermal performance of the building envelope were established (Kalamees et al., 2009, 2011). Also, the durability of RC and brick facades is found to be problematic (Ilomets et al., 2011). Hence, the need for renovation and possibilities of improving hygrothermal performance of the applied renovation measure have to be studied in detail.

1.2 Objective and content of the study

The problems related to the current technical condition of concrete apartment buildings in Estonia are known on general level. In order to apply a renovation scenario, the current need for the renovation of the building envelope and its aspects have to be studied in detail. For that reason, the specific objectives of the thesis were:

- To determine proper indoor hygrothermal loads affecting the building envelope and propose models for indoor boundary conditions;
- To prove the need for renovation due to thermal bridges by presenting the numerical probability of unacceptable performance for Estonian apartment buildings;
- To quantify the proportion of thermal bridges in the total thermal transmittance of the building envelope for the present as well as for the renovated building envelope;
- To study the impact of an additional external thermal insulation composite system (ETICS) on the renovated wall;
- To determine the residual service life restrained by carbonation induced corrosion.

The approach to the research questions in the thesis is based on six peer-reviewed publications – three journal articles and three conference papers, see Figure 1.2 drawn by the author of the thesis. The order of publications from I to VI cover the performance of external wall from indoor to outdoor environment. In publication I, indoor hygrothemal loads were studied in order to have proper

boundary conditions for further analysis. In publication II, these indoor hygrothermal loads were applied to evaluate the probability of unacceptable performance caused by thermal bridges by using statistical analysis. In publication III, thermal bridges were analysed from the aspect of heat loss and both the current situation and the impact of renovation was involved. In publication IV, hygrothermal performance of the concrete wall after applying the ETICS was calculated as well as measured in situ. The calculation model was validated via comparison of simulation results with measured data. In publication V, a method combining existing corrosion propagation models and a hygrothermal simulation tool was validated. Finally, in publication VI, the latter method in combination with a hygrothermal simulation tool was applied to evaluate the corrosion propagation of the RC wall exposed to outdoor climate loads. Also, the effect of installing the ETICS on the corrosion propagation in concrete was analysed at various initial moisture conditions.

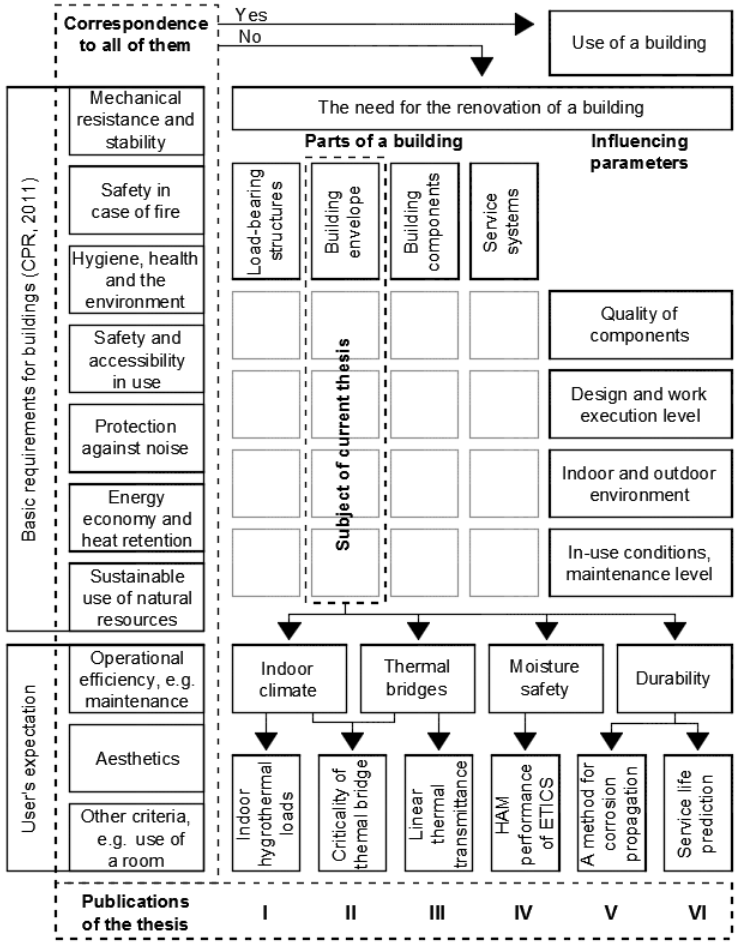

Figure 1.2. Schematic diagram of the bases of the need for renovation and its linkage to factors affecting it treated in six publications of the thesis.

The mapping of the current situation and indoor boundary conditions for further analysis in publication I relied on a broader sampling of buildings. The sample consisted of older, i.e. >30 years old concrete, brick and wooden apartment buildings and newer, i.e. <15 years old apartment buildings as well as detached houses from different periods. The probability of unacceptable performance caused by thermal bridges in publication II was determined for three dominant types of apartment buildings in Estonia. In publications III−VI, the focus was narrowed to proving in detail the need for the renovation of prefabricated RC large-panel apartment buildings based on hygrothermal performance of the building envelope.

Two hypotheses were set in the thesis:

- Indoor hygrothermal loads in combination with thermal bridges cause an inevitable need for renovation;
- The residual service life of carbonated concrete facades is short.

From the first hypothesis, the following research questions arose:

- What are the indoor loads for hygrothermal simulations in Estonian apartment buildings?
- How large is the risk of surface condensation and mould growth in apartment buildings caused by thermal bridges?
- What is the impact of thermal bridges before and after renovating the building envelope of a concrete apartment building?

From the second hypothesis, the following research questions arose:

- How accurately can the hygrothermal performance of the concrete external wall be calculated by using the dynamic heat, air and moisture (HAM) software?
- How accurately can the existing corrosion models be applied to evaluate the corrosion propagation in concrete facades exposed to outdoor climate?
- Does the corrosion process in RC facades activate after the installation of the ETICS?
- What is the numerical value of the residual service life of carbonated concrete facades in case of different cover depths and reinforcement diameters?

1.3 Limitations

The load bearing capacity of the large panels of the external wall and reinforcement corrosion affecting it are not considered in the thesis. Structural stability must always be studied case by case and extra fixing of the external concrete is advisable before installing additional external thermal insulation.

The thesis does not focus on RC balconies and loggias, awnings, overhangs, cornices and eaves because these are not part of the building envelope and therefore were not investigated.

The data on concrete cover depth, carbonation and frost damage collected during the field survey prior to the compilation of the thesis were handled as inputs for the study. Expansion of the field survey data was not an aim of the thesis.

The need for the renovation from the aspect of frost damage of RC facades was not investigated.

The need for the renovation of RC apartment buildings is investigated from the technical point of view only, while social, economic, demographical etc. aspects are not evaluated.

1.4 New knowledge and practical application

The thesis presents the following new knowledge:

- The indoor hygrothermal loads for the whole Estonian housing stock are provided by ranking the factors affecting the moisture production and air change rate in a cold climate. The numerical relationships between the factors affecting the moisture excess as well as moisture production are determined;
- Measured high indoor hygrothermal loads in combination with the detected thermal bridges enable us to numerically determine the probability of surface condensation and mould growth in the three dominant types of apartment buildings;
- A method combining existing corrosion models and a hygrothermal simulation tool is introduced and validated and found to be eligible for evaluating the residual service life of RC facades having outdoor climate loads with wind-driven rain (WDR);
- It is established how corrosion intensity changes after applying an ETICS and what the sensitivity of the results is.

This new knowledge with the developed, tested and validated models and methods in the thesis was/can be implemented for the following practical applications:

- The most dominant factor affecting the indoor humidity load in publication I was applied in the national appendix during the renewal process of EN ISO 13788 (2012);
- The proposed method to evaluate the probability of unacceptable performance caused by thermal bridges is applicable in case of a building, a district or a whole housing stock;
- Numerical values of linear thermal transmittances in publication III are used by the energy auditors in Estonia;
- A calculation model of the concrete wall in the hygrothermal simulation tool can be and is already is used by other researchers for a variety of hygrothermal analyses, for instance by Pihelo et al. (2016);
- The proposed corrosion propagation method can be employed to calculate the residual service life of carbonated RC facades.

2 ON PROBLEMS CONCERNING THE AGEING APARTMENT BUILDINGS

2.1 Overview of the housing stock

Large housing estates have been built all over Europe since 1960, but they became the dominant type of housing in Eastern European countries (Szafrańska, 2013) where the housing stock had been damaged by World War II. The housing stock in Eastern Europe is not old compared to Western or Northern Europe, but it is characterised by much less floor area per inhabitant, lower real estate quality, as well as a lower rate of renovation (Dol and Haffner, 2010; United Nations Publication, 2004). Heating energy consumption in the eastern part of Europe is two to three times higher than in the similar apartment buildings in the West (Balaras et al., 2005b). In Central and Eastern Europe, lower availability of bath/shower, hot running water and central heating is evident based on statistics. The typical occupancy in Eastern Europe is 15−30 m^2/person (30 m^2/person in Estonia) compared to 35−50 m^2/person elsewhere in Europe (Dol and Haffner, 2010). There is a tendency towards increasing level of living area per person, i.e. lower occupancy, in countries with high occupancy. The decreasing average size of households leads to the growing need for the number of dwelling units whilst for Estonia, a decrease of population is forecast (Dol and Haffner, 2010). On the other hand, the growing rate of immigration to Europe, not reflected in recent statistics yet, might increase the population.

Nikulin (2007) studied the residential development, desires and decisions of inhabitants of districts of Tallinn and concluded that a detached or terraced house or an apartment in a new building is not affordable for middle-class residents. Negative examples of large housing estates becoming ethnic minority ghettos can be found in Europe, e.g. France, the Netherlands and Sweden (Szafrańska, 2013) driven by immigration. However,, large housing estates in Estonia have still a relatively good image, social mix of inhabitants and there are no straightforward signs of downgrading (Kährik and Tammaru, 2010).

The existing housing stock and procedures related to it form a substantial share of the economies. It is evaluated that the built environment in Europe represents about half of the national wealth, having therefore enormous economic and technical relevance (Long et al., 2001). In the construction industry, 50% of the turnover serves the maintenance, repair and remedying the damage. Strong pressure to apply progressive measures to modernise the older housing stock in the EU comes from the short-term energy targets set by the year 2020 and by 2050 in a longer perspective. Since the annual renewal of the housing stock is only 1−2% in case of 50−100 years of service life, sustainable renovation scenarios have to be applied to the older, inefficient housing stock. In her thesis, Haapio (2008) claims that the environmental aspects are disregarded in today's renovation. The design of the building should be considered in service life planning, including forthcoming renovations, reuse and recycling.

Future scenarios concerning the ageing housing stock are being discussed throughout Central and Eastern Europe, e.g. in Prague and Warsaw (Terk and Keskpaik, 2015) from the perspective of a whole district, a district via building by building or on the level of a single apartment building. Examples of modernising whole districts can be found from East Berlin (Marzahn-Hellersdorf district) as well as from Helsinki (Jakomäki district) (Terk and Keskpaik, 2015). Three main scenarios have been proposed for discussion in Estonia (Terk and Keskpaik, 2015):

- Demolition and rebuilding by building groups and redesigning the common space between the buildings. This scenario is most progressive, expensive and incommodious for the inhabitants;
- Complete modernisation by building groups via retaining the current RC load-bearing structures by following the example of East Berlin. The floor planning can be renewed and extensions (lifts, balconies, sanitary facilities, common area etc.) added. The cost is lower than for demolition and rebuilding and inhabitants have to leave their homes only for a short period of time;
- Renovation building by buildings. This scenario is similar to what has already started in Estonia. During the renovation, windows are replaced and additional thermal insulation is applied to the external walls and the roof with the upgrading of building services. This scenario is clearly the most affordable and convenient for the inhabitants.

One more scenario that has been executed in a few cases in Estonia is adding an extra storey on top of the building while renovating (EstKONSULT, 1996). This is mostly financed by selling the new apartments built.

Demolishing and rebuilding versus modernising via renovation is being discussed and studied elsewhere in Europe as well. In the UK Power (2008) made a fair comparison between the rebuilding and renovation with a broader overview including environmental, social and economic perspectives. It was stated that rebuilding for energy reasons is greatly weakened if the embodied energy in addition to in-use energy is looked into. In Scandinavia, a significant number of apartment buildings originate from the so-called ‘Million Homes’ project from the 1960s and 1970s (Erlandsson and Levin, 2004). The overall housing quality is better than in former socialist countries, and therefore possibilities and limitations associated with the existing housing stock are evaluated over new buildings. The results indicate that renovation is environmentally a better choice than the construction of a new building (Erlandsson and Levin, 2004). A tool to evaluate sustainable renovation scenarios for Sweden is proposed by Mjörnell et al. (2014). Statistics behind the small number of demolished buildings was studied by Huuhka and Lahdensivu (2016), who found that demolition takes place mostly in the city centres in order to make space for new buildings, irrespective of the building’s age. In Russia, demolishing and rebuilding all run-down buildings is evaluated to be economically impossible; therefore, massive renovation is necessary to prevent housing standards falling further (United

Nations Publication, 2004). In Poland, the cost of modernising older large housing estates is evaluated to be 25−60% of the rebuilding (Gorczyca, 2009). In Lithuania, constructing new buildings would require four to eight times more resources than renovation (Ruzgys et al., 2014). Renovation versus demolishing a five-storey concrete apartment building in terms of energy, economy and environmental impacts was analysed by Kuusk et al. (2014). It was proven that by renovating, a low-energy level and smaller environmental impact with four times less investment can be achieved compared to demolishing and rebuilding. Moreover, it is evaluated that the construction works to replace half of the housing stock will take approximately 20 years (ENMAK 2030, 2016).

2.2 Service life and the need for renovation

According to definition, service life is the period of time after installation during which a building or its parts meet or exceed the performance requirements (ISO 15686, 2000). A standard proposes a framework, principles, requirements and guidelines for the service life planning (ISO 15686, 2000).

At the beginning of the 1960s concrete apartment buildings in Estonia were designed according to Soviet construction norms (SNiP), standards (GOST) and guidelines in Moscow (Poukhonto, 2003; Roitman, 1985). The durability of the structures was designed as regular by setting the requirements for concrete composition, production technology, concrete cover thickness etc. The designed service life of buildings of that time was 50 years as today (EN 1990, 2002), but according to other interpretations of the references up to 125 years (Roitman, 1985). The latter service life is the theoretically calculated so-called averaged value for load-bearing structures. As older buildings have already exceeded the designed service life of 50 years, the question about the current technical condition has arisen. In fact, exceeding the designed service life does not mean that using a building should be finished for at least two reasons:

- Indoor and outdoor climate loads and maintenance conditions affecting the building envelope during the last 50 years were not known at the time of the design;
- Design of the service life is always performed by using safety factors, not median values.

The need for renovation might be due to the requirements set to a building (CPR, 2011), to non-technical as well as to physical performance of the building envelope, see Figure 1.2.

The current technical condition and the future of the housing stock are discussed in many European countries having a similar housing stock. Degrading exterior surface of the building envelope is one of the major concerns why exterior renovation actions are applied (Balaras et al., 2005a). Damage and the need for renovation are pointed out when it comes to RC balconies and facades in Finland (Lahdensivu, 2012; Pentti et al., 1998). Mapping main problems in several Central and Eastern European countries is done in (Raslanas, 2011). In

Russia, the technical condition of apartment buildings is worsening continuously and the volume of necessary renovation is evaluated to be 4−5% of the housing stock (United Nations Publication, 2004). In reality, it was far below 1% at the beginning of the 2000s and has not increased notably since then. In Lithuania, concrete apartment buildings close to 50 years old have had no major repairs over these years. Poor indoor climate due to insufficient ventilation, hygrothermal performance of the building envelope and aesthetic problems are noted in addition to several non-technical and subjective issues. With the high energy consumption and the safety aspects related to degraded non-glazed balconies, buildings are in need of renovation (Raslanas, 2011). Load-bearing structures in Vilnius examined already in 1996 showed 10−30% deterioration (Ignatavicius et al., 2000), which means their fairly good state and possibility of renovation. However, the deterioration rate was higher for overhangs, cornices, balconies and loggias, reaching up to 50%.

2.3 Concrete apartment buildings in Estonia

In Estonia, over three fourths of the dwellings have been built after World War II, primarily in the 1960s, 1970s and 1980s (Statistics Estonia, 2016). Apartment buildings make up 70% of the whole dwelling stock. Apartment buildings are located mostly in urban or suburban areas while detached houses, primarily farmhouses, are the main dwelling types on the outskirts and in rural areas. The dominant apartment building types are brick and prefabricated RC large-panel buildings, accounting for 37% and 36% of all apartment buildings by floor area, respectively (Allikmaa, 2013). However, in the Estonian housing stock, there are also apartment buildings made of autoclaved aerated large blocks (12%), whose characteristics are similar to those of certain brick apartment buildings, and old wooden apartment buildings from the beginning of the 20th century (8%).

Although there are a few such buildings elsewhere, large-panel apartment buildings are concentrated mainly into three districts of Tallinn called Mustamäe, Õismäe and Lasnamäe, see Figure 2.1.

Large-scale industrial construction of RC apartment buildings in Estonia began in the early 1960s in Tallinn (Gritsenko, 2008), see Figure 2.2. The production technology was imported from France but the panels were first designed in the central design institute in Moscow and later locally in Estonia. There were two factories in Tallinn, which had the production capacity of 200 000 m^2 of living area annually.

Figure 2.1. Concrete apartment buildings in districts of Tallinn – Mustamäe (top left), Õismäe (top right), Lasnamäe (bottom left), all from www.taevapiltnik.ee, and a typical 1-464 series building from Mustamäe (bottom right).

The core structure of prefabricated panels mounted in situ with cast junctions has a very high level of structural stability as all the walls (except walls of sanitary rooms) are load-bearing. A reinforcement mesh made of regular smooth steel 3−4 mm in thickness with a tensile strength 500 MPa was placed inside the load-bearing internal as well as the external layer of the concrete. These layers of concrete with a grade of 15 MPa were connected with thicker rods (see Figure 2.2, top left), also made of regular, 'black' smooth steel, subject to corrosion. Higher compressive strength of concrete, predominantly ranging between 25 and 70 MPa, has been detected by measurements (Ilomets et al., 2011). Although only the internal layer was meant to carry the load, cast panels start to act as a whole. This must be kept in mind while designing the renovation and removal of the external layer should not be considered in case of a slender (<75 mm in thickness) internal layer. A technical description of the building envelope in more detail is given in Section 3.1, see also Figure 1.1.

Figure 2.2. Casting the internal layer of concrete into the formwork with steel reinforcement (top left), levelling the rubble bulk of the incoming facade (top right), casting the concrete into the junction in situ (bottom, left) and mounting the panels by crane (bottom right), all from the private collection of Prof. Emer. Karl Õiger.

Mustamäe district was built within approximately ten years between 1962 and 1972 (Gritsenko, 2008). The district was built according to an overall plan, considering its technical and social infrastructure. The district has open planning and green areas forming a natural, characteristic environment, which constitutes 40% of the area (Ojamäe et al., 2009). The visual scene of the built environment is dominated by a limited number of architectural designs. When constructed, the buildings had district heating and apartments were equipped with central cold and hot water and sewage, considered as relevant housing comfort of that time.

Typological series 1-464 apartment buildings in Mustamäe have mostly five, but also nine storeys. One 1-464 typology building consists of four to eight

sections in a row, each having one staircase. The net height of a storey is only 2.5 metres. These buildings have smaller apartments as well as smaller rooms in apartments, especially the kitchen and entry, compared to the later designs from the 1970s and 1980s. Series 1-464 consists of several sub-series from different times; these may differ in the size of the buildings, area of windows and architectural characteristics (Gritsenko, 2008). One of the key shortcomings of the five-storey concrete apartment buildings is the absence of lifts.

The buildings constructed in Õismäe and Lasnamäe districts in the 1970s and 1980s were of series 121. The main difference compared to series 1-464 is the design of sections instead of a building. Hence, a building might be composed of several sections that differ from one another. Each apartment has a balcony.

Series 84 panels were designed and produced exceptionally in Moscow. These buildings can be found in eastern Estonia. In addition, apartment buildings of series 133 and 66 composed of single-layer external wall panels have been erected in various regions of Estonia.

When it comes to ownership, it should be emphasised that the majority of dwelling units (82% in Estonia (Statistics Estonia, 2016)) are in private ownership. A building with a large number of owners makes all decision-making processes concerning renovation very complicated. Such an ownership structure is a result of the privatisation process, which in Estonia took place in the 1990s after the collapse of the Soviet Union. In principle, the right to private property is notably present in the legislation of independent Estonia. During the era of the Soviet Union, real estate such as dwelling units in apartment buildings, were in public ownership. This historical burden has affected the service of buildings, expressed as insufficient maintenance as well as the lack of regular technical condition assessment.

2.4 Indoor hygrothermal loads on the building envelope

Loads affecting the building envelope from inside are temperature, relative humidity (RH), internal moisture excess (depends on moisture production and air change rate) and carbon dioxide, see also Figure 1.1. To prevent dampness-related problems, possible moisture sources should be taken into account in the design phase. As the hygrothermal performance of the building envelope and its surface depends on boundary conditions, a proper evaluation of the indoor hygrothermal loads is crucial. Loads affecting the hygrothermal performance of the building envelope can be expressed in several ways (RH, moisture excess, vapour pressure difference, moisture production and air change rate) and their relation to outdoor climate must be considered.

In deterministic hygrothermal calculations, critical boundary conditions and material properties guarantee that the design solution is on the defined safe side. In-depth studies of indoor hygrothermal loads and their influences are required whereas using the measurements of indoor humidity conditions is advised by Glass and Tenwolde (2009) and Vinha (2007). Currently available deterministic

methodologies (EN ISO 13788, 2012) for measuring hygrothermal performance are insufficient for accurate assessment of functional performance, for instance. Therefore, a research project on the Reliability of Energy Efficient Building Retrofitting – Probability Assessment of Performance and Cost (IEA EBC Annex 55, 2012) was launched. A probabilistic assessment would require the incorporation of both correct critical values and average values with deviations into existing hygrothermal models. IEA EBC Annex 41 shows that it is also possible to use a whole-building indoor climate and energy simulation for hygrothermal modelling (Woloszyn and Rode, 2008). Because whole-building simulation programs use moisture production and air change rate as input parameters, indoor hygrothermal loads should also be reported using these parameters.

Indoor hygrothermal loads in Estonian dwellings were studied in detail in publication I, including the levels of moisture excess for deterministic and stochastic approaches and factors affecting the moisture production and air change rate.

2.5 Thermal bridges

The thermal bridge is a part of the building envelope where the otherwise uniform thermal transmittance is locally significantly larger. From seven essential requirements set in the Construction Products Regulation (EU) No 305 (CPR, 2011), thermal bridges influence the requirements for 'hygiene, health and the environment' and 'energy economy and heat retention'. The main problems caused by thermal bridges are the risk of surface condensation or mould growth, lower thermal comfort and increasing thermal transmittance. As the overall thermal transmittance of the building envelope is reduced while renovating, the ratio of linear thermal transmittance becomes evident. A method how thermal bridges should be accounted for in the heat loss of the building envelope with the default values was proposed already by Olsen and Johennesson (1996). They claimed the computer simulations needed and extra effort put into the better design of the thermal bridges to be very cost effective. Barnes et al. (2013) showed that linear thermal transmittance Ψ, W/(m·K), of the external wall/window junction is highly dependent on the detailing of the window sill in combination with the frame.

The studied buildings have similar architectural and structural typology characteristic of that time, including typical thermal bridges, see Figure 2.3.

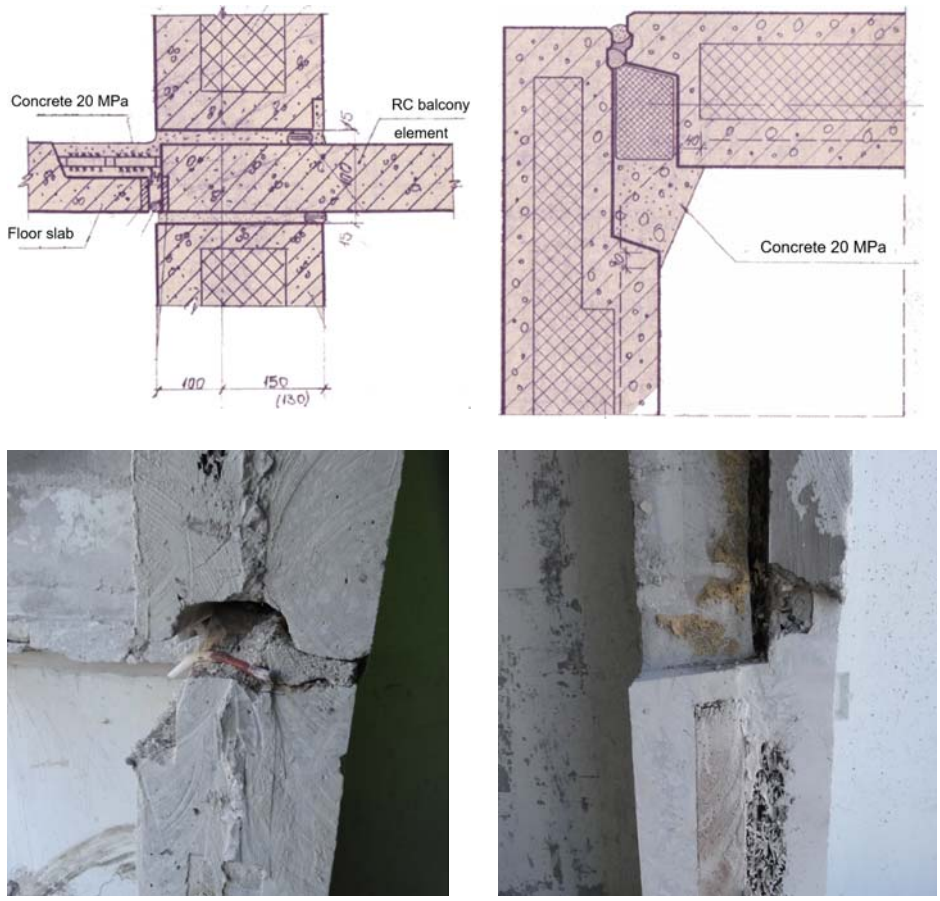

Figure 2.3. Typical thermal bridges caused by discontinuous thermal insulation: the junction of an external wall, inserted floor slab and balcony (top left) and the junction of an external corner (top right) based on original drawings. Photos of an external wall and balcony junction (bottom left, balcony is removed) and external wall, window junction (bottom right).

Suggested structural solutions have turned out problematic in terms of upgraded energy requirements due to large linear thermal transmittances as well as low interior surface temperatures in cold climates. Therefore, elimination of these structural thermal bridges could be one reason for renovation.

For inhabitants and owners of older apartment buildings, the price of renovation design documentation is usually critical; ‘ready to use’ values of linear thermal transmittances can reduce the design time, harmonise the quality and lower the price. Linear thermal transmittances for typical concrete apartment buildings with a common window type would be beneficial for energy audits. As the external wall/window junction is unrivalled in size, it should be the first to concentrate on.

2.6 Degradation mechanisms and durability – reinforcement corrosion

As mechanical resistance and structural stability are the most relevant requirements set to a building, their possible decrease due to corrosion must always be studied. Carbonation reduces the porosity of concrete made with ordinary Portland cement and increases its compressive strength (Lahdensivu, 2012). Decrease of load-bearing capacity of reinforcement bars inside the concrete as well as of bars connecting the layers is evaluated to be minor as the decrease of the cross-section due to corrosion is relatively small compared to the initial cross-section of the reinforcement bar. On the other hand, corrosion diminishes adhesion between the reinforcement bar and concrete. The possible decrease of load-bearing capacity due to corrosion of reinforcement bars must be further monitored.

Corrosion of concrete reinforcement (see Figure 2.4 and oncoming Figure 4.4) can be divided into two main stages: initiation and propagation (Broomfield, 1997; Otieno et al., 2011; Tuutti, 1982).

Figure 2.4. Reinforcement corrosion of the facade, top left and middle (private collection of Prof. Emer. Karl Õiger). Corrosion studied with microscope in laboratory – no corrosion yet, top right, and corroded reinforcement, middle right (Ilomets et al., 2011).

Initiation is the penetration of carbon dioxide following Fick's law into the concrete facing the indoor and outdoor environment. Based on Eq. (1), $n = 0.5$ as the exponent of time while calculating carbonation speed is often applied. Nevertheless, the parameter n is generally $0.2 < n < 0.5$ (Köliö et al., 2016; Parrott, 1987; Tuutti, 1982). Smaller values than $n = 0.5$ could be justified when it comes to the cyclic wetting and drying nature of the concrete facade. The results of Köliö et al. (2016) prove $n = 0.5$ as being proper in spite of large variations within the coefficient. Still, faster carbonation in the beginning in the case of a rubble bulk (exposed aggregate) facade, i.e. $n < 0.5$, is pointed out.

$$d_{carb} = k \cdot \tau^{n} \quad (1)$$

where d_{carb} is carbonation depth (mm); k is carbonation coefficient (mm/√years); τ is time (years); n is exponent of time.

The exponent of time is as a rule smaller than 0.5 in the facade's surface exposed to outdoor climate due to cyclic wetting and drying since the water in concrete pores provides additional resistance up to 10^4 times (Schiessl, 1988) compared to an empty pore, i.e. an ingress of carbon dioxide is faster in concrete that has RH 50−70% (Parrott, 1987). Carbonation is neutralisation of concrete's alkaline pH (CIB W080 Report, 2010; Parrott, 1987). During this chemical reaction, calcium hydroxide and calcium silicate hydrate with carbon dioxide, forming calcium carbonate and water (Johannesson, 1998). A higher level of carbon dioxide due to human activity indoors causes a deeper carbonation front in structures facing the indoor environment (see Figure 1.1). Carbonated structures of the internal layer of walls and inserted floor slabs are harmless as long as these structures stay dry.

The concentration of global atmospheric carbon dioxide has risen from 340 ppm in the beginning of 1980s to 400 ppm today (Dlugokencky and Tans, 2016), having an annual rise of 2 ppm. All future scenarios predict an increase by the year 2050 in the range of 450−550 ppm (IPCC, 2014). Thereafter, it depends on the actions taken to decrease the greenhouse gas emissions and climate warming. However, the scenario having up to 1000 ppm with 4 °C temperature rise by the year 2100 is claimed to be likely (IPCC, 2014). Future climate scenarios for North Europe predict also a worsening situation in terms of corrosion: rise of temperature, higher RH and more precipitation, higher wind speed and less solar radiation (Ruosteenoja et al., 2013). Also extreme weather will be more likely. By the end of the 21st century, the southern parts of Finland will transfer from the boreal *D* climate zone (Köppen-Geiger) to the temperate *C* zone (Ruosteenoja et al., 2013). Therefore, accelerating carbonation of concrete exposed to the outdoor environment is to be considered in durability and service life design of new construction as well as of renovation.

The current thesis evaluates corrosion propagation in porous concrete after the reinforcement has lost its passive film during carbonation. Corrosion starts if the preconditions for the electrochemical process such as presence of moisture and oxygen are fulfilled. Uniform corrosion at the surface of reinforcement forms

anodic and cathodic areas with the pore water as an electrolyte. The electrons move from the anodic area towards the cathodic area creating an electric current (Johannesson, 1998). On the cathodic area, these electrons form hydroxide ions if water molecules are available. Therefore, the corrosion current increases with RH (Bouteiller et al., 2012; Tuutti, 1982) up to a certain level, i.e. RH 90−95% (Yu et al., 2014). Inter alia, the corrosion current depends on the amount of dissolved oxygen, which decreases in concrete saturated with water (Markeset and Myrdal, 2008). Hence, the formation of corrosion products (except black rust) is hindered in wet concrete due to the lack of oxygen. Still, a sufficient quantity of oxygen might be available occasionally while the concrete's surface in contact with outdoor air is not wet (Gjørv, 2009).

Corrosion currents have values between 0 and 10 $\mu A/cm^2$ based on measurements by Lahdensivu et al. (2013) (conducted by Jussi Mattila) and Tuutti (1982). A limit for corrosion current at 2.6 $\mu A/cm^2$ is proposed by Bouteiller et al. (2012). It is also evaluated that high corrosion current $I_{cor} > 1$ $\mu A/cm^2$ (measured seldom) corresponds to annual corrosion penetration depth >10 μm into steel (Andrade and Alonso, 2001), but it depends on temperature.

The critical depth for steel corrosion (cross-section loss) that causes cracks, chipping and spalling of the concrete covering is 15−40 μm (Broomfield, 1997), 15−50 μm (Alonso et al., 1998) or 100 μm (Parrott, 1987). The critical depth depends on the cover thickness, and the lowest value 15 μm occurs in case of a small cover depth while 100 μm is quite typical of large cover depths.

Empirical, numerical or models based on resistivity or oxygen diffusion to calculate the corrosion and service life of a structure have been developed, most of them are reviewed by Ahmad (2003), Jamali et al. (2013) and Raupach (2006). A novel attempt for that time to apply the capability of computer software for predicting the service life of RC was made by Vesikari (1999). Still, the inability to consider cracks and the large calculation unit (50 mm) can be considered as disadvantages. Recently, hygrothermal simulation tool was combined with the corrosion model by the developers of WUFI software in Fraunhofer Institute for Building Physics, Germany. Since the corrosion mechanism is highly complicated and dependent on many factors, calculation results are never accurate and tend to be valid only for the conditions they were developed in (Otieno et al., 2011). This makes validation of the models and their further application highly complicated. Even so, an effort to take a step forward is made in the present thesis.

2.7 Current technical state-of-the-art of concrete apartment buildings

2.7.1 Overview and current technical state-of-the-art of concrete apartment buildings in neighbouring countries

Concrete apartment buildings in Eastern Europe, and especially in the Baltic States, can be characterised as in general similar to those in Estonia, which were described in the previous chapters. As production technology of RC panels was the same in principle, analogous technical solutions can be found in other countries e.g. Czech Republic. Similarities can also be detected when it comes to today`s technical problems related to aging housing stock, such as poor energy performance, winter thermal comfort, mould growth due to insufficient ventilation, water-proofing failures, lack of maintenance etc. (Hejtmánek et al., 2017), see Figure 2.5.

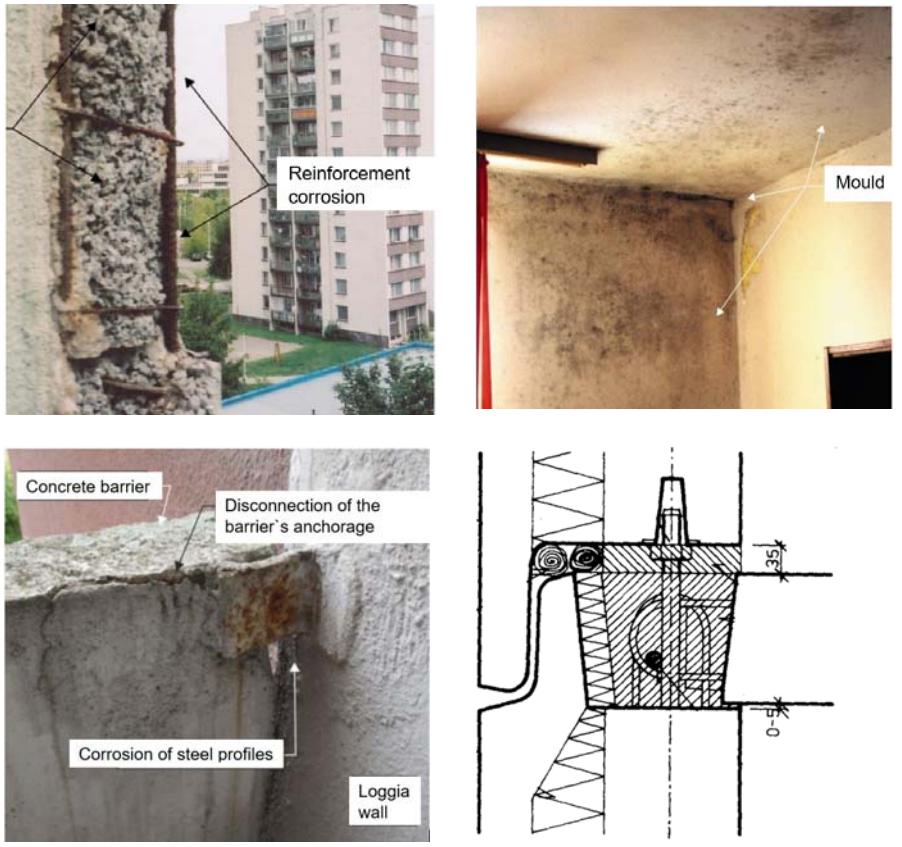

Figure 2.5. Extensive reinforcement corrosion and the concrete cover dropped off (top left) and extensive mould growth on the interior surface of the building envelope (top right). Corroded anchoring detail of the RC loggia barrier (bottom left) and a vertical junction of two external wall panels and the floor slab (bottom right), all from (Witzany, 2016).

Apartment buildings composed of prefabricated RC large panels in Finland as well as in other Nordic countries, have a better construction quality. One of the main differences compared to Estonia is continuous thermal insulation also in junctions (Pentti, 1994), see Figure 2.6. Hence, the problem of thermal bridges is less serious in terms of heat loss as well as the risk of mould growth on the interior surface.

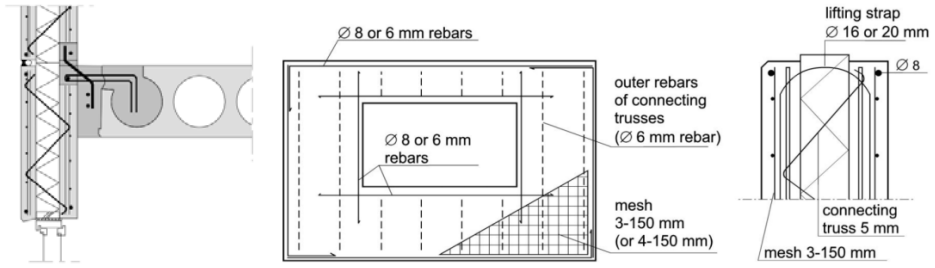

Figure 2.6. Cross-section of a typical junction of the RC external wall and the inserted floor slab (Pentti, 1994) on the left and reinforcement of the outer layer of the RC panel in Finland (Pentti et al., 1998) in the middle and on the right.

When it comes to the current need for renovation, the main problems are related to degradation of facades and balconies, primarily cracking, frost damage and reinforcement corrosion (Al-Neshawy, 2013; Lahdensivu, 2012), see Figure 2.7.

Figure 2.7. Typical carbonation induced corrosion on the left and local frost damage at the edge of an exposed aggregate RC panels on the right (Lahdensivu et al., 2013).

2.7.2 Current technical state-of-the-art of RC apartment buildings in Estonia

The overall technical condition of the RC load-bearing structures was studied already in the 1990s (EKK, 1994) and the results were, in general, satisfactory but threats related to certain types of balconies were pointed out. In the 2000s, a satisfactory condition of load-bearing structures was confirmed with safety aspects of balconies, loggias, awnings, overhangs, cornices and eaves indicated (Kalamees et al., 2009; Õiger, 2006), see Figure 2.8.

Figure 2.8. Severe corrosion propagation of reinforced concrete balconies (Õiger, 2006).

In 2012, a report of mapping the balcony railings was compiled (EKK, 2012) after a RC balcony had dropped down in Tallinn. In 2013, a study about RC balcony and loggia barriers was performed by the Estonian Technical Regulatory Authority (Technical Regulatory Authority, 2013). The report concluded that the poor construction quality, a lack of real estate maintenance and repair combined with unauthorised modifications by inhabitants were the causes of such accidents. Recently, in 2016, a RC awning panel collapsed near Tallinn (see Figure 2.9, right), provoking more discussion about the future of ageing concrete apartment buildings in Estonia.

Figure 2.9. Reinforced concrete awning panel above an entrance door from the 1960s on the left (private collection of Prof. Emer. Karl Õiger) and a collapsed awning panel at Keila near Tallinn (Postimees, 2016).

By the time of completing the thesis, no serious technical problems concerning the safety and residual load-bearing capacity of the external walls had been detected (EKK, 1994, 2012; Kalamees et al., 2009; Õiger, 2006). Having said that, corrosion decreases the cross-section of the reinforcement bar and reduces its load-bearing capacity (Dehoux et al., 2012).

2.7.3 Current technical state-of-the-art of the external walls in Estonia

The technical condition of the building envelopes of concrete apartment buildings in Estonia is satisfactory (Ilomets et al., 2011; Kalamees et al., 2011). Still, junctions of large panels are found to be leaky due to missing or incorrect sealing, enabling water and air infiltration. High thermal transmittance and low indoor surface temperature of the thermal bridges have been detected.

The measured carbonation depth of external concrete is typically 10−40 mm whereas the carbonation of a painted facade was found to be significantly deeper against the rubble bulk finishing (Figure 2.10, left). Reinforcement corrosion is generally minor and it is visually detected only in case of insufficient (<20 mm) cover depth.

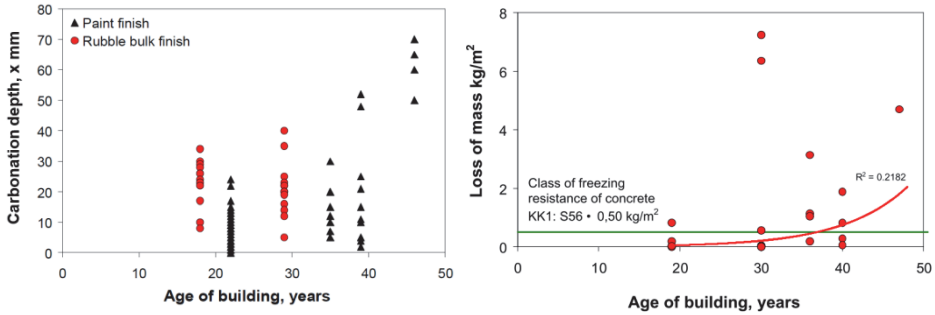

Figure 2.10. Carbonation depth of the external concrete (left) and the loss of mass of concrete after 56 freeze–thaw cycles in laboratory (right) (Ilomets et al., 2011).

No harmful quantities of chlorides and sulphates were detected inside the concrete. Therefore, corrosion can be considered to be carbonation induced.

Both visual inspection of buildings and laboratory tests (Figure 2.10, right) indicated problems with the residual frost resistance of concrete facades. Only half of the specimens fulfilled the criteria for the frost resistance in the XF1 environmental class: loss of mass $M \leq 0.5$ kg/m^2. The frost resistance of older buildings was in a somewhat worse condition (Ilomets et al., 2011).

The hygrothermal performance of the external walls is characterised by some condensation on the interior surface of the external concrete during winter. The calculated quantity of the condensed moisture is rather small and the moisture dries out during spring due to a large heat flux.

The technical need for renovation studied in the thesis comes from the two sides of the building envelope:

- From inside because of the high moisture load, transmission heat loss and low surface temperature; and
- From outside because of climate loads affecting the hygrothermal performance of the building envelope and reinforcement corrosion.

A detailed literature review of the subtopics is included in the publications on which the thesis is based.

3 RESEARCH OBJECTS

3.1 Buildings studied

The initial building sampling was broad-based but was later narrowed throughout the studies due to focussing. Most of the buildings were located in Estonia, except those five used for validating the method concerning the reinforcement corrosion propagation in publication V; these all are located in the Helsinki region, Finland (see Table 3.1 for details). Selection of buildings and dwelling units was random. A general description of the housing stock in Estonia with the focus on reinforced concrete (RC) apartment buildings is given in Section 2.3.

Table 3.1. Distribution of the studied dwelling units

	Number of studied dwelling units	Subdivision of dwelling units
Indoor boundary conditions: temperature and RH (publication I)	180 (+57 detached houses)	32 RC; 45 brick; 42 log; 61 new
Indoor boundary conditions: air change rate (publication I)	80 (+8 detached houses)	13 RC; 24 brick; 23 log; 20 new
Thermal bridges (publications II and III)	48	13 RC; 15 brick; 20 log
Validation of the corrosion method (publication V)	5 buildings	5 RC buildings
HAM performance of RC wall and corrosion (publications IV and VI)	1	1 RC

*RC – reinforced concrete, RH – relative humidity, HAM – heat, air and moisture.

3.1.1 Dwellings involved in indoor climate measurements

The indoor climate measurements were conducted in Estonian apartments and detached houses representative for the housing stock with various occupancies, sizes, ages, structures and types of heating and ventilation, see Table 3.2 and the following description. All 237 dwelling units consisted of an entry, living room, kitchen, sanitary rooms, bedrooms and non-living spaces, e.g. a corridor or storage area. The kitchen area was typically enclosed in a separate room but may also have been integrated with the living room in new apartments. In apartment buildings one-, two- and three-bedroom apartments predominated. In detached houses, three or four bedrooms dominated. All the dwelling units were privately owned.

Table 3.2. Main characteristics of the 237 dwelling units used for indoor climate measurements

	Apartment building, 76% (180 dwelling units)	Detached house, 24% (57 dwelling units)
Net floor area: average ± SD and (min–max)	63±28 m^2 (31–299 m^2)	122±49 m^2 (34–300 m^2)
Occupancy: average ± SD (min–max)	27±15 m^2/person (9–85 m^2/person)	45±22 m^2/person (16–103 m^2/person)
Age of a buildings	<20 years: 35% 20–40 years: 16% 40–70 years: 24% >70 years: 24%	<20 years: 58% 20–40 years: 3% 40–70 years: 4% >70 years: 35%

Structures of external walls of apartment buildings were typically made of RC, brick or wood (see Table 3.1, right column). A combination of different materials was used in 2% of the apartment buildings while walls in detached houses typically consisted of one of two different materials (log 48%, timber frame 52%). Both the natural passive stack ventilation system (51% in apartments and 55% in houses) and the mechanical system (49% in apartments and 45% in houses) were represented in the studied dwellings. Central heating with hydronic radiators was typical (77%) in apartments while in houses many heating systems were represented (stove/fireplace 33%, electrical radiators 20%, hydronic radiators 23%, combined 23%). Mechanical cooling was not used in general in Estonian dwellings.

3.1.2 Apartment buildings involved in the analysis of thermal bridges

The criticality and heat loss of the thermal bridges were studied in apartment buildings composed of RC, brick and log (see Table 3.1 for percentage).

The panels of the external walls of the RC apartment buildings built in the 1960s, 1970s and 1980s are composed of two layers of RC (50–125 mm inner, load-bearing layer, and 30–70 mm outer core, see also Figure 1.1) with thermal insulation of 100–150 mm in between (fibrolite, MW, phenolic foam or EPS). Deviations from the design value of the thickness of the inner layer of RC (e.g. 50 mm instead of 75 mm) exist, caused by large production tolerances and limited total thickness of the panel. Different panels are welded and cast together in situ. The thermal transmittance of solid walls varies in the range $U \approx 0.5$–1.0 W/(m^2·K) and of roofs $U \approx 0.7$–1.0 W/(m^2·K).

The external walls of brick buildings have an inner, load-bearing layer of 250–630 mm in thickness (typically calcium silicate brick), 60–120 mm of MW thermal insulation and a 120 mm external layer (calcium silicate or ceramic brick). The thermal transmittance of solid walls varies in the range $U \approx 0.5$–1.2 W/(m^2·K) and that of roofs $U \approx 0.7$–1.0 W/(m^2·K). In general, slabs on the ground and floor slabs above the cellar are not insulated in these structures.

Typical log dwellings from the first half of the 20th century have 2–3 storeys. The external load-bearing walls are built of horizontal or vertical logs of 120–180 mm in thickness. The inserted floor slabs are usually built of wooden beams. Floor slabs above cellars are also made of RC on steel beams. The thermal transmittance of solid wooden walls varies between ca 0.5 and 0.9 W/(m^2·K). Attics and cellars are generally unheated, and the thermal transmittance of the inserted slabs separating the heated space is $U \approx 0.5$ W/(m^2·K).

Apartment buildings made of autoclaved aerated concrete (included in the evaluation of the heat loss via thermal bridges only) are mainly composed of large blocks that have lime or oil shale ash as the binding agent. Visually similar to some types of brick apartment buildings, these buildings generally have 2–5 storeys. The thermal transmittance of the 300 mm solid walls (density $\rho \approx 800$–1000 kg/m^3) is $U \approx 0.6$–1.1 W/(m^2·K) and that of pitched or flat roofs $U \approx 1.0$–1.5 W/(m^2·K).

In Estonia, it is common that the majority of the original windows having wooden jamb/frame ca 95 mm in thickness have been replaced by the inhabitants in all building types since the late 1990s and early 2000s. Newer windows, characterised often by a narrower, ca 70 mm PVC jamb/frame increase the linear thermal transmittance of external wall/window junction and decrease the air change rate being more airtight.

3.1.3 Buildings involved in the study of corrosion propagation of RC facades

Five prefabricated RC large-panel apartment buildings located in the Helsinki region, Finland, were used for the validation process of corrosion propagation in publication V. Although the principal production technology and general characteristics of the buildings are analogous to those in Estonia, the construction quality (including thermal bridges and frost damage) and overall technical condition are better in Finland. Information for the thesis was collected from the condition investigation reports. These buildings, built between 1968 and 1974 in Siltamäki district, have two to three storeys and concrete facades covered with rubble bulk. As in Estonia, the external wall has two layers of RC and thermal insulation, mostly MW, in between. Data on the building's age, location, concrete cover depth, carbonation depth and corrosion-induced damage with the location of the specimen taken from, were collected.

3.1.4 Hygrothermal performance of a RC external wall

For detailed hygrothermal performance of the external wall, a typical prefabricated RC large-panel wall was used (see Figure 3.1 for illustration and Figure 1.1, Figure 4.2 and Section 2.3 for specific description in addition to publications IV and VI).

Figure 3.1. Reinforced concrete external wall of a case-study building before (left) and after (right) the external thermal insulation composite system was installed.

3.2 Outdoor climate loads

Estonia is located in North-East Europe (59° N, 24° E in case of Tallinn) where maritime-continental climate affected by the Gulf Stream prevails. The temperate zone has four seasons with warm summers and snowy winters with high RH throughout a year (according to Köppen-Geiger (2016) D_{fb} climate classification). The average annual temperature is 5–6 °C, meaning about 4200 heating degree days. The total amount of precipitation varies mostly between 600 and 700 mm according to the Estonian Weather Service. The rainiest months are July and August, although it is often cloudy and rainy during autumn. The dominating winds are south-westerlies of an average wind velocity of approximately 4 m/s. Despite the small area, differences between the rather maritime western and the continental eastern part of Estonia are notable.

Long-term climate data with 1 h frequency from the years 1970–2012 for Estonia and 1979–2009 for Finland measured by the Finnish Meteorological Institute were used, containing the following climate parameters:

- Air temperature, °C;
- Relative humidity, %;
- Wind direction, degree;
- Wind velocity, m/s;
- Rain intensity, mm/h;
- Diffuse solar radiation, W/m^2;
- Direct solar radiation, W/m^2.

4 METHODS

Mixed methods research was used in the thesis. Quantitative methodology by using a large number of studied dwelling units was applied in order to determine indoor hygrothermal loads (publication I) as well as criticality of the thermal bridges (publication II). Qualitative approach was chosen for the in-depth energy performance of different junctions characterised by large variations in publication III. Also profound scientific analysis of corrosion propagation (publications V and VI) can be seen as qualitative research. Qualitative case study field measurements were conducted in order to prove the applicability of the results of the thesis for buildings studied in practice.

Only the main and general methods are reported here to avoid vain duplication. Detailed methods can be found in publications I−VI serving as the basis of the thesis.

4.1 Indoor hygrothermal loads

4.1.1 Measurements

Small data loggers Hobo U12 011 (measurement range from –30 to +70 °C; 5–95% RH; accuracy ±0.35 °C, ±2.5% RH) were used to measure indoor temperature and RH with a 1 h step over the course of one year in the master bedroom and/or living room. Outdoor climate parameters were measured near the buildings or data were obtained from the nearest weather station.

To evaluate the air change rate in bedrooms, measurements of carbon dioxide (CO_2) levels in 13 concrete apartment buildings, one dwelling unit from each building (88 dwelling units in total, see Table 3.1) were conducted over a period of two to three weeks in winter and summer. TelAire 7001 sensors were used for CO_2 measurements with readings at 10 minute intervals. The air change rate was evaluated on the basis of CO_2 measurements (outdoor concentration 350 ppm) and its estimated emissions from inhabitants in bedrooms during the night (approximately 20:00–8:00) following Cui et al. (2015), see Eq. (2):

$$C = C_0 + (C_e + \frac{m}{\dot{V}} - C_0) \cdot (1 - e^{-\frac{\dot{V}}{V}\tau}) \quad (2)$$

where m is CO_2 production (g/h); $\dot{V}$ is the air flow rate (m^3/h); V is the volume of the room (m^3); C_e is CO_2 in the outdoor air (g/m^3); C is CO_2 indoors after measurements (g/m^3); C_0 is the initial CO_2 indoors (g/m^3); τ is time (h).

4.1.2 Calculations

The calculations are based on average night-time human CO_2 emissions (adults: 13 l/h, children: 6.5 l/h) since CO_2 are relatively stable during the night. Average CO_2 emissions for adults while sleeping, at 13 l/h, coincides well with the average figure of 14 l/h (which is valid for a metabolic rate of MET=0.8), as given in EN 15251 (2007). This is supported a figure of by 15 l/h (which included children), found to be representative of Sweden (Bagge et al, 2014). The reliability of the approach has been checked by calculating the CO_2 production levels according to an equation proposed by Tajima et al (2014). This takes the metabolic rate (MET = 0.7 as used in the calculations) and body surface area into account and resulted in 16 l/h as an average for both sexes. The CO_2 tracer gas method which should be suitable for that application is proven by Mikola et al (2017).

Moisture production (moisture source) in bedrooms was calculated based on measured indoor moisture excess and air change rate indoors during the very same night-time period. The volume of the bedroom was used if the bedroom door was closed and the volume of the entire dwelling unit in case the bedroom door was open.

Mechanical exhaust ventilation airflows were measured in the kitchen, toilet and bathroom with an anemometer (SwemaFlow 233). Supply air flow rates were measured with an Alnor/TSI AXD610 Digital Differential Micromanometer.

Survey data were collected for each dwelling unit, covering building characteristics, building materials used, type of building service system and its use, the habits of occupants, typical complaints and health concerns related to indoor air quality. The questionnaire included questions about components affecting both moisture production and air change rate of a dwelling unit.

The value for indoor moisture excess levels, $\Delta\nu$ (g/m^3) (the difference in absolute humidity levels by volume between indoor air ν_i and outdoor air ν_e, also known as moisture supply or vapour excess) was calculated on the basis of the results of indoor and outdoor temperature measurements, along with RH measurements, using Eq. 3):

$$\Delta \nu = \nu_i - \nu_e \tag{3}$$

Moisture production (moisture source) G (g/h) in bedrooms was calculated on the basis of the measured indoor moisture excess and air flow rate indoors, V (m^3/h) (determined from CO_2 decay measurements taken from the very same night-time period), using Eq. (4):

$$G = (\nu_i - \nu_e) \cdot \dot{V} \tag{4}$$

The distribution of data was analysed by using the statistical distribution fitting software, EasyFit, and Pearson's chi-squared test in MS Excel in order to detect whether or not it follows the Gaussian, i.e. normal distribution.

4.2 Thermal bridges

4.2.1 Measurements

To determine typical thermal bridges and their distribution, measurements with a FLIR ThermaCam E320 infrared camera (thermal sensitivity 0.1 °C, measurement range from –20 °C to +500 °C) were conducted in winter in 13 concrete apartment buildings (48 apartment buildings in total). The standard EN 13187 (2001) was followed when the temperature difference between the indoor and outdoor air was at least 20 K.

For the emissivity ε of the surface materials, data from the literature and measurements made by FLIR Systems (2006) were used. From each apartment building, up to four dwelling units (i.e. apartments) were studied.

The presence of mould growth on the internal surface of a thermal bridge was visually inspected combined with the simple tape-lift method (Harris, 2000) and microscopic analysis in the laboratory.

The temperature factor (i.e. the temperature ratio) on the interior surface of the thermal bridge (f_{Rsi}, -) (IEA Annex 14, 1990; EN ISO 10211, 2007; EN ISO 13788, 2012) was used to evaluate the criticality of thermal bridges and the probability of unacceptable performance, see Eq. (5).

$$f_{Rsi} = \frac{t_{si} - t_e}{t_i - t_e} = \frac{R_T - R_{si}}{R_T} \tag{5}$$

where t_{si} is the interior surface temperature, °C; t_e is the outdoor air temperature, °C; t_i is the indoor air temperature, °C; R_T is the total thermal resistance of the building envelope, $m^2 \cdot K/W$; R_{si} is the interior surface resistance of the building envelope, $m^2 \cdot K/W$.

4.2.2 Calculations of the criticality of thermal bridges

The temperature factor f_{Rsi} can be calculated from:

- Thermography measurements $f_{Rsi.res}$ representing the resistance of the thermal bridge;
- Indoor and outdoor climate measurements $f_{Rsi.load}$ representing the load effect on the thermal bridge.

Unacceptable performance (surface condensation or mould growth) occurs if $f_{Rsi.load} > f_{Rsi.res}$, see Figure 4.1. The resulting probability is the overlap of the lowest $f_{Rsi.res}$ and the highest $f_{Rsi.load}$ values. The procedure for calculating critical surface temperature $t_{si.crit}$ or critical temperature factor $f_{Rsi.crit}$ is described in EN ISO 13788, (2012).

The probability of unacceptable performance (P) was calculated according to Eq. (6):

$$P\left(f_{Rsi.res} < f_{Rsi.load}\right) = \int_{0}^{1} f_1(f_{Rsi.load}) \cdot df_{Rsi.load} \cdot \int_{0.26}^{f_{Rsi.load}} f_2(f_{Rsi.res}) \cdot df_{Rsi.res} \quad (6)$$

where f_1, f_2 are probability density functions of $f_{Rsi.res}$ and $f_{Rsi.load}$ respectively; d is differential. The lower limit 0.26 for $f_{Rsi.res}$ should be applied as the worst case possible for the building envelope in case of 0.1 m of concrete around the window frame with the internal surface resistance R_{si} = 0.25 m^{2}K/W.

The probability of unacceptable performance (P) can be easily calculated with MS Excel by inserting Eq. (7):

$$P = \left[NORMDIST\left(1; AVG_{Load}; SD_{Load}; TRUE\right) - NORMDIST\left(0; AVG_{Load}; SD_{Load}; TRUE\right)\right] \cdot$$
$$\cdot \left[NORMDIST\left(f_{Rsi.load}; AVG_{Res}; SD_{Res}; TRUE\right) - NORMDIST\left(0.26; AVG_{Res}; SD_{Res}; TRUE\right)\right] \quad (7)$$

where *normdist* refers to normal distribution; *AVG* is average; *SD* is standard deviation.

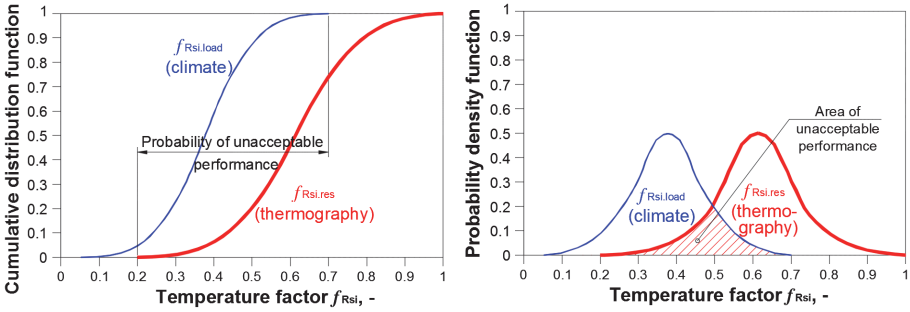

Figure 4.1. Distribution functions from the lowest values of $f_{Rsi.res}$ from each dwelling unit (based on thermography measurements) and the maximum values of $f_{Rsi.load}$ from dwelling units (based on climate measurements).

Normal distribution was chosen by relying on two aspects:

- Data is assumed to approximate to normal distribution as a H0 hypothesis according to the central limit theorem in general. This is valid in case of sufficient sampling and if there is no reason to assume any other distribution;
- For the sake of reasonable simplicity of calculations.

The temperature factors $f_{Rsi.res}$ and $f_{Rsi.load}$ are independent since indoor moisture load does not affect the indoor surface temperature of the building envelope and vice versa – criticality of the thermal bridges does not affect either indoor moisture production or the air change rate.

4.2.3 Calculations of the linear thermal transmittance

Thermal performance of typical thermal bridges was analysed with the two-dimensional (2D) steady-state finite element heat-transfer simulation program THERM 6.0 developed by the Lawrence Berkeley National Laboratory, (2012) and calibrated according to the EN ISO 10211 (2007) standard. The linear thermal transmittance of the thermal bridges Ψ, W/(m·K), was calculated by Eq. (8):

$$\Psi = L_{2D} - \sum_{j=1}^{N_j} U_j \cdot l_j \tag{8}$$

where L_{2D} is the thermal coupling coefficient obtained from the 2D calculation of the component separating the two environments being considered, W/(m·K); U_j is the thermal transmittance of the 1D component j separating the two environments being considered, W/(m^2·K); l_j is the length over which the value U_j applies, m. Length of L_{2D} is equal to Σl_j. Overall internal dimensions of the external envelope according to EVS-EN ISO 13789 (2008) were used in the calculations.

Linear thermal transmittances were calculated for four different building types as original and additionally insulated building envelopes: +100 mm, +150 mm, +200 mm and +300 mm additional external thermal insulation with the thermal conductivity λ = 0.04 W/(m·K). Thermal conductivities of the materials used in the calculations are presented in Table 4.1.

Table 4.1. Thermal conductivity λ, W/(m·K), of the materials used in thermal bridge analysis

Material	Thermal conductivity λ, W/(m·K)
Polyurethane foam	0.024
Additional insulation (mineral wool /expanded polystyrene)	0.040
Phenolic foam (based on phenolic resin)	0.043
Mineral wool of existing building envelope	0.070
Rubber foam, mastics	0.10
Sawdust	0.10
Wood	0.13
Fibrolite (chip cement board)	0.16
Autoclaved aerated concrete	0.23
Dry sand	0.25
Expanded clay concrete	0.30
Hollow calcium silicate masonry	0.70
Ceramic brick masonry	0.70
Calcium silicate brick masonry	0.90
Lime–cement mortar	1.0
Concrete	2.0

In the calculations of linear thermal transmittance, average values of internal surface resistance from the EVS-EN ISO 6946 (2008) standard were used: for roof R_{si} = 0.10 m^{2}K/W, for wall R_{si} = 0.13 m^{2}K/W, for floor R_{si} = 0.17 m^{2}K/W. Thermal resistance R_{se} 0.04 m^{2}K/W was used for all external surfaces.

Transmission heat loss of a building envelope consists of several components: thermal transmittance U, linear thermal transmittance Ψ and point thermal bridges χ. Thermal transmittance can be also presented as an overall reduced (in literature: also 'equivalent') thermal transmittance of a wall U_{red} (W·m^{-2}·K^{-1}), which consists of heat transfer through the 1D opaque wall (excluding windows) and of heat transfer through the 2D thermal bridges divided by the wall area according to Eq. (9):

$$U_{red} = \frac{H}{A} = U + \frac{\sum \Psi_j \cdot l_j + \sum \chi_i \cdot n_i}{A} \tag{9}$$

where H is a specific heat transfer, W/K; A is the area of 1D wall, m^2; U is the thermal transmittance of the 1D wall, W/(m^2·K); Ψ_j is the linear thermal transmittance of the thermal bridge, W/(m·K); l_j is the length of the thermal bridge, m; χ_j is the point thermal transmittance of the thermal bridge, W/K; n is the number of point thermal bridges. Point thermal bridges are not taken into account in this thesis.

4.3 Hygrothermal performance of the external wall

4.3.1 Field measurements of hygrothermal performance of a RC external wall

Temperature and RH inside the concrete wall after the installing of an external thermal insulation composite system (ETICS) were measured in situ to get information for HAM model validation. Two insulation materials, mineral wool (MW) and graphite enhanced expanded polystyrene (EPS), were used. In addition to hygrothermal conditions inside the wall, temperature and RH at the wall surface as well as heat flux and air pressure difference over the building envelope were recorded; see measurement points in Figure 4.2 and illustrative images in Figure 4.3.

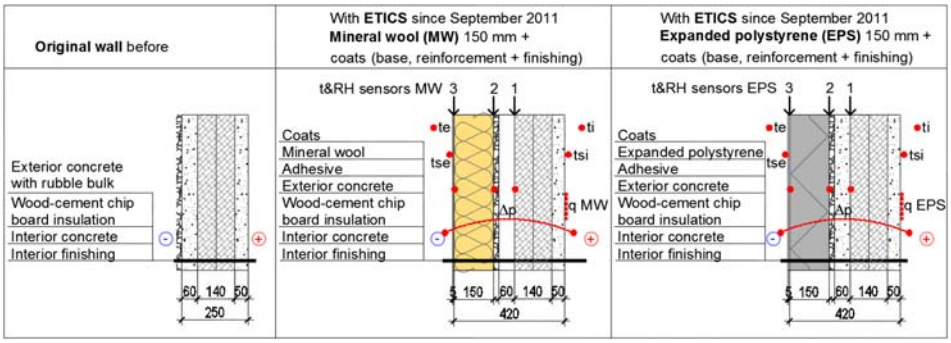

Figure 4.2. Test-wall schematics and measurement points (red dots). ETICS – external thermal insulation composite system; *t&RH* – temperature and relative humidity.

The case study had two aims:

- To study the hygrothermal performance of the concrete wall after applying ETICS;
- To validate the simulation model for further analysis.

Figure 4.3. Illustration of the case study measurements: original reinforced concrete wall covered with rubble bulk and the wiring (left) and the temperature and relative humidity sensor (right).

The heat flux through the external wall was measured with a Ø80 mm Hukseflux HFP01 heat flux plate, measurement range from –2000 to +2000 W/m^2; accuracy +5%/–15%. Surface temperatures were measured by TMC6-HD thermistor (measurement range from –40 to +100 °C; accuracy ±0.25 °C) and TC6-K thermocouple (measurement range from 0 to +285 °C; accuracy ±2.2 °C). Temperature and RH inside the wall were measured by Ø5 mm Rotronic HygroClip SC05, measurement range from –30 to +100 °C; 0–100% RH and accuracy ±0.3 °C, ±1.5% RH. Data were saved by Squirrel Grant SQ2020-1F8 multiple channel data logger placed indoors.

4.3.2 Field study of the corrosion of RC facades

The technical condition of RC facades was surveyed in Siltamäki district near Helsinki in summer 2007 by Tampere University of Technology. All together 44 apartment buildings built in 1968–1974 were studied from which five building were used in the thesis. Buildings had two to three storeys and the RC external core of the three-layer wall was covered with rubble bulk. Both specimens visually not damaged and damaged by cracking or spalling were drilled out from the facades oriented to several cardinal directions. The concrete cover depth, carbonation depth, reinforcement diameter, density, porosity, water uptake and vapour diffusion resistance as well as mechanical characteristics were measured in laboratory.

4.3.3 Calculations by using hygrothermal simulation tool Delphin

The hygrothermal simulation tool Delphin used for simulations was developed in Dresden University of Technology, Germany (Nicolai, 2008). The software is validated (Scheffler, 2008; Sontag et al., 2013) and it is used for simulating coupled heat, air, moisture, pollutants and salt transport. It uses numerical solution which is done by semi-discretisation in space (using a finite/control volume method) and subsequent integration in time. Modelling comprises the description of fluxes in the calculation domain or in the field (between volume elements including material interfaces) and at the boundary (between volume elements and exterior or interior rooms) by physical models. Also models for storage processes such as adsorption, desorption and release are included but hysteresis is excluded.

The moisture mass balance can be written as (Eq. 10):

$$\frac{\partial}{\partial t}\rho_{REV}^{m_{w+v}} = \frac{\partial}{\partial x}\left[j_{conv}^{m_w} + j_{conv}^{m_v} + j_{diff}^{m_v} \right] + \sigma_{REV}^{m_{w+v}} \qquad (10)$$

where $\rho_{REV}^{m_{w+v}}$ is moisture (water + vapour) density in reference to volume kg/m^3; $\sigma_{REV}^{m_{w+v}}$ is moisture source/sink in reference to volume, kg/(m^3·s); j is flux, kg/(m^2·s); *conv* is convective; *diff* is diffusive; v is vapour; *w* is water.

The energy balance is given by Eq. (11):

$$\frac{\partial}{\partial t}\rho_{REV}^{U} = \frac{\partial}{\partial x}\left[j_{diff}^{Q} + u_l j_{conv}^{m_l} + u_g j_{conv}^{m_g} + h_v j_{dif}^{m_v} f + h_{voc,g}\, j_{diff}^{m_{voc,g}} \right] + \sigma_{REV}^{U} \quad (11)$$

where ρ_{REV}^{U} is the internal energy density in reference volume, J/m^3; σ_{REV}^{U} is energy source/sink in reference volume, W/m^3; j_{diff}^{Q} is heat conduction, W/m^2; j is flux, kg/(m^2·s); the subscript *conv* stands for convective, *diff* diffusive, *g* gas, *l* liquid; u is specific internal energy, J/kg; h_v is the specific enthalpy of water vapour, J/kg.

Assumptions of the software are:

- Evaporation equilibrium (the Kelvin equation);
- Diffusive liquid water mass flow, dispersive liquid water and dispersive water vapour mass flow are negligible;
- Pressure equilibrium between all phases (this leads to capillary pressure as well as to defined quantity and to water retention characteristics);
- Distortions of the solid material matrix are negligible;
- Ice does not move.

Versions since 5.8.1 (2013) include an ice model that takes the formation and melting of ice into account, including the enthalpy effect.

Outputs from the software used in the thesis are:

- Temperature t, ˚C;
- Relative humidity RH, %;
- Moisture content w, kg/m^3.

Wind-driven rain (WDR) loads for Delphin are calculated by the user according to Eq. (12):

$$k_{wind} = \begin{cases} 0 \text{ if } \beta_{wind} \geq \pi/2 \text{ or } v_{wind} \leq 0 \\ \dfrac{\cos(\beta_{wind})}{\sqrt{1 + 1141 \cdot \sqrt{\dfrac{3600 \cdot j_{Rain,hor}^{m_w}}{v_{wind}^4}}}} \cdot \exp\left(-\dfrac{12}{5 \cdot v_{wind} \sqrt[4]{3600 \cdot j_{Rain,hor}^{m_w}}} \right) \end{cases} \quad (12)$$

where k_{wind} is local catch ratio of wind-driven rain, β_{wind} is wind angle, degrees; v_{wind} is wind velocity, m/s; $j_{Rain.hor}$ is horizontal rain intensity, kg/(m^2·s).

The presented approach leads to an average local catch ratio of $k_{wind} \approx 0.2$, which is representative for the lower part of the facade in the urban environment for a building up to 20 metres in height (Blocken et al., 2013). This is well consistent with $k_{wind} \approx 0.5$ at wind velocity 10 m/s given by Blocken and Carmeliet (2010). A critical WDR level at the centre of unobstructed facade was achieved via the corrections according to EN ISO 15927-3 (2009) ending up with a catch ratio $\eta \approx 0.43$. A critical WDR level at the top edge of a low rise building

was doubled ($\eta \approx 0.86$), as proposed in (Blocken and Carmeliet, 2010). In the analysis of the applied ETICS, it was assumed, following ASHRAE 160P (2008), that 1% of the WDR load penetrates through the ETICS on the external surface of the original concrete facade.

The material properties used in the calculation of hygrothermal performance of a wall are given in Table 4.2. In addition to fixed values, Delphin's default functions of material properties as depending on the hygric environment were included.

Table 4.2. Material properties used in the calculation of the hygrothermal performance of reinforced concrete external walls

	Concrete	Wood-cement chip board	Adhesive mortar	EPS*	MW*	PIR*	Exterior rendering
Bulk density ρ, kg/m^3	2320	500	700	35	75	35	1270
Porosity θ, m^3/m^3	0.14	0.93	0.73	0.94	0.92	0.91	0.50
Specific heat capacity c, J/(kg·K)	850	1470	945	1500	840	1500	960
Thermal conductivity λ, W/(m·K)	1.5	0.12	0.19	0.035	0.038	0.027	1.0
Water vapour diffusion resistance factor μ, -	19/41	3.8	15	15	2	225	10
Liquid water conductivity k_l, kg/(m·s·Pa)	$4.4 \cdot 10^{-11}$	$16 \cdot 10^{-9}$	$3.2 \cdot 10^{-9}$	0	0	$8 \cdot 10^{-6}$	$0.27 \cdot 10^{-6}$
Air permeability K_g, s	$1 \cdot 10^{-6}$	$7 \cdot 10^{-3}$	$1 \cdot 10^{-5}$	$1 \cdot 10^{-6}$	$1 \cdot 10^{-2}$	0	$1 \cdot 10^{-6}$
Initial moisture w_0, kg·m^{-3}/ RH, %	90–110/ 98.2–99.8	2/ 60	200/ 100	0.6/ 60	3.1/ 60	~0/ 60	300/ 100

* EPS – expanded polystyrene, MW – mineral wool, PIR – polyisocyanurate

4.3.4 Corrosion propagation calculations

The proposed method combines existing corrosion models from the literature and the hygrothermal simulation tool Delphin. The method involves only the period of corrosion propagation, i.e. carbonation of the concrete cover is assumed, see Figure 4.4, left.

The concrete is assumed to be solid, at first without cracks and not deformable. The corrosion process is assumed to be induced by carbonation (i.e. content of chlorides <0.07 weight % of concrete (Gjørv, 2011; Lahdensivu, 2012)) because chlorides were not detected in the concrete specimens drilled in Estonia (Kalamees et al., 2009). The corrosion current inside the external layer of concrete (Figure 1.1) depends primarily on the RH as shown in Figure 4.4, right, and secondly on temperature inside the concrete.

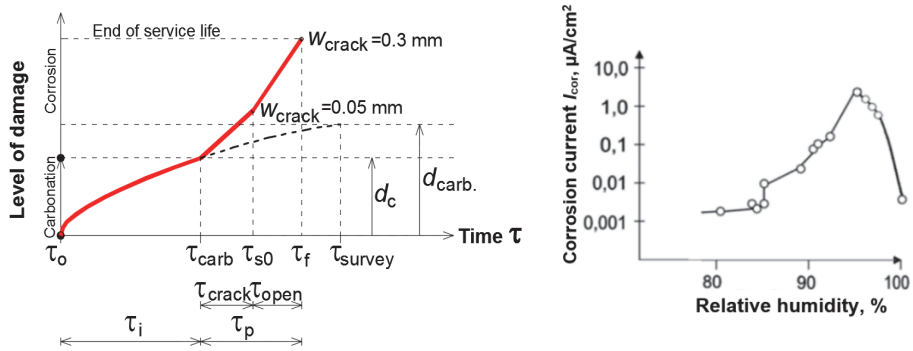

Figure 4.4. Scheme of service life, comprising periods of the initiation (τ_i) and propagation (τ_p) of corrosion (left). On the right, corrosion current depending on the relative humidity (RH) of concrete (valid for a temperature of +5 °C), based on Tuutti (1982).

Corrosion propagation was calculated in the following steps:

- Hourly values for temperature and RH were calculated in the external concrete at the depth of the reinforcement d_c = 20–25 mm by using a dynamic hygrothermal simulation tool;
- Hourly values for corrosion current I_{cor} were calculated from the RH according to Tuutti (1982) in Figure 4.4, right (MS Excel post-processing);
- Hourly values for corrosion current I_{cor} were corrected with the temperature (by 7.5 times with a 10 °C temperature change (Broomfield, 1997) with reference to a 5 °C baseline). Upper limit I_{cor} = 10 µA/cm^2 (i.e. 1 mA/m^2) was set (Künzel, 2015);
- A cross-section loss of the reinforcement was calculated according to Faraday's Law (Eq. 13) from El Maaddawy and Soudki (2007):

$$M_{loss} = \frac{M \cdot I_{cor} \cdot \tau}{z \cdot F} \tag{13}$$

where M_{loss} is the mass of steel dissolved at the anode during the overall time τ, kg/m^2; M is the molecular weight of corroding steel (M = 55.8 g/mol); I_{cor} is the corrosion current, A/m^2; τ is the corrosion duration, s; z is the valence of corroding metal, i.e. the number of electrons involved in the electrochemical reaction (z = 2 for steel); F is Faraday's constant, F = 96487 A·s/mol;

- A cross-section loss x_0 related to the first visible crack (w = 0.05 mm) depends on the cover depth d_c, mm, and the diameter of the reinforcement d, mm, being calculated (see Figure 4.5, left): $x_0 = 7.53 + 9.32 \cdot d_c/d$. The uniform corrosion of a cylinder-shaped d = 3 mm reinforcement mesh (based on condition investigation reports) and the density of the steel ρ = 7850 kg/m^3 are assumed.

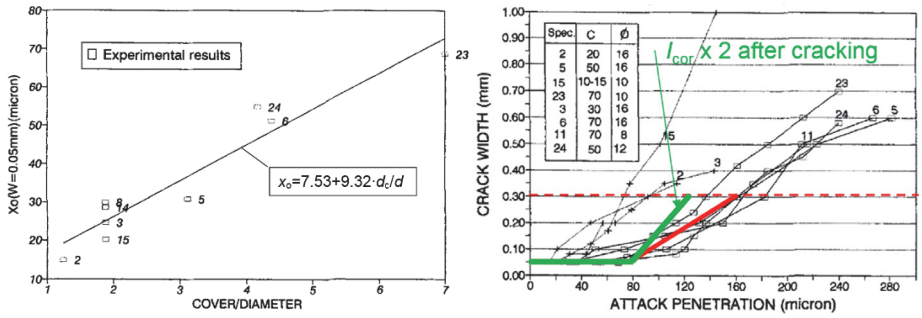

Figure 4.5 The ratio of the concrete cover/reinforcement's diameter causing the first crack (w = 0.05 mm, left) and further crack evolution (w = 0.3 mm, right) modified from Alonso et al. (1998).

- Further attack penetration for the crack's opening, from 0.05 mm up to 0.3 mm (Δ0.25 mm crack width corresponds to Δ80 μm attack penetration), is independent of the cover/diameter ratio from Figure 4.5, right. Corrosion intensity is assumed to double (Δ0.25 mm crack width corresponds to Δ40 μm attack penetration) after the formation of a first crack caused by: i) increased WDR penetration, and ii) dependence of the crack opening on the corrosion current as stated in Alonso et al., (1998).

Several calculation cases were set in order to cover the variability of factors affecting the wall performance (base case is marked with **bold**):

- Calculation period (climate): 1970–1976/**2006–2012**;
- Initial moisture content of the external layer of RC: $w_{initial}$ = **90**/110 kg/m^3;
- Wind-driven rain load: η ≈ **0.43**/0.86;
- Indoor moisture excess: Δν = **3**/5 g/m^3;
- Water vapour diffusion resistance of external RC: μ = **19**/41;
- Three different materials for additional thermal insulation: **EPS**, MW, PIR.

It must also be remembered that the reinforcement corrosion decreases the original safety margin of the load bearing structure. Still, this aspect was not studied in the thesis because the research focused on the performance of the building envelope.

5 RESULTS

Only the core findings of the thesis as a whole are reported here to avoid vain duplication. Detailed results can be found in the publications on which the thesis is based.

5.1 Indoor boundary conditions in Estonian dwellings

5.1.1 Temperature

Temperature measurements (see measurement methods in Section 4.1) show that the heating period ends when the daily average outdoor temperature rises to 10–15 °C and the indoor temperature approximates the outdoor temperature during the warmest summer days. Temperatures in dwellings with central heating and stove/combined heating systems differ: the former have a relatively stable indoor temperature on average at +22 °C throughout the heating period while in the latter the temperature drops to +19 °C with considerable deviations during colder weather. In summer, overheating is generally not a problem due to a reasonable window size and thermal mass of the structures.

The models for the indoor temperature and humidity were developed and validated based on independent field measurements. Two indoor temperature profiles in respect to the outdoor temperature are proposed depending on the heating system, see Figure 5.1. Models representing the average temperature can be used for both the stochastic and the deterministic approach. In case of the stochastic approach, standard deviation is applied. Three types of indoor data sets can be generated:

- T1: variations of indoor temperature t_i between dwelling units where a single line represents the temperature profile for each dwelling unit (SD = 1.8 °C; CV = 0.082 °C);
- T2: variations of indoor temperature t_i within one dwelling unit where each dwelling unit is described with a batch of hourly data (SD = 0.7 °C; CV = 0.032 °C for central heating and SD = 1.4 °C; CV = 0.067 °C for stove heating);
- T3: a combination of T1 and T2 in order to have a batch of lines representing average indoor temperature t_i profiles between dwelling units and a batch of hourly data representing variation of the hourly temperatures within a dwelling unit as well.

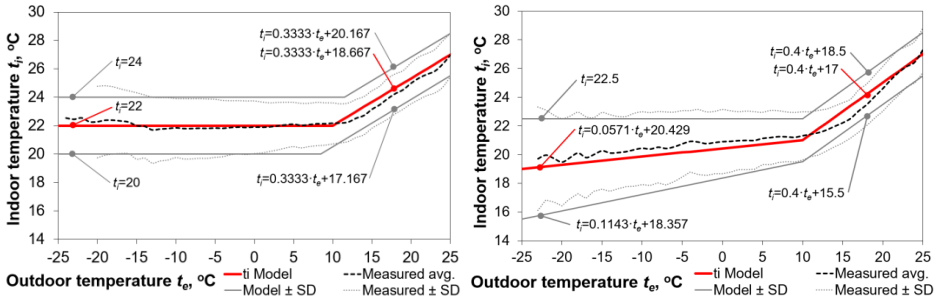

Figure 5.1. Indoor temperature models for dwellings with central heating (left) and stove heating (right).

5.1.2 Humidity

Measurement results of indoor RH show average of all dwelling units around 20% during the coldest time in winter and up to 50–60% in summer with a relatively linear change in between. There are notable deviations of RH (range 10–50% in winter and 40–80% in summer) caused by the range of indoor temperatures as well as large variations of moisture production and air change rate, especially during the heating period.

The average moisture excess based on the measurements was +2.8 g/m^3 (SD ± 1.6 g/m^3; CV ± 0.57 g/m^3) during the cold period ($t_e \leq +5$ °C), +1.4 g/m^3 (SD ± 1.4 g/m^3; CV ± 1.0 g/m^3) during the intermediate period ($+5 < t_e < +20$ °C) and +0.3 g/m^3 (SD ± 0.9 g/m^3; CV ± 3.0 g/m^3) during the warm period ($t_e > +20$ °C).

Like the temperature models, humidity models were developed and validated on the basis of independent field measurements. The M1 model uses occupancy, which is the most important factor influencing indoor humidity loads, as a basis for moisture excess levels. Based on measurements, novel numerical relationships between the moisture excess Δv (g/m^3) and the occupancy O (m^2/person) for the cold period were determined, see Eq. 14 for average and Eq. 15 for 90% critical moisture excess levels:

$$\Delta v = 55 \cdot O^{-0.836} \quad (14)$$

$$\Delta v = 55 \cdot O^{-0.655} \quad (15)$$

For indoor boundary conditions of stochastic hygrothermal analysis, the proposed average values (Figure 5.2, left) and for deterministic analysis, design values at the 90% level (Figure 5.2, right) can be applied. The moisture excess changes in different occupancy groups at 1 g/m^3 step during the cold period and at 0.5 g/m^3 during the warm period. If the dwelling unit's occupancy is unknown, moisture excess value Δv = 6 g/m^3 is proposed for the cold period and 2 g/m^3 for the warm period at the 90% level.

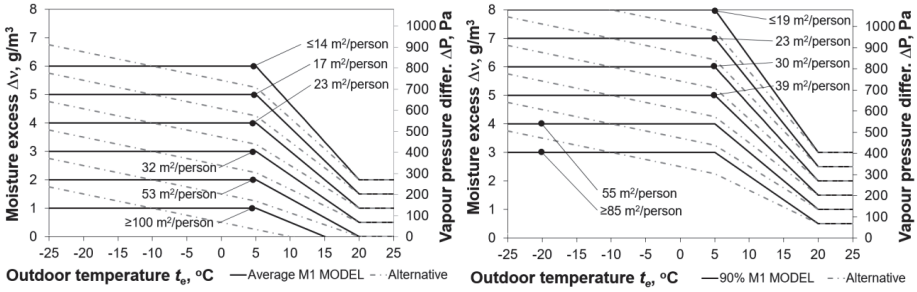

Figure 5.2. Indoor humidity M1 model: the average (left, calculated by using Eq. 14) and 90% design levels (right, calculated by using Eq. 15) of moisture excess correlated with occupancy over the whole outdoor temperature range.

A comparison of the proposed indoor humidity M1 model and the existing EN ISO 13788 (2012) shows that they are similar but with two notable differences: (i) turning points of the graphs (5 °C against 0 °C), and (ii) the levels during warm periods – determining moisture excess levels for warm periods according to the load during cold periods is suggested.

M2 humidity model takes into account in addition to occupancy (primary factor influencing moisture production indoors) secondary factors: air change rate, air leakage rate, the height of the ventilation stack and the age of windows. The numerical relationship between all the factors affecting the indoor humidity load is presented. The M2 model can only be applied if one has measured or predicted data concerning the secondary factors. See details of M2 model in publication I.

Moisture production and air change rate proposed in M3 model can be used as input values for the hygrothermal design by using the whole building simulation models. The model is based on the measurement results in bedrooms during the night: average air change rate $n = 0.60$ (SD 0.43; CV 0.72) h^{-1} and moisture production $G = 72$ (SD 50; CV 0.69) g/h, see Figure 5.3. As there was no significant difference between the moisture excess levels measured during the day and night, the same values are applicable within any period of time.

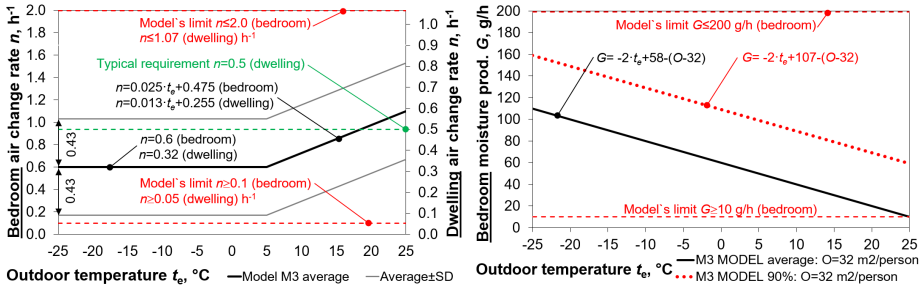

Figure 5.3. The air change rate levels of the bedroom (the primary *y*-axis) and of the entire dwelling unit (the secondary *y*-axis) on the left and moisture production levels for a bedroom as a function of occupancy *O* (right) according to M3 model. The limit value applies for the stochastic approach with average and SD.

Based on the developed M3 model, two novel equations to calculate moisture production G (g/h) based on occupancy O (m^2/person) (for different outdoor temperatures t_e) are proposed: Eq. (16) for a deterministic approach at 90% level and Eq. (17) for a stochastic approach:

$$G = -2 \cdot t_e + 107 - (O - 32) \tag{16}$$

$$G = -2 \cdot t_e + 58 - (O - 32) \tag{17}$$

Based on measurements, the critical value for the air change rate at the 10th percentile was 0.20 h^{-1} for bedrooms and 0.11 h^{-1} for the entire dwelling unit. The critical value for moisture production at the 90th percentile was 121 g/h.

Studying indoor hygrothermal loads in Estonian dwellings had two main aims. First, to get proper indoor boundary conditions for analysis conducted for the thesis. Secondly, long-term and wide-spread indoor climate measurements in cold climates are necessary in order to get more reliable indoor boundary condition models. Indoor moisture loads were proven to depend on the occupancy and the numerical relationship was determined. Two novel temperature models and three humidity models were proposed and their contradiction to the existing standard was denoted.

5.2 Thermal bridges

5.2.1 A method to evaluate the criticality of thermal bridges

The first result to present about the thermal bridges is a novel method combining the measured values of indoor hygrothermal loads and the temperature factor of thermal bridges. The procedure for calculating critical surface temperature $t_{si.crit}$ or critical temperature factor $f_{Rsi.crit}$ is described in (EN ISO 13788, 2012). An example of critical temperature factor based on indoor and outdoor climate measurements of a dwelling unit throughout a year is shown in Figure 5.4.

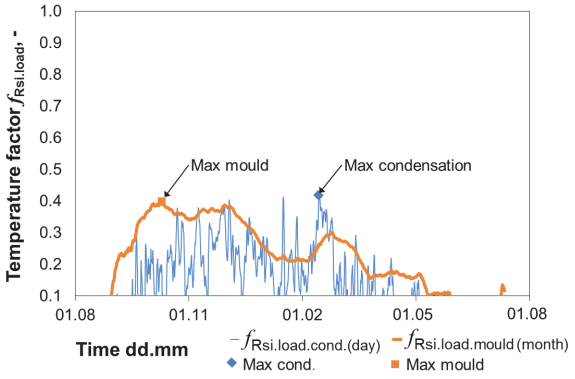

Figure 5.4. Critical temperature factors $f_{Rsi.load(cond.mould)}$ of one dwelling unit during a one-year period. Daily average was used for condensation criterion and monthly average for mould growth criterion.

The probabilistic approach, presuming the normal distribution of measured temperature factors $f_{Rsi.res}$ and critical temperature factors $f_{Rsi.load}$, was used to evaluate the risk of mould growth in concrete apartment buildings, see Figure 4.1. Critical temperature factors were calculated according to indoor and outdoor climate measurements of these buildings in publication I.

5.2.2 Practical application of the proposed method – Estonia's apartment building stock

The proposed method was applied for the whole apartment building stock. The results for concrete apartment buildings are shown in Figure 5.5. The most critical thermal bridge is at the external wall/window junction, but three other junctions characterised by large differences are also critical for the low humidity load.

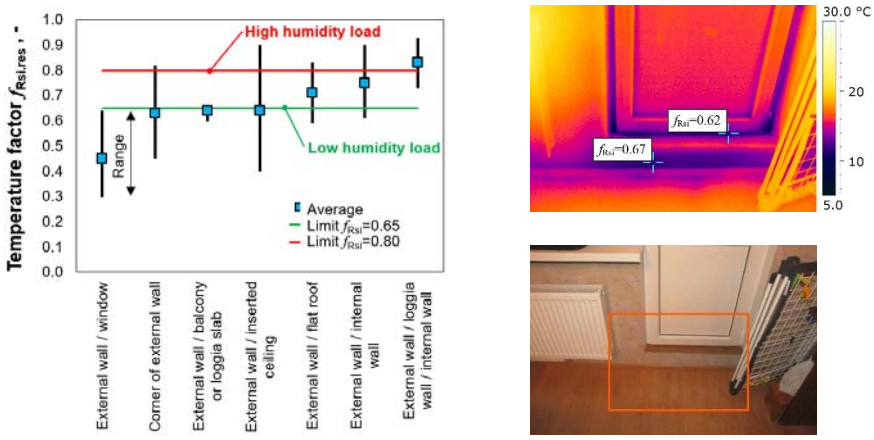

Figure 5.5. Measured temperature factors of different junctions of concrete apartment buildings (left) and sample thermography of an external wall/balcony slab – thermal image (top right) and regular image (bottom right).

Critical temperature factors were calculated based on indoor and outdoor climate (temperature and RH) and the evaluation criterion (surface condensation or mould growth), see Figure 5.6. Significant variations between different dwelling units in concrete apartment building can be seen, ranging between 0.21 and 0.81 for surface condensation and from 0.18 to 0.99 for mould growth, indicating extreme humidity loads in some dwelling units. The temperature factor at 90% level reaches up to $f_{Rsi.load} \approx 0.8$ with a mould growth criterion. As expected, the load of the condensation criterion is the highest during the coldest period in winter and the risk of mould growth is high until the daily average outdoor temperature falls to 10–15 °C in autumn, see also Figure 5.4.

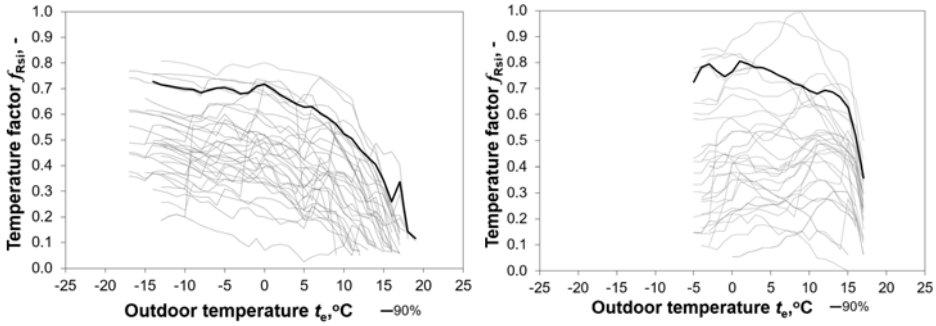

Figure 5.6. Measured temperature factors $f_{Rsi.load(cond.mould)}$ for surface condensation (left) and mould growth (right). Each thin curve represents the maximum daily (for surface condensation) or monthly average (for mould growth) temperature factor in one dwelling unit.

The probability of mould growth was calculated by comparing the distribution of the lowest temperature factors from each dwelling unit $f_{Rsi.res}$ and the highest critical temperature factors $f_{Rsi.load}$ according to Eqs. (6) and (7). The cumulative distribution curves presented in Figure 5.7 show average temperature factors

around 0.56 with large variations (SD 0.21; CV 0.38), especially in case of $f_{Rsi.load.mould}$. The calculated probability of surface condensation was 51%. The calculated mould growth resulted in 54% against visually detected mould growth 46% at the interior surface of the building envelope. As presented distribution of the temperature factors $f_{Rsi.load.mould}$ somewhat differs from the ideal normal distribution, the numerical result might not be exactly 54% but the result close to 50% is unacceptably high anyway.

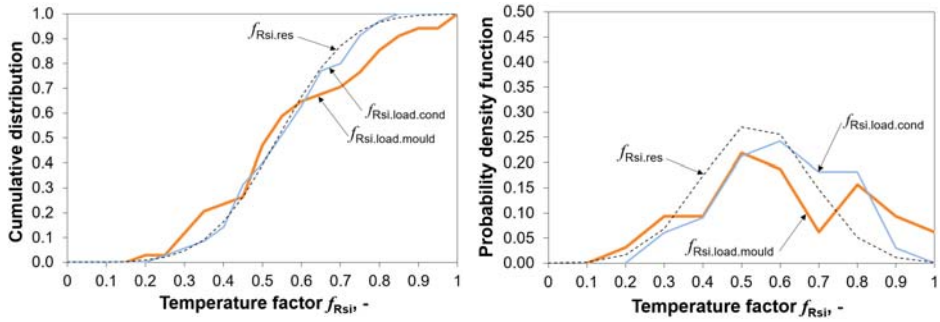

Figure 5.7. Distributions of the temperature factors measured with thermography $f_{Rsi.res}$ and the temperature factors determined from indoor climate measurements $f_{Rsi.load}$ (see Figure 5.4 and Figure 5.6) in the studied concrete apartment buildings.

The main scientific value of publication II is that the inevitability of renovation was proven. Existing concrete apartment buildings characterised by serious thermal bridges in combination with present indoor hygrothermal loads do not fulfil the requirements set to buildings according to CPR, (2011). The proposed method can be used in stochastic analysis if the present need for renovation or designed renovation alternatives are under consideration.

5.2.3 Linear thermal transmittances

The junctions of the external walls of concrete apartment buildings contain a variety of geometrical and structural thermal bridges originating already from the original design drawings. The results of calculated linear thermal transmittances Ψ, W(m·K), in the thesis are applicable for energy audits. Numerical values for the current, pre-renovation concrete apartment buildings (upper row in Table 5.1) as well as the impact of renovation (lower row in Table 5.1) on the thermal transmittance of the building envelope are presented.

Since large variations were found in the original design drawings of buildings of different typology, the results are given as a range instead of a concrete value. The value in brackets in Table 5.1 is valid for a junction that can be considered as being the most probable; if no value in brackets is given, it is advisable to apply the average of the range.

Table 5.1. Calculated linear thermal transmittances Ψ_{oi}, W/(m·K), of various external wall junctions by using overall internal dimensions of the building envelope (in brackets the most probable value)

Junction of external wall	Original wall/ +200 mm insulation	Calculated linear thermal transmittances Ψ_{oi}, W/(m·K)
External corner of external walls	Original wall/	0.50…(0.70)…1.30
	+200 mm insulation	0.12…0.18
External wall/ internal wall	Original wall/	0.12…(0.30)…1.10
	+200 mm insulation	0.00…0.02
External walls/ inserted floor slab	Original wall/	0.25…(0.50)…0.70
	+200 mm insulation	0.00…0.03
External walls/ floor slab above cellar	Original wall/	0.25…(0.50)…0.70
	+200 mm insulation	0.04…0.06
External walls/ inserted floor slab at loggia or balcony	Original wall/	0.15…(0.20)…0.65
	+200 mm insulation	0.18…(0.30)…0.65
External wall/ pitched roof	Original wall/	0.40…(0.55)…1.0
	+200 mm insulation	0.20…0.55
External wall/ flat roof with parapet	Original wall/	0.20…(0.25)…0.90
	+200 mm insulation	0.17…0.50
External walls/ windows (at original position)	Original wall/	0.06…(0.13)…0.30
	+200 mm insulation	0.20…0.50
External walls/ windows (windows inside insulation)	Original wall/	0.06…(0.13)…0.30
	+200 mm insulation	0.01…0.03

The impact of linear thermal bridges on the total thermal performance of a building envelope can be taken into account separately, but can also be considered as a part of the thermal transmittance of a wall.

In case of a so-called bad practice renovation (see Figure 5.8), windows are left in their original position in the wall and concrete balcony slabs are not insulated during renovation.

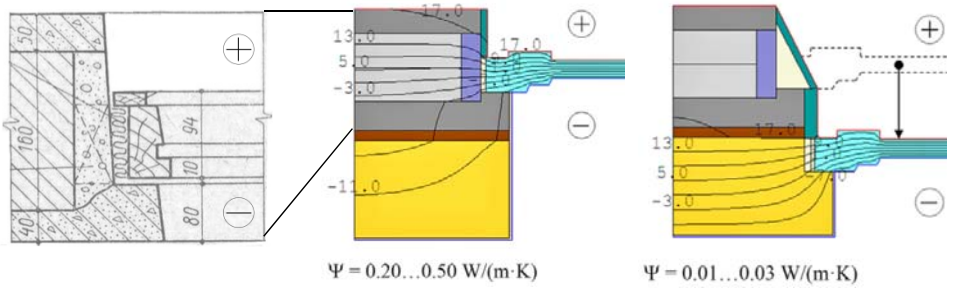

Figure 5.8. An original design drawing of an external concrete wall/window junction (left) with examples of bad practice (middle) and best practice with windows positioned in the plane of additional thermal insulation (right).

In case of a best practice renovation, old windows are replaced and new windows are positioned in the same plane as the additional thermal insulation. Old concrete balcony slabs are demolished and rebuilt or entirely covered with thermal insulation. The latter might be difficult in practice.

The relative significance of the linear thermal transmittances of a typical five-storey concrete element apartment building before and after renovation is presented in Figure 5.9. In case of the bad practice approach, the percentage of thermal bridges in transmission heat loss increases with the level of additional insulation, reaching up to 34% with typical insulation thickness of +200 mm.

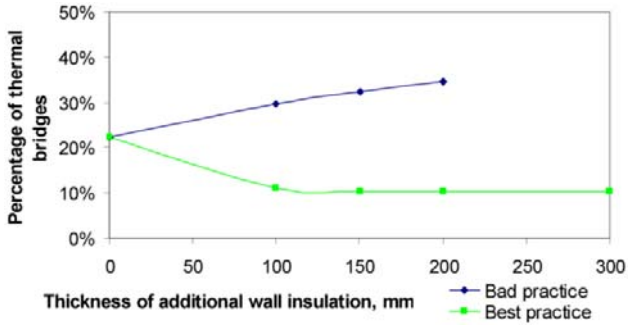

Figure 5.9. Percentage of thermal bridges in transmission heat loss (through the whole building thermal envelope including thermal bridges).

Hence, the new knowledge gained in addition to numerical values proposed for the linear thermal transmittances is that windows should be repositioned in order to attain a reasonable share of thermal bridges in the total transmission heat loss of the building envelope. In theory, thermal insulation is designed to the external side of a window jamb. In practice, it is possible to install insulation only 5–20 mm in thickness, as found in a case study in publication IV.

5.3 Hygrothermal performance of an additionally insulated external wall – a case study

5.3.1 Thermal performance

Thermal transmittance was measured (see measurement methods in Section 4.3) and calculated for concrete walls with ETICSs in which MW or EPS was used for insulation. Average thermal transmittance during winter was ca 0.19 W/(m^2·K) for MW and ca 0.17 W/(m^2·K) for EPS. These results are in accordance with what was expected based on the thermal conductivity of the insulation materials. The measured value for MW is even lower than calculated. This is probably due to the fact that the declared thermal conductivity is higher than average.

Calculated and measured temperatures of both walls match quite well. In the case of MW, calculated temperatures at measurement points 1 and 2 are up to

1 °C lower than measured and in the case of EPS, up to 1 °C higher than measured, see Figure 5.10.

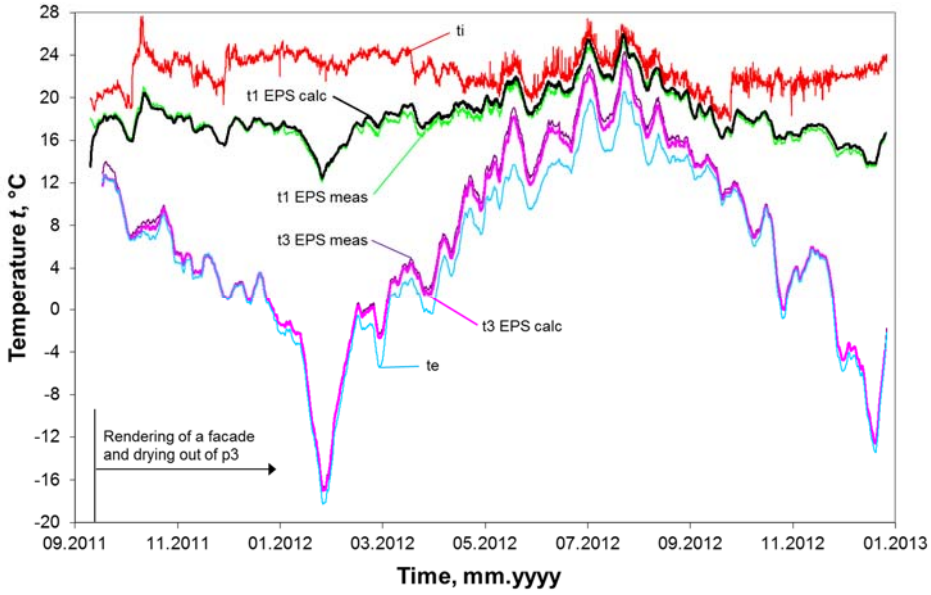

Figure 5.10. Measured and calculated temperature *t*, °C in the wall additionally insulated with the EPS-ETICS. See numbers of measurement points (p) in Figure 4.2. Temperature in point 2 (not shown for clarity's sake) is similar to that in point 1.

5.3.2 Moisture performance

A fair agreement between the measured and calculated results was achieved in terms of RH and vapour pressure. These results fit the steady-state distribution of the wall according to EN ISO 13788 (2012) during the stable boundary conditions as well.

After first calculations, there was a mismatch concerning the drying out period. According to field measurements, moisture in the wall (hygroscopic moisture in the external layer of RC and additional moisture from adhesive mortar) dried out within 3–4 months. In the calculations, however, moisture did not dry out until the next summer, see Figure 5.11. These drying out times are supported by findings of Künzel (2015), according to which drying out took approximately 6 months after the installation of ETICS with MW and 2 years in case of EPS-ETICS.

Since the measured drying out indicated fast and similar behaviour for both insulation materials, diffusion could not be the dominant phenomenon due to very different vapour diffusion resistance of MW ($\mu = 2$) and EPS ($\mu = 15–20$).

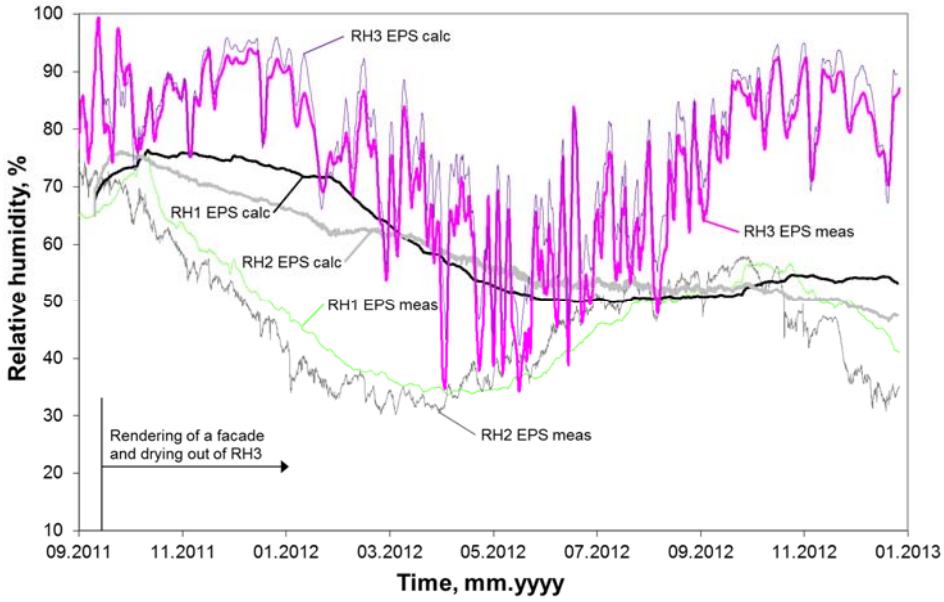

Figure 5.11. Comparison of measured and calculated relative humidity (RH) only by diffusion of the EPS-ETICS.

For that reason, another moisture transfer phenomenon had to be present. Since the measured RH inside the wall was too low for the liquid flux, air convection must have been the reason for faster drying out. Therefore, air gaps 1 mm in width were introduced between the measurement points 1 and 2 (Figure 4.2) with the air pressure difference as the driving potential. This enabled the measured and calculated results to converge, see Figure 5.12.

At this point, a correcting upgrade is made in the thesis compared to publication IV. Namely, there was little information about material properties of concrete and EPS, e.g. vapour diffusion resistance μ at the time of calculations in the year 2012. Since that time, measurement results in Estonia, Finland and elsewhere have become available, referring to values μ = 30–70 for concrete and μ = 20–40 for EPS. Therefore, an additional analysis was performed to evaluate the impact of the material's vapour diffusion resistance on the validated model.

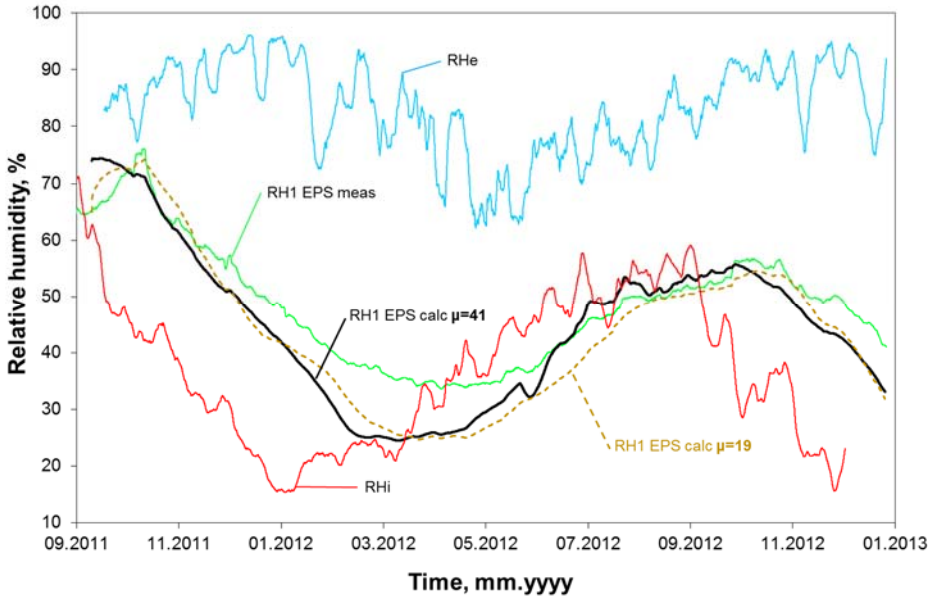

Figure 5.12. Measured and calculated relative humidity (RH) in the EPS-ETICS wall and the impact of different vapour resistances of concrete (μ = 19 vs μ = 41).

The relevant new knowledge gathered from the field measurements and computer simulations is as follows:

- Other moisture transfer phenomena in addition to diffusion might be present;
- Applying a sufficient layer of thermal insulation on a window jamb is problematic in practice.

5.4 Corrosion propagation

5.4.1 Validation of the method

Validation of the method was presented in Section 4.3.4 and in publication V. The calculated propagation periods $\tau_{p,c}$ and real propagation periods $\tau_{p,r}$ are presented in Figure 5.13. Each of the five points represents one degradation case from one facade. Average calculated propagation periods of $\tau_{p,c} = 20.4$ (SD 8.5; CV 0.42) years compared to the average real-time propagation period of $\tau_{p,r} = 19.8$ years with a notable deviation (SD 6.5; CV 0.33). Three calculated results out of five underestimate the progress of corrosion and two estimate it as being on the safe side. Introducing a safety margin, say, factor 0.5 for calculated results, could be discussed.

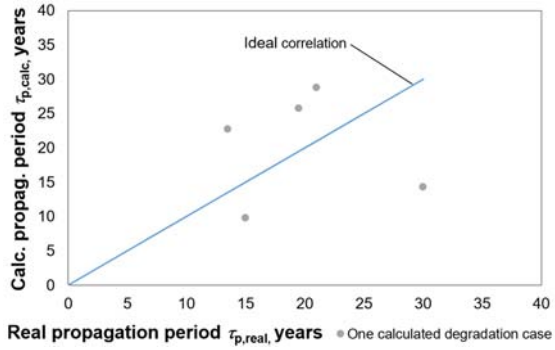

Figure 5.13. Comparison of real-time and calculated propagation periods.

The proposed method demonstrates an ability to evaluate the corrosion propagation and can be applied to evaluate the degradation, service life and need for the renovation of RC facades.

5.4.2 Hygrothermal performance of exterior concrete

The results show that the temperature inside the RC after applying an ETICS is relatively stable and does not drop below +10 °C even in Estonian winter with temperatures below –20 °C. Hence, no more freeze–thaw cycles in RC will appear after the installation of additional external thermal insulation, see Figure 5.14.

A delay of approximately ten days between the WDR hitting the original facade and an increase of the RH at 20–25 mm from the concrete's surface was observed. The RH inside the concrete stays rather high (>95%) compared to the surface during most of the year and dries out to some extent in spring and summer. This is similar to what was found by Saar (2013) and Pihelo et al. (2016) although expressed as moisture content w in the latter, e.g. $w \approx 80$ kg/m^3 corresponds to RH ≈ 95%. Most of the initial moisture in the RC dries out during the first year and the rest during the second year via vapour diffusion.

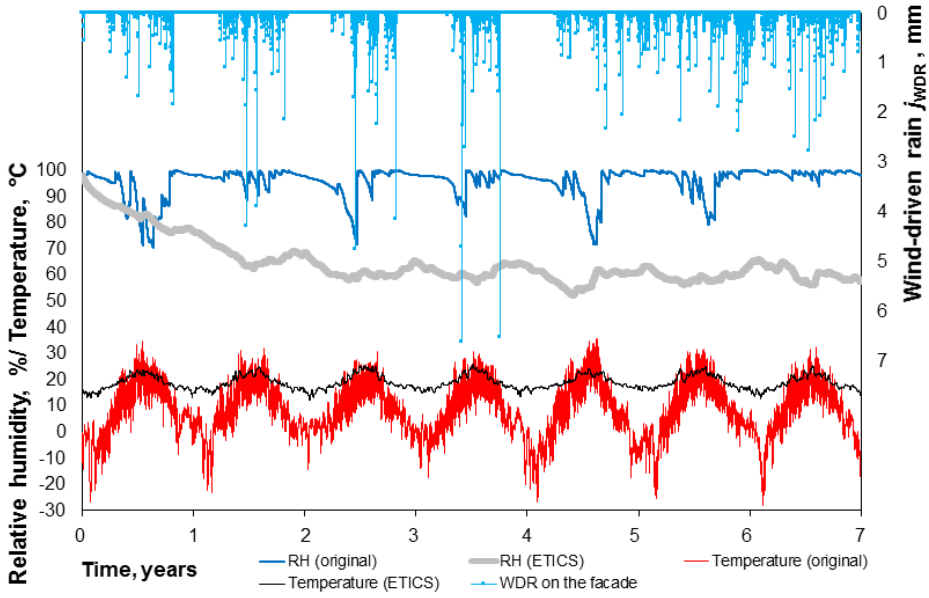

Figure 5.14. Temperature and relative humidity (RH) inside the external layer of reinforced concrete at 20–25 mm from the facade surface.

5.4.3 Corrosion propagation of concrete facades after applying an ETICS

The method proposed in publication V was applied to evaluate the corrosion propagation in RC facades. The corrosion propagation in the external layer of RC concerning the current, pre-renovation conditions as well as the impact of applying ETICS was focused on.

The results show that summer periods, characterised by high temperatures and severe WDR loads, are responsible for most of the corrosion propagation and a limit state $I_{cor} = 10$ µA/cm^2 is reached, see Figure 5.15.

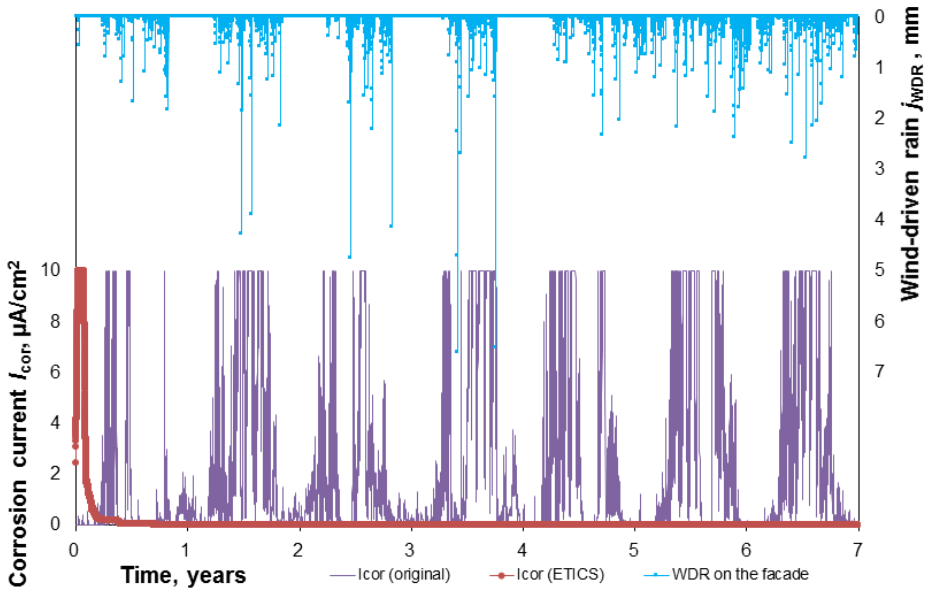

Figure 5.15. Corrosion current of an original wall before renovation and the impact of applying an external thermal insulation composite system (ETICS).

Corrosion current (Figure 5.15) was summarised for the total corrosion current, see Figure 5.16 and Figure 5.17. This enables us evaluating whether the total corrosion propagation causes cracking of RC or not. The residual service life of an original RC wall facing south-west and not sheltered from WDR is approximately three to six years after the carbonation depth has reached the reinforcement (Figure 5.16 and Figure 5.17). The exact duration depends mostly on the outdoor climate, hygrothermal properties of concrete, but also on the ratio of concrete cover depth against the reinforcement diameter. The most intense time of the year in terms of corrosion for the original RC facade is summer, characterised by a high level of rainfall and outdoor temperature and autumn with a higher moisture content of the concrete compared to summer but lower temperatures. Variations between the corrosion current at a different depth from the surface (10–15 mm; 15–20 mm; 20–25 mm) in Figure 5.16 are rather small whereas a higher and more stable RH level deeper inside the concrete leads to faster corrosion. In the case of a small cover depth, say 10 mm, or thick reinforcement, say Ø8 mm, cover depth d_c diameter d ratio is only 2–3, meaning a residual service life of 3–4 years.

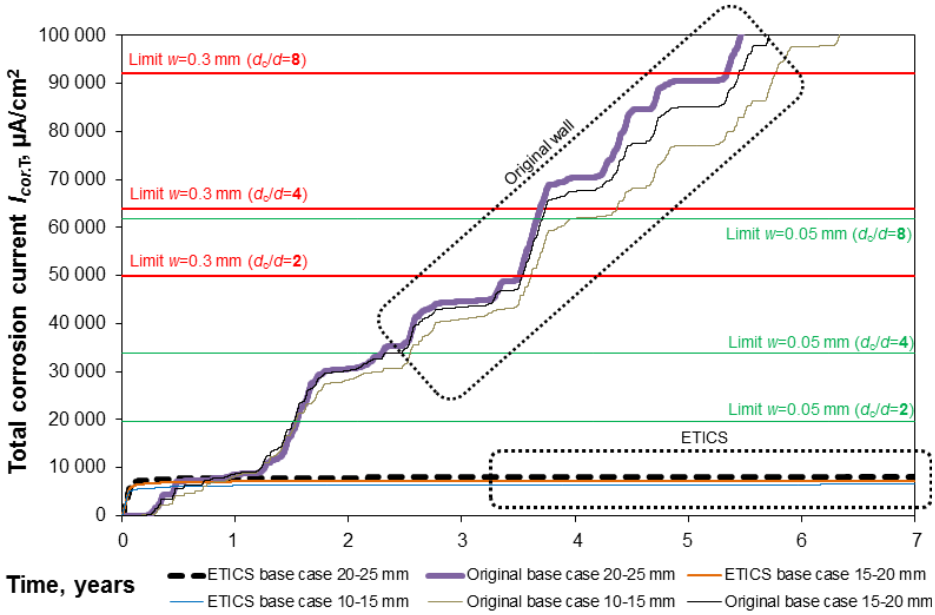

Figure 5.16. Total corrosion current at different depths from the surface without ETICS (original wall) and after applying ETICS. Horizontal lines stand for the limit criteria for different ratios of concrete cover depth d_c against reinforcement diameter d.

The results presented narrow down to two batches, referring to small variations within both calculation cases: an original wall as well as a wall having an ETICS. Small deviation of the results concerning different climatic years, WDR load, material properties, and indoor moisture excess in Figure 5.17 increase the reliability of the calculated residual service lives. As expected, increasing the moisture excess from base value $\Delta v = 3$ g/m^3 (see end of Section 4.3.4) to $\Delta v = 5$ g/m^3 accelerates the corrosion propagation but none of the changed parameters (time period, catch ratio) leads to any significant alteration.

Installation of ETICS (another, lower group of results in Figure 5.16 and Figure 5.17) increases the corrosion propagation during a short period of time while the moisture dries out. Anyhow, the total corrosion of reinforcement in carbonated RC after applying an ETICS of all calculation cases (see Figure 5.17) is so slow that no cracking will happen. The largest effect on the drying out, and hence, on the corrosion propagation, is the vapour diffusion resistance of the thermal insulation (PIR, $\mu = 225$) used for the ETICS. Levels of total corrosion have similar behaviour in the case of high initial moisture content of concrete ($w_0 = 110$ kg/m^3), reaching much higher levels compared to the ETICS base case. From the criterion of corrosion propagation (crack width $w = 0.3$ mm), all three thermal insulation materials used for ETICS are fair. Still, the durability of ETICS, especially frost damage in the case of mineral wool, has to be further

analysed in terms of large moisture flux originating from the concrete while drying out.

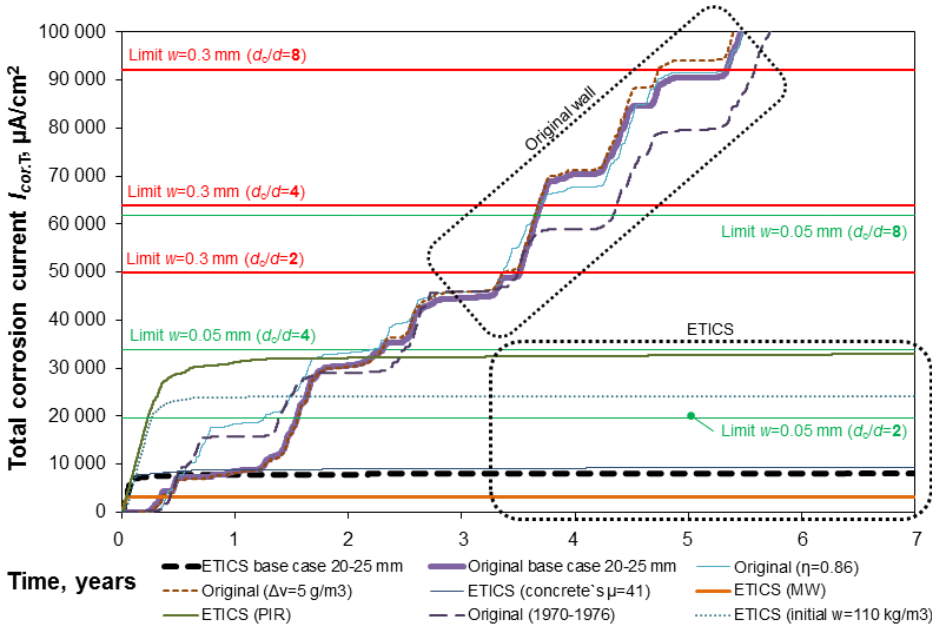

Figure 5.17. Total corrosion current of different calculation cases against the limit criteria and the impact of applying ETICS at a 20–25 mm cover depth. Each calculation case represents one deviation from the base case – changed parameter named in the parentheses.

Since only one parameter was changed at the time to study its effect, using PIR insulation in combination with high initial moisture content might lead to unacceptable performance and therefore it should be avoided.

The scientific contribution of publications V and VI consists in showing that it is possible to calculate the degradation of RC facades although the accuracy and reliability of the calculated results are yet to be improved. The method allows for an evaluation to be carried out on degradation, residual service life, and the need for the renovation of RC facades.

6 DISCUSSION

6.1 Indoor hygrothermal loads

In general indoor climate measurements resulted in similar indoor hygrothermal loads as presented in the summary of latest measurements (Kumaran et al., 2008; later references see in publication I) and in the existing standards EN 15026 (2007) and EN ISO 13788 (2012): the levels of moisture excess during colder periods are higher compared to the warm season. On the one hand, this comes from the lower ventilation rates (set by the occupants or maintenance manager as declared during the interviews in buildings with mechanical ventilation) to save heating energy, achieve better thermal comfort and avoid extremely low indoor RH. On the other hand, this caused by the higher moisture production due to an increased level of indoor activities during the colder period. Lower ventilation air change rates are supported by Bekö et al. (2010), who found occupant behaviour to be a stronger predictor of the ventilation air change rate than building characteristics. Indoor humidity design loads have changed since the revision of the latest version of standard EN ISO 13788 (2012): moisture excess during summer has risen from $\Delta\nu$ 0 to 0.7 g/m^3. Nevertheless, the current study showed similar results with a previous authoritative study in Finland (Vinha, 2007), according to which a higher humidity load during the cold period resulted in a higher humidity load also during the warm period. Another difference between the proposed model and EN ISO 13788 (2012) is the turning point of the moisture excess graphs (5 °C against 0 °C). Therefore, a different indoor hygrothermal model was proposed into the national annex of EN ISO 13788 (2012). These differences may describe national living peculiarities, living style or building properties. The impact of moisture excess and moisture production during the daily and weekly cycle was found to be insignificant.

A novel outcome of the thesis is the possibility of choosing the moisture excess level based on occupancy and at any probability of an average based on all the data as well as a critical value based on weekly maximums. Although the dependence of the indoor humidity load on occupancy has been known before, in the thesis the parameters affecting the moisture excess are quantified and the numerical relationships between the moisture excess and occupancy as well as moisture production and occupancy, are determined.

Differently from the Finnish study by Vinha (2007) showing that new apartment buildings have a lower moisture excess, the Estonian study did not reveal such performance. Therefore, occupancy is proposed as the main selection parameter for moisture excess and moisture production in the thesis. This makes the designer's work also more straightforward and simulation more adequate. The moisture excess for the design of the building envelope is proposed to be $\Delta\nu$ 6 g/m^3 during the cold period and $\Delta\nu$ 2 g/m^3 during the warm period if occupancy appears to be unknown. As this is a higher indoor humidity load than for Finnish apartment buildings (RIL 107, 2012), structural solutions imported from Finland should be checked before using them in Estonia. Although occupancy may vary

between the apartments, the building envelope should be sufficiently performing and durable also for higher loads.

In addition to the improvement of the EN ISO 13788 (2012) standard, data was generated also for designers who make whole building heat, air and moisture simulations and need moisture production data (instead of moisture excess). The volume of the room to evaluate the air change rate and moisture production depends on whether the bedroom door is open or closed. This might cause some inaccuracy in the results since there is probably some air transfer within the apartment although the door is closed. The average bedroom moisture production 72 g/h is mostly the moisture emitted by the occupants. This does not include other sources such as cooking, showering, cleaning, drying laundry, plants, aquarium etc.

In most cases an insufficient air change rate and large variations within the results indicate the need for better control and adjusting with assuring the required level of ventilation. Therefore, mechanical ventilation at a tolerable sound level with the heat recovery as a solution that is less dependent on the outdoor climate conditions should be installed during renovation. The indoor humidity load should be reduced and the performance of ventilation improved as both of them affect the occupants' heath. A recent Swedish cross-sectional study showed that asthma attacks are less common in buildings with a higher ventilation rate and respiratory infections are more common in homes with a higher humidity load (Wang et al., 2016).

6.2 Thermal bridges

6.2.1 Criticality of thermal bridges

The analysis of criticality of thermal bridges showed thermal bridges in combination with high indoor humidity loads in Estonian old apartment buildings to be a serious problem. Therefore, additional external thermal insulation is inevitable in the renovation of old apartment buildings. In countries with milder climate or with a better original thermal quality of building envelopes, additional external thermal insulation has not been mandatory in the renovation of old facades. The current renovation grant scheme (RT I, 31.12.2015, 2016) requires additional thermal insulation for external walls to guarantee thermal transmittance $U \leq 0.22–0.25$ W/(m²·K) depending on the percentage of subsidy.

The method developed to evaluate the criticality of thermal bridges uses thermography measurements in the determination of temperature factor $f_{\mathrm{Rsi.res}}$. This advantage enables avoiding uncertainties in the calculation of surface temperatures from three-dimensional (3D) junctions because the actual long-wave radiation emitted from the surface (i.e. surface temperature if the surrounding environmental conditions are known) is measured. The lowest indoor surface temperature was measured at 3D corners, and the detected mould growth confirmed that these were the most critical. A low temperature factor at the roof junction is related to a somewhat higher probability of unacceptable

performance as the top storeys of naturally ventilated buildings have a small stack height, which leads to lower air change rates.

Paint and wallpaper often used for the interior finishing in bedrooms and living rooms of the studied concrete apartment buildings have emissivity values $\varepsilon = 0.84–0.97$ according to FLIR Systems (2006). Although each of the surface materials was not validated for the exact emissivity, the given range is close to the averaged emissivity $\varepsilon = 0.90–0.95$ used in measurements as well as in post-processing. As found by Barreira and de Freitas (2007), differences of thermal images were not very significant in case of specimen's emissivity $\varepsilon = 0.85–0.95$. In the referred study, as small as 1 °C temperature difference between the object and the surrounding environment is detectable. Since the measured interior surface temperatures in the thesis were typically 5–10 °C lower than the indoor air temperature, the measurement accuracy with the thermal sensitivity 0.1 °C of the thermal camera is good. Wallpaper belongs to the class 'sensitive', and the detected mould growth is consistent with the classes proposed by Ojanen et al. (2010), indicating that the used monthly average critical RH = 80% is valid also for surface materials in the studied concrete apartment buildings. The findings in the thesis (Figure 5.6) prove the earlier results of by Kalamees (2006): to avoid mould growth and surface condensation in dwelling units with high indoor humidity loads (publication I), the temperature factor should be $f_{Rsi} > 0.8$ at the 10% critical level.

A sufficient quantity of the measured interior surface temperatures and indoor loads should be analysed in order to decrease uncertainty due to variation. At least 10 apartments from at least 10% of all apartment buildings is proposed as the sufficient quantity for thermography measurements. Direct measurements of indoor air temperature and RH as well as internal surface temperature by using thermography could be utilised as a regular, non-destructive, relatively simple and inexpensive process in the assessment of the technical condition of a single dwelling unit, a building, a district, or a whole housing stock. If direct measurements are not possible to conduct, a consultant can use indoor hygrothermal models presented in publication I. Also the distribution function of the data should always be examined because the method assumes normal distribution.

Awareness about lessons learnt from low interior surface temperature already has expanded, and probably will continue expanding, and be helpful in the renovations to come. Structural solutions of the building envelope in a cold climate should not be designed without thermal insulation in the junctions. Until the building envelope stays as built, proper ventilation considering occupancy and indoor activities must be guaranteed. Installation of interior thermal insulation should be prohibited since in addition to risks related to building physics, it would also lower the interior surface temperature of the neighbouring apartments.

6.2.2 Linear thermal transmittance

Calculations show that thermal bridges increase the transmission heat loss of the walls of a typical five-storey concrete apartment building by approximately 66% whereas thermal transmittance of a similar, not yet renovated building envelope is unreasonably large already. Installing additional external thermal insulation on the building envelope during renovation decreases the total transmission heat loss considerably but the relative significance of thermal bridges increases. Therefore it is not possible to discard the heat flow through the junctions of the building envelope and use only reduced or averaged thermal transmittances in energy-renovation of Estonian old apartment buildings. It was common practice in history that using external dimensions of the building envelope compensates for the heat flow through the thermal bridges (external corners, connections of roof and wall). However, this method does not take into account the heat flow through non-geometrical junctions as the wall's connection with windows and balconies.

The external wall/window junction should be especially emphasised – 85% of the transmission heat loss of thermal bridges in a five-storey building originates from this junction due to the length of the window perimeter. In case of a nine-storey building, the ratio would be even higher as the percentage of the wall area in the total building envelope is higher. In addition to the increased relative share of thermal bridges, also the absolute value of the linear thermal transmittance at the external wall/window junction is increased after applying additional thermal insulation (Figure 5.8). Large linear thermal transmittance cannot be compensated for with thicker insulation of the building envelope. Therefore, this aspect should be focused on while designing technical solutions and performing economic analysis in order to achieve the level of energy performance required today. Naturally, choosing a low overall thermal transmittance of the window itself is essential (Barnes et al., 2013). To avoid thermal bridges around windows, the current renovation grant scheme (RT I, 31.12.2015, 2016) requires new windows to be positioned in the same plane as the additional external thermal insulation layer. If this is not possible (no consensus between the occupants for example), linear thermal transmittance should be $\Psi \leq 0.05$ W/(m·K).

Concerning the linear thermal transmittance of the external wall/balcony or loggia junctions, applying additional thermal insulation on these components is complicated in practice. Also, the current width of the balcony or loggia of approximately 1 metre would decrease to about 0.8–0.7 m after adding external thermal insulation, becoming clearly too narrow for practical and convenient usage. Due to the poor technical condition and safety aspects of RC loggias and balconies (see Section 2.7), considering the demolition of the latter (and rebuilding, if decided) is advised as a sustainable renovation measure.

As similar concrete apartment buildings and structural solutions were widely used with only a few local changes made, results presented in Table 5.1 are useful also in other countries of the former Soviet Union. Still, before using the values

presented in this thesis, similarities and differences due to local typology, materials and workmanship practice related to junctions must be considered.

6.3 Hygrothermal performance of the ETICS

Applying an ETICS is a possible renovation measure to avoid thermal bridges and to protect facades. Temperature and RH inside the three-layer concrete large-panel external wall were measured in situ as a case study and calculated in order to validate the HAM model for future corrosion propagation simulations. Initial simulation results considering only vapour diffusion showed higher humidity levels than the measured levels. As shown in the results section, measured and calculated results started to correlate after introducing an air gap with the air pressure difference driven by the air densities across the original wall as well as across the ETICS. The reason for this air transfer and its quantities along the wall cannot be declared for sure since these were not measured. Anyhow, an air gap might appear:

- Between the adhesive mortar of the ETICS and rough rubble bulk of the facade;
- Through the shrinkage cracks inside the external layer of RC (see Figure 4.2, Figure 4.3, left and Figure 1.1) caused by heating the panel for faster hydration;
- Air leakages at the junctions of RC panels.

Jansson and Hansén (2015) showed an extensive amount of water leakage through the holes or defects around the ETICS facade details, such as windows, window sills, doors, balcony supports, shades, ventilation ducts etc. in buildings throughout the whole Sweden. Liisma et al. (2016) reported that different cracks are common also in renovated facades with an ETICS in Estonia. This indicates that the hygrothermal performance of the ETICS should be analysed together with air and water (WDR) transfer.

Air and water transfer inside the ETICS might influence its thermal performance and durability. Measurements in the present thesis showed that the impact of air convection inside the wall was small enough not to appear in the results of the thermal transmittance of the wall in practice. In the worst case, it might be large enough for the convective moisture from indoors to condensate inside the ETICS. Therefore, airtight adhesion between the thermal insulation and the original wall as well as airtightness of the ETICS and its detailing at the foundation wall and roof should be carefully designed and executed.

In addition, covering the facade with a ETICS or any other additional external thermal insulation and finishing improves the indoor thermal comfort as well as the aesthetics of the built environment.

6.4 Corrosion propagation of reinforced concrete facade

6.4.1 Validation of the method

Carbonated concrete is one of the presumptions for corrosion propagation in the RC facade. During the sensitivity analysis, alternative exponents of time in addition to $n = 0.5$ as used in calculating the carbonation coefficient k were studied. Measured and calculated corrosion propagation periods were confluent by using rather 0.3 than 0.4 or 0.5 as the exponent of time during carbonation and by taking a crack width $w = 0.3$ mm as the criterion. However, considering large deviations and rather limited sampling (five cases), the author of the thesis is reserved about suggesting exponent of time 0.3 as a research result over 0.5 that is generally used. The results are sensitive to the exponent of time and the crack width as the failure criterion. The impact of changing the exponent of time is found to be relevant whereas it tends to be linear when it comes to corrosion propagation. Sensitivity analysis of material properties detected a notable impact of liquid water conductivity of concrete: the higher the value, the longer the propagation period due to a lower RH inside the concrete. The reason for this is the faster moisture drying out process for a RH value that is close to 100% (liquid moisture flux) dominating over the higher water uptake of the surface. Only a fraction of the WDR hitting the surface is absorbed, the rest of it runs off.

The appearance of the first crack $w = 0.05$ mm (Alonso et al., 1998) is supported by recent solid result as $w = 0.054$ by Köliö et al. (2015). The limiting state criterion for the crack width ($w = 0.3$ mm as used in the thesis), upon which the propagation period depends, has a notable impact. The crack width, say 0.1–1 mm, may be discussed but its further opening after the crack's initial ($w = 0.05$ mm) emergence should be included by all means in order to achieve a more accurate prediction. Accelerated crack opening by the factors of two between 0.05–0.3 mm takes firstly into account the increased WDR penetration caused by the crack itself and secondly, the dependence of the crack development on the corrosion current as shown by Alonso et al. (1998). Crack width $w = 0.3$ mm was chosen on the basis of 0.2–0.4 mm proposed by Teplý and Vořechovská (2012) and 0.3 mm by Al-Neshawy, (2013); Khan et al., (2014) supported by Eurocode 2. Shinohara and Aryanto (2014) confirmed the crack width $w = 0.3$ mm valid for approximately 0.2 mm corrosion penetration, which is in accordance with the approach used in the thesis (Figure 4.5).

6.4.2 Calculated corrosion propagation in reinforced concrete facade

As carbonation depths exceeding the cover depths have already been found in Estonia, the race against time has started. The results of calculated corrosion propagation in a reinforced concrete facade (see Figure 5.16 and Figure 5.17) indicate that the residual service life after the carbonisation of the RC wall is very short (approximately three to six years). This is well in accordance with the propagation period of five years in LNEC E465, (2007) valid for humid environmental class XC4 (cyclic wet and dry) with 30 mm cover depth. This is a

very worrying result because the external surface of older RC facades is mostly carbonated (Kalamees et al., 2011). Therefore addition of external thermal insulation is inevitable in the renovation of old apartment buildings with RC facades in Estonia. Re-alkalisation of carbonated concrete (González et al., 2011) could be another renovation measure, but this is more suitable for historic buildings (Bertolini et al., 2008).

As modernisation of the housing stock in Estonia is evaluated to last for decades (ENMAK 2030, 2016) due to the huge capacity, an urgent and wide-spread monitoring of the carbonation depth and cover depth is advised. According to Hradil et al. (2014), an effort to prolong the service life of the original concrete core is pointless if the limit state of the service life has already been reached at the time of renovation. The small deviation of the results in case of a different climate, WDR load, material properties and indoor moisture excess in present thesis increases the reliability of the statement. An increase of the WDR load ($\eta = 0.86$) gives a somewhat surprising result: the total corrosion current decreases. This can be explained by the dependence of corrosion current on RH, as shown in Figure 4.5. An increase of the WDR causes too high levels of RH in terms of corrosion current, close to 100%. Anyhow, a high initial moisture content can cause biological degradation inside the wall after applying additional external thermal insulation if materials sensitive to mould growth are used (Pihelo et al., 2016). Also, a high moisture flux from the external concrete (in both directions at first and outwards later on) might damage the rendering of the ETICS.

Vapour convection detected in the case study analysis of publication IV was rejected in the current analysis because convection might, or might not, take place. Drying out is the slowest when the insulation material with the highest vapour diffusion resistance ($\mu = 225$ for PIR) is used. Drying out is the fastest, respectively, if the most vapour permeable material is used ($\mu = 2$ for MW). As the base case EPS ($\mu = 20$) was used. Different vapour diffusion resistance of concrete ($\mu = 19$ vs $\mu = 41$) has no significant impact on corrosion propagation.

6.5 Synthesis

Several drawbacks concerning the building envelope were discovered originating already from the initial design and production technology of concrete apartment buildings. Fast mass production with accelerated concrete drying, the quality and availability of the materials (first of all the choice of steel reinforcement) and varying and often small cover depths are some of the examples. In addition, absence of eaves and balconies without glazing combined with poor waterproofing are the architectural factors affecting the quantity of outdoor climate loads on the building.

When it comes to the service of the buildings, lack of a manager in charge, monitoring, small-scale repairs and the awareness of inhabitants have led to the downgrading that would have been easy and cheap to prevent. For instance, water leakages of roofs and wall joints, rainfall drainage and tins, maintenance of

windows and doors, e.g. repainting, a variety of problems related to heating and ventilation as well as other building services should have been handled when appearing. Deplorably, unauthorised actions by inhabitants such as installation of internal thermal insulation or changing the building structures have been executed.

As carbonation is faster in the zones of lower WDR loads, parts of the facade below balconies, awning, eaves etc. have deeper carbonation depths. Therefore, this is what one should bear in mind while future actions and renovation scenarios are considered: the removal of the protective element above carbonated concrete leads to extensive corrosion propagation.

When an additional external thermal insulation or other facade elements is designed, previous actions concerning the building must be known. Current technical aspects and circumstances, including moisture conditions of the building envelope, must be studied and renovation scenarios analysed. Here, the durability and load-bearing capacity of the connections between the internal and external concrete are pointed out as being the subject of corrosion. Removing the original external concrete and thermal insulation is restricted if the thickness of the internal concrete appears to be insufficient for structural stability, e.g. <75 mm.

As this thesis shows, ageing concrete apartment buildings do not fulfil the expected performance requirements because of (i) insufficient air change rate, (ii) high risk of mould growth and (iii) poor energy performance.

6.6 Suggestions for the future research

Research questions posed at the beginning of the studies were predominantly answered as results of the thesis. In addition, the thesis showed that future research and development are necessary to specify the need for the renovation of old concrete apartment buildings. The subtopics to be studied further are presented in the following sections.

The moisture production indoors was calculated assuming a common behaviour and living style of inhabitants. In other words, the results of moisture production were pointed out in the thesis while the reasons and the quantities of contributing sources were not. Moisture production values and their variations could be further studied more deeply. This can be done by laboratory studies (measurements in controlled conditions for a certain moisture production activity) or by field measurements (inhabitants write down their moisture production activities). This helps to develop a more detailed indoor humidity model that can be used in deterministic or stochastic analysis. A detailed indoor moisture production model helps also to determine humidity based ventilation airflow values. Performance criteria could be mould growth (Hukka and Viitanen, 1999; Ojanen et al., 2010), dust mites (Arlian et al., 2001; Hart, 1998; Korsgaard, 1983), dryness of the eyes and skin (Norback et al., 2000; Reinikainen and Jaakkola, 2003; Sato et al., 2003; Sunwoo et al., 2006) or other parameters.

The heat flow through the point thermal bridges and three-dimensional building envelope connection becomes meaningful for future Nearly Zero Energy Buildings where all heat flows should be taken into account in detail. In the assessment of the criticality of thermal bridges, a steady-state heat flow gives some safety margin, especially for a massive building envelope. The formation of interior surface temperature is a quintessentially dynamic phenomenon with several heat transfer phenomena and a fixed state might not be reached with dynamic boundary conditions. Therefore, its dynamic calculation would enable more precise evaluation with shorter periods of time.

The present thesis showed that HAM performance of the additional external thermal insulation systems such as the ETICS, but not solely, should be further studied. As this thesis shows, the component of air might have a significant impact on the HAM performance: possible air transfer between the original wall and the ETICS contributes to the drying out of the built-in moisture. To make more detailed analysis, air flow resistance of the air layer between the original wall and additional thermal insulation should be measured. This can be done in laboratory conditions in the same way as airflow performance of a ventilated sub flooring system is measured (Kalamees et al., 2007). Air velocity measurements and pressure conditions over the thermal insulation layer can be determined in field conditions.

Reinforcement corrosion of RC is a multi-parameter process. Validation of the corrosion model gave approximate results that can provide guidance in future research. However, the variation between field investigations and simulations was rather large. Stochastic simulations are proposed as the next step to find a better agreement between field investigations and the model. Stochastic analysis with varying parameters (indoor and outdoor climate, material properties, carbonation speed, cover depth etc.) could give a better overview about the residual service life of the facades that cannot be additionally insulated. Hygrothermal properties of concrete as well as other materials and surface coatings and their variations should be measured in order to expand the database. Also, the extent of corrosion propagation should be studied in depth. For instance, measurements of corrosion penetration of the reinforcement, type and chemical content of the corrosion products, porous zone at the intersection of concrete and reinforcement and cracking of the concrete cover should be made.

Frost damage in case of different facade coatings and areas under severe WDR loads is advised to focus on. Surface scaling and interior degradation of the concrete specimen should investigated using modulus of elasticity, compressive and tensile strength, pore size distribution and specific area, critical degree of saturation etc. Also, more appropriate and reliable methods to evaluate these properties and the extent of degradation (e.g. the mass loss of the surface scaling) should be developed.

Alternatives to renovation such as demolition and rebuilding or extending the existing building could be perspectives of modernising the ageing housing stock. We cannot ignore this reality, especially in towns where population conditions

demand some modernisation. It is suggested that a sample case study by demolishing a concrete apartment building be considered, driven by the poor technical condition of the building, unattractive location or socio-economic reasons. A building to be demolished would be a valuable on-site research object in terms of extent of degradation mechanisms, detailed structural solutions, material properties etc. Also, it could be a lesson to learn at a more general level, non-technical level such as financing, juridical and relocating the inhabitants.

7 CONCLUSIONS

The thesis discusses problems concerning the need to renovate the ageing housing stock in Estonia. The focus is on the renovation of building envelopes of prefabricated concrete large-panel apartment buildings. In terms of the current physical performance, this need might originate from both sides of the building envelope – interior and exterior.

From the interior side, indoor hygrothermal loads were studied in order to have proper boundary conditions, and temperature and humidity models were proposed based on the measurements. The results show that indoor temperature profiles differ depending on whether a building has central heating or a stove or combined heating system. The determined average moisture excess value, 2.8 g/m^3 with standard deviation (SD) of 1.6 g/m^3 and coefficient of variation (CV) of 0.57 g/m^3 for cold periods, can be used in stochastic calculations. In the deterministic analysis, critical values for moisture excess at the 90th percentile range between 3 and 8 g/m^3, depending on occupancy, which is the main factor affecting the indoor moisture production. The other factor responsible for moisture excess – air change – is significantly affected by air change rate, air leakage rate, height of the ventilation stack and windows (original or replaced). Levels of moisture excess are reported at different percentiles for average and weekly maximums. Moisture excess during warm periods depends on the value during the cold period, meaning considerable distinctness compared to the EN ISO 13788 (2012) standard. Moisture excess during summer is close to 0 g/m^3 while it has a level of ≈ 2 g/m^3 during winter. Moisture excess has a positive value during summer with higher levels, i.e. > 2 g/m^3 during winter. Average moisture production in bedrooms during cold periods is 72 g/h (SD 50 g/h; CV 0.69) and the critical value at the 90th percentile is 121 g/h. The average air change rate in bedrooms is 0.6 h^{-1} (SD 0.43 h^{-1}; CV 0.72 h^{-1}) and the critical value at the 10th percentile is 0.20 h^{-1}. The corresponding average air change rate for the entire dwelling unit is 0.32 h^{-1} (SD 0.23 h^{-1}; CV 0.72 h^{-1}) and the critical value at the 10th percentile is 0.11 h^{-1}. It is concluded that the air change rate poses a serious problem as it is insufficient for roughly 2/3 of the dwelling units according to the European standard EN-15251 (2007).

Measurements of thermal bridges show that unacceptably low interior surface temperatures exist in all types of apartment buildings. The worst results were obtained for reinforced concrete (RC) apartment buildings where average temperature factors $f_{Rsi.res} < 0.65$ exist for several junctions. For the worst dwelling unit the temperature factors from indoor hygrothermal loads are as high as $f_{Rsi.load} = 0.99$ and $f_{Rsi.load} = 0.80$ at the 90% reliability level for mould growth. The calculated risk for surface condensation is 51% for RC apartment buildings and the probability of mould growth is 54%. The calculated results are confirmed by detected mould growth in 46% of the studied dwelling units. Notable thermal bridges from the thermal performance aspect exist in all building types whereas the situation is the worst for RC apartment buildings. As a result of neglecting the external wall/window and the external wall/balcony junctions as typical bad

practice renovation, the percentage of thermal bridges in the transmission heat loss of a building envelope is 30–34%, depending on the thickness of additional thermal insulation. Large linear thermal transmittance of the thermal bridges in certain junctions cannot be compensated for by thicker insulation of the building envelope. As another extreme, the share of thermal bridges in transmission heat loss might be only 10% as best practice. Hence, windows have to be replaced and positioned in the same plane as the additional external thermal insulation and balconies should be rebuilt or insulated from top and bottom in order to fulfil energy performance requirements and to achieve, e.g. the low-energy level.

When it comes to the need for renovation from outside, carbonation induced corrosion is one of the key problems in terms of the future service of RC apartment buildings. A method to evaluate the corrosion propagation phase by combining the existing models and the dynamic hygrothermal simulation tool was proposed and validated based on field measurements.

The corrosion propagation time of the original RC facade exposed to severe WDR loads before renovation is approximately three to six years after the carbonation depth has reached the reinforcement. The exact duration depends mostly on the outdoor climate, hygrothermal properties of concrete, but also on the ratio of concrete cover depth against the reinforcement diameter. Most intense times of a year in terms of corrosion are summer, characterised by high levels of outdoor temperature and rainfall, and autumn with a higher moisture content of the concrete compared to summer but lower temperatures.

The results also show that the ETICS with all the studied thermal insulation materials do not increase the reinforcement corrosion in long term. Corrosion of reinforcement in carbonated concrete after applying ETICS rises for about a year but becomes low later on, and therefore, no cracking will occur. Drying out moisture or vapour diffusion from indoor air is not able to propagate the corrosion of reinforcement in carbonated concrete if it has not started yet before installing ETICS. Temperature of external layer of old concrete facade after applying external thermal insulation remains above +10 °C throughout the year, meaning no more freeze-thaw damage. High initial moisture content of concrete (w_0 >90 kg/m^3) in combination with high water vapour resistance of the additional external thermal insulation (e.g. $\mu = 225$) might cause corrosion induced cracking and is therefore advised to avoid.

Therefore, an additional external thermal insulation together with the improvement of ventilation is advised in order to eliminate critical thermal bridges and to stop degradation mechanisms. In addition, covering the facade with thermal insulation and finishing improve the indoor thermal comfort but also the aesthetics of the built environment. This can be done only within a limited time-frame due to the ongoing degradation accelerated by the adverse future climate scenarios and a huge construction capacity of the existing housing stock.

8 REFERENCES

Ahmad S (2003) Reinforcement corrosion in concrete structures, its monitoring and service life prediction — a review. *Cement & Concrete Composites 25* 25: 459–471.

Al-Neshawy F (2013) Computerised prediction of the deterioration of concrete building facades caused by moisture and changes in temperature. Aalto University. Doctoral thesis.

Allikmaa A (2013) Typology and improvement of energy performance of Estonian detached houses (Eesti väikeelamute iseloomustus ja energiatõhususe parandamine). Master thesis. Tallinn University of Technology (in Estonian).

Alonso C, Andradel C and Diez JM (1998) Factors controlling cracking of concrete affected by reinforcement corrosion. *Materials and Structures* 31(September): 435–441.

Andrade CU and Alonso C (2001) On-site measurements of corrosion rate of reinforcements. *Construction and Building Materials* 15: 141–145.

Arlian LG, Neal JS, Morgan MS, et al. (2001) Reducing relative humidity is a practical way to control dust mites and their allergens in homes in temperate climates. *Journal of Allergy and Clinical Immunology*, Elsevier 107(1): 99–104.

ASHRAE 160P (2008) *Criteria for Moisture Control Design Analysis in Buildings*. *Standard*, Atlanta GA.

Bagge H, Johansson D and Lindstrii L (2014) Measured indoor hygrothermal conditions and occupancy levels in an arctic Swedish multi-family building. *HVAC&R Research* 20(4): 376–383.

Balaras CA, Droutsa K, Dascalaki E, et al. (2005a) Deterioration of European apartment buildings. *Energy and Buildings* 37(5): 515–527.

Balaras CA, Droutsa K, Dascalaki E, et al. (2005b) Heating energy consumption and resulting environmental impact of European apartment buildings. *Energy and Buildings* 37(5): 429–442.

Barnes B, Liesen R and Yu J (2013) Window related thermal bridges. In: *Proceedings of XII International Conference on Performance of Exterior Envelopes of Whole Buildings: Florida, USA, December 1-5, 2013.*, Clearwater Beach: ASHRAE.

Barreira E and de Freitas VP (2007) Evaluation of building materials using infrared thermography. *Construction and Building Materials* 21(1): 218–224.

Bekö G, Lund T, Nors F, et al. (2010) Ventilation rates in the bedrooms of 500

Danish children. *Building and Environment* 45(10): 2289–2295.

Bertolini L, Carsana M and Redaelli E (2008) Conservation of historical reinforced concrete structures damaged by carbonation induced corrosion by means of electrochemical realkalisation. *Journal of Cultural Heritage* 9(4): 376–385.

Blocken B and Carmeliet J (2010) Overview of three state-of-the-art wind-driven rain assessment models and comparison based on model theory. *Building and Environment* 45(3): 691–703.

Blocken B, Derome D and Carmeliet J (2013) Rainwater runoff from building facades : A review. *Building and Environment*, Elsevier Ltd 60: 339–361. Available from: http://dx.doi.org/10.1016/j.buildenv.2012.10.008.

Bouteiller V, Cherrier J and Hostis VL (2012) Influence of humidity and temperature on the corrosion of reinforced concrete prisms. *European Journal of Environmental and Civil Engineering* 16(3): 471–480.

Broomfield JP (1997) *Corrosion of steel in concrete – understanding, investigation and repair.* London: E&FN Spon.

CIB W080 Report (2010) *WG3 Test Methods for Service life Prediction*. Daniotti B and Re Cecconi F (eds), *Cib*, CIB Publication no 331.

CPR (2011) Construction Products Regulation. *Official Journal of the European Union. Regulation (EU) No. 305/2011*: 39.

Cui S, Cohen M, Stabat P, et al. (2015) CO2 tracer gas concentration decay method for measuring air change rate. *Building and Environment* 84: 162–169.

Dehoux A, Bouchelaghem F, Berthaud Y, et al. (2012) Micromechanical study of corrosion products layers. Part I: Experimental characterization. *Corrosion Science*, Elsevier Ltd 54(1): 52–59. Available from: http://dx.doi.org/10.1016/j.corsci.2011.08.048.

Dlugokencky E and Tans P (2016) NOAA/ESRL (National Oceanic & Athomispheric Administration/Earth System Reasearch Laboratory) - Trends in Atmospheric Carbon Dioxide. Available from: http://www.esrl.noaa.gov/gmd/ccgg/trends/global.html#global_data (accessed 19 July 2016).

Dol K and Haffner M (2010) *Housing Statistics in the European Union 2010*. Available from: http://www.bmwfw.gv.at/Wirtschaftspolitik/Wohnungspolitik/Documents/housing_statistics_in_the_european_union_2010.pdf.

EKK (1994) *Condition investigation of concrete large-panel buildings in Mustamäe and renovation proposals (Mustamäe suurelamute konstruktsioonide seisukorra ekspertiisi ning renoveerimise ettepanekud)*. Tallinn. Constructional Engineering and Testing LTD. Tallinn. Report. (in

Estonian).

EKK (2012) *Mapping the balcony railings typology of apartment buildings from 1960-1990. Part I. (1960-1990 Ehitatud korterelamute rõdude esipiirdepaneelide tüüpide kaardistamine. I etapp)*. Constructional Engineering and Testing LTD. Tallinn. Report nr 1211P02 (in Estonian). Available from: http://www.tja.ee/ekspertiisid-ja-uuringud/.

El Maaddawy T and Soudki K (2007) A model for prediction of time from corrosion initiation to corrosion cracking. *Cement & Concrete Composites* 29: 168–175.

EN 13187 (2001) *Thermal performance of buildings - Qualitative detection of thermal irregularities in building envelopes - Infrared method*. Brussels, Belgium.

EN 15026 (2007) *Hygrothermal performance of building components and building elements - Assessment of moisture transfer by numerical simulation*. Brussels, Belgium.

EN 15251 (2007) *Indoor environmental input parameters for design and assessment of energy performance of buildings addressing indoor air quality, thermal environment, lighting and acoustics*. Brussels, Belgium.

EN 1990 (2002) *Eurocode - Basis of structural design*. Brussels, Belgium.

EN ISO 10211 (2007) *Thermal bridges in building construction - Heat flows and surface temperatures - Detailed calculations*. Brussels, Belgium.

EN ISO 13788 (2012) *Hygrothermal performance of building components and building elements – Internal surface temperature to avoid critical surface humidity and interstitial condensation – Calculation methods.* Brussels, Belgium.

EN ISO 13789 (2008) *Thermal performance of buildings - Transmission and ventilation heat transfer coefficients - Calculation method*. Brussels, Belgium.

EN ISO 15927-3 (2009) *Hygrothermal performance of buildings - Calculation and presentation of climatic data - Part 3: Calculation of a driving rain index for vertical surface from hourly wind and rain data*. Brussels, Belgium.

EN ISO 6946 (2008) *Building components and building elements - Thermal resistance and thermal transmittance - Calculation method*. Brussels, Belgium.

ENMAK 2030 (2016) Scenarios of housing stock (Hoonefondi stsenaariumid). *(in Estonian)*. Available from: http://www.energiatalgud.ee/index.php?title=ENMAK_2030._Hoonefondi_stsenaariumid&menu-185 (accessed 4 July 2016).

Erlandsson M and Levin P (2004) Environmental assessment of rebuilding and possible performance improvements effect on a national scale. *Building and Environment* 39(12): 1453–1465.

EstKONSULT (1996) *Reconstruction of apartment buildings in Mustamäe district in Tallinn (Tallinna Mustamäe linnaosa elamute rekonstrueerimine)*. Tallinn (in Estonian).

FLIR Systems (2006) FLIR Systems. Publ. No 1558407.

Gjørv OE (2009) *Durability design of concrete structures in severe environments.* Taylor & Francis, 220 p.

Gjørv OE (2011) Durability of concrete structures. *Arabian Journal for Science and Engineering* 36(2): 151–172.

Glass S V. and Tenwolde A (2009) Review of moisture balance models for residential indoor humidity. In: *12th Canadian Conference on Building Science and Technology*, Montreal, pp. 231–246.

González F, Fajardo G, Arliguie G, et al. (2011) Electrochemical Realkalisation of Carbonated Concrete: an Alternative Approach to Prevention of Reinforcing Steel Corrosion. *Int. J. Electrochem. Sci* 6: 6332–6349.

Gorczyca K (2009) *Przestrzenne aspekty rewitalizacji – śródmieścia, blokowiska, tereny poprzemysłowe, pokolejowe i powojskowe*. Instytut Rozwoju Miast, Krakow (in Polish with English summary).

Gritsenko S (2008) The research of pre-cast large-panel dwellings of the Soviet Union`s mass serial construction (Nõukoguaegsete tüüpsete suurpaneelelamute uuring). Bachelor thesis. Tallinn University of Applied Sciences (in Estonian).

Haapio A (2008) Environmental assessment of buildings. Doctoral thesis. Helsinki University of Technology. Espoo, Finland.

Harris JL (2000) Safe, low-distortion tape touch method for fungal slide mounts. *Journal of clinical microbiology* 38(12): 4683–4.

Hart BJ (1998) Life cycle and reproduction of house-dust mites: environmental factors influencing mite populations. *Allergy*, Blackwell Publishing Ltd 53(s48): 13–17.

Hejtmánek P, Volf M, Sojková K, et al. (2017) First Stepping Stones of Alternative Refurbishment Modular System Leading to Zero Energy Buildings. *Energy Procedia* 111(September 2016): 121–130. Available from: http://linkinghub.elsevier.com/retrieve/pii/S1876610217300310.

Hradil P, Toratti T, Vesikari E, et al. (2014) Durability considerations of refurbished external walls. *Construction and Building Materials*, Elsevier Ltd 53: 162–172. Available from: http://dx.doi.org/10.1016/j.conbuildmat.2013.11.081.

Hukka A and Viitanen H (1999) A mathematical model of mould growth on wooden material. *Wood Science and Technology* 33(6): 475–485.

Huuhka S and Lahdensivu J (2016) Statistical and geographical study on demolished buildings. *Building Research & Information* 44(1): 73–96. Available from: http://dx.doi.org/10.1080/09613218.2014.980101.

IEA Annex 14 (1990) *Condensation and Energy, Guidelines and Practice*. Hens H (ed.). Available from: http://www.ecbcs.org/docs/annex_14_guidelines_and_practice.pdf.

IEA EBC Annex 55 (2012) Reliability of Energy Efficient Building Retrofitting -Probability Assessment of Performance and Cost. Hagentoft CE (ed.).

Ignatavicius Č, Zavadskas EK and Ustinovicius L (2000) *Modernization of Large-panel Houses in Vilnius*. Vilnius Gediminas Technical University, Lithuania.

Ilomets S, Kalamees T, Agasild T, et al. (2011) Durability of concrete and brick facades of apartment buildings built between 1960-90 in Estonia. In: Freitas VP, Corvacho H, and Lacasse M (eds), *12th International Conference on Durability of Building Materials and Components*, Porto. Portugal 12-15 April: FEUP Faculdade de Engenharia da Universidade do Porto, pp. 1171–1178.

IPCC (2014) *Climate Change 2014. Synthesis report*.

ISO 15686 (2000) Buildings and constructed assets— Service life planning. Geneva, Switzerland.

Jamali A, Angst U, Adey B, et al. (2013) Modeling of corrosion-induced concrete cover cracking : A critical analysis. *Construction and Building Materials* 42: 225–237. Available from: http://dx.doi.org/10.1016/j.conbuildmat.2013.01.019.

Jansson A and Hansén M (2015) *Putsade enstegstätade regelväggar: Erfarenheter från undersökningar som SP har utfört.* SP Report. Borås (in Swedish).

Johannesson B (1998) Modelling of transport processes involved in service life prediction of concrete: important principles. *Report TVBM 3083. Lund University*. Available from: http://lup.lub.lu.se/record/526302.

Kalamees T (2006) Critical values for the temperature factor to assess thermal bridges. *Proceedings of the Estonian Academy of Sciences. Engineering* 12(3–1): 218–229.

Kalamees T, Kurnitski J and Helenius T (2007) Airflow performance of ventilated sub flooring system. *Building and Environment* 42(10): 3708–3716.

Kalamees T, Õiger K, Kõiv T-A, et al. (2009) *Technical condition and service*

life of the Estonian prefabricated concrete large panel apartment buildings (Eesti eluasemefondi suurpaneel-korterelamute ehitustehniline seisukord ning prognoositav eluiga).

Kalamees T, Õiger K, Kõiv T, et al. (2011) Technical Condition of Prefabricated Concrete Large Panel Apartment Buildings in Estonia. In: Freitas VP, Corvacho H, and Lacasse M (eds), *Proceedings of the 12DBMC - International Conference on Durability of Building Materials and Components*, Porto, Portugal. 12th-15th April 2011: FEUP Faculdade de Engenharia da Universidade do Porto, pp. 973–981.

Khan I, Francois R and Castel A (2014) Prediction of reinforcement corrosion using corrosion induced cracks width in corroded reinforced concrete beams.pdf. *Cement and Concrete Research* 56: 84–96.

Korsgaard J (1983) House-Dust Mites and Absolute Indoor Humidity. *Allergy*, Blackwell Publishing Ltd 38(2): 85–92.

Kumaran K, Sanders C, Tariku F, et al. (2008) *Boundary conditions and whole Building HAM analysis IEA Annex 41 MOIST-ENG Subtask 3*.

Kuusk K, Ilomets S, Kalamees T, et al. (2014) Renovation vs. demolition of an old apartment building: energy use, economic and environmental analysis. In: Arfvidsson J, Harderup L-E, Kumlin A, et al. (eds), *NSB 2014 10th Nordic Symposium on Building Physics*, 15-19 June 2014, Lund, Sweden.

Kährik A and Tammaru T (2010) Soviet Prefabricated Panel Housing Estates : Areas of Continued Social Mix or Decline ? The Case of Tallinn. *Housing Studies* 25(2): 201–219.

Köliö A, Honkanen M, Lahdensivu J, et al. (2015) Corrosion products of carbonation induced corrosion in existing reinforced concrete facades. *Cement and Concrete Research*, Elsevier Ltd 78: 200–207. Available from: http://dx.doi.org/10.1016/j.cemconres.2015.07.009.

Köliö A, Niemelä PJ and Lahdensivu J (2016) Evaluation of a carbonation model for existing concrete facades and balconies by consecutive field measurements. *Cement and Concrete Composites* 65: 29–40.

Köppen-Geiger (2016) Köppen-Geiger climate classification. Available from: http://koeppen-geiger.vu-wien.ac.at/ (accessed 30 June 2016).

Künzel HM (2015) *Moisture control design by hygrothermal simulation*. Fraunhofer IBP in 19 th Annual Westford Symposium on Building Science.

Lahdensivu J (2012) Durability Properties and Actual Deterioration of Finnish Concrete Facades and Balconies. Doctoral thesis. Publication 1028. Tampere University of Technology.

Lahdensivu J, Köliö A, Pakkala T, et al. (2013) Betonijulkisivun kuntotutkimus BY42 (Field survey of concrete facades). Suomen Betoniyhdistys r.y. Helsinki (in Finnish).

Lahdensivu Jukka, Varjonen S, Pakkala T, et al. (2013) Systematic condition assessment of concrete facades and balconies exposed to outdoor climate. *International Journal of Sustainable Building Technology and Urban Development*.

Lawrence Berkeley National Laboratory (2012) THERM 6.0. Available from: https://windows.lbl.gov/Software/therm/6/index.html.

Liisma E, Sepri R, Raado L-M, et al. (2016) Defect analysis of renovated facade walls with ETICS solutions in cold climate conditions. In: Hajek, P.; Tywonjak, J.; Lupišek, A.; Sojkova K (ed.), *Central Europe towards Sustainable Building*, Prague, Czech Republic. 22-24.06.2016: Grada Publishing, a.s. for Czech Technical University in Prague.

LNEC E465. (2007) *Concrete. Methodology for estimating the concrete performance properties allowing to comply with the design working life of the reinforced or pre-stressed concrete structures under environmental exposures XC and XS.* Lisbon: LNEC.

Long AE, Henderson GD and Montgomery FR (2001) Why assess the properties of near-surface concrete? *Construction and Building Materials* 15(2–3): 65–79.

Markeset IG and Myrdal R (2008) *Modelling of reinforcement corrosion in concrete - State of the art*. SINTEF. COIN Project report 7.

Mikola A, Kõiv T and Rehand J (2017) The Usage of CO2 Tracer Gas Methods for Ventilation Performance Evaluation in Apartment Buildings. In: *'Environmental Engineering' 10th International Conference*, Vilnius, Lithuania.

Mjörnell K, Boss A, Lindahl M, et al. (2014) A tool to evaluate different renovation alternatives with regard to sustainability. *Sustainability (Switzerland)* 6(7): 4227–4245.

Nicolai A (2008) Modeling and Numerical Simulation of Salt Transport and Phase Transitions in Unsaturated Porous Building Materials. Doctoral thesis. Syracuse University.

Nikulin P (2007) Residential development and planning ahead for a sustainable Tallinn. Book of Fulbright program. Tallinn University of Technology.

Norback D, Wieslander G, Nordstrom K, et al. (2000) The effect of air humidification on symptoms and nasal patency, tear film stability, and biomarkers in nasal lavage: A 6 weeks' longitudinal study. *Indoor and Built Environment*, SAGE Publications 9(1): 28–34.

Ojamäe L, Paadam K and Liias R (2009) Regeneration of Mustamäe. In: Holt-Jensen A and Pollock E (eds), *Urban Sustainability and Governance: New Challenges in Nordic-Baltic Housing Policies*.

Ojanen T, Viitanen H, Peuhkuri R, et al. (2010) Mold growth modeling of

building structures using sensitivity classes of materials. In: *XI International Conference on Performance of Exterior Envelopes of Whole Buildings*, Clearwater Beach, Florida: ASHRAE.

Olsen L and Johennesson G (1996) A Guidance of the Treatment of Thermal Bridges in Building Practice. In: *4th Nordic Symposium in Building Physics*, 9-10 September, Espoo, Finland: VTT Building Technology, pp. 247–253.

Otieno MB, Beushausen HD and Alexander MG (2011) Modelling corrosion propagation in reinforced concrete structures – A critical review. *Cement and Concrete Composites*, Elsevier Ltd 33(2): 240–245. Available from: http://dx.doi.org/10.1016/j.cemconcomp.2010.11.002.

Parrott L. (1987) *Review of carbonation in reinforced concrete*. Cement and Concrete Association. Wexham Springs. 42 pWexham Springs. 42 p.

Pentti M (1994) *Repair of building envelope.* In Kaivonen, J.-A. (editor). Repair techniques and economy of buildings. Saarijärvi. Rakennustieto Oy. Pp.

Pentti M, Mattila J and Wahlman J (1998) *Repair of concrete facades and balconies. Part 1: Structures, degradation and condition investigation*. Publication 87. 156p. Tampere University of Technology (in Finnish).

Pihelo P, Lelumees M and Kalamees T (2016) Potential of Moisture Dry-out from Concrete Wall in Estonian Climate. In: *International RILEM Conference on Materials, Systems and Structures in Civil Engineering. Conference segment on Moisture in Materials and Structures. 22-24 August 2016, Technical University of Denmark, Lyngby, Denmark.*

Postimees (2016) 'Balcony awning drop down in Keila'. *Uwe Gnadenteich 23.05.2016 http://tallinncity.postimees.ee/3704901/keilas-kukkus-alla-korterelamu-varikatus/5425921*, Keila. Available from: http://tallinncity.postimees.ee/3704901/keilas-kukkus-alla-korterelamu-varikatus/5425921.

Poukhonto L. (2003) *Durability of Concrete Structures and Constructions (translated from Russian)*. A.A. Balkema Publishers.

Power A (2008) Does demolition or refurbishment of old and inefficient homes help to increase our environmental, social and economic viability? *Energy Policy* 36(12): 4487–4501.

Raslanas S (2011) Residential areas with apartment houses : analysis of the condition of buildings, planning issues, retrofit strategies and scenarios. *International Journal of Strategic Property Management* 15(2): 152–172.

Raupach M (2006) Models for the propagation phase of reinforcement corrosion – an overview. *Materials and Corrosion* 57(8): 605–613.

Reinikainen LM and Jaakkola JJK (2003) Significance of humidity and temperature on skin and upper airway symptoms. *Indoor Air*, Munksgaard International Publishers 13(4): 344–352.

RIL 107 (2012) *Rakennusten veden- ja kosteudeneristysohje (Buildings water and moisture protection guide)*. Finnish Association of Civil Engineers RIL ry (in Finnish).

Roitman A. (1985) *Reliability of building structures service*. Moscow: Stroyizdat (in Russian).

RT I, 31.12.2015 8 (2016) The conditions for support for reconstruction of apartment buildings (Korterelamute rekonstrueerimise toetuse andmise tingimused). *Riigi Teataja - State Gazette of the Republic of Estonia (in Estonian)*.

Ruosteenoja K, Räisänen J, Jylhä K, et al. (2013) *Maailmanlaajuisiin CMIP3-malleihin perustuvia arvioita Suomen tulevasta ilmastosta*. Finnish Meteorological Institute. Report 2013:4 (in Finnish).

Ruzgys A, Volvačiovas R, Ignatavičius Č, et al. (2014) Integrated evaluation of external wall insulation in residential buildings using SWARA-TODIM MCDM method. *Journal of Civil Engineering and Management* 20(1): 103–110. Available from: http://www.tandfonline.com/doi/abs/10.3846/13923730.2013.843585.

Saar J (2013) Evaluation of corrosion propagation phase in reinforced concrete facades (Raudbetoonfassaadi armatuurterase aktiivse korrosiooni analüüs). Master Thesis. Tallinn University of Technology (in Estonian).

Sato M, Fukayo S and Yano E (2003) Adverse Environmental Health Effects of Ultra-low Relative Humidity Indoor Air. *Journal of Occupational Health* 45(2): 133–136.

Scheffler G (2008) Validation of hygrothermal material modelling under consideration of the hysteresis of moisture storage. Doctoral thesis. Dresden University of Technology.

Schiessl P (1988) *Corrosion of Steel in Concrete*. RILEM.

Shinohara Y and Aryanto A (2014) Effect of confinement and concrete strenght upon crack behavior induced by corrosion-product. In: Quattrone M (ed.), *XIII Conference on Durability of Building Materials and Components. 2-5 September, Sao Paolo, Brazil*, pp. 417–424.

Sontag L, Nicolai A and Vogelsang S (2013) Validierung der Solverimplementierung des hygrothermischen Simulationsprogramms Delphin 2013 (in Deutch). Available from: www.qucosa.de/fileadmin/data/qucosa/documents/12896/DelphinValidierung.pdf (28.09.2015).

Szafrańska E (2013) Large Housing Estates in Post-Socialist Poland as a Housing Policy Challenge. *European Spatial Research and Policy* 20(1). Available from: http://www.degruyter.com/view/j/esrp.2013.20.issue-1/esrp-2013-0006/esrp-2013-0006.xml.

Statistics Estonia (2016) www.stat.ee/en. Available from: www.stat.ee/en (accessed 20 June 2016).

Sunwoo Y, Chou C, Takeshita J, et al. (2006) Physiological and subjective responses to low relative humidity in young and elderly men. *Journal of Physiological Anthropology* 25(3): 229–238.

Tajima M, Inoue T and Ohnishi Y (2014) Derivation of equation for personal carbon dioxide in exhaled breath intended to estimation of building ventilation. In: *35th AIVC Conference ' Ventilation and airtightness in transforming the building stock to high performance', 24-25 September*, Poznań, Poland.

Technical Regulatory Authority (2013) *Reinforced concrete balconies and loggia barriers of apartment buildings constructed 1960-1990. Part II. 1960 – 1990 ehitatud korterelamute rõdude ja lodžade raudbetoonist eenduvate esipiirdepaneelide uuring. II etapp. Report (in Estonian)*. Tallinn. Available from: http://www.tja.ee/ekspertiisid-ja-uuringud/.

Teplý B and Vořechovská D (2012) Reinforcement corrosion: Limit states, reliability and modelling. *Journal of Advanced Concrete Technology* 10(11): 353–362. Available from: http://japanlinkcenter.org/DN/JST.JSTAGE/jact/10.353?from=Google.

Terk E and Keskpaik A (2015) *Tallinn`s housing scenarios and the future of districts (Tallinna elamispinnastsenaariumid ja „magamislinnaosade" tulevik) final report (in Estonian)*. Tallinn University. Available from: http://uuringud.tallinnlv.ee/document.aspx?id=11538.

Tuutti K (1982) *Corrosion of steel in concrete.* Stockholm. Swedish Cement and Concrete Research Institute. CBI Research 4:82. 304 p.

United Nations Publication (2004) *Country Profiles on the Housing Sector - Russian Federation*. *Economic Commission for Europe*, New York and Geneva.

Wang J, Engvall K, Smedje G, et al. (2016) Rhinitis, asthma and respiratory infections among adults in relation to the home environment in multi-family buildings in Sweden. In: Laverge J (ed.), *Indoor Air*, Ghent, Belgium. July 3-8: International Society of Indoor Air Quality and Climate - ISIAQ.

Vesikari E (1999) Prediction of service life of concrete structures by computer simulation. Licentiate's thesis. Helsinki University of Technology.

Vinha J (2007) Hygrothermal performance of timber-framed external walls in Finnish climatic conditions: A method of determing a sufficient water vapour resistance of the internal lining of a wall assembly. Doctoral thesis. Publication 658. Tampere University of Technology.

Witzany J (2016) *List of the most common and characteristic defects and faults of panel houses (in Czech)*. Prague. Available from:

http://www.sfrb.cz/fileadmin/user_upload/CHARAKTERISTICK__VADY_komplet_final.pdf.

Woloszyn M and Rode C (2008) *Final report of IEA Annex 41, Subtask 1: Modelling principles and common exercises.* Leuven, Belgium: K.U. Leuven. Department of Civil Engineering Laboratory of Building Physics.

Õiger K (2006) Examination of service life and serviceability of concrete element houses. In: *ESCS*, Espoo, Finland.

Yu B, Yang L, Wu M, et al. (2014) Practical model for predicting corrosion rate of steel reinforcement in concrete structures. *Construction and Building Materials* 54: 385–401.

CURRICULUM VITAE

Personal data

Name:	Simo Ilomets
Date and place of birth:	07.02.1984, Tartu, Estonia
Nationality:	Estonian
E-mail address:	simo.ilomets@ttu.ee, simo.ilomets@gmail.com

Education

Educational institution	Graduation year	Education (field of study/degree)
Tallinn University of Technology	2009	Civil Engineering, MSc
Pärnu Raeküla Gymnasium	2002	Secondary education
Pärnu Raeküla Gymnasium	1999	Lower secondary education
Surju Primary School	(1990–1998)	Lower secondary education

Language competence/skills

Language	Level
Estonian	Native language
English	Fluent
Finnish	Average
Russian	Basic

Special courses

Period	Educational or other organisation
13.-16.12.2010	Net ZEB and on-site renewable energy, Aalto University, Finland
09.-14.01.2011	Urban Physics Winter School, ETHZ, Ascona, Switzerland
15.-23.03.2011	Renovation of Buildings, Tallinn University of Technology
20.04-15.12.2011	Moisture in Materials and Structures, Lund University, Sweden
10.-26.04.2013	2nd PhD international school on Buildings Physics, Pontifical Catholic University of Parana, Curitiba, Brazil
10.-14.06.2013	EnTool 2013 Symposium, Workshop & Summer School, TU Dresden, Germany
Autumns 2012 and 2013	Visiting doctoral student in Tampere University of Technology, Finland

Professional employment

Period	Organisation	Position
2015 − ...	Tallinn University of Technology	Lecturer
2010 − 2015	Tallinn University of Technology	Researcher/Teaching Assistant
2007 − 2008	Architectural design office	Technician
2007 − 2007	Structural design office	Engineer
2005 − 2007	Real estate company	Assistant of civil engineer
2004 − 2005	Structural design office	Technician
2004 − 2004	Geodesy office	Technician

ELULOOKIRJELDUS

Isikuandmed

Nimi:	Simo Ilomets
Sünniaeg ja -koht:	07.02.1984, Tartu
Kodakondsus:	Eestlane
E-posti aadress:	simo.ilomets@ttu.ee, simo.ilomets@gmail.com

Haridustee

Õppeasutus	Lõpetamise aeg	Haridus (eriala/kraad)
Tallinna Tehnikaülikool	2009	Tööstus- ja tsiviilehitus, magister
Pärnu Raeküla Gümnaasium	2002	Keskharidus
Pärnu Raeküla Gümnaasium	1999	Põhiharidus
Surju Põhikool	(1990–1998)	

Keelteoskus

Keel	Tase
Eesti	Emakeel
Inglise	Sorav
Soome	Kesktase
Vene	Baastase

Täiendusõpe

Õppimise aeg	Korraldaja või kursuse nimetus
13.-16.12.2010	Liginullenergiahooned ja taastuvenergia, Aalto Ülikool, Soome
09.-14.01.2011	Linnafüüsika Talvekool, ETH Zürich, Ascona, Šveits
15.-23.03.2011	Hoonete renoveerimine, Tallinna Tehnikaülikool
20.04-15.12.2011	Niiskus materjalides ja tarindites, Lundi Ülikool, Rootsi
10.-26.04.2013	Ehitusfüüsika alane teine rahvusvaheline doktorantide suvekool, Parana Piiskoplik Katoliiklik Ülikool, Curitiba, Brasiilia
10.-14.06.2013	EnTool 2013 Sümpoosion, Töötuba & Suvekool, Dresdeni Tehnikaülikool, Saksamaa
Sügis 2012 ja 2013	Külalisdoktorant Tampere Tehnikaülikoolis, Soome

Teenistuskäik

Töötamise aeg	Tööandja nimetus	Ametikoht
2015 − ...	Tallinna Tehnikaülikool	Lektor
2010 − 2015	Tallinna Tehnikaülikool	Teadur/Assistent
2007 − 2008	Arhitektuuribüroo	Tehnik
2007 − 2007	Konstrukts. projekteerimise firma	Insener
2005 − 2007	Kinnisvara firma	Ehitusinseneri assistent
2004 − 2005	Konstrukts. projekteerimise firma	Tehnik
2004 − 2004	Geodeesia firma	Tehnik

Publications

Articles in journals

Kalamees, T.; Jylhä, K.; Tietäväinen, H.; Jokisalo, J.; **Ilomets, S**.; Hyvönen, R.; Saku, S. (2012). Development of weighting factors for climate variables for selecting the energy reference year according to the EN ISO 15927-4 standard. Energy and Buildings, 47, 53−60, 10.1016/j.enbuild.2011.11.031.

Ilomets, S., Kalamees, T. Evaluation of the criticality of thermal bridges. Journal of Building Pathology and Rehabilitation (2016) 1:11.

Kuusk, K.; Kalamees, T.; Link, S.; **Ilomets, S**.; Mikola, A. (2016). Case-study analysis of concrete large-panel apartment building at pre- and post low-budget energy-renovation. Journal of Civil Engineering and Management, 23:1, 67−75, 10.3846/13923730.2014.975741.

Ilomets, S., Kuusk, K., Paap, L., Arumägi, E., Kalamees, T. Impact of linear thermal bridges on thermal transmittance of renovated apartment buildings. Journal of Civil Engineering and Management (2017) 23:1, 96-104.

Ilomets, S., Kalamees, T. Indoor hygrothermal loads for the deterministic and stochastic design of the building envelope for dwellings in cold climates. (Submitted to Journal of Building Physics, 06.05.2016 and resubmitted after reviewing 17.04.2017).

Articles in conference proceedings

Ilomets, S.; Kalamees, T.; Kõiv, T-A. (2010). Analysis of energy use in detached houses to determine energy performance requirements in Estonia. In: Proceedings of Clima2010 10th Rehva World Congress "Sustainable Energy Use in Buildings", Antalya, 9-12.05.2010.: Turkey, Antalya, 9-12.05. [Rowman & Littlefield]; Lexington Books.

Kalamees, T.; Kõiv, T-A.; Arumägi, E.; **Ilomets, S**. (2010). Indoor temperature and humidity conditions in Estonian old multi-storey apartment buildings composed of prefabricated concrete elements. In: Proceedings of “Clima2010 10th Rehva World Congress "Sustainable Energy Use in Buildings", Antalya, 9-12.05.2010. (8). [Rowman & Littlefield]; Lexington Books.

Ilomets S, Kalamees T, Agasild T, et al. (2011) Durability of concrete and brick facades of apartment buildings built between 1960–90 in Estonia. In: Freitas VP, Corvacho H, and Lacasse M (eds), 12th International Conference on Durability of Building Materials and Components, Porto. Portugal 12-15 April: FEUP Faculdade de Engenharia da Universidade do Porto, pp. 1171–1178.

Ilomets, S.; Kalamees, T.; Paap, L. (2011). Evaluation of the thermal bridges of prefabricated concrete large-panel and brick apartment buildings in

Estonia. 9th Nordic Symposium on Building Physics, 29 May - 2 June 2011, Tampere, Finland, 3. Tampere University of Technology, 943−950.

Kalamees, T.; Niemelä, J.; Kurnitski, J.; Tark, T.; Vuolle, M.; **Ilomets, S**. (2011). Strategy for Achieving Low-energy Houses in Estonia. . PHN11, 4th Nordic Passive House Conference, 17 - 19 October, 2011 Helsinki, Finland. (1−10). Finnish Association of Civil Engineers RIL.

Kalamees, T.; **Ilomets, S**.; Arumägi, E.; Alev, Ü.; Kõiv, T.-A.; Mikola, A.; Kuusk, K.; Maivel, M. (2011). Indoor Hygrothermal Conditions In Estonian Old Multi-storey Brick Apartment Buildings. In: The 12th International Conference on Indoor Air Quality and Climate: June 5-10. Austin, Texas, USA.

Arumägi, E.; **Ilomets, S**.; Kalamees, T.; Tuisk, T. (2011). Field Study of Hygrothermal Performance of Log Wall with Internal Thermal Insulation. In: International Conference on Durability of Building Materials and Components. Proceedings: XII DBMC. International Conference on Durability of Building Materials and Components, Porto, Portugal, 2011. FEUP Edicoes, 811−819.

Kalamees, T.; Jylhä, K.; Tietäväinen, H.; Jokisalo, J.; **Ilomets, S**.; Ruosteenoja, K.; Hyvönen, R.; Saku, S.; Hutila, A. (2011). Principles to select new test reference year assessing the annual energy for heating and cooling of buildings in Finland. In: The 12th International Conference on Air Distribution in Rooms: June 19-22, Trondheim, Norway.

Alev, Ü.; Kalamees, T.; Arumägi, E.; **Ilomets, S**. (2012). Comparison of thermal performance of mineral wool and reflective insulation on internally insulated log wall. In: Proceedings of Healthy Buildings 2012: Healthy Buildings 2012. Brisbane, Austraalia 8.-12. juuli 2012. Brisbane, Austraalia: Queensland University of Technology, 1−6.

Ilomets, S; Kalamees, T; Raado, L-M (2012). Performance testing of frost damage model by hygrothermal simulation. In: Proceedings of the 5th International Building Physics Conference (IBPC). Kyoto, Japan, May 28-31, 2012: 5th International Building Physics Conference. Kyoto, Japan, May 28-31, 2012. Ed. The 5th IBPC organizing committee. 73−80.

Kalamees, T; Arumägi, E; Thalfeldt, M; **Ilomets, S**; Klõšeiko, P; Alev, Ü. (2012). The analysis of indoor hygrothermal loads based on measurements in multi-storey wooden apartment buildings. Proceedings of 5th IBPC: International Building Physics Conference, The Role of Building Physics in Resolving Carbon Reduction Challenge and Promoting Human Health in Buildings.. Kyoto, Japan, May 28-31, 225−232.

Kalamees, T.; **Ilomets, S**.; Kuusk, K.; Paap, L. (2013). Indoor Temperature and Humidity Conditions in Modern Estonian Apartment Buildings. Proceedings of 11th REHVA World Congress and the 8th International Conference on Indoor Air Quality, Ventilation and Energy Conservation in Buildings: Prague, Czech Republic, on June 16 – 19. Elsevier [to be published].

Ilomets, S., Kalamees, T. Case-study analysis on hygrothermal performance of ETICS on concrete wall after low-budget energy renovation. In: Proceedings of XII International Conference on Performance of Exterior Envelopes of Whole Buildings, Florida, USA, 01−05.12.2013, ASHRAE.

Ilomets, S., Kalamees, T., Lahdensivu, J. Validation of the method to evaluate the corrosion propagation stage by hygrothermal simulation. In: Proceedings of Central Europe towards Sustainable Building 2016; Innovations for Sustainable Future, 22−24.06.2016, Prague.

Ilomets, S., Kalamees, T., Lahdensivu, J., Klõšeiko, P. Impact of ETICS on corrosion propagation of concrete facade. In: SBE16 Tallinn and Helsinki Conference. Build Green and Renovate Deep 5–7 October 2016, Tallinn and Helsinki / Energy Procedia 96 (2016) 67–76.

PUBLICATIONS

PUBLICATION I

Ilomets, S., Kalamees, T. Indoor hygrothermal loads for the deterministic and stochastic design of the building envelope for dwellings in cold climates. Submitted to Journal of Building Physics, 06.05.2016 and resubmitted after reviewing 17.04.2017

Indoor hygrothermal loads for the deterministic and stochastic design of the building envelope for dwellings in cold climates

Simo Ilomets*& Targo Kalamees

Nearly Zero Energy Buildings Research Group, Department of Civil Engineering and Architecture, Tallinn University of Technology. Ehitajate tee 5, Tallinn, Estonia 19086

* Simo Ilomets is the author to whom correspondence should be addressed: email via simo.ilomets@ttu.ee, or phone: +372 6202 402

Abstract

In this study, several years of field measurements of indoor hygrothermal loads in 237 dwelling units are analysed. Moisture excess is calculated from hourly values of temperature and relative humidity measured both indoors and outdoors. Air change rate and moisture production in bedrooms are calculated on the basis of CO_2 measurements. It is found that indoor temperature profiles differ depending on whether a building has central heating, a stove or combined heating system. The determined average moisture excess value, 2.8 g/m^3 with a standard deviation of 1.6 g/m^3 for cold periods, can be used in stochastic calculations. Critical values for moisture excess at the 90th percentile, ranging from 3–8 g/m^3, depending upon occupancy rates, can be used in the deterministic analysis. Averages and weekly maxima of moisture excess in the study are reported at different percentiles. Considerable deviations from the EN ISO 13788 (2012) standard are discovered, concerning the breaking point depending on outdoor temperature and moisture excess during the summer. The average and critical moisture production in bedroom is presented and insufficient ventilation determined based on measurements. During the heating period the air change rate is relatively stable while moisture production levels increase along with the dropping outdoor temperature. Two indoor temperature and three humidity models with different levels of detail and influencing factors are proposed. Temperature and humidity loads derived using the proposed models can be used to determine the indoor hygrothermal boundary conditions for the building envelope of dwellings in cold climates.

Keywords

Indoor hygrothermal load, moisture excess, moisture production, ventilation air change, stochastic, deterministic, occupancy.

Introduction

Problem statement

According to the European Construction Products Regulation (CPR, 2011), health and safety aspects which are connected to the use of a building during its entire life cycle must be taken into account when assessing the performance of that building. Moisture-related problems in buildings (such as with dampness) increase the risk of there being adverse health effects, such as respiratory problems, asthma, and allergies both in adults and children (Bornehag et al, 2004). According to meta-analyses (Fisk et al,

2007), approximately 30–50% of the increases in a variety of respiratory and asthma-related health problems are linked to building dampness and mould. Dampness is defined as a range of moisture problems in buildings, including high relative humidity (RH), condensation, water ponding, and other signs of excess moisture or microbial growth (IOM, 2004). In order to be able to prevent dampness-related problems, possible moisture sources should be taken into account in the design phase. As the hygrothermal performance of the building envelope and its surface depend upon boundary conditions, a proper evaluation of hygrothermal loads is crucial. In terms of indoor moisture load and the risk of moisture damage occurring, two room types can be found in a dwelling unit, these being the bathroom and all other rooms. The moisture load in bathrooms is higher in general but, on the other hand, it also has waterproofing or a moisture barrier on the interior surface of the building envelope. As moisture loads in bedrooms have so far been subject to less study until now, these were chosen as the object of this study.

When assessing indoor hygrothermal loads on the building envelope, it is important to consider indoor temperature and humidity conditions and their dependence on the outdoor climate. Indoor humidity levels are dependent upon the rate of moisture production (caused primarily by indoor human activities), the air change rate, and moisture exchange with hygroscopic materials inside the building. Recorded air change rates in five hundred bedrooms in Denmark (Bekö et al, 2010) showed that occupant behaviour is a stronger predictor of the ventilation rate than it is of building characteristics. Kalamees et al (2006) compared moisture production values as calculated from the average air change rate and moisture excess levels, with values which had been predicted on the basis of questionnaire results. Only 45% of the predictions were correct (with an accuracy of ±25%). As the designer cannot rely on knowledge of the future behaviour of the occupants or the building's occupancy, the only recourse is to use moisture levels, determined in dwellings which are already in use. In order to acquire reliable data, what is needed are large-scale, long-term, and wide-spread indoor climate measurements from dwellings with different characteristics. Moisture excess levels (Δv), represented as the difference between indoor and outdoor air vapour content by volume (the potential for vapour diffusion), is a good indicator of the indoor humidity load.

Literature review

Indoor boundary conditions in cold climates have been measured in a good many countries and these involve various circumstances. Rousseau et al (2007) studied indoor temperature and humidity conditions in the cold climate of Canada, but a higher temperature load and RH levels did not translate into a more frequent occurrence of moisture-related problems, and more in-depth studies are required in this area. Arena et al (2010) measured the monthly average temperature, RH levels, and the humidity ratio in sixty homes in different climate zones in the USA. In addition to bathrooms, moisture-related problems were most often detected around windows. However, due to the small sample size being taken, they were unable to show a strong correlation between the characteristics of houses and indoor humidity levels. Covering the period up to 2006, a solid literature review concerning moisture excess levels and moisture production is given in Kalamees et al (2006). From there on, an overview of relevant literature concerning indoor temperature and humidity levels with the numerical results available is given in Table 1.

Some studies have concentrated on indoor temperature and thermal comfort, but not on humidity levels. Literature concerning temperature levels is reviewed and generalised by Peeters et al (2009), who claim that bedrooms which are used only for sleeping in winter are colder when set against bedrooms which are used for other activities besides sleeping. In the former type, bedrooms used only for sleeping,

comfortable indoor air temperatures are predominantly between +15 °C and +17 °C but may drop as low as +12 °C. Lower temperature limit +16 °C for bedrooms and +18 °C for all other rooms of a dwelling is proposed.

Table 1. Average indoor boundary conditions during cold periods as shown in various studies since 2006

	t, °C	RH, %	Moisture excess Δv, g/m^3	Household moisture prod. G, kg/d	Comments (country or region)
Kalamees et al (2006)	21–23		1.8	5.9	Bedrooms and living rooms (Finland), occupancy 43 m^2/person
Janssens and Vandepitte (2006)	15–20 20–21 18–20		2.2 2.3 2.8		Bedrooms (Belgium) Living rooms Bath rooms Both t and Δv dependent on outdoor temperature
Zhang et al (2007)	16–22	42–43	2.8–6.1		(Japan)
Glass and Tenwolde (2009)				3–15	
(Becker and Paciuk 2009)	20	40			(Israel)
Peeters et al., (2009)	15–20 20–21				Bedrooms (Belgium) Living rooms
Francisco and Rose (2010)			2.8 3.2		Rooms above ground (Rhode Island, USA), Playroom Bedroom
Geving and Holme (2011)	17 22 22	43 35 35	1.8 1.6 2.2		Bedrooms, (Norway) Living rooms: >50 m^2/person Living rooms: <50 m^2/person
(Tariku and Simpson, 2014)	17–21 17–24		2.3–4.5 2.4–4.9		Bedrooms (Canada) All other rooms
Bagge et al (2014).			1.8		Central exhaust ventilation (northern Sweden), occupancy 71 m^2/person

In deterministic hygrothermal calculations, critical climatic loads and material parameters ensure that the design solution is within the margins of safety. The International Energy Agency (IEA) EBC Annex 24 (Sanders 1996) has recommended applying a 10% critical level. This means that hygrothermal loads which are higher than their normative value should not appear in more than 10% of cases. Cornick and Kumaran (2008) compared empirical indoor climate models (ASHRAE 160P 2008; EN ISO 13788:2012; Jones 1993) against data collected from 25 houses (Rousseau et al, 2007) and found that, relative to the data measured, all of the models generally overestimated RH levels. Therefore, when taking a deterministic approach to hygrothermal design, in-depth studies of indoor loads and their influences are essential. An effect of moisture buffering with a literature review concerning constant versus cyclic moisture production is discussed in Labat and Woloszyn (2016). In addition, an advantage of using the stochastic approach over the deterministic one is something that is emphasised. Glass and Tenwolde (2009) concluded in their review paper that design moisture production rates are currently based on a rather limited data set, and more data is needed concerning the relationship between the number of occupants and indoor moisture production levels.

Uncertainties are widespread in terms of climatic loads and material parameters. The currently available deterministic methodologies for measuring hygrothermal performance are insufficient for the accurate assessment of variations in energy use, functional performance, and life-cycle costs. Therefore a research project was launched by the IEA on the 'Reliability of Energy Efficient Building Retrofitting – a Probability Assessment of Performance and Cost' (IEA EBC Annex 55, 2012). For stochastic hygrothermal simulations, load variations are important input parameters. A probabilistic assessment would require the incorporation into existing hygrothermal modelling both of correct critical values and average values with deviations. Pallin (2013) and Tariku et al (2011) took the first steps towards this goal. Bishara et al (2014) developed and validated a tool based on the simplified energy and moisture balance of a building to calculate indoor temperature and RH levels. IEA Annex 41 has shown that it is also possible to use a whole-building indoor climate and energy simulation for hygrothermal modelling (Woloszyn and Rode, 2008). Because these simulation programs use moisture production levels and air change values as input parameters, indoor hygrothermal loads must also be reported using these parameters.

The present study contributes to this approach by providing comprehensive measurements for indoor hygrothermal loads in the case of 237 dwelling units across a range of building types. Factors were studied in depth where they affected moisture excess levels, moisture production levels, and the air change rate. Three different indoor hygrothermal boundary condition models have been proposed, each with a different granularity, including a deterministic, stochastic, and whole-building HAM approach.

Methods

The buildings studied

The process of recording measurements was conducted in Estonia (24°E, 59°N; in north-eastern Europe), using apartments and detached houses of various occupancies, sizes, ages, structures, and types of heating and ventilation (see Table 2). All 237 dwellings consisted of an entry hall, living room, kitchen, sanitary rooms, bedrooms, and non-living spaces, such as a corridor or storage area. The kitchen area was typically enclosed in a separate room but may also have been integrated into the living room in newer apartments. One, two, and three-bedroom apartments predominated. All of the apartments and detached houses were privately owned.

Table 2. The main characteristics of the 237 dwellings being studied

	Apartment building, 76% (180 apartments)	Detached house, 24% (57 houses)
Net surface area: average ± SD, (min-max)	63±28 m^2 (31–299 m^2)	122±49 m^2 (34–300 m^2)
Occupancy: average ± SD, (min-max)	27±15 m^2/person (9–85 m^2/person)	45±22 m^2/person (16–103 m^2/person)
Building age	<20 years: 35% 20–40 years: 16% 40–70 years: 24% >70 years: 24%	<20 years: 58% 20–40 years: 3% 40–70 years: 4% >70 years: 35%

The structures of the external walls in apartment buildings typically consisted of one of three different materials (concrete 39%, brick 34%, log 25%, or a combination of any of the three 2%), while walls in detached houses typically consisted of one of two different materials (log 48%, or timber frame

52%). The interior surface of the external wall was covered with plaster in the case of concrete or brick apartment buildings, and then painted or covered with wallpaper as an interior finishing. Buildings involving wooden structures may have wood or gypsum on the interior, and may also be covered with paint or wallpaper.

Natural passive stack ventilation systems (51% in apartments and 55% in houses) and mechanical systems (49% in apartments and 45% in houses) were both represented in the dwellings being studied. Apartments typically used central heating with hydronic radiators (77%), while houses used a variety of heating systems (a stove or fireplace 33%, electrical radiators 20%, hydronic radiators 23%, or combined 23%). The requirement for a ventilation air change rate according to the old Soviet SNiP was n=1.0 h^{-1} for bedrooms and living rooms (Mikola et al, 2013). That gives us about n=0.5 h^{-1} for the whole dwelling, conforming well with other Nordic countries from that era (Dimitroulopoulou, 2012).

Measurements

Small data loggers (Hobo U12 011) were used to measure indoor temperatures and RH levels with a 1 h step over the course of one year in a room used for sleeping - the master bedroom and/or living room. Data for the exterior climate was measured near the buildings or was taken from the nearest weather station.

Indoor carbon dioxide (CO_2) levels were measured in 88 apartments in order to be able to evaluate the air change rate in bedrooms at ten minute intervals over a period of two to three weeks in winter and summer. The air change rate was evaluated on the basis of CO_2 measurements and its estimated emissions from inhabitants (known as the CO_2 tracer gas method) in bedrooms during the night (≈20:00-08:00), as reported by Cui et al (2015), see equation (1):

$$C = C_0 + (C_e + \frac{m}{\dot{V}} - C_0) \cdot (1 - e^{-\frac{\dot{V}}{V}\tau}) \qquad (1)$$

where m is the CO_2 production (g/h); $\dot{V}$ is the air flow rate (m^3/h); V is the room's total volume (m^3); C_e is CO_2 in the exterior air (g/m^3); C is CO_2 indoors after measurements have been taken (g/m^3); C_0 is CO_2 indoors before the measurements are taken (g/m^3); and τ is time (h).

The calculations are based on average night-time human CO_2 emissions (adults: 13 l/h and children: 6.5 l/h), since CO_2 emissions are relatively stable during the night. Average CO_2 emissions for adults while sleeping, at 13 l/h, coincides well with the average figure of 14 l/h (which is valid for a metabolic rate of MET=0.8), as given in (EN 15251, 2007). This is supported a figure of by 15 l/h (which included children), found to be representative of Sweden (Bagge et al, 2014). We also checked on the reliability of the approach by calculating the CO_2 production levels according to an equation proposed by Tajima et al (2014). This takes the metabolic rate (MET=0.7 as used in the calculations) and body surface area into account and resulted in 16 l/h as an average for both sexes. The CO_2 tracer gas method which should be suitable for that application is proven by Mikola et al (2017).Mechanical exhaust ventilation airflows were measured in the kitchen, toilet, and bathroom with an anemometer (SwemaFlow 233). Supply air flow rates were measured with an Alnor/TSI AXD610 Digital Differential Micromanometer. The air leakage rate for the building envelope was measured using the fan pressurisation method (EN 13829, 2000).

Survey data was collected for each dwelling, including building characteristics, the building materials used, the type of building service system and its use, the habits of the building's occupants, typical complaints, and health concerns related to indoor air quality. The questionnaire contained questions about moisture production and the air change rate in the dwelling.

An assessment of indoor hygrothermal loads

The value for indoor moisture excess levels, Δv (g/m^3) (the difference in absolute humidity levels by volume between indoor air v_i and outdoor air v_e, also known as moisture supply or vapour excess) was calculated on the basis of the results of indoor and outdoor temperature measurements, along with RH measurements, using equation (2):

$$\Delta v = v_i - v_e \qquad (2)$$

Moisture production (moisture source) G (g/h) in bedrooms was calculated on the basis of the measured indoor moisture excess and air change rate indoors, $\dot{V}$ (m^3/h) (determined from CO_2 decay measurements taken from the very same night-time period), using equation (3):

$$G = (v_i - v_e) \cdot \dot{V} \qquad (3)$$

The temperature, RH levels, and moisture excess levels were expressed in relation to the outdoor air temperature t_e with a 1 °C step as a daily average. The values for moisture excess levels have been reported in this paper as a weekly average over the entire year, since a week is a complete living cycle and represents the indoor climate more accurately than, for example, a month. Data in this paper has been reported in two ways: firstly, for the purposes of deterministic modelling, based on weekly maximums, where critical loads must be taken into account; and secondly, based on all measurements, where the average and standard deviation (SD) are presented for the purposes of stochastic modelling. The second approach also includes data for those periods in which the dwelling was not being used and there was no humidity load, and on the calculation of moisture flow through the building envelope.

Statistical analysis

The statistical significance of parameters which may have been effecting the indoor humidity load was investigated using a student's T test. The values for moisture excess levels were first separated into two arrays according to the median value. Next, other values were tested in order to achieve the smallest possible P value in order to be able to evaluate the strength of the correlation between those arrays which are under comparison. The significance level was set at 5%, i.e. $p<0.05$. The distribution of data was analysed by using the statistical distribution fitting software, EasyFit, and Pearson's chi-squared test in MS Excel in order to detect whether or not it follows the Gaussian, i.e. normal distribution.

Two ranges of outdoor air temperature ($t_e \leq +10$ °C; $t_e > +10$ °C) were used for the indoor air temperature, and three ranges of outdoor air temperature ($t_e \leq +5$ °C; $+5 < t_e < +20$ °C; $t_e > +20$ °C) were used for moisture excess levels. The key parameters which effect moisture excess (g/m^3) levels (X, Y, Z, etc) were determined using regression analysis, based on measurements taken from 88 dwellings (A, B, C, etc are linear regression coefficients). The moisture excess levels can be expressed in terms of these parameters and their respective regression coefficients, as in equation (4):

$$\Delta v = A \cdot X + B \cdot Y + C \cdot Z \ldots \qquad (4)$$

Results

Temperature

The effect of the exterior, outdoor temperature on the indoor temperature was dependent upon the type of heating used in the dwelling. Central heating ensured a relatively stable indoor temperature level during the heating period ($t_e \leq +10$ °C) - see Figure 1., left. It was also found that the indoor temperature tended, on average, to be between 1–2 °C higher in dwellings which were built after 2000. Clearly, without central heating during the cold period (i.e. when a stove or combined heating is used) - see Figure 1., right - the indoor temperature depends upon outdoor temperature thanks to cyclic heating, insufficient heating capacity, and large building envelope heat losses. As expected, the indoor temperature started to approximate the outdoor temperature during the warm period ($t_e > +10$–15 °C), irrespective of the heating system in use. When the daily average outdoor temperature exceeded approximately +10 °C, the indoor temperature exceeded +21–22 °C, and the summer period began. According to indoor climate Class III (EN-15251 2007) (shown as straight bold lines in Figure 1), this is acceptable for older dwellings in which temperatures between +19 °C and +25 °C should be maintained. As can be seen, many dwellings are under-heated or over-heated during the heating period. Indoor temperatures during the warm period ($t_e > +10$ °C) also match up to the ASHRAE 55 (2004) standard, which proposes temperatures of +21 °C at t_e+10 °C up to approximately +26 °C at t_e+25 °C for an average indoor operative temperature.

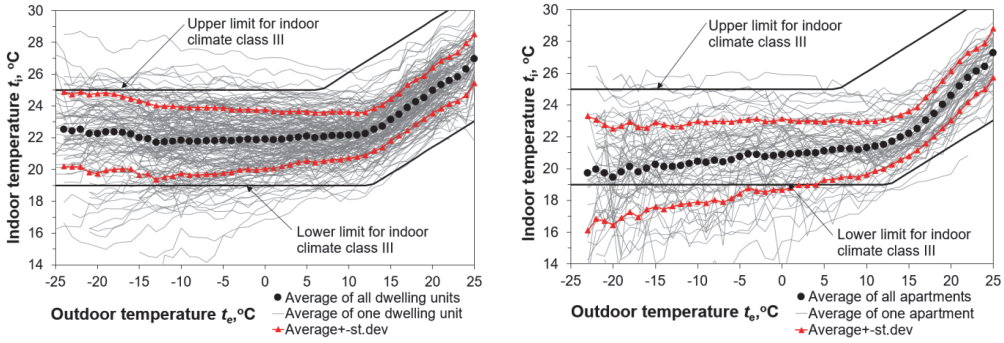

Figure 1. Indoor air temperature for 190 dwelling units with central heating (left) and 66 units using a stove or combined heating system (right)

Moisture excess levels

The average moisture excess levels in the 237 dwellings was calculated to be +2.8 g/m^3 (SD ±1.6 g/m^3) during the cold period ($t_e \leq +5$ °C), +1.4 g/m^3 (±1.4) during the intermediate period ($+5 < t_e < +20$ °C), and +0.3 g/m^3 (±0.9) during the warm period ($t_e > +20$ °C). The small dots in Figure 2, left, show the relation between hourly indoor moisture excess levels and daily outdoor temperature in one dwelling over a one year period. The round dotted line shows average indoor moisture excess levels, while the square dotted line shows weekly maximum indoor moisture excess levels. The thin lines in Figure 2, right, show the average moisture excess levels for each dwelling. The round dotted line shows the average, while the lines with triangles show the average ± SD for all dwellings.

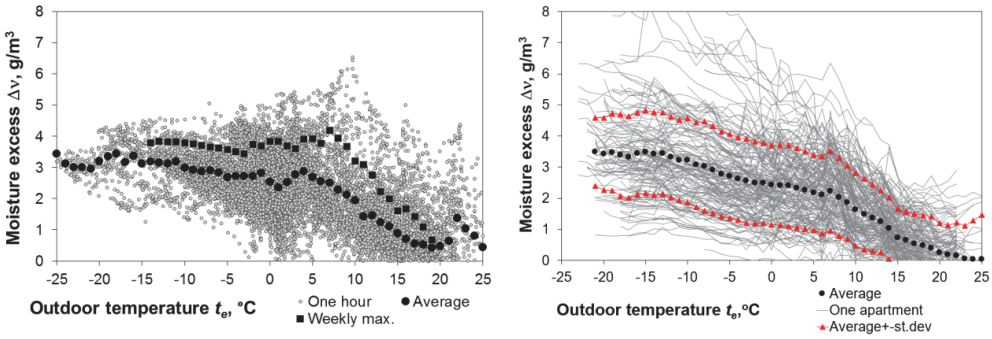

Figure 2. Hourly data for moisture excess levels for one dwelling (left) and weekly data for all 237 dwellings (right)

Using the full dataset in Figure 3, left, and the weekly maximums in Figure 3, right, curves were calculated with their corresponding percentiles to show the distribution of moisture excess levels over the whole dataset. Trend lines (straight lines) for moisture excess levels based on the full dataset and weekly maximums during the cold period (t_e≤+5 °C) are shown as rounded moisture excess values which range from one to 6 g/m^3.

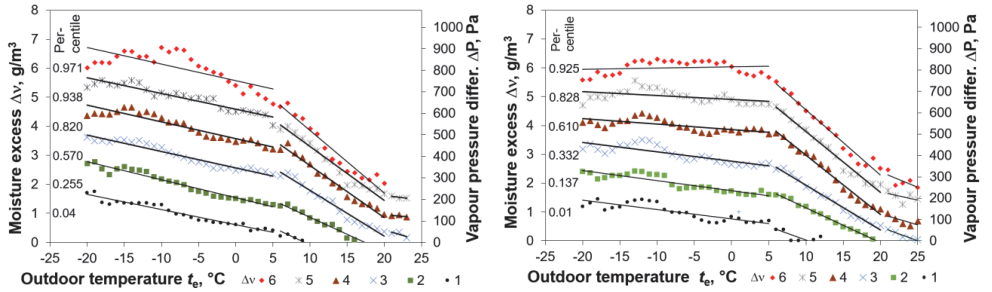

Figure 3. Moisture excess levels based on the full dataset (left) and for the weekly maximums for 237 dwelling units (right). The column of values beside the rounded moisture excess values on the primary y-axis shows the corresponding percentiles. The straight lines are linear trend lines for moisture excess levels during cold, intermediate, and warm periods

The dependence of moisture excess levels on the outdoor temperature is clearly visible in Figure 3. On the basis of these curves, a change in moisture excess levels was observed of 1 g/m^3 during the cold period (t_e≤+5 ºC) and 0.5 g/m^3 during the warm period (t_e>+20 ºC). The average moisture excess levels Δv was 2.8 g/m^3 (±1.6) during the cold period and 0.3 g/m^3 (±0.9) during the warm period. The 90th percentile for weekly maximums (Figure 3, right) was 5.7 g/m^3 during the cold period and 2.0 g/m^3 during the warm period. The higher moisture excess levels during the cold period could have been due to a difference in air change performance and/or moisture production.

Moisture excess levels for the full dataset (Figure 3, left) tend to decrease at outdoor temperatures of around 0 °C mainly because the full dataset also includes data which was collected when the apartments were unoccupied (when there was no moisture production). Another reason for higher measured moisture excess levels during very cold periods in Figure 3, left, is vapour desorption from surrounding surfaces, something which is driven by the low indoor RH levels. An important outcome of the analysis is the determination of the level of moisture excess levels during the intermediate and

warm periods, and the ascertaining of its dependence on the cold period's value. At low moisture loads ($\Delta v \approx 2$ g/m^3 during winter), the moisture excess levels were around 0 g/m^3 in summer but with considerable fluctuation. Moisture excess levels had a positive value in summer under high moisture loads.

Air change rate and moisture production

The average air change rate during winter in a bedroom (n) was 0.6 h^{-1} (see Figure 4, left), which is remarkably below the requirement at the time of construction where n=1.0 h^{-1} as well as for the indoor climate Class III (EN-15251 2007) requirement of 0.86 h^{-1}, i.e. 0.6 l/(s·m^2) with a room height of 2.5 m. In each dwelling air change measurements were carried out on different days which may serve to amplify the large deviation shown in Figure 4, left. Each point in Figure 4, right, shows the measurement during one night at the corresponding average outdoor temperature. The thin lines represent linear trend lines for these results in one dwelling, while the thick line represents the average for all dwellings. During the winter period the air change rate did not change remarkably (see Figure 4, right). The bedroom air change rate was 0.2 h^{-1} with the whole dwelling unit producing a figure of 0.1 h^{-1} at the 10th percentile.

Average moisture production (G) in master bedrooms was found to be 72±50 g/h (1.7±1.2 kg/day) during the winter period (see Figure 5), with higher values on colder days. The assumption of constant moisture production within a period of 24 hours is based on a finding which showed that the buffering-corrected values which were measured for moisture excess levels in bedrooms were not significantly different between day and night. Moisture production levels at the 90th percentile based on the full data set was at 121 g/h and 2.9 kg/day. The unexpectedly low average moisture production in some dwellings could have been due to the bedrooms being temporarily unoccupied or to a moisture buffering effect. Overall moisture production across the entire dwelling was naturally greater since not all moisture sources were located in the bedroom.

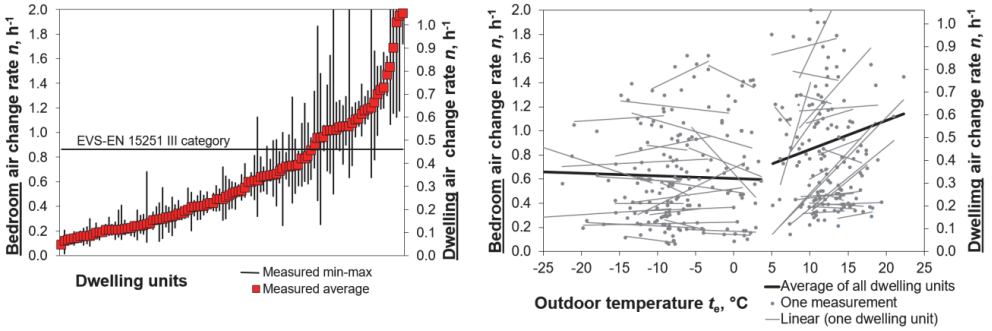

Figure 4. The average air change rate (shown in bold dots) and variability (the vertical lines) during winter in bedrooms at night (left) and the dependence of the air change rate upon the outdoor temperature (right)

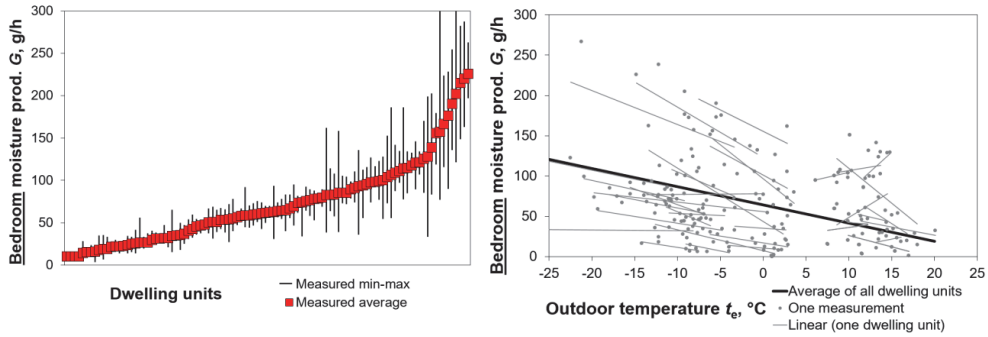

Figure 5. The average moisture production level (dots) and variability (vertical lines) during winter in bedrooms at night (left) and the dependence of moisture production levels on the outdoor temperature (right)

The analysis of moisture production dynamics within the period of a week showed small fluctuations: moisture production was somewhat higher on Fridays and Saturdays, but the difference was statistically insignificant.

Factors affecting indoor humidity load

Data from the 237 dwellings was used to study those factors which may be affecting moisture excess levels (moisture production: Table 3; air change: Table 4) during the cold period ($t_e \leq +5$ °C). Occupancy was the most significant factor ($p=4.1 \cdot 10^{-11}$) when it came to affecting moisture excess levels (see Figure 6 left). Since occupancy affected the values for other factors, those subgroups with restricted occupancy (<27; >27 m^2/person) were investigated separately.

A secondary moisture production parameter which significantly influenced moisture excess levels was that of cooking ($P<0.05$). The type of ventilation being used also significantly influenced the ventilation air change rate: in dwellings with mechanical ventilation, the air change rate was higher. The height of the natural ventilation stack and the age of windows also had a significant impact upon indoor moisture excess levels. The effect of window opening was contrary to that expected: in rooms with higher moisture excess levels the windows had been opened in order to ventilate the room.

The dependency of moisture excess levels on occupancy is shown in Figure 6, left. The data can be sorted by moisture excess levels or by occupancy. Equations 5 and 6 are both a combination of two trend lines (with the data sorted by moisture excess levels and occupancy) by using the data point to provide higher moisture excess levels.

A 90% moisture excess level (g/m^3) depending on occupancy O, m^2/person:

$$\Delta v = 55 \cdot O^{-0.655} \qquad (5)$$

Average moisture excess level (g/m^3) depending on occupancy O, m^2/person:

$$\Delta v = 55 \cdot O^{-0.836} \qquad (6)$$

It turns out that the 90% critical level is approximately 1.5 g/m^3 higher than the average in the case of low occupancy levels, but the difference increases with higher occupancy levels. Moisture excess distributions for different building typologies are shown graphically in Figure 6, right, where a large

deviation can be seen with values between 0–8 g/m^3. Some building types (Figure 6, right) have steeper slopes, especially in the case of old (pre-1940) detached houses, but also in the case of apartment buildings which were constructed using wood. It appears that detached houses show significantly lower moisture excess levels ($p=3.2\cdot10^{-6}$) - due to lower occupancy levels this was at 45 m^2/person on average - and apartments have higher moisture excess levels - with an occupancy of 27 m^2/person on average.

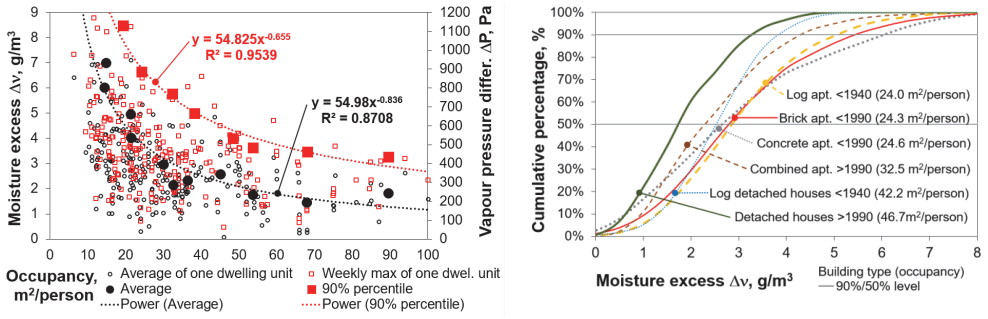

Figure 6. The dependence of moisture excess levels on occupancy (left). Cumulative distributions of moisture excess according to building typology during the cold period ($t_e \leq +5$ °C) (right) based on all measurements. Apt-apartments

Old (pre-1990) concrete apartment buildings exhibited the highest moisture excess levels at the 90th percentile, reaching ~6 g/m^3. This was due mainly to poor ventilation (with the average for a bedroom being n=0.35 h^{-1}) and high occupancy levels (25 m^2/person). Ventilation stacks in concrete apartment buildings were composed of multiple vertical stack elements which were neither airtight nor exactly aligned, as revealed during the assessment of the technical condition of these buildings.

Table 3. Factors influencing moisture excess levels and production during the cold period ($t_e \leq +5$ °C)

Factor studied (**bold** indicates statistically significant differences, i.e. p<0.05	No. of dwellings	All occupancy		Restricted occupancy				Restricted occupancy			
		Avg.	90th%	Avg.		90th%		Avg.		90th%	
				O<27	*O*>27	*O*<27	*O*>27	*O*<27	*O*>27	*O*<27	*O*>27
		Moisture excess Δv, g/m^3						Moisture prod. *G*, g/h			
Occupancy, *O*											
≤27 m^2/person	121	**3.28**	**6.08**	N/A				N/A			
>27 m^2/person	116	**2.16**	**4.17**	N/A				N/A			
Cooking											
≤once per day	102	**2.52**	5.66	3.12	2.03	6.63	4.423.	85	52	232	153
≥twice a day	70	**2.95**	5.55	3.40	2.26	5.67	74	76	61	221	161
Laundry drying											
yes	76	2.68	6.04	3.46	2.07	6.86	4.10	62	42	143	121
no	43	2.27	5.49	2.94	1.77	6.42	4.36	65	33	186	98
Shower use											
≤once per day	81	2.55	5.88	3.27	2.07	6.46	4.13	84	51	269	177
≥three times a day	48	2.98	5.65	3.34	2.21	5.67	4.22	93	69	225	157

Table 4. Factors influencing moisture excess levels and air change during the cold period (t_e≤+5 °C)

Factor studied (**bold** indicates statistically significant difference ie. p<0.05	No. of dwellings	All occupancy		Restricted occupancy				Restricted occupancy			
		Avg.	90th%	Avg.		90th%		Avg.		10th%	
				O<27	*O*>27	*O*<27	*O*>27	*O*<27	*O*>27	*O*<27	*O*>27
		Moisture excess Δv, g/m^3						Air change rate *n*, h^{-1}			
Air change *n*											
<0.3 h^{-1}	25	**3.50**	**7.19**	**4.34**	2.54	**7.73**	**4.25**	N/A			
>0.6 h^{-1}	49	**2.48**	**4.95**	**2.90**	1.91	**5.06**	**3.49**	N/A			
Ventilation type											
passive stack	63	3.13	**6.47**	3.41	**3.23**	7.11	4.96	**0.50**	**0.26**	**0.10**	**0.15**
mechanical	61	2.78	**5.34**	3.16	**2.28**	5.47	4.60	**0.87**	**0.84**	**0.50**	**0.22**
Ventilation stack height											
≤1 m	31	**3.81**	**7.28**	**4.20**	**2.98**	**8.24**	**5.55**	**0.47**	0.58	**0.20**	0.24
>4 m	79	**2.50**	**4.91**	**2.71**	**2.08**	**5.41**	**3.72**	**0.71**	0.68	**0.14**	0.20
Window airing											
≤2 times/day	91	**2.62**	5.31	3.10	2.18	5.78	4.16	0.65	0.60	0.14	0.24
≥3 times/day	80	**3.09**	6.05	3.47	2.37	6.38	5.45	0.61	0.70	0.20	0.17
Age of windows											
≤10 years	92	**3.40**	**6.02**	3.02	2.16	6.39	5.42	0.59	0.39	0.13	0.15
>10 years	48	**2.70**	**5.42**	3.33	2.42	5.46	4.28	0.64	0.68	0.20	0.28
Air leakage rate q_{50}											
≤4 m^3/(h·m^2)	82	2.79	6.34	3.69	2.09	7.77	4.27	0.57	0.62	0.18	0.21
>4 m^3/(h·m^2)	91	2.55	4.89	3.08	2.03	5.38	3.64	0.71	0.63	0.20	0.20

Indoor hygrothermal models

Temperature model

Model description

The indoor temperature model is based on the average indoor temperature. Since there was an indoor temperature turning point at which the outdoor temperature was around +10–15 °C, the model is for the heating period (t_e≤+10 °C) and for the summer period (t_e>+10 °C). Since the heating system strongly affected the indoor temperature during the heating period (see Figure 1.), two different temperature models have been proposed for the indoor air temperature. The average indoor temperature curve in dwellings with central heating (Figure 7, left) was stable at +22 °C during the heating period (t_e≤+10 °C) and rose up to +27 °C (at t_e +25 °C) during the summer. In the case of a stove heating system (Figure 7, right), average indoor temperature rose linearly from about +19 °C (at t_e -25 °C) to +21 °C (at t_e +10 °C) during the heating period, reaching +27 °C during the summer as well - see equation (7):

$$t_{i,central\ heating} = \begin{cases} t_e \le +10\,^oC \Rightarrow t_i = 22\,^oC \\ t_e > +10\,^oC \Rightarrow t_i = 0.3333 \cdot t_e + 18.667\,^oC \end{cases}$$

$$t_{i,stove\ heating} = \begin{cases} t_e \le +10\,^oC \Rightarrow t_i = 0.0571 \cdot t_e + 20.429\,^oC \\ t_e > +10\,^oC \Rightarrow t_i = 0.4 \cdot t_e + 17\,^oC \end{cases} \quad (7)$$

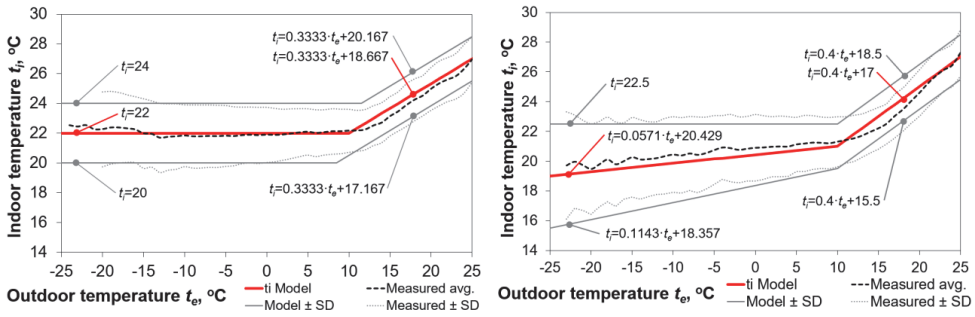

Figure 7. Indoor temperature models for dwellings with central heating (left) and stove heating (right), dependent upon the daily average outdoor temperature. Lines representing the measured results for each dwelling unit have been omitted for the sake of clarity

The same heating-system-dependent indoor temperature model can be used for all indoor hygrothermal models. The variability of the indoor climate for the stochastic approach can be generated by using the SD values at corresponding outdoor temperatures. Normal distribution of temperatures in order to use the average and SD was ascertained via Pearson's chi-squared test, which resulted in a p-value of 0.33>0.05. If one has a reliable indoor temperature profile which is valid for certain buildings in a certain climate, then this should always be preferred over the models proposed in this study.

The variation demonstrates possible differences in the behaviour of occupants on the one hand, and differences in the performance of the heating system on the other. The SD used in the stochastic approach has a larger value (±2 °C for central heating and ±3.5 °C for stove heating) for low outdoor temperatures and a smaller value (±1.5 °C for both heating systems) for higher outdoor temperatures (t_e≥+10 °C). It is possible to generate three types of indoor temperature data for stochastic simulations:

- T1: variation of t_i between dwellings. The same average indoor temperature equations are used for the whole year, and one dwelling is described by a single line, e.g. the t_i in Figure 1. One line of the model consists of two straight parts with a breaking point at t_e= +10°C. The random variation is shown by using SD=1.8 °C for different dwellings. Each subsequent simulation is handled using a different average temperature. This describes the situation when the variation falls between different dwellings with different temperatures;
- T2: variation of t_i within one dwelling. The random variation is expressed using SD for each hour - SD=0.7 °C in the case of central heating and SD=1.4 °C in the case of stove heating. This shows a larger variation for the indoor temperature over the course of one year, and each dwelling is described using an hourly batch of data, e.g. Figure 8, right;
- T3: a combination of methods T1 and T2. This shows a variation in the average temperature between dwellings and a variation of indoor temperatures at the same outdoor temperature range within a dwelling.

Validation of the indoor temperature models

The indoor temperature data sets were generated on the basis of outdoor temperatures during the measurement period. Calculated values and measured data sets were compared for model validation. Figure 8, left, shows a comparison of model T1 with the date gained through measurements in Estonian and Finnish dwellings which had central heating. The model T1 is can be considered to be representative by having R^2>0.8 for average measured indoor temperatures in Finnish detached houses and for Estonian

dwelling units but not for Finnish apartment buildings. Hence, representative indoor temperature t_i=23 °C for cold period was used in validation in case of these dwelling units.

Figure 8, right, shows a comparison of model T2 against the measured hourly data for one dwelling. Square dots represent the average indoor temperature which was calculated using the outdoor temperature and the measured data set. The average and distribution of measured and calculated temperatures are in good agreement.

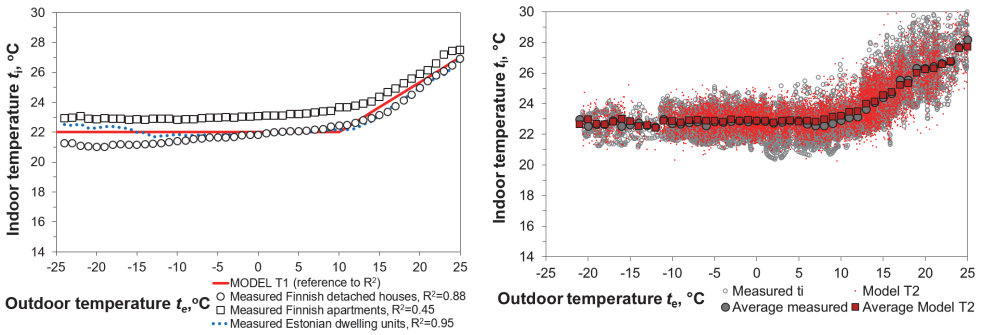

Figure 8. Indoor temperature model T1 and measured average of different dwelling groups with central heating (left) and a comparison of the measured hourly data against calculated values within one dwelling unit using model T2 (right)

The indoor M1 humidity model based on moisture excess levels

Model description

It is possible to calculate indoor air humidity by volume (or by water vapour pressure) by adding moisture excess levels (or vapour pressure difference) to outdoor air humidity. We propose the use of occupancy (as the most important factor influencing indoor humidity loads) as the basis for calculating the moisture excess level. For stochastic hygrothermal analysis the average values can be applied (Figure 9, left); for the deterministic hygrothermal design of the building envelope, values at the 90% level are applicable (Figure 9, right). The dotted line represents an alternative model to be discussed which has a 1.5 g/m^3 moisture excess difference in the cold season, -25<t_e<+5 °C.

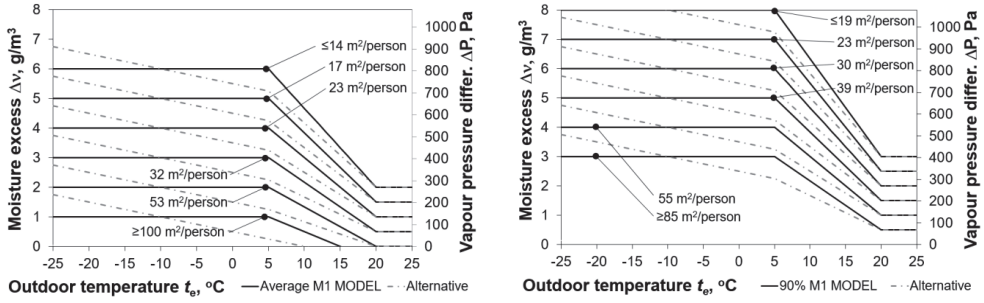

Figure 9. The average (left) and 90% design levels (right) for moisture excess levels as agreed against occupancy rates over the whole outdoor temperature range (see also Figure 6, left)

The dependency of design moisture excess curves on the outdoor temperature was determined from measurements (Figure 3). The moisture excess levels were calculated for three outdoor temperature intervals ($t_e \leq +5$ °C for the cold period; $+5 < t_e < +20$ °C for the intermediate period; and $t_e > +20$ °C for the warm period). The design value for moisture excess levels for other outdoor temperatures was calculated using the value for the cold period ($t_e \leq +5$°C). This also made it possible to obtain moisture excess values for the other periods. When moisture excess changed in different occupancy groups by steps of 1 g/m^3 during the cold period, it changed by 0.5 g/m^3 during the warm period. The number of rooms (bedrooms, living room, cabinets, etc, but not kitchen, entryway, or toilet) is a simple rule of thumb used to calculate the number of persons when this may be unknown, e.g. buildings which are still being designed. The dotted lines in Figure 9 represent a modification of the model which is to be discussed. This is something that would be in conflict with the current EN ISO 13788, (2012) standard, but it would certainly provide better agreement with the measurements.

The indoor climate for stochastic analysis of the dwellings can be calculated using the average moisture excess levels at different occupancy rates (Figure 9, left) with an SD of 1.6 g/m^3 (limitation: $\Delta v > 0$ g/m^3 during the cold period). The SD for hourly data for the moisture excess levels within one dwelling was 1 g/m^3 ($t_e > +5$ °C) and this decreased linearly during the cold period to a value of 0.5 g/m^3 as $t_e = -25$ °C (see Figure 10, left). Resolutions about the moisture excess levels for different building types were doubtful when following the normal distribution pattern according to the EasyFit software. For instance, normal distribution in the case of wooden apartment buildings was placed seventeenth out of 37 distributions in total with the Kolmogorov-Smirnov statistic of 0.049.

Model M1 validation

The indoor RH levels as measured were used to validate the indoor humidity M1 model. Firstly, the proposed model which was based on data for 237 dwellings was verified using the same sampling in order to ensure that the model was mathematically correct. Secondly, the model's performance was studied and the model was validated using independent data from Finland. Indoor RH levels were calculated using the following procedure:

- While the actual occupancy is unknown (in the case of a new building which is still being designed), the total surface area of a dwelling unit is the only parameter available - hence the latter was used as a basis for calculating the indoor moisture load;
- A representative running trend line between the number of occupants N against total surface area A of the dwelling unit was used to calculate occupancy - $N = 1.83 * \ln(A) - 6.51$;
- Using the calculated occupancy rates ($O = A/N$), the moisture excess curves were selected for the average indoor climate (Figure 9, left) or 90% level hygrothermal design (Figure 9, right);
- The moisture excess levels were added to outdoor humidity levels in order to derive the indoor humidity levels by volume;
- The indoor temperature was calculated using models T1 and T2 for both heating system types (central heating or stove/combined heating);
- The saturation humidity by volume was calculated using the indoor temperature;
- The indoor RH levels were calculated using actual and saturation values for indoor humidity levels (see Figure 10, right).

Both verification and validation showed that all of the calculated indoor RH values (Figure 11, left) were somewhat lower than those measured at very cold temperatures and higher than those measured under warm outdoor conditions. This was due to a simplification of our moisture excess model which is taken horizontal during the entire cold period (up to a deflection point of +5 °C) while the measured values for moisture excess levels tend to rise at very low outdoor temperatures (see Figure 3).

The temperature model for central heating systems showed less agreement, while that for a stove or combined heating system (not presented graphically) at cold temperatures showed greater agreement due to a lower indoor temperature profile (Figure 7), which caused higher indoor RH levels.

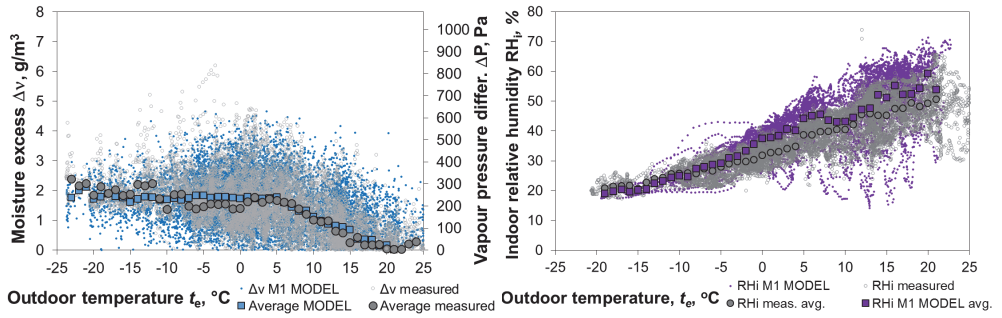

Figure 10. The comparison between measured hourly indoor moisture excess (left) and indoor RH levels (right) against calculated values for one dwelling unit using T2 and stochastic M1 models

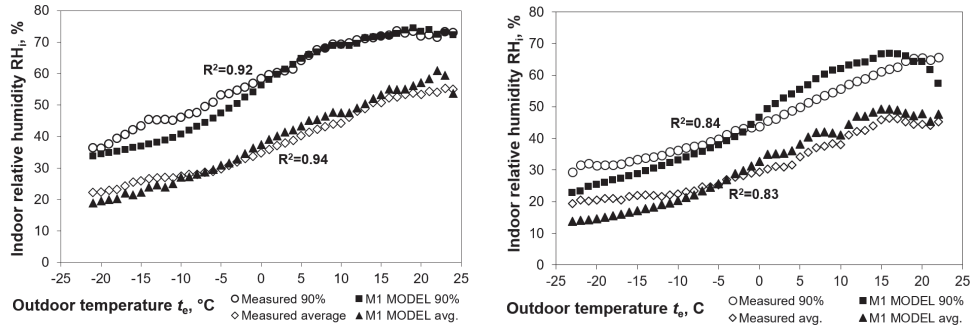

Figure 11. The verification results by using Estonian data (left) and validation by using the Finnish data via the measured average indoor RH levels as well as daily maximums at the 90th percentile using T1 and M1 models for dwellings which are equipped with central heating

Indoor humidity M2 model based on moisture excess factors

Model description

Although occupancy has the greatest impact on moisture excess, other factors can also be taken into account when determining the average indoor humidity loads. Responses by residents to a questionnaire provided more information on those factors which can influence indoor humidity loads (such as the height of the ventilation stack, or the age of windows), without requiring any actual measurements to be taken.

In addition to occupancy levels (the primary factor influencing moisture production indoors), the M2 model takes into account secondary factors: air change rate, air leakage rate, the height of the ventilation stack, and the age of windows. In order to calculate the numerical values for moisture excess levels during the cold period, the average and SD rate for the design values for occupancy and other factors have to be assumed by the user of the M2 model (see Table 5).

Table 5. Factors affecting moisture excess levels in the M2 model

Factor affecting moisture excess levels	Average	Standard deviation	Limitation
Occupancy O, m^2/person	32.0	18.9	≥ 5.0
Air change rate (dwelling) n, h^{-1}	0.32	0.23	≥ 0.05
Air leakage rate q_{50}, $m^3/(h \cdot m^2)$	6.0	5.4	≥ 0.8
Height of ventilation stack h, m	7.8	7.6	≥ 1.0
Age of windows A, '1' as >10 years; '2' as <10 years	1.6	0.42	1 or 2

The coefficients which were derived using linear regression analysis are expressed in eq. (8):

$$\Delta v_{M2} = \Delta v_{M1}(O) + \Delta v(O) \cdot \left[-0.29 \left(\frac{n_{user} - n_{default}}{SD_n} \right) - 0.19 \left(\frac{q_{50,user} - q_{50,default}}{SD_{q50}} \right) - 0.13 \left(\frac{h_{user} - h_{default}}{SD_h} \right) + 0.12 \left(\frac{A_{user} - A_{default}}{SD_A} \right) \right] \quad (8)$$

Where Δv_{M2} is the moisture excess level according to the M2 model, corrected using secondary factors, and $\Delta v_{M1}(O)$ is the base value for moisture excess levels as a function of occupancy (see the equation in Figure 6, left); n, q_{50}, h, A are all variables (see Table 5); and SD is the standard deviation for the variables given in Table 5 (n, q_{50}, h, A). Thanks to this, the procedure is as follows, according to the M2 model for calculating moisture excess levels Δv_{M2} during cold periods:

- Determine the occupancy value as was carried out for the M1 model. A questionnaire is the safest and most reliable solution. If unavailable, the number of persons can be taken as being equal to the number of rooms;
- Calculate the moisture excess base value as a function of occupancy using the equations given in Figure 6 left, or the levels in Figure 9, left;
- Determine the values for the secondary factors given in Table 5. If information on secondary factors is unavailable, no correction for secondary factors can be applied, and the M2 model is not applicable;
- Calculate the moisture excess level Δv_{M2} using equation 8;
- Note that moisture excess Δv_{M2} is an average value. Conversion to 90% critical values for moisture excess levels can be carried out for the same occupancy (see Figure 6 left, and Figure 9).

M2 model validation

The moisture excess value was calculated on the basis of occupancy using the M1 model. Secondary factors (such as air change rate, air leakage rate, the height of the ventilation stack, and the age of the windows) were taken into account in the M2 model using average values (see Figure 12).

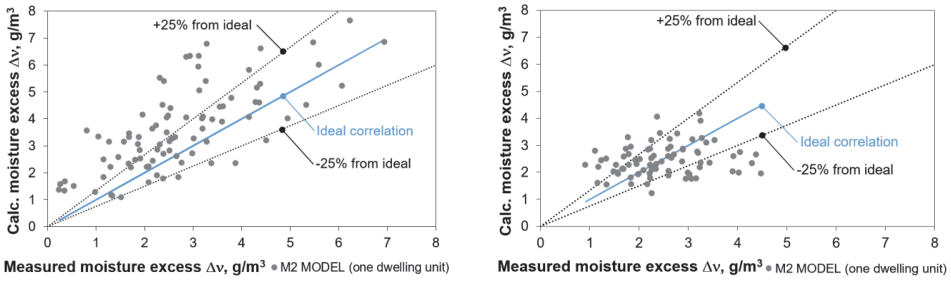

Figure 12. Measured and calculated moisture excess levels using the M2 model - verification using the Estonian data (left) and validation using the Finnish data (right)

The deviation in calculated values from the measured values decreased due to the inclusion of secondary factors but was still relatively large - 49% of the data within a range ±25% in the case of Estonian dwellings and 53% of the data within a range ±25% using the Finnish dwellings. The rate of deviation remains in place due to the stochastic nature of the factors which have been affecting moisture excess levels.

The indoor M3 humidity model based on air change and moisture production rates

Model description

Indoor climate and energy simulation models calculate the indoor air temperature in a zone which takes into account internal and external heat sinks and sources, and the thermal transmittance of the building envelope, while the temperature is stabilised by the thermal capacity. The moisture balance in a zone depends upon moisture production and the air change rate and is stabilised by moisture buffering due to interior surfaces (IEA Annex 14, 1991). Thanks to this, hygrothermal design using whole building simulation models requires moisture production and air change rates as input values in place of moisture excess levels, which are used in standardised hygrothermal calculations (EN 15026, 2007; EN ISO 13788, 2012). The M3 model provides such a solution.

As the measured air change rate in Estonian dwellings was found to be predominantly lower than the requirement for the whole dwelling n=0.5 h^{-1}, similarly to what was found elsewhere in Europe (Dimitroulopoulou, 2012), hygrothermal analysis should be carried out using the measured levels. Hence, the proposed M3 model is based on the measurement results (Figure 4 and Figure 5) for the average air change rate n=0.60 h^{-1} (SD 0.43) and moisture production rates G=72 g/h (SD 50) in bedrooms (see Figure 13). This corresponds to n=0.32±0.23 h^{-1} for the whole dwelling in this study (due to the flow of ventilation air from inlets towards rooms which have an exhaust outlet). Moisture excess levels which are measured in bedrooms can be assumed to be the same within a single apartment or detached house (except in the bathroom or sauna). If the air flow rate $\dot{V}$ (m^3/h) is required, the designer will calculate this using the air change rate n and the geometrical dimensions for the dwelling as a whole. The critical load at the 90th percentile based on measurements in the bedroom was at G=121 g/h. The air flow rate was calculated using 35 m^3 as the representative effective volume of a master bedroom with a closed bedroom door. It was not proven that the air change rate corresponded to the normal distribution rate in Figure 4 when using Pearson's chi-squared test (with a p-value of 0.002<0.05) but was close to the limit value (p=0.026<0.05) in the case of moisture production in Figure 5. On the other hand, the cumulative distribution curve for the measured air change rate as well as for moisture production was representative when compared against the cumulative distribution rates for an ideal normal distribution (R^2>0.8).

With this in mind, the procedure one should carry out according to the M3 model (see Figure 13) in order to be able to calculate the air change rate and moisture production levels is as follows:

- If the deterministic approach is taken, use the average air change rate (n=0.6 h^{-1} during the cold period) and an increased moisture production rate according to equation (9), depending upon the occupancy;
- If the stochastic approach is taken, use the average and SD for the air change rate and moisture production rate according to equation (10). Generate one curve for the air change rate and another for moisture production for each dwelling.

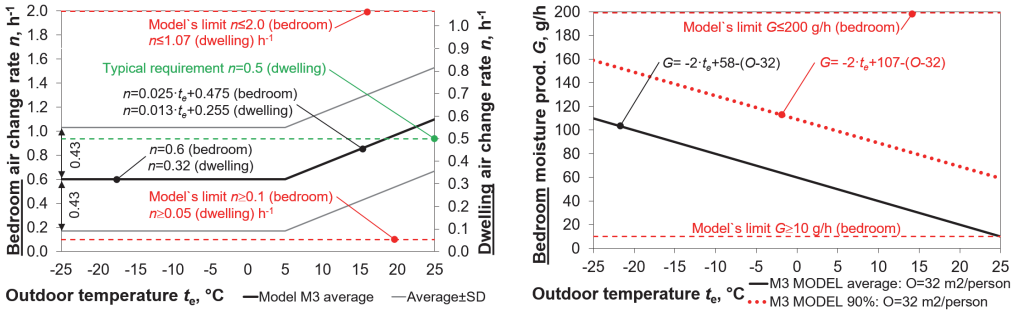

Figure 13. The dependency of air change rate levels for the bedroom (the primary y-axis) as well as for the entire dwelling (the secondary y-axis) on the left and moisture production levels for a bedroom as a function of occupancy *O* (right) according to the M3 model

Equation (9) for 90% moisture production (g/h):

$$G = -2 \cdot t_e + 107 - (O - 32) \qquad (9)$$

Equation (10) for average moisture production (g/h):

$$G = -2 \cdot t_e + 58 - (O - 32) \qquad (10)$$

Validation for the M3 model

The performance of the indoor M3 humidity model was also studied by comparing measured and calculated indoor RH levels (see results in Figure 14). The verification procedure itself was similar to that used for the M1 model but was based on data for 88 Estonian dwellings, where information about the air change rate was available. Validation was based on eighty Finnish dwellings. The validation procedure was similar to that used for the M1 model and consisted of the following:

- Since the total surface area of a dwelling unit is the only parameter available in the case of a new building, the latter was used as the basis for calculating the indoor moisture load;
- A representative running trend line between the number of occupants *N* against the total surface area *A* of the dwelling unit was used to calculate occupancy - *N*=1.83*ln(*A*)-6.51;
- Using the calculated occupancy (*O*=*A*/*N*), the moisture production rates as depending upon the outdoor temperature were selected by using Equations 9 or 10;
- The moisture excess level was added to the outdoor humidity rates in order to derive the indoor humidity by volume;
- The indoor temperature was calculated using models T1 and T2 for both heating system types (central heating or stove/combined heating);
- The saturation humidity by volume was calculated using the indoor temperature;
- The indoor RH levels were calculated using actual and saturation values for indoor humidity levels.

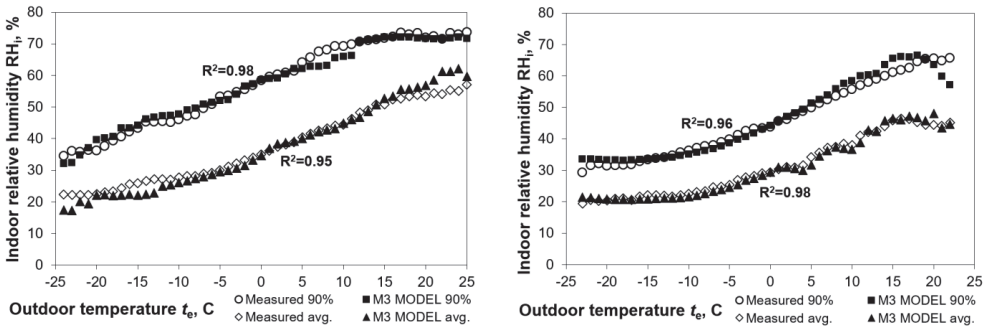

Figure 14. A comparison of measured and calculated indoor RH levels for Estonian dwellings which are equipped with central heating (left) and for Finnish dwellings (right) using the M3 model

Discussion

Methodology

Indoor humidity is sometimes represented by the RH levels. Indoor RH levels, however, are highly dependent upon the temperature and outdoor climate and are therefore unsuitable for representing the indoor humidity load. The indoor absolute humidity level cannot be used either, since this value also depends upon the outdoor humidity level. Therefore, the moisture excess (or water vapour pressure difference) was used to evaluate moisture loads, as the latter is a driving potential for vapour diffusion.

Since the properties of indoor air had been measured, the data already takes into account the buffering effect of the walls, floors, and furniture. Mlakar and Stancar (2013) also report that the presence of hygroscopic materials helps to reduce variations in RH levels. Hence, the values measured in the study are actually 'buffering corrected moisture excess' and 'buffering corrected moisture production', but shorter terms are used down the line for the sake of simplicity. Considering the uncertainties present in moisture production and air change rate, Glass and Tenwolde (2009) have evaluated the role of buffering to be rather insignificant and, therefore, simplified modelling is justified.

EN ISO 13788 review

A comparison of the proposed indoor M1 humidity model (Figure 9) with the existing model described by EN-ISO 13788 (2012) shows that they are similar. This is because moisture excess depends upon outdoor air temperature - during colder periods, when moisture excess levels are higher. This is due in part to the lower ventilation rates which are set by the occupants in order to save heating energy and achieve better thermal comfort, but they are also due to an increased level of indoor activity. Since approximately half of the buildings studied had natural ventilation, a higher rate of air change should have been detected, driven by the difference between indoor and outdoor air densities during the winter. Our detailed analysis of the air change rate versus the outdoor temperature seems to show, however, that this stack effect is secondary to the effect shown by the behaviour of the inhabitants, with the latter resulting in a rather constant air change rate during the cold period. As revealed by responses to a questionnaire, residents took action to reduce the air change rate during the winter in order to reduce energy consumption levels and create a better thermal indoor environment. Higher moisture excess levels when the outdoor temperature was very low was due primarily to higher moisture production levels arising from indoor activity but also due to desorbed moisture. Wind velocity during the coldest

period of the winter was rather low since climatic high-pressure systems were often present. Differences between the proposed model and that described by EN-ISO 13788 (2012) include the turning points in the graphs (5 °C versus 0 °C) and the levels during warm periods. We propose that moisture excess levels be determined for warm periods according to the load during cold periods - a low base load such as 2 g/m^3 would result in about 0 g/m^3 (valid for low occupancy levels), and a high base load (valid for high occupancy levels), for example, a figure of 6 g/m^3 would result in 2 g/m^3 during the warm period. This latter high moisture excess level may result in very high RH levels in some cases during the warm period, but this should not be considered a failure of the model since a single hour or even a single day are not representative time units for mould growth as a criterion. Lower calculated indoor RH levels than those measured during the validation of the M1 model, but not in the case of the M3 model, indicates an increase of moisture excess levels when the outdoor temperature drops. The latter observation is also supported by our measurement results and by many previous studies. This means that some modification is advised of the EN ISO 13788 (2012) standard so that this perspective is accepted.

The measured air change rate is insufficient for roughly two thirds of dwellings, according to the European standard, EN-15251 (2007) - see Figure 4, left. In the case of a few apartments, the low air change rate may have been due to the apartments being temporarily unoccupied. In the majority of cases, the insufficient air change rate (including infiltration) was indicative of comprehensive and serious deficiencies where air change was concerned. A similar problem was discovered by Kotol et al (2014), who found that ventilation was insufficient in 73% of bedrooms in Greenland.

Novelty and contribution

Any given temperature profile was proven to be dependent upon the heating system being used - central heating or stove. A novel outcome of the approach presented in this paper is the ability to choose the moisture excess level for any probability. This is valid both for an average based on all the data (Figure 3, left), and for a critical value (Figure 3, right) based on weekly maximums. It was found that average moisture excess levels during the heating period in bedrooms and living rooms, 2.8 g/m^3 (±1.6), were nearly the same or were somewhat higher than that reported in earlier studies. Although the availability of data on occupancy levels is very limited, occupancy in our sampling of buildings (with a median of 27 m^2/person with an SD of 15 m^2/person for apartments and 45±22 m^2/person for detached houses) was somewhat high, resulting in a rather high moisture excess level.

One of our aims was to examine those factors which were influencing moisture excess levels and moisture production. Although our finding that occupancy is the dominant factor was itself fairly predictable, we were able to quantify its relation to moisture excess and moisture production. We also found other factors which have a significant impact on moisture excess levels and which can be quantified using linear regression. Since we demonstrated that moisture excess levels depend upon occupancy rates, a baseline design value is recommended both for average and critical values. A simple or detailed model can be selected, depending upon data availability, and the ranges for moisture production and air change rates can be used for whole-building modelling. Measuring the actual dynamic moisture production rates on a source-by-source basis is proposed for the future research.

The validated models can be applied to determine the hygrothermal boundary conditions for dwellings in cold climates, assuming similar climate conditions and comparable building characteristics. In order to use the results proposed in this paper for other countries, it is recommended that comparisons be made of the data (Table 2) and results (Table 5) against findings for the country of origin.

Conclusions

The indoor hygrothermal loads for 237 dwelling units were analysed, determined upon the basis of hourly indoor and outdoor climate measurements which were carried out over a span of several years. The air change rate and moisture production levels in bedrooms were calculated on the basis of CO_2 measurements.

It was found that indoor temperature profiles vary depending upon whether a building has central heating or a stove or a combined heating system. The determined average moisture excess value, 2.8 g/m^3 with an SD of 1.6 g/m^3 for cold periods, can be used in stochastic calculations. Critical values for moisture excess at the 90th percentile, ranging predominantly between 3 g/m^3 and 8 g/m^3, depending upon occupancy rates, can be used in the deterministic analysis. Levels of moisture excess are reported at different percentiles for average and weekly maximums. It appears that moisture excess levels during warm periods depend upon the value during the cold period, marking a significant departure from the EN ISO 13788 (2012) standard. Moisture excess levels during the summer were close to 0 g/m^3 with a low moisture excess level of about 2 g/m^3 during the winter, but the result was in positive figures for higher moisture excess levels.

Average night-time moisture production in bedrooms during cold periods was at 72 g/h with an SD of 50 g/h. The critical value at the 90th percentile was 121 g/h. The average air change rate in bedrooms was 0.6±0.43 h^{-1}, and the critical value at the 10th percentile was 0.20 h^{-1}. The corresponding average air change rate for the entire dwelling unit was 0.32±0.23 h^{-1}, and the critical value at the 10th percentile was 0.11 h^{-1}.

Two indoor temperature and three humidity models were proposed with different levels of detail. Our analysis of factors which may be affecting moisture excess and moisture production levels indicates that occupancy is the dominant factor. Therefore, occupancy should be the basis for the selection of the design value for any indoor humidity load. In addition to occupancy, the air change rate and air leakage rate, the height of the ventilation stack, and the age of windows all had a significant level of impact. The temperature and humidity load determined using the proposed models can be used to calculate indoor hygrothermal boundary conditions for the building envelope of dwellings in cold climates.

Acknowledgements

The authors would like to thank Associate Professor Margus Pihlak PhD, and Endrik Arumägi PhD, for their assistance with the statistical analysis, and doctoral candidates Üllar Alev MSc and Alo Mikola MSc for their help with the data analysis, all of Tallinn University of Technology. Thanks should go to Juha Vinha DSc of Tampere University of Technology for sharing Finnish data which was used in the validation of the models.

Declaration of a conflict of interest

The authors declare that there are no conflicts of interest.

Funding

This research was supported by the Estonian Centre of Excellence in Zero Energy and Resource Efficient Smart Buildings and Districts (ZEBE), Grant No TK146, which was funded by the European Regional Development Fund, and by the Estonian Research Council, with institutional research funding grant No IUT1-15.

References

Arena L, Mantha P and Karagiozis AN (2010) Monitoring of Internal Moisture Loads in Residential Buildings. In: *Proceedings of Building Enclosure Scienbce and Technology (BEST2)*, Portlenad, USA, pp. 1–28.

ASHRAE 160P (2009) *Criteria for Moisture Control Design Analysis in Buildings*. *Standard*, Atlanta GA.

ASHRAE 55 (2004) Thermal environmental conditions for human occupancy. Atlanta GA.

Bagge H, Johansson D and Lindstrii L (2014) Measured indoor hygrothermal conditions and occupancy levels in an arctic Swedish multi-family building. *HVAC&R Research* 20(4): 376–383. Available from: http://www.tandfonline.com/doi/full/10.1080/10789669.2014.888367#abstract.

Becker R and Paciuk M (2009) Thermal comfort in residential buildings – Failure to predict by Standard model. *Building and Environment* 44: 948–960.

Bekö G, Lund T, Nors F, et al. (2010) Ventilation rates in the bedrooms of 500 Danish children. *Building and Environment* 45(10): 2289–2295.

Bishara a., Haupl P and Hansel F (2014) Model and program for the prediction of the indoor air temperature and indoor air relative humidity. *Journal of Building Physics* 38(2): 103–120. Available from: http://jen.sagepub.com/cgi/doi/10.1177/1744259114532614.

Bornehag CG, Sundell J, Bonini S, et al. (2004) Dampness in buildings as a risk factor for health effects, EUROEXPO: a multidisciplinary review of the literature (1998-2000) on dampness and mite exposure in buildings and health effects. *Indoor air* 14(4): 243–57.

Cornick SM and Kumaran MK (2008) A Comparison of Empirical Indoor Relative Humidity Models with Measured Data. *Journal of Building Physics* 31(3): 243–268.

CPR (2011) Construction Products Regulation. *Official Journal of the European Union. Regulation (EU) No. 305/2011*: 39.

Cui S, Cohen M, Stabat P, et al. (2015) CO2 tracer gas concentration decay method for measuring air change rate. *Building and Environment* 84: 162–169.

Dimitroulopoulou C (2012) Ventilation in European dwellings : A review. *Building and Environment*, Elsevier Ltd 47: 109–125. Available from: http://dx.doi.org/10.1016/j.buildenv.2011.07.016.

EN 13829 (2000) *Thermal performance of buildings - Determination of air permeability of buildings - Fan pressurization method*. Brussels, Belgium.

EN 15026 (2007) *Hygrothermal performance of building components and building elements - Assessment of moisture transfer by numerical simulation*. Brussels, Belgium.

EN 15251 (2007) *Indoor environmental input parameters for design and assessment of energy performance of buildings addressing indoor air quality, thermal environment, lighting and acoustics*. Brussels, Belgium.

EN ISO 13788 (2012) *Hygrothermal performance of building components and building elements – Internal surface temperature to avoid critical surface humidity and interstitial condensation – Calculation methods.* Brussels, Belgium.

Fisk WJ, Lei-Gomez Q and Mendell MJ (2007) Meta-analyses of the associations of respiratory health effects with dampness and mold in homes. *Indoor air* 17(4): 284–96.

Francisco PW and Rose WB (2010) Temperature and Humidity Measurements in 71 Homes Participating in an IAQ Improvement Program. In: *Thermal Performance of the Exterior Envelopes of Whole Buildings XI International Conference*, Clearwater Beach, FL: ASHRAE.

Geving S and Holme J (2011) Mean and diurnal indoor air humidity loads in residential buildings. *Journal of Building Physics* 35(4): 392–421.

Glass S V. and Tenwolde A (2009) Review of moisture balance models for residential indoor humidity. In: *12th Canadian Conference on Building Science and Technology*, Montreal, pp. 231–246.

IEA Annex 14 (1991) *Condensation and Energy, Sourcebook*. Leuven, Belgium.

IEA EBC Annex 55 (2012) Reliability of Energy Efficient Building Retrofitting -Probability Assessment of Performance and Cost. Hagentoft CE (ed.).

IOM (2004) *Damp indoor spaces and health. Health San Francisco*, Washington, DC: The National Academy of Sciences Press.

Janssens A and Vandepitte A (2006) *Analysis of indoor climate measurements in recently built Belgian dwellings*. Annex 41 Moist-Eng Working Meeting Lyon October, 25-27 2006.

Jones R (1993) Modelling water vapour conditions in buildings. *Building Services Engineering Research and Technology* 14(3): 99–106.

Kalamees T, Vinha J and Kurnitski J (2006) Indoor Humidity Loads and Moisture Production in Lightweight Timber-frame Detached Houses. *Journal of Building Physics* 29(3): 219–246.

Kotol M, Rode C, Clausen G, et al. (2014) Indoor environment in bedrooms in 79 Greenlandic households. *Building and Environment* 81: 29–36. Available from: http://www.sciencedirect.com/science/article/pii/S0360132314001528 (accessed 30 April 2016).

Labat M and Woloszyn M (2016) Moisture balance assessment at room scale for four cases based on numerical simulations of heat – air – moisture transfers for a realistic occupancy scenario. *Journal of Building Performance Simulation* 1493(Vol. 9, No. 5): 487–509. Available from: http://dx.doi.org/10.1080/19401493.2015.1107136.

Mikola A, Kõiv T and Kalamees T (2013) Quality of ventilation systems in residential buildings: status and perspectives in Estonia. In: *International Workshop Securing the quality of ventilation systems in residential buildings: status and perspectives*, Brussels, Belgium: INIVE, AIVC, TightVent.

Mikola A, Kõiv T and Rehand J (2017) The Usage of CO2 Tracer Gas Methods for Ventilation Performance Evaluation in Apartment Buildings. In: *'Environmental Engineering' 10th International Conference*, Vilnius, Lithuania.

Mlakar J and Štrancar J (2013) Temperature and humidity profiles in passive-house building blocks. *Building and Environment* 60: 185–193.

Pallin S (2013) Risk Assessment of Hygrothermal Performance - Building Envelope Retrofit. Chalmers University of Technology. Doctoral thesis.

Peeters L, Dear R De, Hensen J, et al. (2009) Thermal comfort in residential buildings : Comfort values and scales for building energy simulation. *Applied Energy* 86: 772–780.

Rousseau M, Manning M, Said MN, et al. (2007) Characterization of Indoor Hygrothermal Conditions in Houses in Different Northern Climates. *Thermal Performance of Exterior Envelopes of Whole Buildings X International Conference*: 1–14.

Sanders C (1996) *Heat, Air and Moisture Transfer in Highly Insulated Building Envelopes (HAMTIE). Report, Volume 2, Task 2: Environmental conditions.*

Zhang H, Yoshino H, Murakami S, et al. (2007) Investigation of actual humidity conditions in houses and evaluation of indoor environment by fungal index. In: *The 6th International Conference on Indoor Air Quality, Ventilation & Energy Conservation in Buildings IAQVEC*, Oct. 28 - 31 2007, Sendai, Japan, p. 6.

Tajima M, Inoue T and Ohnishi Y (2014) Derivation of equation for personal carbon dioxide in exhaled breath intended to estimation of building ventilation. In: *35th AIVC Conference ' Ventilation and airtightness in transforming the building stock to high performance', 24-25 September*, Poznań, Poland.

Tariku F and Simpson WY (2014) Temperature and humidity distributions in a mid-rise residential building suite. In: *14th Canadian Conference on Building Science and Technology*, Toronto, Canada, pp. 419–428.

Tariku F, Kumaran K and Fazio P (2011) Determination of indoor humidity profile using a whole-building hygrothermal model. *Building Simulation* 4(1): 61–78.

Woloszyn M and Rode C (2008) *Final report of IEA Annex 41, Subtask 1: Modelling principles and common exercises.* Leuven, Belgium: K.U. Leuven. Department of Civil Engineering Laboratory of Building Physics.

About the authors

Simo ILOMETS. He is a researcher/lecturer in 'Nearly Zero Energy Buildings Research Group' at Tallinn University of Technology. His fields of research include building physics and the durability and renovation of buildings. He has an MSc in civil engineering and is currently a doctoral candidate.

Targo KALAMEES. He is a professor of building physics in 'Nearly Zero Energy Buildings Research Group' at Tallinn University of Technology. His fields of research include the hygrothermal behaviour of buildings structures, boundary conditions for hygrothermal simulations and experiments, indoor climates, building energy consumption and healthy building design, and building renovation.

PUBLICATION II

Ilomets, S., Kalamees, T. Evaluation of the criticality of thermal bridges.
Journal of Building Pathology and Rehabilitation (2016) 1:11

J Build Rehabil (2016) 1:11
DOI 10.1007/s41024-016-0005-6

RESEARCH ARTICLE

Evaluation of the criticality of thermal bridges

Simo Ilomets[1] · **Targo Kalamees**[1]

Received: 27 May 2016 / Accepted: 14 September 2016

Abstract Thermal bridges can be an important reason for the renovation of old apartment buildings. This study presents a method for the critical analysis of thermal bridges. The risk of failure, i.e., surface condensation or mould growth, is evaluated by using the temperature factor $f_{Rsi.load}$ based on indoor hygrothermal loads and the temperature factor $f_{Rsi.resistance}$ from thermography measurements. The proposed method is employed for two practical applications—a case study analysis of the entire Estonian apartment building stock and a case study concerning the thermal bridges before and after the renovation of a precast concrete large-panel apartment building. The results show that critical thermal bridges caused by low surface temperature exist in all types of apartment buildings. The measured temperature factors were as low as $f_{Rsi.res} < 0.65$ for several junctions in concrete buildings and for the external wall/window junctions of brick buildings. The temperature factors from indoor hygrothermal loads are as high as $f_{Rsi.load} = 0.99$ for the worst dwelling unit and $f_{Rsi.load} = 0.80$ at a 90% reliability level for mould growth in concrete buildings. The calculated risk for surface condensation is 45–51% and for mould growth is 45–54%; this is highest in concrete buildings for both criteria. The calculated results are confirmed by visually detected mould growth, which ranges between 28 and 46% depending on the type of building. The proposed method can be used in stochastic analysis if the present need for renovation or designed renovation alternatives is under consideration.

Keywords Thermal bridge · Temperature factor · Mould growth · Probabilistic · Risk of failure · Thermography

Introduction

A thermal bridge is a part of the building envelope where the thermal transmittance is significantly larger at a local level in comparison to the surrounding area. Thermal bridges are mainly caused by geometrical or structural reasons or due to a full or partial discontinuation of the thermal insulation. Thermal bridges may lead to surface damage and hygiene problems, such as mould growth, surface condensation and the staining of surfaces. The fact that thermal bridges in a building envelope can cause considerable heat loss was detailed in the 1980s [1–3]. This factor should also be considered in the design of modern buildings [4, 5] because the relative significance of heat loss through thermal bridges is increased when there is a general decrease in thermal transmittance [6–9]. In short, the parameters that influence the criticality and probability of thermal bridges are presented in Fig. 1.

In the qualitative evaluation of the criticality of thermal bridges, the temperature factor on the internal surface (f_{Rsi}, −) [10–12] can be used. The temperature factor (also referred as the temperature ratio in research publications) on the internal surface depends on the ratio of total thermal resistance of the building envelope R_T (m^2 K/W) without the internal surface resistance R_{si} (m^2 K/W) to the total thermal resistance of the building envelope. The temperature factor can be calculated as the difference between the internal surface temperature (t_{si}, °C) and the outdoor air temperature (t_e, °C) divided by the

✉ Simo Ilomets
simo.ilomets@ttu.ee

[1] Department of Structural Design, Chair of Building Physics and Energy Efficiency, Faculty of Civil Engineering, Tallinn University of Technology, Ehitajate tee 5, 19086 Tallinn, Estonia

Published online: 31 October 2016

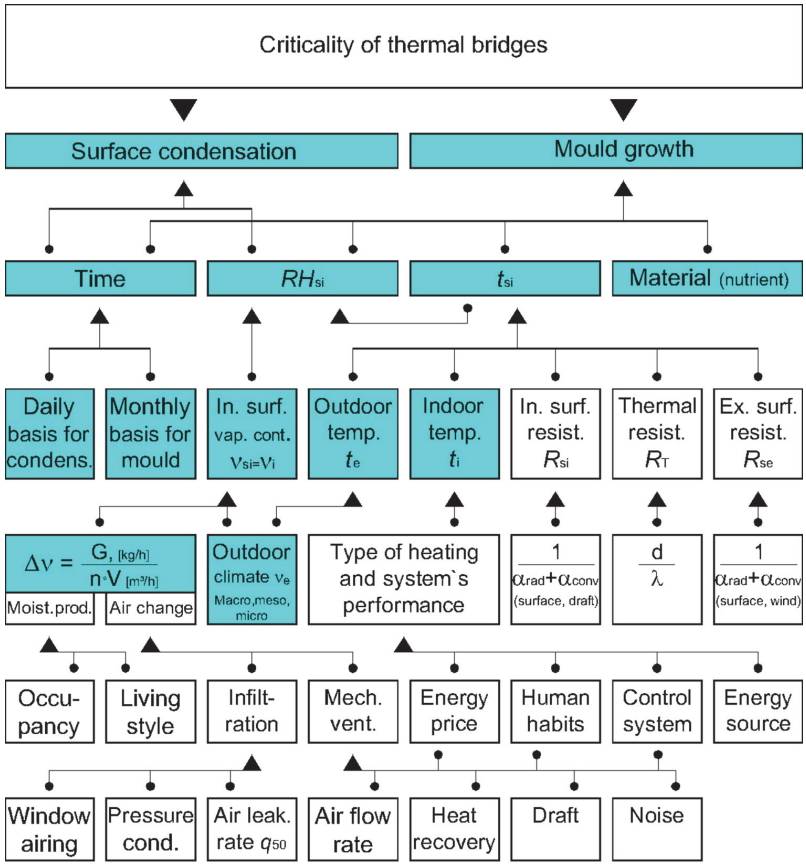

Fig. 1 Parameters that influence the criticality of thermal bridges

difference between the indoor air temperature (t_i, °C) and the outdoor air temperature, Eq. 1. The surface temperature of thermal bridges can be either calculated [12] or measured [13, 14].

$$f_{Rsi} = \frac{t_{si} - t_e}{t_i - t_e} = \frac{R_T - R_{si}}{R_T} \quad (1)$$

The limit value of the temperature factor depends on the indoor hygrothermal loads, outdoor climate, specific junction, hygrothermal criteria and other factors, and it varies between 0.6 and 0.8 depending on the country [15–20].

Many old buildings, especially those built before the first energy crisis in the 1970s, contain serious thermal bridges [21, 22]. Many of these buildings were constructed according to standard design with similar architectural and structural typology, including typical thermal bridges. The elimination of these structural thermal bridges could be one reason for renovation.

This study presents a methodology to determine the criticality of thermal bridges based on statistical analysis of the temperature factors by using distributions of thermal bridges measured with thermography and indoor hygrothermal loads. The methodology presented could be used in the risk assessment and analysis of the need for renovation of both an individual building level and the whole building stock. It is necessary to analyse thermal bridges in order to make decisions regarding the technical solutions of building envelope renovation.

Methods

Buildings studied

Apartment buildings (blocks of flats) from different eras and typology were included in the analysis of thermal bridges. Based on external wall material, three different

types were studied: precast concrete large-panel (hereafter: concrete) (13 buildings), brick (15 buildings) and wooden log (20 buildings).

The external walls of concrete buildings built between 1962 and 1990 are composed of two layers of reinforced concrete (50–130 mm inner, load-bearing layer and 50–80 mm outer core) with thermal insulation of 100–150 mm in between (fibrolite, mineral wool, phenolic foam or expanded polystyrene). Different elements are welded and casted together in situ. The thermal transmittance U of solid walls varies between 0.5 and 1.0 W/(m^2 K), and 0.7 and 1.0 W/(m^2 K) for roofs.

The external walls of brick buildings have an inner, load-bearing layer of 250–630 mm in thickness (typically calcium silicate brick), 60–120 mm of mineral wool thermal insulation and a 120 mm external layer (calcium silicate or ceramic brick). The thermal transmittance of solid walls varies between 0.5 and 1.2 W/(m^2 K) and 0.7 and 1.0 W/(m^2 K) for roofs. In general, slabs on the ground and cellar ceilings are uninsulated in these structures.

Typical wooden log dwellings from the first half of the twentieth century have 2–3 storeys. The external walls are built with a horizontal or vertical load-bearing log wall of 120–180 mm in thickness. The inserted ceilings are usually built of wooden beams. Cellar ceilings are also made of concrete on steel beams. The thermal transmittance of solid wooden walls varies between 0.5 and 0.9 W/(m^2 K). Attics and cellars are generally unheated, and the thermal transmittance of those inserted ceilings that separate the heated space is $\sim$0.5 W/(m^2 K).

Measurements

To determine typical thermal bridges and their distribution, measurements with a FLIR ThermaCam E320 infrared camera (thermal sensitivity of 0.1 °C, measurement range from −20 to +500 °C) were conducted during the winter in 48 buildings. European standard EN 13187 [14] was followed when the temperature difference between the indoor and outdoor air was at least 20 K. Up to four dwelling units (i.e., apartments) were studied in each apartment building.

The presence of mould growth on the internal surface of a thermal bridge was visually inspected using the simple tape-lift method [23] and microscopic analysis in the laboratory.

The indoor humidity loads in apartments were determined based on indoor climate measurements with small data loggers for temperature and relative humidity (RH) (HOBO U12-013; temperature measurement range: −20 and +70 °C with an accuracy of ±0.35 °C; RH measurement range: 5 and 95% with an accuracy of ±2.5% in the 10–90% RH range) at 1-h intervals over a 1-year period in the master bedroom and/or living room. The long-term outdoor climate was measured near the building or obtained from the nearest weather station.

Evaluation of the probability of failure

A lower surface temperature on a thermal bridge leads to higher RH on the surface. Two types of failure were used in this study:

- surface condensation: $f_{(\text{relative humidity: (water vapour pressure, saturation vapour pressure))}}$;
- mould growth: $f_{(\text{temperature, relative humidity, time, nutrient (surface material))}}$.

The temperature factor at the internal surface (f_{Rsi}, −) was used to evaluate the criticality of thermal bridges and the probability of failure. The temperature factor can be calculated from the following:

- thermography measurements $f_{\text{Rsi.res}}$ that represent the resistance of the thermal bridge;
- indoor and outdoor climate measurements $f_{\text{Rsi.load}}$ that represent the hygrothermal load effect on the thermal bridge.

Failure (surface condensation or mould growth) occurs if $f_{\text{Rsi.load}} > f_{\text{Rsi.res}}$. The resulting probability of failure is the probability of low $f_{\text{Rsi.res}}$ values and high $f_{\text{Rsi.load}}$ values simultaneously (Fig. 2).

The probabilistic approach, presuming the normal distribution of measured temperature factors $f_{\text{Rsi.res}}$ with thermography and critical temperature factors $f_{\text{Rsi.load}}$ based on indoor climate measurements, was used to evaluate the risk of mould growth in the three building types. Critical temperature factors were calculated according to the long-term and large-scale indoor and outdoor climate measurements of Ilomets and Kalamees [24]. The probability of the risk of failure was calculated according to Eq. (2):

$$P(f_{Rsi.res} < f_{Rsi.load}) = \int_0^1 \int_0^{f_{Rsi.res}} f_1(f_{Rsi.res}) \cdot f_2(f_{Rsi.load}) \cdot \mathrm{d}f_{Rsi.res} \cdot \mathrm{d}f_{Rsi.load} \quad (2)$$

where: P is probability for the risk of failure; f_1, f_2 are probability density functions of $f_{\text{Rsi.res}}$ and $f_{\text{Rsi.load}}$ respectively; d is differential.

The probability of an event can be easily calculated in MS Excel by inserting Eq. (3):

$$= norndist(0, AVG_{fRsi.res} - AVG_{fRsi.load}, sqrt(SD_{fRsi.res} \cdot SD_{fRsi.res} + SD_{fRsi.load} \cdot SD_{fRsi.load}), true) \quad (3)$$

where: *normdist* refers to normal distribution; *AVG* is average; *sqrt* is square root; *SD* is standard deviation.

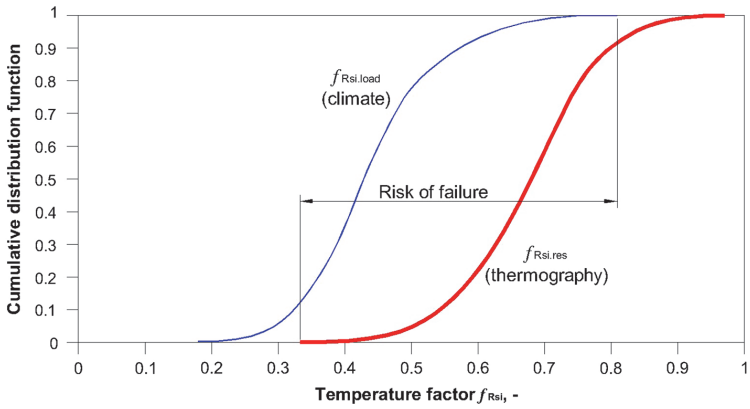

Fig. 2 Cumulative distribution functions from the lowest values of $f_{Rsi.res}$ from each dwelling unit (based on thermography measurements) and the values of $f_{Rsi.load}$ from each dwelling unit (based on climate measurements)

Nutrient availability (substrate), moisture state and temperature are the three most important factors on which mould growth depends [25]. The presence of oxygen is also necessary due to the aerobic nature of mould. It is possible to draw a trend line of mould growth on a building material with various hygrothermal conditions [25]. While surface condensation starts at the RH of 100%, the limit value for RH in relation to mould growth is from 75 to 95%, depending on temperature variations over time and the group of materials [26–30]. Several mould growth models have been developed, such as the so-called VTT model by Hukka and Viitanen [28], Sedlbauer's isopleths [31], Moon's mould germination method [32] and others. Vereecken and Roels have given a detailed description and studied the impact of the models on the results [33]. As the VTT model has proven to be consistent with the temperature factor approach, it was chosen for the present study. The critical RH for wood, as proposed by Hukka and Viitanen [28], see Eq. 4, may therefore be written as the following:

$$RH_{crit},\% = \begin{cases} 100 & if\ t < 0^\circ C; \\ -0,00267 \cdot t^3 + 0,160 \cdot t^2 - 3,13 \cdot t + 100 & if\ 0^\circ C \le t \le 20^\circ C; \\ 80 & if\ t > 20^\circ C; \end{cases} \quad (4)$$

where: t is temperature, °C.

Results

A method to evaluate the probability of surface condensation or mould growth on thermal bridges was developed during the course of this study. In the following, the method is described and its application at both building stock and single apartment level is then presented.

Method to evaluate the probability of surface condensation or mould growth on thermal bridges

The method is based on temperature factor f_{Rsi}, which should be calculated in order to avoid surface condensation and mould growth. The following procedure for calculating critical surface temperature $t_{si.crit}$ or critical temperature factor $f_{Rsi.crit}$ is described in EN ISO 13788 [11]. First, the indoor vapour content is calculated from the indoor temperature and RH. Then, with the maximum acceptable RH_{crit} (depends on temperature, see Eq. 4) at the thermal bridge surface, the maximum acceptable absolute humidity should be calculated. From that, the minimum acceptable surface temperature, i.e., saturation temperature corresponding to absolute humidity, should be calculated. Using this minimum acceptable surface temperature, outdoor temperature and indoor temperature, the minimum temperature factor should be calculated according to Eq. 1. As the mould growth depends on time, average monthly climate data could be used. The calculation procedure employed for selecting the critical temperature factor to avoid surface condensation was the same, though the average daily climate values and the maximum acceptable RH at the thermal envelope's surface RH_{si} 100% was used. If the variations of all these parameters in Fig. 1 are known, it is possible to make detailed stochastic calculations.

This study was generalised so that only the main sphere of influencing parameters (shaded in Fig. 1) was taken into account:

- $f_{Rsi.res} = (t_{si} - t_e)/(t_i - t_e)$ is the result of the following parameters:
  outdoor air temperature t_e (in macro, meso and micro scale) to be measured during thermography measurements near the studied building;
  indoor air temperature t_i to be measured during

thermography measurements (strongly depends on the performance of the heating systems);
internal surface temperature t_{si} to be measured by thermography is the result of the following parameters (in addition to indoor and outdoor air temperatures);
internal and external surface resistance R_{si}, R_{se} (depends on convective and radiative heat transfer coefficients);
thermal resistance of a building fabric (depends on the thermal transmittance of the building envelope or thermal bridge, i.e., thermal conductivity λ and the thickness d of building materials).

- $f_{Rsi.load(cond.mould)} = (t_{si.crit(cond.mould)} - t_e)/(t_i - t_e)$ is the result of the following parameters:
time: condensation to be calculated from the daily average (short time, i.e., less frequent than daily, surface condensation is acceptable) and mould growth to be calculated from monthly average (mould germination needs time);
outdoor air temperature t_e (in macro-, meso- and micro-scale) to be taken from the nearest weather station;
indoor air temperature t_i to be measured by data loggers in bedrooms over a 1-year period (strongly depends on the performance and type of heating systems: source and price of energy, the control system and human habits);
critical internal surface temperature $t_{si.crit}$ to be calculated by using indoor (=internal surface) vapour content and critical RH_{crit} (Eq. 4), see the first paragraph of this chapter.

Practical application I: a case study on Estonia's apartment building stock

Thermography measurements to determine $f_{Rsi.res}$

Thermography measurements in buildings showed that the critical thermal bridges are located in the following places (see also Fig. 3):

- the junction of the external wall and windows/doors;
- the junction of the external wall and cellar ceiling;
- the junctions of the external wall (especially end sides) and flat roof;
- the bonds of the inner and outer layers of the external wall elements;
- the external corners of two external walls;
- the junctions of the external wall and the balcony slab (valid for concrete and brick buildings);
- the horizontal and vertical joints between external wall elements (valid for concrete buildings);
- the junction of the external wall and inserted ceiling (mostly for concrete buildings).

In the worst cases, mould growth was visually detected on the internal surface of the thermal bridges, see Fig. 4.

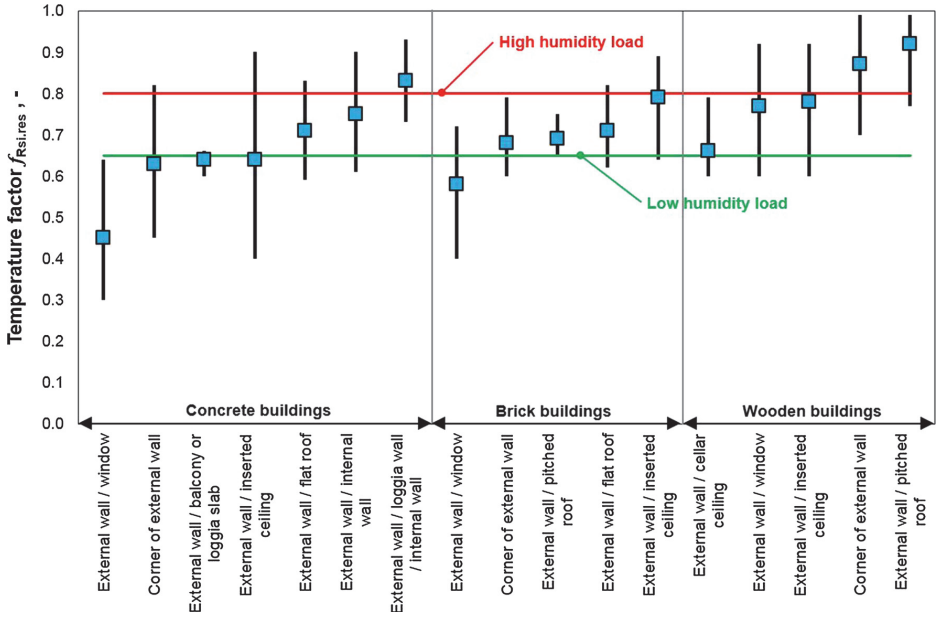

Fig. 3 Measured (by thermography) results of the temperature factors $f_{Rsi.res}$ of thermal bridges. The *horizontal lines* represent the minimum acceptable values for high/low humidity loads in Estonia [16]. The *black vertical line* shows the range of the results

Fig. 4 Example of a precast concrete large-panel apartment building (*upper left*) with discontinued insulation in the junction of the external wall and floor (*lower left*). Visible mould growth at the corners of a building envelope (*upper right*) is caused by the thermal bridge (*lower right*) and high indoor humidity load

Indoor climate measurements to determine $f_{Rsi.load}$

Critical temperature factors were calculated based on the indoor and outdoor climate (temperature and RH) and the evaluation criterion (surface condensation or mould growth), see Fig. 5. There are significant variations between different dwelling units according to the hygrothermal loads. Each thin curve represents the maximum daily average (for surface condensation) or monthly average (for mould growth) temperature factor $f_{Rsi.load(cond.mould)}$ at the corresponding outdoor temperature. The maximum temperature factors $f_{Rsi.load}$ from different dwelling units for surface condensation (left column in Fig. 5) were in the range of 0.21–0.81 for concrete, 0.38–0.79 for brick and 0.40–0.83 for wooden apartment buildings. For mould growth (right column in Fig. 5), temperature factors $f_{Rsi.load}$ were in the range of 0.18–0.99 for concrete, 0.26–0.84 for brick and 0.36–0.95 for wooden apartment buildings. The temperature factor at 90% level is around $f_{Rsi.load} \approx 0.7$ but reaches 0.8 for concrete buildings with a mould growth criterion. As expected, the load of the condensation criterion is highest during the coldest period in winter, while the risk of mould growth is high up to a daily average outdoor temperature of 10–15 °C.

Probability of failure due to thermal bridges in Estonia's apartment buildings

The presence of mould growth on the internal surfaces of thermal bridges was inspected visually and calculated statistically according to Eq. 3. The probability of mould growth was calculated by comparing the distribution of the lowest temperature factors from each dwelling unit measured with the infrared camera $f_{Rsi.res}$ and the highest critical temperature factors calculated from indoor climate measurements $f_{Rsi.load}$. Figure 6 presents the results of three common apartment building types where the temperature factors $f_{Rsi.res}$ measured with thermography on the horizontal axes should be as near as possible to 1, with small

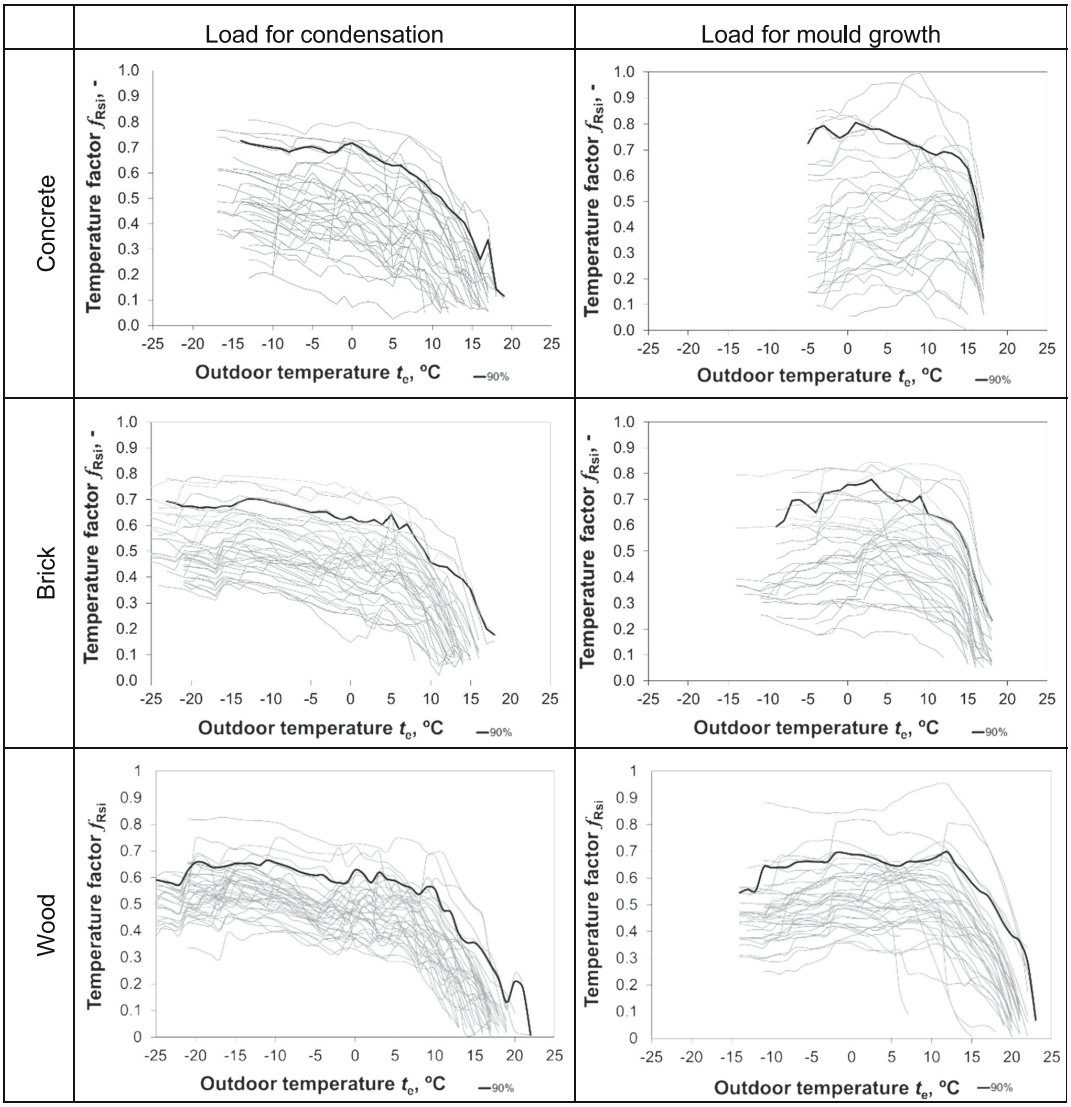

Fig. 5 Temperature factors $f_{Rsi.load(cond.mould)}$ for surface condensation (*left column*) and mould growth (*right column*) in dwelling units (each thin curve) located in concrete apartment buildings (*upper row*), brick buildings (*middle row*) and wooden buildings (*bottom row*)

deviation. Temperature factors $f_{Rsi.load}$ from climate loads come from Fig. 5 and should be oriented in the middle of the horizontal axes. The presented cumulative distribution curves show that deviation within the temperature factors $f_{Rsi.res}$ is smallest in the case of brick buildings, where it is expressed as the steepest angle ranging between approximately 0.4 and 0.75 of the line in Fig. 6, middle. There are also no dwelling units with extraordinarily high indoor climate loads over $f_{Rsi.load} > 0.8$ in Fig. 5, middle right. The largest variations of temperature factors $f_{Rsi.res}$ and $f_{Rsi.load}$ with the extreme values of <0.3 and 1 are in concrete buildings. The high values close to 1 for mould growth $f_{Rsi.load.mould}$ come from a few dwelling units that have extreme indoor loads (Fig. 5, top right).

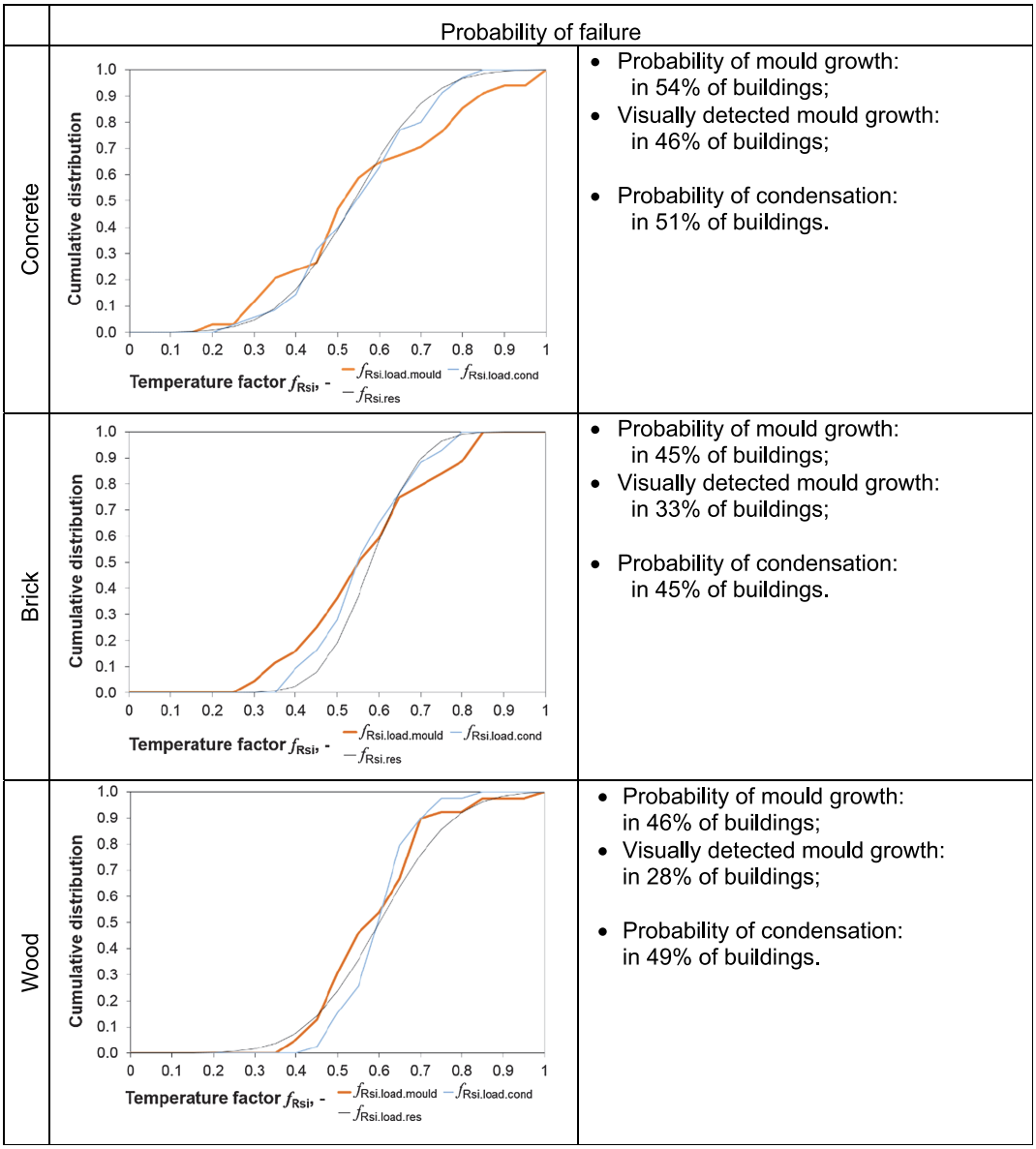

Fig. 6 Distribution of the temperature factors measured with thermography and the temperature factors determined from indoor climate measurements in the studied building types for both failure criteria—surface condensation and mould growth

Since temperature factors $f_{Rsi.res}$ of >0.8 can be considered acceptable, ventilation must be considerably improved in these dwelling units to effect a decrease in the humidity loads. In wooden buildings, one dwelling unit (Fig. 5, bottom, right) is responsible for a drastic temperature factor $f_{Rsi.load.mould}$ close to 1. That said, the temperature factor $f_{Rsi.res}$ is unacceptably low across the board in all building types.

Practical application II: a case study on a concrete apartment building

The method to determine the risk of failure due to thermal bridges was also tested on a precast reinforced concrete large-panel apartment building that was renovated due to high energy use and poor indoor climate [34, 35], see Fig. 7. This particular type of construction was common in Estonia and other countries in East and North-East Europe from 1961 to 1990. About two million m^2 of precast concrete large-panel apartment buildings were built in Estonia during that period. The method introduced could also have been applied to a single dwelling unit, but only the presence of risk (or absence thereof) can be evaluated instead of the numerical value for the risk of failure.

Thermography measurements to determine $f_{Rsi.res}$

In our case study, the thermography measurements in six dwelling units (including ground and top storeys) showed that the critical thermal bridges before the renovation are located in:

- horizontal and vertical joints between external wall elements: $f_{Rsi.res}$ 0.68–0.80;
- the outer corner of external walls: $f_{Rsi.res}$ 0.60–0.73;
- the junction of the external wall and the balcony slab;
- the junction of the external wall (especially end sides) and flat roof (3D corner): $f_{Rsi.res}$ 0.61–0.65;
- bonds of the inner and outer layers of the external wall elements;
- the external wall/foundation wall elements (3D corner): $f_{Rsi.res}$ 0.43–0.62;
- the junction of the external wall and the window/door (3D corner): $f_{Rsi.res}$ 0.66–0.70.

As an example, the improvement after installing ETICS in the course of the renovation increased the temperature factor of the window/wall sample junction from $f_{Rsi.res} = 0.68$ to $f_{Rsi.res} = 0.84$, see Fig. 8.

Indoor climate measurements to determine $f_{Rsi.load}$

Available information about the present situation of $f_{Rsi.load}$ was collected by measuring the indoor air temperature and

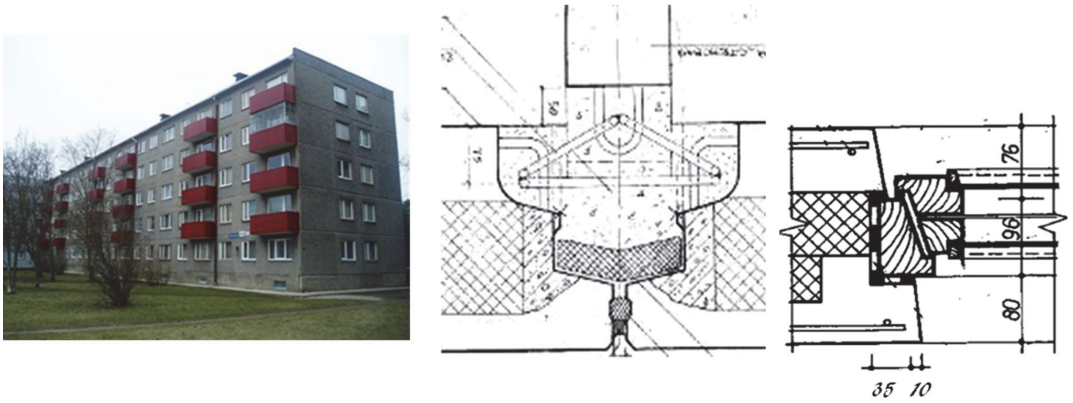

Fig. 7 The studied concrete large-panel apartment building before renovation (*left*) and its original design drawings—junction of external wall/internal wall (*middle*) and junction of external wall/window (*right*)

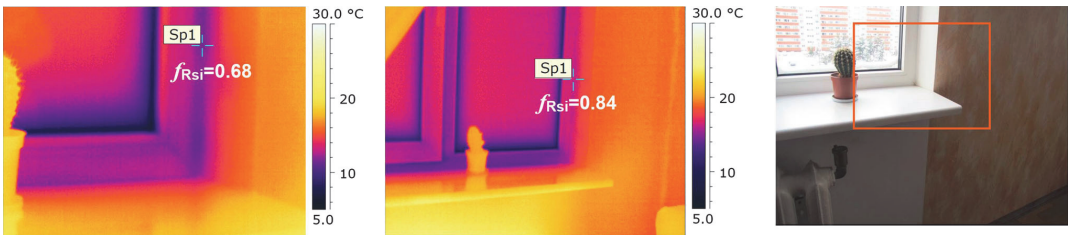

Fig. 8 Measured (by thermography) results of the temperature factors $f_{Rsi.res}$ of thermal bridges before (*left*) and after the renovation (*middle*) of the external wall/window junction (illustrating picture of a junction in the *right*). The window was not replaced during the renovation

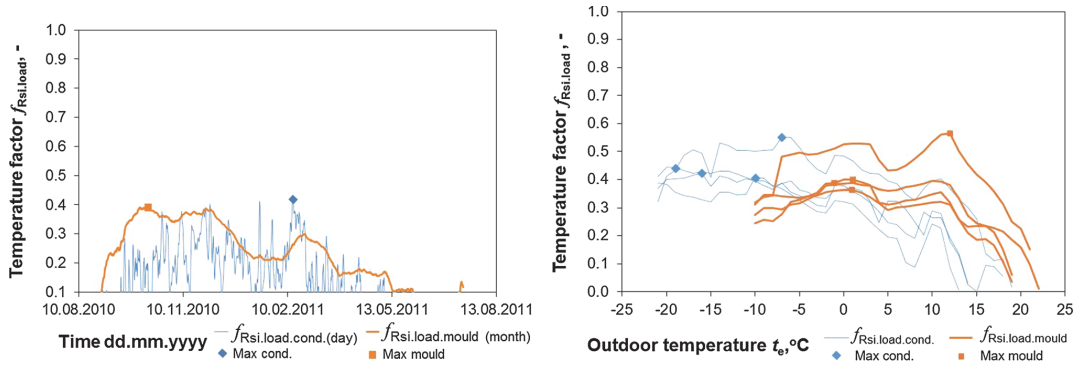

Fig. 9 Critical temperature factors $f_{Rsi.load(cond.mould)}$ of one dwelling unit during a 1-year period (*left*) and the same for four dwelling units arranged according to outdoor air temperature before the renovation (*right*)

RH over the course of a year prior to the renovation. Measurements and thermography were taken in the same dwelling units.

Critical temperature factors were calculated based on the indoor and outdoor climate (temperature and RH) data and the assessment criterion (surface condensation or mould growth), (Fig. 9, based on example of Fig. 5). The critical temperature factor for surface condensation $f_{Rsi.load(cond.)}$ is highest during the winter; see Fig. 9, left. In terms of mould growth, $f_{Rsi.load(mould)}$ becomes significant during the autumn. The risk of mould growth is relatively low in spring, although the outdoor temperature is similar to that in autumn; however, the RH of outdoor air is much lower in spring. Each curve in Fig. 9, right, represents the maximum daily average (for surface condensation) or monthly average (for mould growth) temperature factor $f_{Rsi,load(cond.mould)}$ at the corresponding outdoor temperature. One dwelling unit on an upper storey has higher indoor hygrothermal loads in comparison to the other three units. The maximum temperature factors $f_{Rsi.load}$ from different dwelling units before the renovation varied between 0.40 and 0.55 for surface condensation and 0.36–0.57 for mould growth. Compared to concrete buildings in a whole building stock level, our case study building had quite average indoor hygrothermal loads prior to renovation. Although the heating and ventilation systems were upgraded during the renovation, the indoor climate is assumed to remain the same in order to analyse the improved performance of the building envelope.

Probability of failure due to thermal bridges in a case study building

The probability of surface condensation and mould growth was calculated according to Eq. (3), by comparing

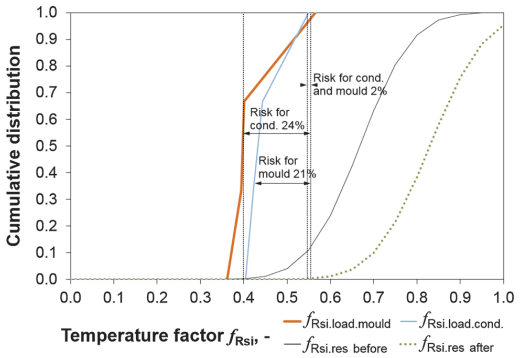

Fig. 10 Distribution of the temperature factors $f_{Rsi,load}$ and temperature factors measured with thermography $f_{Rsi,res}$, before and after the renovation. The temperature factor $f_{Rsi,load}$ from the indoor climate before and after renovation remained unchanged

the distribution of the temperature factors measured with the infrared camera $f_{Rsi.res}$ and the critical temperature factors calculated from the indoor climate measurements $f_{Rsi.load}$. Figure 10 presents the probability of surface condensation before the renovation as 24% and of mould growth as 21%. The risk of both is unacceptably high and the energy renovation of the building must cover the thermal bridges.

We were also able to measure the temperatures factors $f_{Rsi.res}$ after the renovation. The probability of surface condensation and mould growth after renovation resulted in 2% for both criteria, as presented graphically in Fig. 10. A target of 0% for the risk level was chosen, which was assumed to be reached with all the temperature factors $f_{Rsi.res}$ at >0.8. This target was not achieved since some of the measured temperature factors were lower than those calculated.

Discussion

The method proposed in this study and its application to evaluate the criticality of thermal bridges can be advised. The calculated risk for mould growth does not differ much from the percentage actually detected in dwelling units by visual observations and later confirmed to be mould in the laboratory. The advantage of the method is its ability to avoid uncertainties emanating from 2D vs 3D junctions, since the actual long-wave radiation emitted from the surface (i.e., surface temperature) is measured. When calculating the impact on thermal bridges due to renovation, the 3D approach should be performed. A sufficient quantity (48 dwelling units were used in this study) of the measured indoor surface temperatures and indoor loads should be analysed in order to decrease this uncertainty. The distribution function of the data should always be examined.

As Figs. 3 and 6 shows, the lowest temperature factors $f_{\mathrm{Rsi.res}}$ measured by thermography exist in concrete apartment buildings. The calculated probability for the surface condensation exceeded 50% for concrete and was close to 50% for wooden and brick buildings. The calculated probability (and also visually detected) of mould growth is also the highest for concrete buildings; though it is somewhat lower for wooden and brick buildings, it is still at an unacceptably high level. Most frequently, mould growth was found on the 3D corners of different junctions of the external wall. The criterion for mould growth $\mathrm{RH_{crit}} = 80\%$ (Eq. 4) was developed by Hukka and Viitanen [28] using wooden samples. The model was updated by Ojanen et al. [30] who proposed $\mathrm{RH_{crit}} = 80\%$ as a proper value for building materials that are "sensitive" to mould growth. Wooden based wallpaper and boards covered with paper were often used for the interior finishing in bedrooms, living rooms and kitchens of dwellings in the present study. These materials belong to the "sensitive" class and detected mould growth is consistent with the classes proposed by Ojanen. Furthermore, to eliminate problems caused by thermal bridges, additional thermal insulation of 150 mm is sufficient, as shown in Ilomets and Kalamees [35]. In light of more strict energy efficiency requirements today and in the future, thicker insulation, e.g., $\geq$200 mm for external walls, is advised. This would notably increase the building envelope's internal surface temperature and improve indoor thermal comfort.

The results of temperature factors $f_{\mathrm{Rsi.res}}$ in Fig. 3, measured by infrared thermography, refer to extremely low levels and significant variations within each junction, especially in terms of window junctions. The significant variations within the results indicate deficiencies in the quality of workmanship and variations in structural junctions due to different building types and series.

The present measurements prove the results of the previous study by Kalamees [16]: to avoid mould growth and surface condensation in dwellings with high indoor humidity loads [24], the temperature factor should be $f_{\mathrm{Rsi}} > 0.8$ at 10% critical level. The lines at higher temperature factors (Fig. 5) correlate with the higher moisture excess Δv, g/m^3 calculated from indoor and outdoor climate measurements. Also, the findings are largely consistent with $f_{\mathrm{Rsi}} > 0.7$ at 5% critical level [33], especially for wooden buildings.

The proposed method is a useful tool for evaluating the renovation need of the building envelope of old apartment buildings that are characterised with high indoor humidity loads and/or low temperature factors f_{Rsi}. Measuring indoor air temperature and RH as well as internal surface temperature by using thermography could be utilised as a regular, non-destructive, relatively simple and inexpensive process in the assessment of the technical condition of a single dwelling unit, a building, a district, or a whole housing stock. The impact of upgrading the building envelope or lowering humidity loads via improving ventilation can be analysed during the renovation design.

Overall, a building's low energy performance in the twentieth century, a historical lack of high quality building materials and workmanship, and poor records of operation and maintenance are the main reasons why the majority of older housing stock fail to meet today's standards. The largest shortcomings are related to indoor climate and energy performance as well as natural degradation mechanism, e.g., carbonation induced corrosion and frost damage [36]. As this study proves, the poor hygrothermal performance of a building envelope is also characterised by critical thermal bridges. Therefore, a situation has been reached whereby a huge number of buildings are in need of inevitable renovation.

Conclusions

The study had two aims—first, to propose a method and, second, to evaluate the criticality of thermal bridges by using the proposed method based on the temperature factor f_{Rsi}. The risk of surface condensation and mould growth was calculated from the measured results of $f_{\mathrm{Rsi.res}}$ by using thermography and from measured indoor hygrothermal loads expressed as $f_{\mathrm{Rsi.load}}$.

The results show that critical thermal bridges caused by a low surface temperature exist in all types of apartment buildings. The measured temperature factors were as low as $f_{\mathrm{Rsi.res}} < 0.65$ on average for several junctions of concrete buildings and for the external wall/window junctions of brick buildings. The temperature factors from indoor hygrothermal loads were as high as $f_{\mathrm{Rsi.load}} = 0.99$ for the

worst dwelling unit and $f_{Rsi.load} = 0.80$ at 90% reliability level for mould growth in concrete buildings. The calculated risk for surface condensation is 51% for concrete buildings and close to 50% for wooden and brick buildings. The probability of mould growth in concrete buildings is 54%, in wooden buildings 46% and in brick buildings 45%. The calculated results are confirmed by detected mould growth ranging between 28 and 46% in the studied dwelling units.

One of the main reasons for renovating old apartment buildings in Estonia is to eliminate critical thermal bridges that cause mould growth. Furthermore, additional external thermal insulation reduces heat loss, leads to a higher internal surface temperature that improves thermal comfort and protects the building façade against outdoor climate loads.

Acknowledgements This research was supported by the Estonian Centre of Excellence in Zero Energy and Resource Efficient Smart Buildings and Districts, ZEBE, grant TK146 funded by the European Regional Development Fund, and by the Estonian Research Council, with Institutional research funding grant IUT1-15.

References

1. Birkeland O (1979) Energy losses through thermal bridges. Batim Int Build Res Pract 7:284. doi:10.1080/09613217908550792
2. Andersson AC (1980) Insulation and the thermal bridge effect. Batim Int Build Res Pract 8:222. doi:10.1080/09613218008550868
3. Fang JB, Grot RA, Childs KW, Courville GE (2008) Heat loss from thermal bridges. Batim Int Build Res Pract 12:346–352. doi:10.1080/09613218408545298
4. Varga T, Ingeli R (2016) The effect of thermal bridges on energy balance of wood frame houses. Appl Mech Mater 824:323–330. doi:10.4028/www.scientific.net/AMM.824.323
5. Mend'an R, Pavčeková M (2016) The influence of thermal bridges on the energy need for heating after renewal: a case study. Appl Mech Mater 824:307–314. doi:10.4028/www.scientific.net/AMM.824.307
6. Ge H, Baba F (2015) Dynamic effect of thermal bridges on the energy performance of a low-rise residential building. Energy Build 105:106–118. doi:10.1016/j.enbuild.2015.07.023
7. Berggren B, Wall M (2013) Calculation of thermal bridges in (Nordic) building envelopes—risk of performance failure due to inconsistent use of methodology. Energy Build 65:331–339. doi:10.1016/j.enbuild.2013.06.021
8. Altan H, Kim YK (2014) Non Repeating Thermal Bridges and the Impact on Overall Heating Energy Consumption in a Typical UK Home. In: Dincer I, Midilli A, Kucuk H (eds) Progess in sustainable energy technologies, vol II. Springer International Publishing, Cham, pp 109–122. doi:10.1007/978-3-319-07977-6
9. Janssens A, Van Londersele E, Vandermarcke B, Roels S, Standaert P, Wouters P (2007) Development of limits for the linear thermal transmittance of thermal bridges in buildings. Therm. Perform. Exter. Envel. Whole Build. X Int. Conf., Clearwater, Florida
10. IEA Annex 14 (1990) Condensation and energy, guidelines and practice. In: Hens H (ed) Laboratory for building physics, Belgium, KU Leuven, p 55
11. EN ISO 13788 (2012) Hygrothermal performance of building components and building elements—internal surface temperature to avoid critical surface humidity and interstitial condensation—calculation methods
12. ISO 10211 (2007) Thermal bridges in building construction—heat flows and surface temperatures—detailed calculations
13. ISO 6781-3 (2015) Performance of buildings—detection of heat, air and moisture irregularities in buildings by infrared methods—Part 3: qualifications of equipment operators, data analysts and report writers
14. EN 13187 (2001) Thermal performance of buildings—qualitative detection of thermal irregularities in building envelopes—infrared method
15. STM 545 (2015) Sosiaali- ja terveysministeriön asetus asunnon ja muun oleskelutilan terveydellisistä olosuhteista sekä ulkopuolisten asiantuntijoiden pätevyysvaatimuksista. Helsinki
16. Kalamees T (2006) Critical values for the temperature factor to assess thermal bridges. Proc Est Acad Sci Eng 12:218–229
17. DIN 4108-2 (2013) Wärmeschutz und Energie-Einsparung in Gebäuden—Teil 2: Mindestanforderungen an den Wärmeschutz
18. SIA-180 (1999) Wärme- und Feuchteschutz im Hochbau. Schweizerische Ingenieur- und Architektenverein. Zürich
19. Ward TJ (2006) Assessing the effects of thermal bridging at junctions and around openings. BRE information paper IP 1/06. BRE Press, Garston, Glasgow, Scotland. https://www.brebookshop.com/details.jsp?id=190162
20. Wouters P, Schietecat J, Standaert P (2003) Practical guide for the hygrothermal evaluation of thermal bridges. Project document. Eurokobra
21. Ilomets S, Kuusk K, Paap L, Arumägi E, Kalamees T (2016) Impact of linear thermal bridges on thermal transmittance of renovated apartment buildings. J Civ Eng Manag. doi:10.3846/13923730.2014.976259
22. Mend'an R, Vavrovič B (2013) Renewal of envelope constructions of panel residential houses as a tool for elimination of hygienic problems of thermal bridges. Adv Mater Res 855:89–92. doi:10.4028/www.scientific.net/AMR.855.89
23. Harris JL (2000) Safe, low-distortion tape touch method for fungal slide mounts. J Clin Microbiol 38:4683–4684
24. Ilomets S, Kalamees T (2016) Indoor hygrothermal loads for the deterministic and stochastic design of the building envelope of dwellings in cold climates. J Build Phys (**in process after minor revision**)
25. Li Y (2014) System model of mould growth on building materials. XIII Conf. Durab. Build. Mater. Components, pp 231–5
26. Johansson P, Ekstrand-Tobin A, Svensson T, Bok G (2012) Laboratory study to determine the critical moisture level for mould growth on building materials. Int Biodeterior Biodegradation 73:23–32. doi:10.1016/j.ibiod.2012.05.014
27. Johansson P, Ekstrand-Tobin A, Bok G (2014) An innovative test method for evaluating the critical moisture level for mould growth on building materials. Build Environ 81:404–409. doi:10.1016/j.buildenv.2014.07.002
28. Hukka A, Viitanen H (1999) A mathematical model of mould growth on wooden material. Wood Sci Technol 33:475–485. doi:10.1007/s002260050131
29. IEA EBC Annex 41 (2008) Whole building heat, air and moisture response (MOIST-EN)
30. Ojanen T, Viitanen H, Peuhkuri R, Vinha J, Salminen K (2010) Mold growth modeling of building structures using sensitivity classes of materials. XI Int. Conf. Perform. Exter. Envel. Whole Build
31. Sedlbauer K (2002) Prediction of mould growth by hygrothermal calculation. J Build Phys 25:321–336. doi:10.1177/075424202025004093

32. Moon HJ (2005) Assessing mold risk in buildings uncertainty. Georgia Institute of Technology
33. Vereecken E, Roels S (2014) Mould risk assessment for thermal bridges: what is the impact of the mould prediction model? XIII Conf. Durab. Build. Mater. Components, pp 599–606
34. Kuusk K, Kalamees T, Link S, Ilomets S, Mikola A (2016) Case-study analysis of concrete large-panel apartment building at pre- and post low-budget energy renovation. J Civ Eng Manag. pp 1–9. doi:10.3846/13923730.2014.975741
35. Ilomets S, Kalamees T (2013) Case-study analysis on hygrothermal performance of ETICS on concrete wall after low-budget energy-renovation. Proc. XII Int. Conf. Perform. Exter. Envel. Whole Build. Florida, USA, December 1–5, 2013, ASHRAE
36. Ilomets S, Kalamees T, Agasild T, Õiger K, Raado L (2011) Durability of concrete and brick facades of apartment buildings built between 1960–90 in Estonia. 12th Int. Conf. Durab. Build. Mater. Components, vol. III, Porto, pp 1171–8

PUBLICATION III

Ilomets, S., Kuusk, K., Paap, L., Arumägi, E., Kalamees, T. Impact of linear thermal bridges on thermal transmittance of renovated apartment buildings. Journal of Civil Engineering and Management (2017) 23:1, 96−104

JOURNAL OF CIVIL ENGINEERING AND MANAGEMENT
ISSN 1392-3730/eISSN 1822-3605
2017 Volume 23(1): 96–104
https://doi.org/10.3846/13923730.2014.976259

IMPACT OF LINEAR THERMAL BRIDGES ON THERMAL TRANSMITTANCE OF RENOVATED APARTMENT BUILDINGS

Simo ILOMETS, Kalle KUUSK, Leena PAAP, Endrik ARUMÄGI, Targo KALAMEES

Faculty of Civil Engineering, Department of Structural Design, Tallinn University of Technology, Ehitajate tee 5, 19086 Tallinn, Estonia

Received 12 May 2014; accepted 16 Jul 2014

Abstract. Renovation of old apartment buildings is a topic of current research interest throughout the Eastern Europe region where similar typology is derived from the period of 1960–1990. Thermal bridges, essential components of the transmission heat loss of a building, have to be properly evaluated in the energy audit during current state-of-the-art situation as well as in the comparison of renovation solutions. Resulting from field measurements and calculations, we propose linear thermal transmittances Ψ of thermal bridges for four types of apartment buildings: prefabricated concrete large panel element, brick, wood (log), and autoclaved aerated concrete. Our results show that thermal bridges contribute 23% of the total transmission heat loss of a building envelope before renovation. After renovation thermal bridges account for only 10% if windows are repositioned into additional external thermal insulation and balconies are rebuilt as best practice. Inversely, impact of the thermal bridges might be up to 34%, depending on the wall insulation thickness. We have also found that the relative percentage of thermal bridges after renovation increases and the negative impact of the thermal bridges of certain junctions cannot be compensated with thicker wall insulation. Results obtained in this paper are useful for energy audits.

Keywords: thermal bridge, apartment building, large-panel, brick, wood, AAC, linear thermal transmittance, transmission heat loss, need for renovation.

Introduction

The thermal bridge is a part of the building envelope where the otherwise uniform thermal transmittance is locally significantly larger. The European Directive on the Energy Performance of Buildings (EPBD 2010) states that the methodology for calculating the energy performance of buildings should also take into account thermal bridges. All EU Member States plus Norway consider thermal bridges in the energy performance assessment of new buildings, but to a lesser extent in the assessment of existing buildings that undergo major renovation (Erhorn *et al.* 2010). From seven essential requirements set in the Construction Products Regulation (EU) No 305/2011 (2011), thermal bridges influence the requirements for "hygiene, health and the environment" and "energy economy and heat retention".

The share of thermal bridges in the transmission heat loss depends on the climate and construction. In warm France and Greece the influence of thermal bridges is in a range of 5–35% (Déqué *et al.* 2001; Theodosiou, Papadopoulos 2008). In cold Sweden, the impact of thermal bridges may be accounted for by the increasing heat transfer between 20% and 38% for precast concrete sandwich walls and between 12% and 26% for wooden frame walls (Berggren, Wall 2013) in terms of internal dimensions of the building envelope.

The better the insulation of the building envelope, the larger the relative contribution of thermal bridges on the overall transmission heat loss of the building and the more important it is to develop improved constructional details (Janssens *et al*. 2007). Comprehensive research about evaluating thermal bridges by a quantitative approach with a new method is introduced in Asdrubali *et al.* (2012).

There are many methods to determine linear thermal transmittance of thermal bridges: numerical calculations (typical accuracy ±5%), thermal bridge catalogues (±20%), manual calculations (±20%), and default values (0–50%) (EN ISO 13789:2008; EN ISO 14683:2008).

Linear thermal transmittance values of thermal bridges for new buildings are to be calculated by the designer or can be commonly taken from a standard EN ISO 14683:2008 (2008), database or catalogue (Tilmans, Orshoven 2009). Regression equations for thermal bridges of typical junctions are presented in Capozzoli *et al.* (2013) and Ben Larbi (2005). Thermal bridges were analysed in a guarded hot box testing facility by Martin *et al.* (2012a) who demonstrated the methodology

Corresponding author: Simo Ilomets
E-mail: *simo.ilomets@ttu.ee*

Taylor & Francis
Taylor & Francis Group

(Martin *et al.* 2012b) to calculate an equivalent wall, which has the same dynamic thermal behaviour as the thermal bridge. A pragmatic approach was used in Roels *et al.* (2011) to incorporate the effect of thermal bridging within the EPBD (2010) regulation. It is stated that thermal bridges are a crucial point in the energy analysis of the building envelope. Most of the studies are applicable to the design of new buildings rather than to energy renovation of old apartment buildings.

Renovation of an old building envelope is important because it offers a huge (60 Mtoe by 2030 for the EU28) potential for energy savings (Lechtenböhmer, Schüring 2010). To simplify design, which is anyhow undervalued and derogated concerning time and money, a simplified approach to thermal bridges would be preferable in older buildings under major renovation.

Renovation/modernisation of old apartment buildings is a topic of current interest in the whole Eastern Europe region with similar buildings. In Lithuania, as reported in Biekša *et al.* (2011), the current shape and tendencies of multi-apartment building renovation are far from completion and further improvement and recommendations are needed. Almost a decade ago, Zavadskas *et al.* (2004) developed a method with a multi-criteria approach in order to analyse renovation scenarios of old apartment buildings. Recently they have proposed a more general but still a multi-criteria approach for all construction works (Zavadskas *et al.* 2014). A relevant factor to be considered is the form of ownership in the Baltic States that differs from most of Europe – each apartment has a different owner.

Before renovation, the proper evaluation of the technical condition and energy performance of a building with possible energy savings is essential. A relevant approach is presented in Ignatavičius *et al.* (2007) in the context of case-study analysis and results. To select energy saving measures properly and to evaluate their efficiency, the consumed and calculated heat amounts "before" and "after" the renovation should be divided into components (Čiuprinskas, Martinaitis 2003). Further, linear thermal transmittance of the thermal bridges should be taken into account when calculating energy consumption of a building.

Many older apartment buildings in Eastern Europe were constructed according to a standard design with similar architectural and constructional typology, including typical thermal bridges. Therefore, for typical apartment building series, similar values of the linear thermal transmittance of thermal bridges may be used. This can help energy auditors and designers to choose a proper quantity of the thermal bridges in order to improve energy calculations. Regarding to inhabitants and owners of older apartment buildings, the cost of renovation design documentation is usually critical, "ready to use" values of linear thermal transmittances can reduce the design time, harmonise the quality and lower the cost.

This paper evaluates the impact of thermal bridges in the transmission heat loss. Different levels of building envelope insulation were analysed for apartment buildings composed with prefabricated reinforced concrete large-panel elements, bricks, wood and autoclaved aerated concrete large-blocks, mostly built during the constructional wave between 1960 and 1990. We have calculated the true impact of thermal bridges in the transmission heat loss of a building envelope before and after renovation. Numerical values of proposed linear thermal transmittances are useful for energy audits.

1. Methods

1.1. Buildings studied

Based on the main construction material, four different building types were analysed: prefabricated reinforced concrete large-panel element (hereafter: concrete element) (13 example buildings), brick (15 buildings), wood (log 20 buildings), and autoclaved aerated concrete (AAC) large-blocks (1 building). Typical buildings with different construction, service systems, ages and number of storeys were selected. External walls of concrete element buildings (Fig. 1 left) are composed of two layers of reinforced concrete (50–130 mm inner load-bearing layer and 50–80 mm outer core) and 100–150 mm thick insulation layer in between (fibrolite, mineral wool, phenolic foam or expanded polystyrene). Different elements are welded and concreted together in-situ. Thermal transmittance of walls varies between $U = 0.5–1.0$ W/(m^2·K) and that of roofs 0.7–1.0 W/(m^2·K). Thickness of the inner load-bearing layer in brick buildings (Fig. 1 right) is 250–630 mm (typically calcium silicate brick), 60–120 mm mineral wool thermal insulation, and 120 mm of external layer (calcium silicate or ceramic brick). Also, thick brick walls without insulation material were analysed. Thermal transmittance of brick walls varies between 0.5–1.2 W/(m^2·K) and that of roofs 0.7–1.0 W/(m^2·K). In general, slabs on the ground and cellar ceilings are uninsulated.

The two- and three-storeyed wooden apartment buildings studied were built in the first half of the 20th century (Fig. 2 left). The external wall is built with a horizontal or vertical load-bearing log wall with a thickness of 120–180 mm. Inserted ceilings are usually built from wooden beams, whereby cellar ceilings can be also made of concrete on steel beams. Thermal transmittance

Fig. 1. Typical prefabricated reinforced concrete large-panel element apartment building (left) and brick apartment building (right)

Fig. 2. Typical wooden apartment building (left) and autoclaved aerated concrete large-block building (right)

of solid wooden walls varies between U = 0.5–0.9 W/(m^2·K). Attics and cellars are generally unheated, and the thermal transmittance of those inserted ceilings separating heated space is ~0.5 W/(m^2·K).

Apartment buildings composed of autoclaved aerated concrete (AAC) are mainly (Fig. 2 right) composed of large-blocks that have lime or oil shale ash as a binding agent. Visually similar to some types of brick apartment buildings, these buildings generally have 2–5 storeys. Thermal transmittance of 300 mm solid walls (density ρ~800–1000 kg/m^3) varies between U = 0.6–1.1 W/(m^2·K) and that of pitched or flat roofs 1.0–1.5 W/(m^2·K).

1.2. Calculation methods

Thermal performance of typical thermal bridges was analysed with the two-dimensional (2D) steady-state finite element heat-transfer simulation program THERM 6.0 developed by the Lawrence Berkeley National Laboratory and calibrated according to the EN ISO 10211:2007 (2007) standard. The linear thermal transmittance of the thermal bridges Ψ, W/(m·K) was calculated by Eqn (1):

$$\Psi = L_{2D} - \sum_{j=1}^{N_j} U_j \cdot l_j, \text{ W/(m·K)}, \quad (1)$$

where L_{2D} is the thermal coupling coefficient obtained from the 2D calculation of the component separating the two environments being considered, W/(m·K); U_j is the thermal transmittance of the 1D component j separating the two environments being considered, W/(m^2·K); l_j is the length over which the value U_j applies, m. Length L_{2D} is equal to $\sum l_j$. Overall internal dimensions of the external envelope according to EN ISO 13789:2008 (2008) was used in the calculations.

In the calculations of linear thermal transmittance, average values of internal surface resistance from the EN ISO 6946:2007 (2007) standard were used: for roof R_{si} 0.10 m^{2}K/W, for wall R_{si} 0.13 m^{2}K/W, for floor R_{si} 0.17 m^{2}K/W. Thermal resistance R_{se} 0.04 m^{2}K/W was used for all external surfaces. Thermal conductivities of the materials used in the calculations are presented in Table 1.

Linear thermal transmittances were calculated for four different building types as original and additionally insulated building envelopes: +100 mm, +150 mm, +200 mm and +300 mm additional external thermal insulation with the thermal conductivity λ = 0.04 W/(m·K).

Table 1. Thermal conductivity λ, W/(m·K) of the materials used

Material	Thermal conductivity λ, W/(m·K)
Polyurethane foam (PU)	0.024
Additional insulation (mineral wool/ EPS)	0.040
Phenolic foam (based on phenolic resin)	0.043
Mineral wool of exist. building envelope	0.070
Rubber foam, mastics	0.10
Sawdust	0.10
Wood	0.13
Fibrolite (chip cement board)	0.16
Autoclaved aerated concrete (AAC)	0.23
Dry sand	0.25
Expanded clay concrete	0.30
Hollow calcium silicate masonry	0.70
Ceramic brick masonry	0.70
Calcium silicate brick masonry	0.90
Lime-cement mortar	1.0
Concrete	2.0

Transmission heat loss (also heat flow rate, W) of a building envelope consists of several components – thermal transmittance U, linear thermal transmittance Ψ and point thermal bridges χ. Thermal transmittance can be also presented as an overall reduced (in literature: also "effective") thermal transmittance of a wall U_{red} that consists of heat transfer through the 1D opaque wall (excluding windows) and of heat transfer through the 2D thermal bridges divided by the wall area according to Eqn (2):

$$U_{red} = \frac{H}{A} = U + \frac{\sum \Psi_j \cdot l_j + \sum \chi_j \cdot n_j}{A}, \text{ W/(m}^2\text{·K)}, \quad (2)$$

where H is a specific heat transfer, W/K; A is the area of 1D wall, m^2; U is the thermal transmittance of the 1D wall, W/(m^2·K); Ψ_j is the linear thermal transmittance of the thermal bridge, W/(m·K); l_j is the length of the thermal bridge, m; χ_j is the point thermal transmittance of the thermal bridge, W/K; n is the number of point thermal bridges. Point thermal bridges are not taken into account in this paper.

1.3. Field measurement methods

Buildings were surveyed first by assessing the technical condition and secondly by using infrared thermography. Original design drawings were collected (see Fig. 3) and inhabitants and operators interviewed. Surface temperatures were measured to enable the comparison of calculation results and to increase the reliability of the calculated linear thermal transmittances.

To determine the thermal bridges and their distribution, measurements with an infrared image camera FLIR ThermaCam E320 (thermal sensitivity of 0.1 °C, measurement range from –20 °C to +500 °C) were conducted

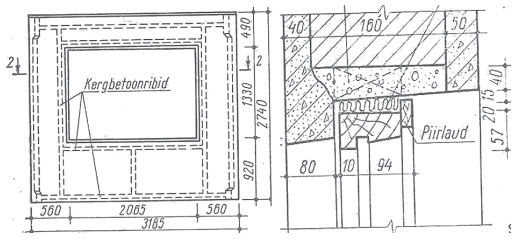

Fig. 3. Original design drawings of reinforced concrete large-panel element building – external wall element (left) and external wall/ window junction (right)

in 49 buildings. Measurements were done according to the standard EN 13187:2001 (2001) during the winter while the temperature difference between the indoor and outdoor air was at least 20 K. For the emissivity ε of the surface materials, data from the infrared literature and measurements made by FLIR Systems (2006) were used. Air pressure difference was consciously not created, but it existed to some extent due to wind and different densities of the indoor and outdoor air.

2. Results

2.1. Measurement results

Field measurements in concrete element buildings showed that the critical thermal bridges are located in:

- horizontal and vertical joints between external wall elements, see Figure 4 (top);
- junctions of the external wall and the balcony slab, see Figure 4 (top);
- junctions of the external wall (especially end sides) and the flat roof, see Figure 4 (top and bottom);

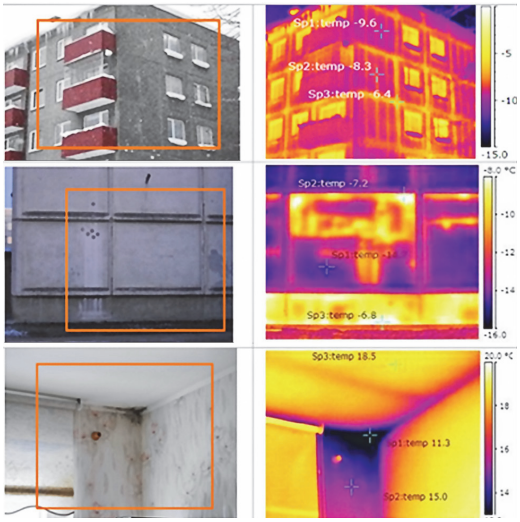

Fig. 4. Thermal bridges of a concrete element apartment building from outside (top and middle) and from inside (bottom)

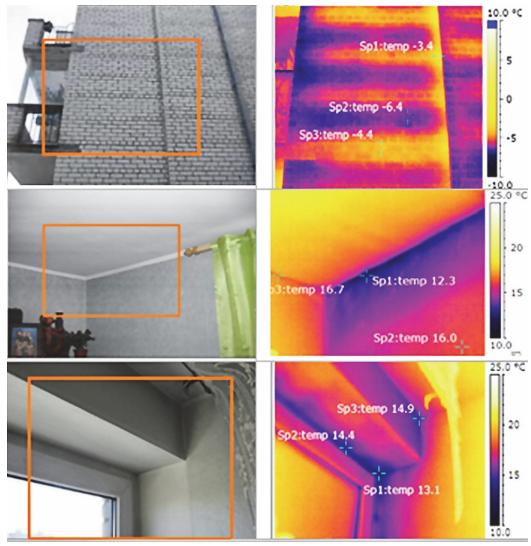

Fig. 5. Thermal bridges of a brick building from outside (top) and from inside (middle and bottom)

- bonds of element`s inner and outer layers of the external walls, see Figure 4 (top);
- foundation wall elements, see Figure 4 (middle);
- junction of the external wall and the window/door, see Figure 4 (top).

Also, wall elements with missing or poor insulation existed, see Figure 4 (middle). In the worst cases, mould growth was visually detected on the internal surface of the thermal bridges, see Figure 4 (bottom).

Field measurements in brick apartment are presented in Figure 5.

Field measurements in brick buildings showed that the thermal bridges are located in:

- junctions of the external wall and the flat or pitched roof;
- junctions of the external wall and the balcony or loggia slab and wall;
- junctions of the external wall and the window/ door, see Figure 5 (bottom);
- junction between the foundation wall elements and the external wall;
- junctions of the external wall/inserted ceiling, see Figure 5 (middle);
- bonding bricks, see Figure 5 (top).

Field measurements in the old wooden (log) apartment buildings showed that the most critical thermal bridge is located at the junction of the external wall and the cellar ceiling. This is caused by the large thermal transmittance of limestone foundation that the log wall lies on. Since leaky 2-frame windows were typically used in wooden buildings, low surface temperatures caused by air leakage rather than by the thermal bridge were determined around the windows.

Table 2. Calculated linear thermal transmittances Ψ_{oi}, W/(m·K) of various external wall junctions for different building types by using overall internal dimensions of a building envelope. Upper row is for pre-renovation situation and lower row for post-renovation situation with +200 mm thermal insulation as an example. Values are given as a range, and at substantial variation, with a third value in between as the most probable (in brackets)

Junction of external wall	Original wall/ +200 mm insulation	Calculated linear thermal transmittances Ψ, W/(m·K)			
		Concrete element building:	Brick building:	Wooden (log) building:	AAC (building):
External corner of external walls	Original/	0.50…(0.70)…1.30	0.25…0.30	0.04…0.06	0.13…0.15
	+200 mm insulation	0.12…0.18	0.13…0.17	0.04…0.06	0.09…0.11
External wall/ internal wall	Original/	0.12…(0.30)…1.10	0.00…0.03	0.00…0.02	0.00…0.02
	+200 mm insulation	0.00…0.02	0.00…0.01	0.00…0.01	0.00…0.01
External walls/ inserted ceiling	Original/	0.25…(0.50)…0.70	0.00…0.02	0.00…0.02	0.25…0.35
	+200 mm insulation	0.00…0.03	0.00…0.01	0.00…0.01	0.05…0.07
External walls/ cellar ceiling	Original/	0.25…(0.50)…0.70	0.01…0.03	0.15…0.20	0.30…0.40
	+200 mm insulation	0.04…0.06	0.00…0.02	0.04…0.08	0.05…0.07
External walls/ inserted ceiling at loggia or balcony	Original/	0.15…(0.20)…0.65	0.01…0.02	Not typical	0.30…0.35
	+200 mm insulation	0.18…(0.30)…0.65	0.10…0.15		0.27…0.33
External wall/ pitched roof	Original/	0.40…(0.55)…1.0	0.30…0.60	0.13…0.17	0.25…0.40
	+200 mm insulation	0.20…0.55	0.40…0.50	0.11…0.15	0.09…0.25
External wall/ flat roof with parapet	Original/	0.20…(0.25)…0.90	0.25…0.50	Not typical	Not typical
	+200 mm insulation	0.17…0.50	0.20…0.25		
External walls/ windows (at original position)	Original/	0.06…(0.13)…0.30	0.35…0.50	0.00…0.02	0.06…0.08
	+200 mm insulation	0.20…0.50	0.35…0.50	0.01…0.10	0.12…0.18
External walls/ windows (windows inside insulation)	Original/	0.06…(0.13)…0.30	0.35…0.50	0.00…0.02	0.06…0.08
	+200 mm insulation	0.01…0.03	0.01…0.04	0.01…0.10	0.01…0.05

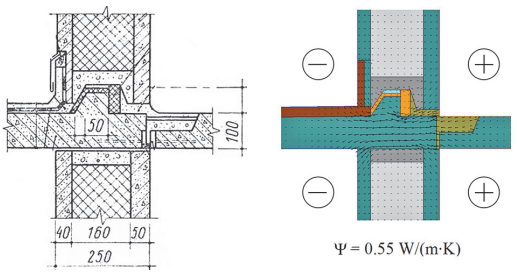

Fig. 6. Original drawing from the design documentation of the external wall/inserted ceiling at balcony junction (left) and heat flux vectors with the calculated linear thermal transmittance Ψ (right)

2.2. Calculation results

Calculation results of linear thermal transmittances for four building types with varying junctions are shown in Table 2. Calculations were based on the original drawings of the buildings and information from the field survey. Results of calculations (values of the linear thermal transmittance Ψ rounded to 0.01 if the value ≤ 0.20 and rounded to 0.05 if the value > 0.20 W/(m·K)) are presented as a range instead of an average value. This approach was chosen because of variations and uncertainty at junctions caused by the variability of thermal properties, thickness of materials, constructional technology and other reasons. A calculation example with the best possible solution of an external wall/inserted ceiling at balcony is shown in Figure 6. At a wide range of values (e.g. concrete element buildings), also the third number in between is proposed, which can be considered as the most probable. Without any information available, that value can be used in the energy audit as the first approximation. At the external wall/roof junction both or only one can be insulated.

3. Impact of thermal bridges

Impact of thermal bridges on the thermal performance of a building can be taken into account separately, but for emphasis it is considered as a part of thermal transmittance of a wall. Relative significance of the thermal bridges of a typical five-storeyed concrete element apartment building (Fig. 1 left, and more detail in Ilomets and Kalamees (2013)) before the renovation is:

$$U_{red.1} = U_{original} + \frac{\sum \Psi_j \cdot l_j}{A} =$$

$$\frac{1}{0.13 + 0.11/2 + 0.14/0.16 + 0.04} +$$

$$\frac{43 + 163 + 166 + 64/2 + 26 + 58/2 + 6/2 + 189}{1091} =$$

$$0.91 + 0.60 = 1.51 \text{ W}/\left(\text{m}^2\text{K}\right)$$

and after the renovation with +200 mm insulation (λ = 0.04 W/(mK)):

$$U_{red.2} = U_{+200mm} + \frac{\sum \Psi_j \cdot l_j}{A} =$$

$$\frac{1}{0.13 + 0.11/2 + 0.14/0.16 + 0.2/0.04 + 0.04} +$$

$$\frac{7 + 6 + 6 + 4/2 + 46 + 22/2 + 4/2 + 442}{1091} =$$

$$0.16 + 0.48 = 0.64 \text{W}/\left(\text{m}^2\text{K}\right).$$

The results obtained – 1.51 W/(m^{2}K) before and 0.64 W/(m^{2}K) after renovation indicate that thermal transmittance of a **wall** increases about 66% before and approximately three times after renovation derived from thermal bridges. Thus, the relative significance of thermal bridges in the transmission heat loss increases with an improved level of insulation. It must be noted here that only half of the linear thermal transmittance Ψ was taken into account at the external wall/roof and the external wall/cellar ceiling junctions because the other half is the thermal transmittance related to the roof or the cellar ceiling, respectively. Results of $\Psi_j \cdot l_j$ in calculation of U_{red} given above the line follow the order of junctions as presented in Table 2. Quantity 442 W/K after renovation originates from external wall/window (and door) junction and it forms 85% of the transmission heat loss through all thermal bridges.

Figure 7 shows the impact of thermal bridges depending on the insulation thickness where the percentage of thermal bridges in the transmission heat loss of the **building envelope** is presented.

In typical bad practice renovation (Fig. 8, left) insufficient attention is paid to thermal bridges – windows are left to original position and concrete balcony slabs are not insulated during renovation (hereafter: bad practice). With best practice, windows are repositioned into additional thermal insulation (Fig. 8, right) and old concrete balcony slabs have been demolished and rebuilt (hereafter: best practice). In case of bad practice approach, percentage of thermal bridges in transmission heat loss increases with the level of additional insulation (Fig. 7), reaching up to 34% with typical insulation thickness +200 mm.

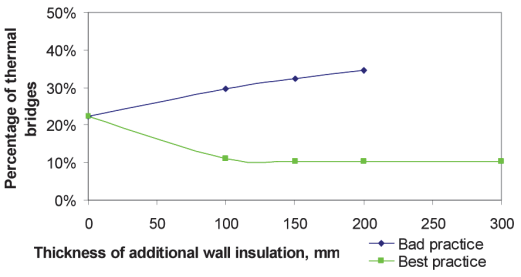

Fig. 7. Percentage of thermal bridges in transmission heat loss (through the whole building thermal envelope including thermal bridges)

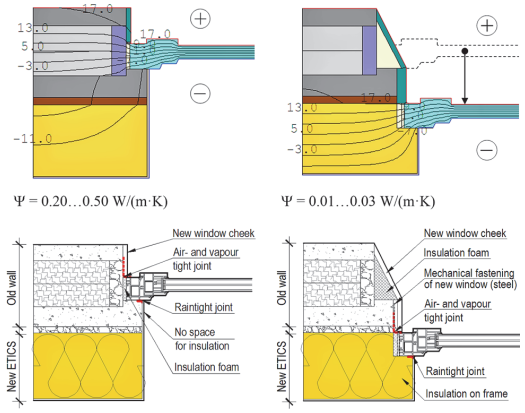

Fig. 8. Examples of bad practice (left) and best practice – windows are repositioned into additional insulation (right). Isotherms in both cases are presented in upper row and designed principal renovation solution in bottom row

We also analysed the effect of thicker additional insulation of a wall required to compensate the impact of thermal bridges. In other words, how much extra wall insulation is needed to achieve equal linear thermal transmittance of the thermal bridges. In buildings renovated under bad practice, the external wall/window (numerous window perimeter length) and external wall/balcony junction have the largest impact on the thermal bridges. Theoretical thickness of additional wall insulation needed to compensate linear thermal transmittance of thermal bridges ends up at infinity at bad practice renovation if it is impossible to insulate the window jamb (also named window cheek), as was found in the analysis of our renovation case study (Ilomets, Kalamees 2013), see also Figure 8, bottom left. During best practice renovation where windows are repositioned and balconies rebuilt, additional insulation has to be 390 mm instead of 200 mm in order to compensate high thermal transmittance of thermal bridges.

4. Discussion

In this study we have evaluated the share of thermal bridges in the transmission heat loss of old apartment buildings based on Estonian example. As similar solutions were widely used in many parts of Eastern Europe and former Soviet Union with only few local changes made, results are useful also in other countries. Still, before using the values presented in this study, similarities and differences due to local typology, materials and workmanship practice related to junctions must be considered.

Both measurements and calculations show that the problem with thermal bridges is extremely serious especially for concrete element but also for brick buildings since constructional thermal bridges were already designed in original solutions. Most of the thermal bridges can be minimised by applying additional external ther-

mal insulation and paying special attention to the external wall/window and the external wall/balcony junctions. As compared to concrete element buildings, the situation in brick buildings is somewhat better and in wooden and ACC buildings substantially better since there are fewer constructional joints (no in-situ concrete casting). Also, insulation is continuous at the external wall/internal wall and the external wall/inserted ceiling junctions in brick buildings.

Results of wooden apartment buildings indicate that the critical thermal bridge exists at the external wall/foundation wall junction. Under renovation, the foundation wall should be additionally insulated from outside. Also, new windows with a similar width of a jamb should be carefully designed and installed with additional insulation during renovation.

In AAC buildings also critical thermal bridges exist, but the problem is somewhat less serious compared to concrete and brick buildings, mainly because of smaller thermal conductivity of the AAC blocks. Often in older apartment buildings, thermal bridge is a combination of a geometrical and a constructional thermal bridge.

Two main factors have worsened the situation related to thermal bridges during the last decade. First, inhabitants have replaced their windows, but usually a narrow 70 mm jamb is installed instead of an old wooden window with a wide jamb (ca 130 mm in wooden buildings and ca 95 mm in all other building types). Secondly, installation of additional external insulation with windows left at their original position has increased the linear thermal transmittance at the external wall/window junction. It must be emphasised that in addition to increased relative share of thermal bridges, also absolute value of linear thermal transmittance at external wall/window junction is increased after applying additional insulation.

Although the total thermal performance of a building during renovation is improved, we found that the relative percentage of thermal bridges increases with the thickness of insulation. From 23% for a current state-of-the-art building, we reached up to 34% with +200 mm additional insulation during bad practice renovation as windows are the major source of the transmission heat loss. Large impact of thermal bridges can be emphasised by the ratio of linear thermal transmittances of the thermal bridges and the thermal transmittance of the walls, which results in a rate of 3. This means that the heat flow rate from the heated space through the thermal bridges is three times larger than the heat flow rate of the opaque wall. The share of thermal bridges would have been even higher with a thicker layer of insulation, but insulation >200 mm is not typical as windows kept to original position as bad practice. The same tendency (percentage of thermal bridges in the transmission heat loss is growing with the level of insulation) has been found in Berggren and Wall (2013). Our share of 34% is in good correlation with 30–35% reported in Theodosiou and Papadopoulos (2008) and Erhorn *et al.* (2010). Also, Berggren and Wall (2013) found the impact between 20–38% for concrete element buildings – the same building type as used in our analysis. In addition, Kauppinen *et al.* (1997) found that thermal transmittance is valid only for 50% due to thermal bridges considering the heat loss of the whole building envelope and Al-Sanea and Zedan (2012) and Desjarlais and McGowan (1997) similarly claim that thermal resistance can be reduced twice by using internal dimensions of a building envelope.

The share of thermal bridges in the transmission heat loss of the building envelope after renovation depends strongly on the insulation on the window jamb under bad practice. This is caused by the large perimeter of the external wall/window junction. If the windows remain in their original position, the original linear thermal transmittance (up to Ψ = 0.30 W/(m·K)) will increase (up to Ψ = 0.50 W/(m·K)) because of the insulation applied. Thermal performance of the external wall/window junction has been studied in Cappalletti *et al.* (2011) who reported a similar result – linear thermal transmittance up to Ψ = 0.40 W/(m·K) depending on the position of a window. Our renovation case-study analysis (Ilomets, Kalamees 2013) has shown that in practice it is impossible to sufficiently insulate a window jamb due to limited space (ca 10 mm) for insulation. Unacceptably poor thermal performance of windows and balconies can be concluded by comparing the values of linear thermal transmittances presented in Table 2 and the results of Janssens *et al.* (2007). Limit value Ψ = 0.10 W/(m·K) is proposed to represent a sufficient level of linear thermal transmittance of junctions which is also supported by the default value in EN ISO 14683:2008 (2008). Since external dimensions of a building envelope were used in the referred sources, comparison is valid only for non-geometrical thermal bridges as junctions of the window and the balcony.

An impact as small as 10% (Fig. 6) is achieved only by installing windows in a new position inside the additional insulation and removing existing concrete slab balconies. Since total transmission heat loss after renovation is already small, 10% of it means very small absolute quantity. Therefore, this solution can be suggested for sustainable complete best practice renovation and the share of 10% tends not to change with the thickness of insulation. In addition to the window junction, also the remaining external wall/balcony slab without thermal insulation can have a significant impact. Our study has found that the transmission heat loss of the building envelope rises by 5–9% when considering only the impact of old balconies. This is close to the result of 9–18% found by Ge *et al.* (2013).

Since the relative impact of thermal bridges enlarges with insulation thickness, focus during renovation should be on the minimisation of thermal bridges rather than on using thicker insulation to achieve the target, e.g. low-energy level in cold climate. Minimising the effect of thermal bridges at the junctions of the building envelope in existing buildings is a major challenge and therefore careful design is essential.

In addition to improved thermal performance, additional external thermal insulation improves thermal indoor environment and decreases the risk for mould growth in the corners because of higher surface temperature. New external insulation also protects the building envelope against climate loads and improves aesthetics.

Conclusions

Linear thermal bridges in the transmission heat loss were evaluated in four apartment building types – prefabricated reinforced concrete large-panel elements, bricks, wood (log), and autoclaved aerated concrete large-blocks. Range and typical values of the linear thermal transmittance of the thermal bridge (by using overall internal dimensions of a building envelope) was calculated for various junctions of four building types by using the 2D heat transfer simulation tool. Results are useful for many countries in Eastern Europe with similar non-renovated housing stock that are facing problems related to today's energy performance requirements.

Based on the thermography field measurements and calculations, we found that notable thermal bridges from the thermal performance aspect exist in all building types. The situation is the worst for concrete element buildings, where the linear thermal transmittance of the thermal bridge might be up to Ψ = 1.30 W/(m·K) as maximum and Ψ = 0.70 W/(m·K) as the most probable value to be used in the energy audit. Overlooking the external wall/ window and the external wall/balcony junctions as typical bad practice renovation, share of thermal bridges in the transmission heat loss of a building envelope is 30–34%, depending on the thickness of additional insulation. Large linear thermal transmittance of the thermal bridges in certain junctions cannot be compensated with thicker insulation of the building envelope. As another extreme, share of thermal bridges in transmission heat loss might be only 10% in best practice.

In conclusion, windows have to be replaced (and repositioned into additional thermal insulation) and balconies should be rebuilt or insulated from top and bottom in order to fulfil energy performance requirements and to achieve, e.g. low-energy level. Linear thermal transmittance of the thermal bridges must be properly taken into account while conducting the energy audit or comparing the scenarios before the renovation.

Acknowledgements

This research was supported by the EU through the European Regional Development Fund. The research has been conducted as a result of the IUT1−15 project "Nearly-zero energy solutions and their implementation on deep renovation of buildings" (financed by the Estonian Research Council) and "Reducing the environmental impact of buildings through improvements of energy performance" (3.2.0801.11-0035, financed by SA Archimedes).

References

Al-Sanea, S. A.; Zedan, M. F. 2012. Effect of thermal bridges on transmission loads and thermal resistance of building walls under dynamic conditions, *Applied Energy* 98: 584–593. http://dx.doi.org/10.1016/j.apenergy.2012.04.038

Asdrubali, F.; Baldinelli, G.; Bianchi, F. 2012. A quantitative methodology to evaluate thermal bridges in buildings, *Applied Energy* 97: 365–373. http://dx.doi.org/10.1016/j.apenergy.2011.12.054

Ben Larbi, A. 2005. Statistical modelling of heat transfer for thermal bridges of buildings, *Energy and Buildings* 37(9): 945–951. http://dx.doi.org/10.1016/j.enbuild.2004.12.013

Berggren, B.; Wall, M. 2013. Calculation of thermal bridges in (Nordic) building envelopes – risk of performance failure due to inconsistent use of methodology, *Energy and Buildings* 65: 331–339. http://dx.doi.org/10.1016/j.enbuild.2013.06.021

Biekša, D.; Šiupšinskas, G.; Martinaitis, V.; Jaraminienė, E. 2011. Energy efficiency challenges in multi-apartment building renovation in Lithuania, *Journal of Civil Engineering and Management* 17(4): 467–475. http://dx.doi.org/10.3846/13923730.2011.622408

Cappalletti, A.; Gasparella, A.; Romagnoni, P.; Baggio, P. 2011. Analysis of the influence of installation thermal bridges on windows performance: the case of clay block wall, *Energy and Buildings* 43(6): 1435–1442. http://dx.doi.org/10.1016/j.enbuild.2011.02.004

Capozzoli, A.; Gorrino, A.; Corrado, V. 2013. A building thermal bridges sensitivity analysis, *Applied Energy* 107: 229–243. http://dx.doi.org/10.1016/j.apenergy.2013.02.045

Čiuprinskas, K.; Martinaitis, V. 2003. Correction of a designed building's heat balance according to its real heat consumption, *Journal of Civil Engineering and Management* 9(2): 98–103. http://dx.doi.org/10.1080/13923730.2003.10531311

Construction Products Regulation (EU) No 305/2011 of the European Parliament and of the Council repealing Council Directive 89/106/EEC [online], [cited 05 May 2014]. Available from Internet: http://eur-lex.europa.eu/legal-content/EN/TXT/?uri=CELEX:32011R0305

Desjarlais, A.; McGowan, A. 1997. Comparison of experimental and analytical methods to evaluate thermal bridges in wall systems, in *3rd ASTM Symposium on Insulation Materials: Testing and Applications*, 15–17 May 1997, Quebec, Canada. Report No CONF-970582–2.

Déqué, F.; Ollivier, F.; Roux, J. J. 2001. Effect of 2D modelling of thermal bridges on the energy performance of buildings: numerical application on the Matisse apartment, *Energy and Buildings* 33(6): 583–587. http://dx.doi.org/10.1016/S0378-7788(00)00128-6

EN ISO 10211:2007 Thermal bridges in building construction – Heat flows and surface temperatures – Detailed calculations. European Committee for Standardization (CEN). Geneva, 2007. 45 p.

EN 13187:2001 Thermal performance of buildings – Qualitative detection of thermal irregularities in building envelopes – Infrared method. European Committee for Standardization (CEN). Geneva, 2001. 16 p.

EN ISO 13789:2008 Thermal performance of buildings – Transmission and ventilation heat transfer coefficients – Calculation method. European Committee for Standardization (CEN). Geneva, 2008. 18 p.

EN ISO 14683:2008 Thermal bridges in building construction – linear thermal transmittance – simplified methods and default values. European Committee for Standardization (CEN). Geneva, 2008. 23 p.

EN ISO 6946:2007 Building components and building elements – Thermal resistance and thermal transmittance – Calculation method. European Committee for Standardization (CEN). Geneva, 2007. 28 p.

EPBD Directive 2010/31/EU of the European Parliament and of the Council of 19 May 2010 on the energy performance of buildings, *Official Journal of the European Union*, 2010, L153/13–L153/35.

Erhorn, H.; Erhorn-Kluttig, H.; Citterio, M.; Cocco, M.; Orshoven, D.; Tilmans, A. 2010. *An effective handling of thermal bridges in the EPBD context (ASIEPI report) 2010:69* [online], [cited 05 May 2014]. Available from Internet: http://www.buildup.eu/publications/8832

FLIR Systems 2006. *FLIR ThermaCam E320 user's manual*. Publ. No 1558407. 170 p.

Ge, H.; McClung, V. R.; Zhang, S. 2013. Impact of balcony thermal bridges on the overall thermal performance of multi-unit residential buildings: a case study, *Energy and Buildings* 60: 163–173. http://dx.doi.org/10.1016/j.enbuild.2013.01.004

Ignatavičius, Č.; Zavadskas, E.; Ustinovičius, L. 2007. Modernization of large-panel houses in Vilnius, in *Proc. of the 9th International Conference of Modern Building Materials, Structures and Techniques*, 16–18 May 2007, Vilnius, Lithuania, 258–264.

Ilomets, S.; Kalamees, T. 2013. Case-study analysis on hygrothermal performance of ETICS on concrete wall after low-budget energy-renovation, in *Proceedings of XII International Conference on Performance of Exterior Envelopes of Whole Buildings*, 2013, Florida, USA. ASHRAE. 14 p.

Janssens, A.; van Londersele, E.; Vandermarcke, B.; Roels, S.; Standaert, P.; Wouters, P. 2007. Development of limits for the linear thermal transmittance of thermal bridges in buildings, in *Proceedings of Thermal Performance of the Exterior Envelopes of Whole Buildings X*, 2007, Atlanta, GA, USA. American Society of Heating, Refrigerating and Air-Conditioning Engineers. 10 p.

Kauppinen, T.; Hyratt, J.; Sasi, L. 1997. Thermal performance of prefabricated multistory house in Tallinn, Estonia, based on IR survey, in *Proceedings of Thermosense XIX*, 4 April 1997, Orlando, USA. 12 p.

Lechtenböhmer, S.; Schüring, A. 2010. The potential for large-scale savings from insulating residential buildings in the EU, *Energy Efficiency* 4(2): 257–270. http://dx.doi.org/10.1007/s12053-010-9090-6

Martin, K.; Campos-Celador, A.; Escudero, C.; Gomez, I.; Sala, J. M. 2012a. Analysis of a thermal bridge in a guarded hot box testing facility, *Energy and Buildings* 50: 139–149. http://dx.doi.org/10.1016/j.enbuild.2012.03.028

Martin, K.; Escudero, C.; Erkoreka, A.; Flores, I.; Sala, J. M. 2012b. Equivalent wall method for dynamic characterisation of thermal bridges, *Energy and Buildings* 55: 704–707. http://dx.doi.org/10.1016/j.enbuild.2012.08.024

Roels, S.; Deurinck, M.; Delghust, M.; Janssens, A.; van Orshoven, D. 2011. A pragmatic approach to incorporate the effect of thermal bridging within the EPBD-regulation, in *Proceedings of 9th Nordic Symposium on Building Physics (NSB 2011)*, 2011, Tampere, Finland, 1009–116.

Tilmans, A.; Orshoven, D. 2009. *Software and atlases for evaluating thermal bridge*. ASIEPI project 2009:10 [online], [cited 05 May 2014]. Available from Internet: http://www.buildup.eu/publications/5657

Theodosiou, T. G.; Papadopoulos, A. M. 2008. The impact of thermal bridges on the energy demand of buildings with double brick wall constructions, *Energy and Buildings* 40(11): 2083–2089. http://dx.doi.org/10.1016/j.enbuild.2008.06.006

Zavadskas, E. K.; Kaklauskas, A.; Gulbinas, A. 2004. Multiple criteria decision support web-based system for building refurbishment, *Journal of Civil Engineering and Management* 10(1): 77–85. http://dx.doi.org/10.1080/13923730.2004.9636289

Zavadskas, E. K.; Vilutienė, T.; Turskis, Z.; Šaparauskas, J. 2014. Multi-criteria analysis of projects' performance in construction, *Archives of Civil and Mechanical Engineering* 14(1): 114–121. http://dx.doi.org/10.1016/j.acme.2013.07.006

Simo ILOMETS. He is a researcher/teaching assistant in Chair of Building Physics and Energy Efficiency in Tallinn University of Technology. His research fields are building physics, durability and renovation of buildings. He has MSc in civil engineering. Currently his is a PhD candidate with a topic "The need for renovation of the building envelope of concrete apartment buildings".

Kalle KUUSK. He is a researcher in Chair of Building Physics and Energy Efficiency in Tallinn University of Technology. His research fields are building's service systems, indoor climate and energy performance of buildings. Currently his is a PhD candidate with a topic "Renovation of apartment buildings toward nearly zero energy buildings".

Leena PAAP. She is an engineer in Chair of Building Physics and Energy Efficiency in Tallinn University of Technology. Her research fields are building physics and renovation of buildings. She has MSc in civil engineering.

Endrik ARUMÄGI. He is a researcher in Chair of Building Physics and Energy Efficiency in Tallinn University of Technology. His research fields are indoor climate, hygrothermal and energy performance of historical buildings. Currently his is a PhD candidate with a topic "Sustainable renovation of historical buildings to provide better hygrothermal performance, energy efficiency and indoor climate".

Targo KALAMEES. He is the professor of Building Physics and head of Chair of Building Physics and Energy Efficiency in Tallinn University of Technology. His research fields are hygrothermal behaviour of buildings structures (computer simulations, laboratory experiments, field studies); boundary conditions for hygrothermal simulations and experiments; indoor climate and indoor air quality of residential-, office-, and heritage buildings; building's energy consumption and healthy building design; renovation of buildings.

PUBLICATION IV

Ilomets, S., Kalamees, T. Case-study analysis on hygrothermal performance of ETICS on concrete wall after low-budget energy renovation. In: Proceedings of XII International Conference on Performance of Exterior Envelopes of Whole Buildings, Florida, USA, 01−05.12.2013, ASHRAE

Case-Study Analysis on Hygrothermal Performance of ETICS on Concrete Wall after Low-Budget Energy Renovation

Simo Ilomets **Targo Kalamees, PhD**

ABSTRACT

Hygrothermal performance of mineral wool and expanded polystyrene external thermal insulation composite system (ETICS/EIFS) was studied in field conditions and by computer simulations with the Delphin program. Temperature and relative humidity were measured in a additionally insulated large panel concrete element wall from September 2011 to January 2013 in the cold climate of Estonia. Measurements of indoor climate, air leakage, and thermal bridges through building fabric were conducted before and after the low-budget energy renovation pilot project of an apartment building.

Results showed that indoor climate and thermal comfort were not improved a lot in all aspects and the same was true for airtightness. Unacceptable thermal bridges remained at external wall/balcony, external wall/foundation wall junction, and also around the windows because they stayed in their original position. Built-in moisture of the whole wall dried out during the first heating season. Better agreement was found between measured and results if the convective moisture flow in addition to diffusion was taken into account in simulations. Average measured thermal transmittance during the winter was U_{wall} *0.17 W/(m²·K) in the case of graphite enhanced EPS and 0.19 W/(m²·K) with mineral wool. Long-term durability of ETICS in cold climate and under wind driven rain loads need further investigation.*

INTRODUCTION

It is estimated that there are 200 million dwellings and 25 billion m^2 of useful floor space in the EU27, Switzerland, and Norway (Dol and Haffner 2010; Economidou et al. 2011). In Europe, especially in Eastern Europe, a large number of buildings were constructed after the second World War. About 70% of the residential building stock is over 30 years old and about 35% are more than 50 years old (Balaras 2005). A general characteristic of dwellings in Eastern Europe constructed after the second World War and before the energy crisis in the 1970s is that buildings are generally poorly insulated compared to today's requirements for energy performance. Apartment buildings constructed in the late 1970s and 1980s typically have a much higher energy consumption. The energy-renovation measures of old apartment buildings are under discussion internationally (Hagentoft 2010; Silva et al. 2013; Nemry et al. 2010; Dall'O' et al. 2012; Uihlein and Eder 2010) as well as in Estonia (Kalamees et al. 2009).

In Estonia 65% of people live in apartment buildings. Nearly half of the apartment buildings constructed between 1961 and 1990 are composed of large panel prefabricated concrete elements. The condition of concrete façades is mainly satisfactory, except the low frost resistance and corrosion of reinforcement when the carbonation depth has reached close to reinforcement; steel connections of balconies and awnings have turned out to be problematic in some cases (Kalamees et al. 2009; Ilomets et al. 2011). In combination with the high indoor humidity load and thermal bridges, mould can grow at internal surfaces building envelope. Thermal transmittance of original external walls is 0.7–1.0 W/(m²·K), being 3–5 times higher than considered reasonable today. Therefore, energy-renovation and better understanding of renovation solutions of apartment building is needed.

Simo Ilomets *is a PhD student and chair of Building Physics & Energy Efficiency, Tallinn University of Technology, Tallinn, Estonia.* ***Targo Kalamees*** *is a professor and chair of Building Physics & Energy Efficiency, Tallinn University of Technology.*

The aim of the study was to explore hygrothermal performance of the existing concrete wall insulated with ETICS and to get data for calibrating a hygrothermal computer model for ETICS to permit applying the model to other climatic conditions and other structural dimensions. Other outcomes from energy-renovation pilot project are discussed briefly.

METHODS

An energy-renovation pilot project "Healthy and Cost-Saving Home" was started in spring 2010 in co-operation with two financing institutions together with a ministry, an energy company, a local municipality, and a university. The global purpose was to carry out an example renovation of a typical apartment building to demonstrate energy saving and improve indoor climate as well to motivate people to renovate their buildings. The renovation works lasted from summer to the end of 2011.

The case-study building is a five-story block of flats (Figure 1) constructed during 1966 with prefabricated large panel concrete elements. That type of construction was typical in Estonia during the period between 1961–90. Approximately half of apartment buildings in Estonia are composed of prefabricated concrete large panel elements.

Renovation Solution

Renovation solution was selected based on the energy and economical calculations:

- Improvement of building envelope:
  - External walls: +15 cm graphite enhanced expanded polystyrene (EPS) in the external thermal insulation composite system (ETICS): $U_{\text{external walls}} = 0.17$ W/(m^2·K);
  - Basement walls: +10 cm EPS covered with drained and ventilated cladding: $U_{\text{basementwall}} = 0.36$ W/(m^2·K);
  - Roof: +30 cm EPS above the roof $U_{\text{roof}} = 0.11$ W/(m^2·K);
  - Replacing of 33% of the old windows: $U_{\text{old window}} = 1.8$ W/(m^2·K), $U_{\text{new window}} = 1.0$ W/(m^2·K); because only 1/3 of the windows were replaced with new; all windows were left at their original position: inboard of the exterior concrete core of the external wall;
- Ventilation system: new exhaust ventilation with heat recovery (exhaust air [water to water] heat pump);
- Heating system: new hydronic radiator heating with thermostats.

Measurements

Measurements on the case-study building concentrated on the indoor climate, energy performance, and hygrothermal performance of the building envelope. During the study the following measurements were taken:

- The values of indoor temperature (t) and relative humidity (RH) conditions were measured with small data loggers at 1 h intervals over a 2 year period;
- Surface temperature of thermal bridges were measured by using infrared image camera "FLIR ThermaCam E320" (EN 13187) with minimum indoor and outdoor temperature difference at least 20 K. Tabulated surface emissivities from FLIR ThermaCam E320 user's manual was used;
- The air leakages of the building fabric of the apartment were measured with the standardized fan pressurization method (EN 13829), using "Minneapolis Blower Door Model 4" equipment; hygrothermal performance of east facing external wall (see Figure 1 and Figure 2), additionally insulated with ETICS, was studied using temperature and relative humidity sensors and heat flux plates.

Figure 1 *View to the external wall with measurement areas of ETICS.*

Hygrothermal performance of face sealed, non-drainable external thermal insulation composite system (ETICS) (also called exterior insulation and finish systems, EIFS) with two different insulation materials was compared in two test-walls: mineral wool (MW) and graphite enhanced expanded polystyrene (EPS), see Figure 1 and Figure 2. All the other components (adhesive, base coat, reinforcement [glass fiber mesh], mineral finishing coat, paint coating) of two test-walls were the same. Test-walls were located exterior to the same room so that both test-walls experienced the same climatic conditions. Two walls were separated from each other with polyurethane (PU) foam insulation to minimize wall-direction moisture movement. The location of the test-walls at the upper corner of the wall was selected based on it having the highest driving rain intensity.

Simulations

The temperature and humidity measurement results from test-walls were compared with a hygrothermal simulation model Delphin 5.7.4 (Nicolai 2008):

- to validate the simulation model for future simulations with different initial and climatic conditions as well as with different dimensions of the building envelope;
- to understand better the performance of the external thermal insulation composite system.

Modified material properties were used from the Delphin's database. Table 1 shows the properties of materials used as compared to measured and simulated results when the best correlation was obtained. The dependency of hygrother-

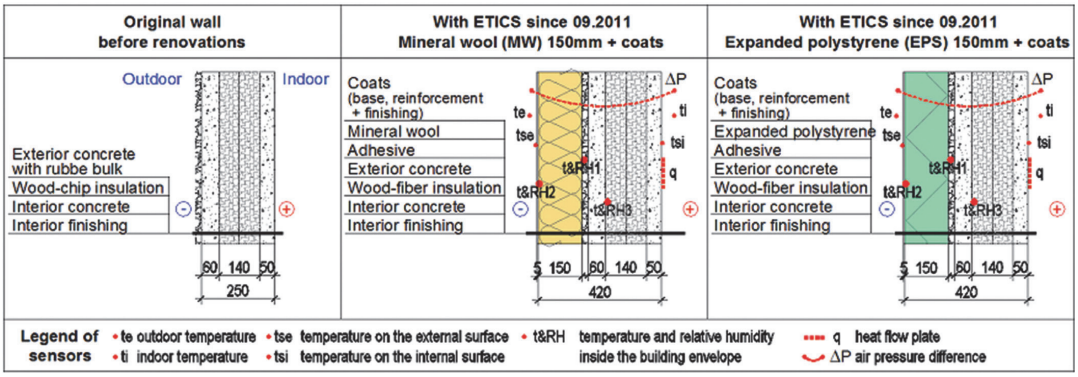

Figure 2 *Test-wall schematics and measurement points (red dots).*

Table 1. Main Hygrothermal Properties of Materials Used in the Simulation

	Concrete	Wood-Cement Chip Board	Adhesive Mortar	EPS	MW	Exterior Coating
Bulk density ρ , kg/m^3	2320	500	700	35	75	1270
Porosity *f*, m^3/m^3	0.14	0.93	0.73	0.94	0.92	0.50
Specific heat capacity *c*, J/(kg·K)	850	1470	945	1500	840	960
Thermal conductivity* λ, W/(m·K)	1.5	0.12	0.19	0.035	0.038	1.0
Water vapour diffusion resistance factor* μ, —	19	3.8	15	15	2	10
Liquid water conductivity* *k*, kg/(m·s·Pa)	$44\cdot10^{-12}$	$16\cdot10^{-9}$	$3.2\cdot10^{-9}$	0	0	$0.27\cdot10^{-6}$
Air permeability Kg, s	$1\cdot10^{-6}$	$7\cdot10^{-3}$	$1\cdot10^{-5}$	$1\cdot10^{-6}$	$1\cdot10^{-2}$	$1\cdot10^{-6}$
Built-in moisture *w*, kg/m^3 / rh, %	48 / 65	27 / 60	200 / 100	0.6 / 60	3.1 / 60	300

*Dry material

mal properties on the environmental conditions was taken into account: water vapour permeability, liquid water conductivity, thermal conductivity dependent on water content of a material (example of concrete is shown in Figure 3 [left]). Cross-section of simulated wall is presented in Figure 3 (right).

Thermal bridges before and after the renovation were evaluated by using a thermal camera and two-dimensional heat-transfer simulation software THERM 6.3 according to standard EN ISO 10211. Thermal bridges were assessed using the temperature factor (EVS-EN ISO 13788). The limit value for temperature factor in a dwelling with high or unknown humidity loads is considered to be ≥0.8 (Kalamees 2006).

RESULTS

Technical Condition of External Walls

External walls of the analysed building were composed of large-panel prefabricated concrete elements. Fourteen centimeters of wood-cement chip board (thermal conductivity λ ~0.12 W/[m·K]) was used for insulation between two layers of concrete and external surface is covered with rubble bulk. The main problems related to external walls are thermal bridges, corrosion of reinforcement, frost resistance, and large thermal transmittance. The layer between insulation and external concrete core is not ventilated but slightly drained (small tubes installed into the intersection of movement joints). The external core can become wet due to vapour condensation and wind-driven rain. This means that frost damages of concrete and corrosion of reinforcement can occur. Structures and technical condition of a building are shown in Figure 4–6.

Indoor Climate Conditions

Temperature and relative humidity were measured in four apartments before and after the renovation. There was significant difference ($P < 0.001$) in temperature measurement results, see Figure 7 left. A new adjusted heating system has even temperatures during a whole heating season after the renovation while there was a clear overheating before. There was no significant ($P = 0.3$) difference in RH before and after the renovation. Moisture excess (the difference between vapour content of the indoor and outdoor air), Δ v, g/m^3 was calculated from indoor and outdoor climate, Figure 7 (right). Somewhat surprisingly, moisture excess was not lower but even higher (significant difference [$P < 0.001$]) after the renovation, especially during very cold days with outdoor air temperature lower than –10°C. Still, the level of moisture excess being up to ~3 g/m^3 on average and up to ~4 g/m^3 at 90% level are lower than in these types of buildings in general.

Thermal Bridges

Thermographic measurements before the renovation (see Figure 8) show very low surface temperatures (temperature factors f_{Rsi} ~0.6–0.7) that cannot be accepted in the cold climate of Estonia. In addition to lower average value of the temperature factor, the range of measurement results is wider before the renovation. After renovation and installation of additional thermal insulation, all thermal bridges were decreased. Thermal bridges that ended up being lower than the limit value of 0.8 after the renovation were at the external wall/window, external wall/balcony, and external wall/foundation wall junction.

Because before the renovation already 2/3 of windows were replaced, it was decided to change only remaining 1/3 windows. Therefore all windows were left at their original position (see Figure 9 left). That solution is comfortable from the point of view of inhabitant living conditions during the renovation (less work inside the apartment), but it is unreasonable in terms of energy efficiency, hygrothermal performance, and esthetics since serious thermal bridges remain at the junction of window/external wall.

If windows remain at their original position, linear thermal transmittance of external wall/window increases, see Figure 9. For that reason, this junction remains a domi-

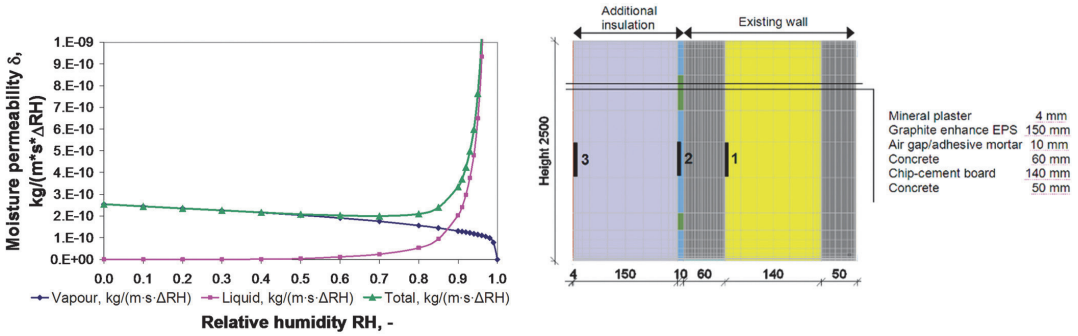

Figure 3 *Moisture permeability of concrete as liquid and vapour at different RHs (left). Example of wall section in simulation tool Delphin with measurement points of temperature and RH 1, 2, 3 (right).*

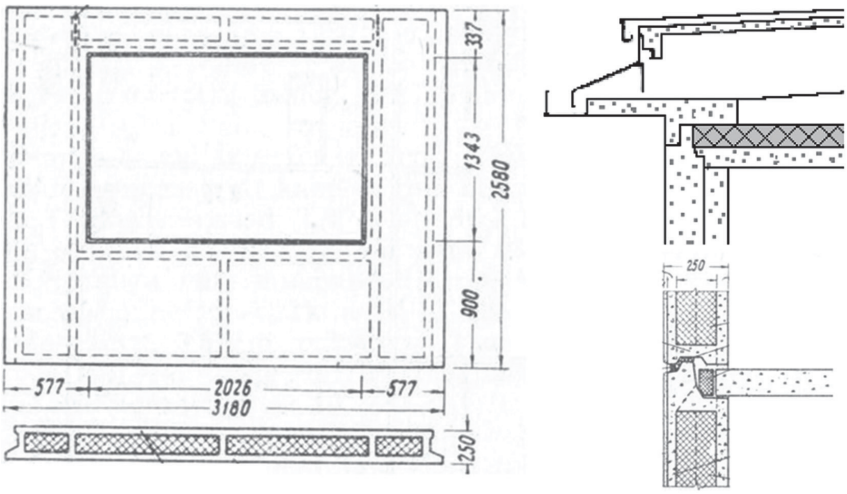

Figure 4 *Original design drawing of a large panel prefabricated concrete element (left). External wall/roof junction (right top) and external wall/inserted ceiling (right bottom).*

Figure 5 *Reinforcement steel between layers of concrete has started to corrode (left and middle). In principle, this steel should be cast into expanded clay concrete, but in reality it is often not so. Cross-section of a concrete wall element (right).*

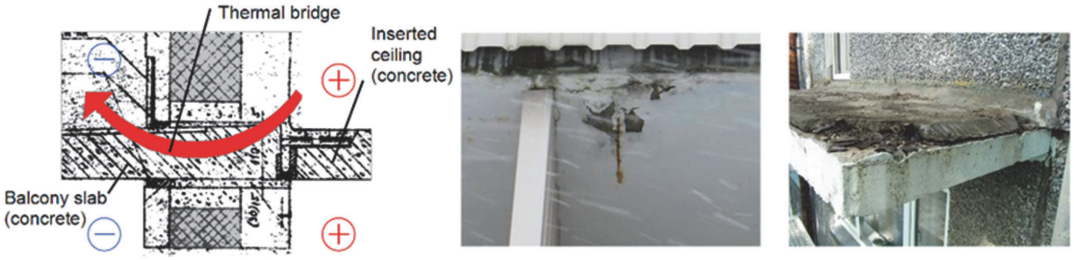

Figure 6 *Original drawing of an external wall/console balcony junction with a thermal bridge (left) and a picture of a degrading balcony (middle and right).*

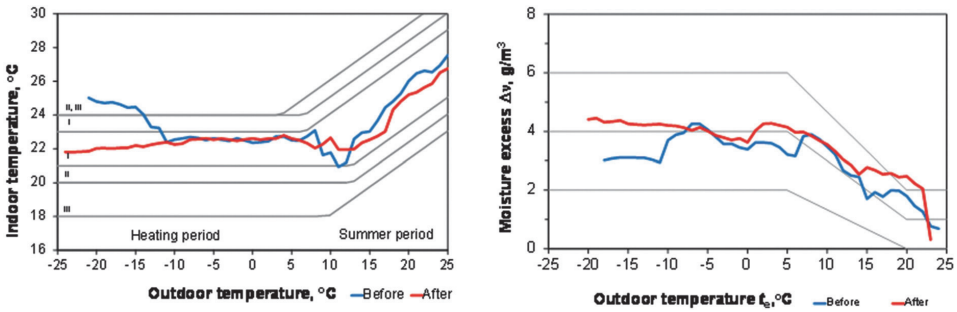

Figure 7 *Measurement results of indoor air temperature (left) and moisture excess (right) depending on the outdoor air's temperature before and after the renovation.*

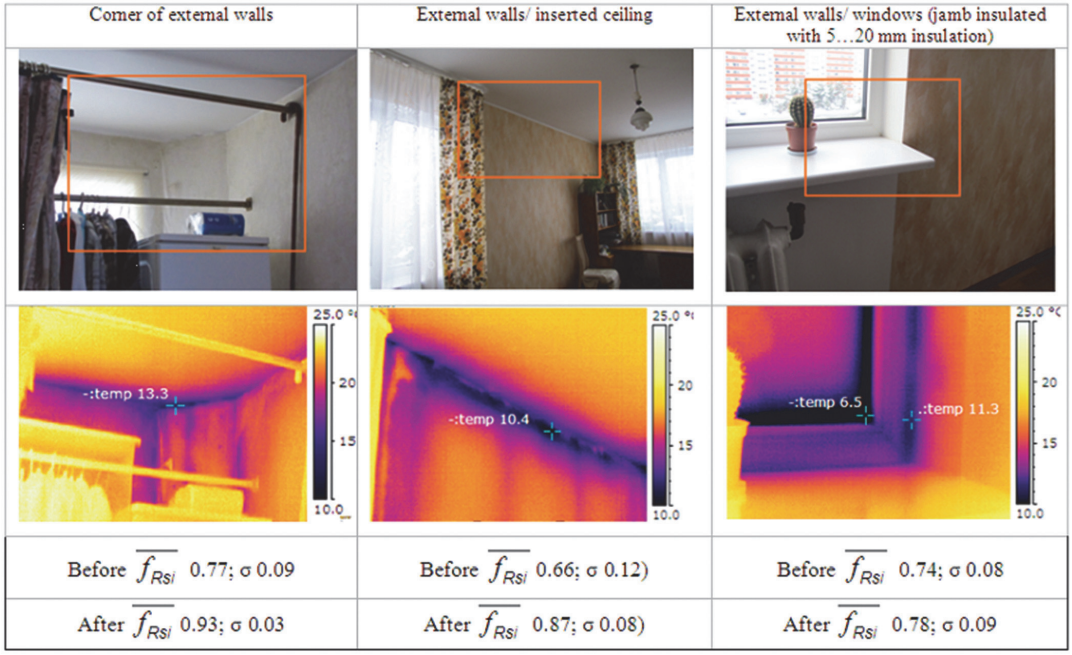

Figure 8 *Measured range of temperature factor f_{Rsi}, of thermal bridges with average and standard deviation σ . Pictures were taken before the renovation.*

nant thermal bridge in terms of heat loss. Results are very sensitive about the thickness of insulation on a window's jamb (cheek) (window return).

It is not possible to install a sufficient layer of insulation (>30 mm) to the window jambs because of the shape of the concrete element that windows are attached to, see Figure 10. To avoid serious thermal bridges around the windows, all the windows should be placed to the external side of the existing concrete element that moves them more in-line with the additional exterior insulation.

Hygrothermal Performance of External Walls

Temperature and RH were measured in both test-walls: MW and EPS external thermal insulation composite systems

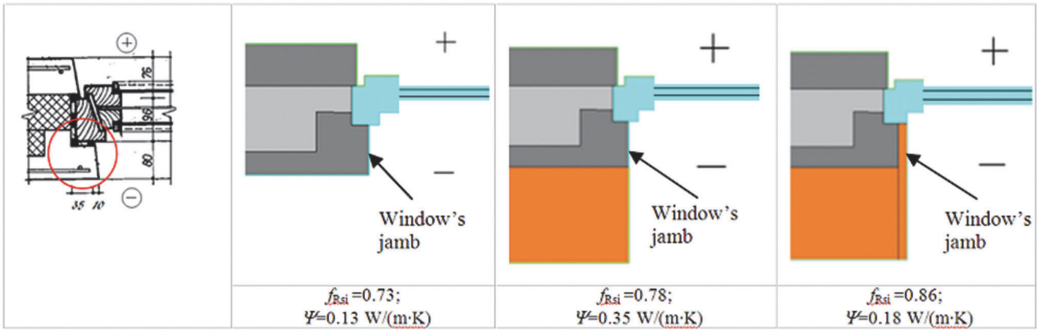

Figure 9 *Calculation results of temperature factor f_{Rsi} and linear thermal transmittance ψ of the external wall/window junction. Inside area of original drawing (left) the red circle shows the proportion of the jamb of a window covered.*

Figure 10 *Picture of an old window (left) and of new windows placed at their original position. Most of the jamb is covered and only a thin layer of insulation (5…20 mm) can be attached to the jamb.*

(ETICS). Measurements lasted for one and a half heating periods from September 2011 until December 2012. Hygrothermal performance of both walls was also simulated by Delphin 5.7.4.

In general, agreement of temperature, vapour pressure, and RH between the measurements and calculations was good, except RH between mineral wool insulation and plaster (measuring point 3, see Figure 14) where the measured value was higher. Results presented in Figure 12–Figure 14 of the cold period fit also with steady-state distributions of temperature, vapour pressure, and RH. After first calculations, there was also a mismatch about the drying out period. According to the measurements, moisture in the wall (existing moisture in the external core and additional moisture from adhesive mortar) dried out during within 3–4 months, mainly by diffusion and with minor convection. We ended up with acceptable agreement after adding small air gaps between measurement points 1 and 2 with air pressure difference at outdoor climate conditions in cross-section 2, see Figure 3 right. The effect of moisture movement without convection can be seen in Figure 11. If in fact moisture in measuring points 1 and 2 dried out during half of heating season it was much slower by diffusion only according to calculations. There is also some difference in the beginning of the second winter.

Calculated and measured temperatures of both walls match quite well. In the case of MW, calculated temperatures at measurement point 1 and 2 are up to 1°C lower than measured (Figure 12) and up to 1°C higher than measured in the case of EPS (Figure 15). Measured temperatures of two test-walls are similar, maximum 0.5°C higher in the case of EPS.

Also, vapour content/vapour pressures were calculated from the measured temperature and RH in both test-walls and calculated with software. Results for MW are shown in Figure 13 and for EPS Figure 16, respectively. Vapour pressure starts to increase right after the beginning of the heating season in the second half of October 2011 but then starts to decrease. Measurement point nr 2 is not graphically presented. It behaves as point nr 1 but its level is somewhat lower.

Results of measured and calculated RH are presented in Figure 14 for MW and in Figure 17 for EPS. As it

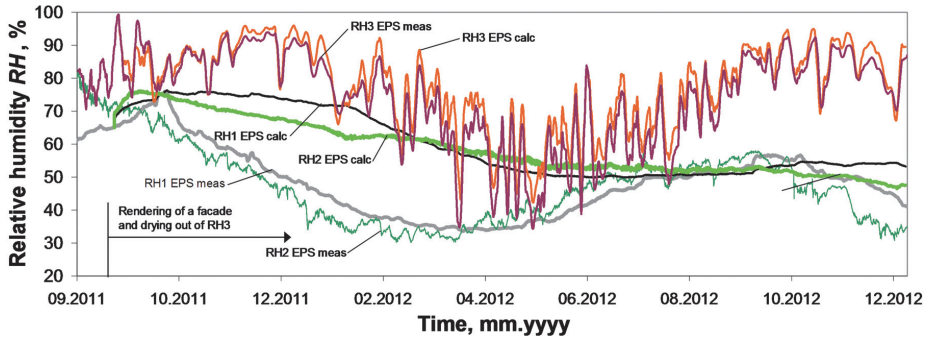

Figure 11 *Comparison of measured (meas) RH and calculated (calc) RH moisture movement only by diffusion of ETICS with graphite enhanced EPS.*

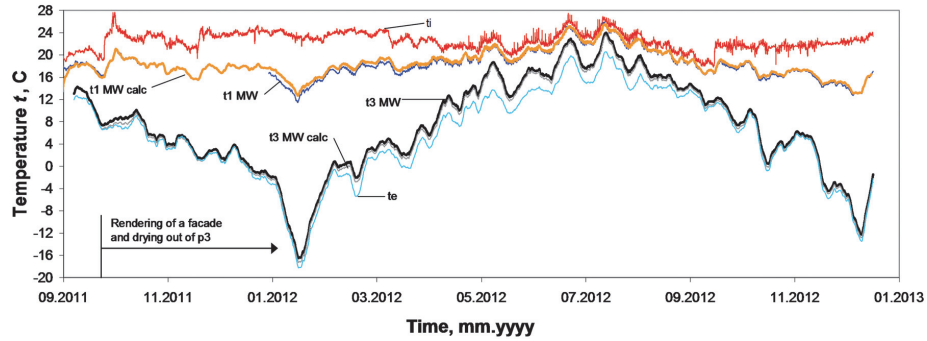

Figure 12 *Measured and calculated temperature (t) in the wall additionally insulated with MW. Location of measurement points see in Figure 2.*

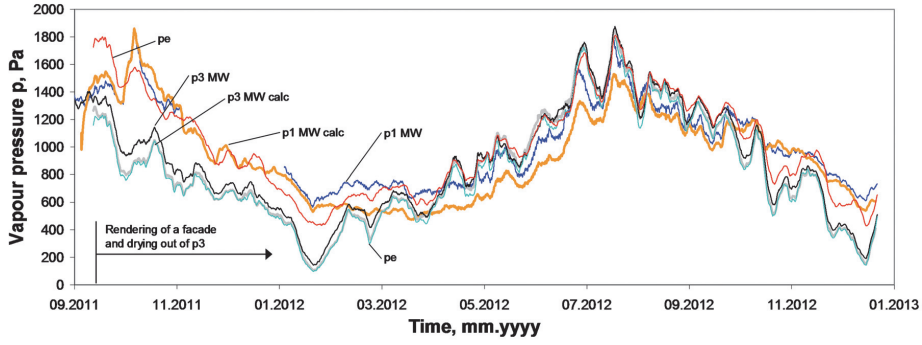

Figure 13 *Measured and calculated vapour pressure (p) in the wall additionally insulated with MW.*

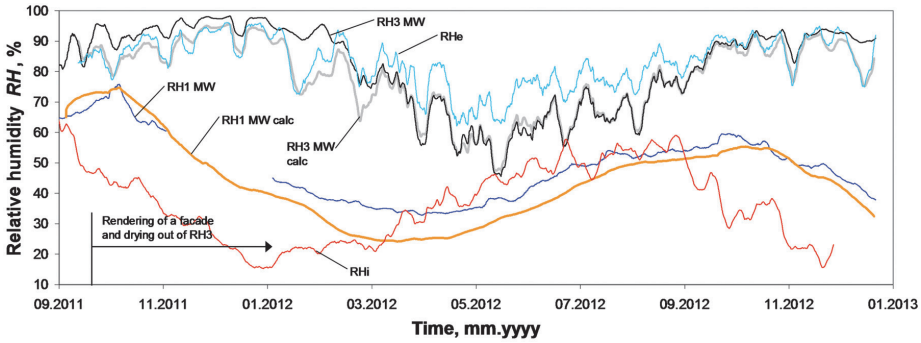

Figure 14 *Measured and calculated RH in the wall additionally insulated with MW.*

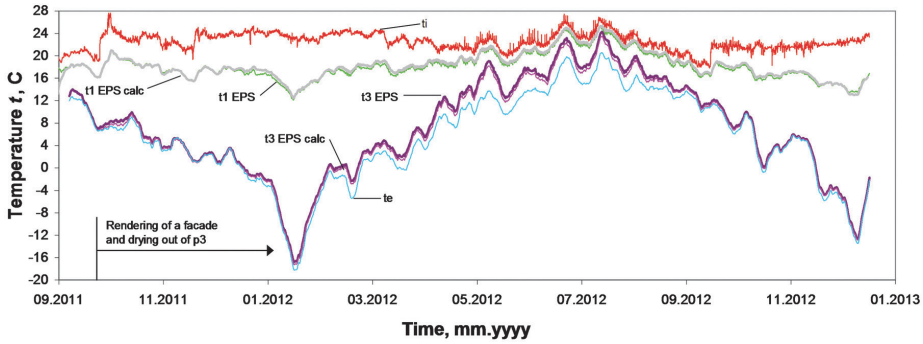

Figure 15 *Measured and calculated temperature in the wall additionally insulated with expanded polystyrene (EPS). Location of measurement points see in Figure 2.*

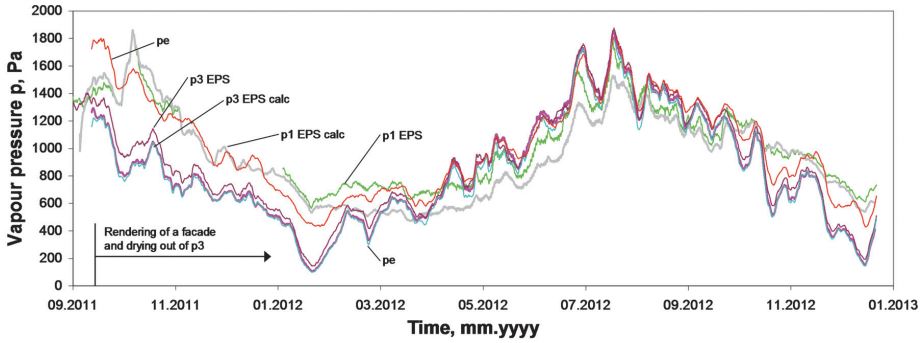

Figure 16 *Measured and calculated vapour pressure in the wall additionally insulated with EPS.*

appears, measured RH at point 3 with MW is somewhat higher than calculated during winter period. In spring measured RH at point 1 is somewhat higher than calculated with both insulation materials. Correlation in summer period is very good, especially in the case of MW. To the contrary, agreement with EPS is better at winter time. Results of measuring point 2 follow the results of point 1 but at 10%–15% lower level. That is a result of higher vapour pressure at point 1 compared to point 2 at almost same temperatures.

Results of thermal transmittance of walls are presented in Figure 18. It can be seen that the calculated thermal transmittance of MW is substantially higher than the rest of three lines. Fluctuation of measurement results appears probably because solar radiation affects temperature of the external surface of the wall. Average thermal transmittances of winter months are 0.17 W/(m^2·K) for EPS and 0.19 W/(m^2·K) for MW.

One of the important research questions was the drying out period of the external core of the original external wall. Analysis of time for drying out period at different initial moisture conditions (from 80% to 100% rh) is shown in Figure 19.

DISCUSSION

Indoor Climate and Thermal Comfort

Indoor climate measurements before and after the retrofit showed small improvement at air temperatures, where no overheating appears at very cold period because of better adjustment of a new heating system.

Natural passive stack ventilation was changed into mechanical exhaust ventilation with exhaust air heat pump. Recovered heat was used for domestic hot water and heating. The air change did not improve after the renovations. It can be seen from moisture excess (Figure 7 right). There are several reasons that are more or less related to each other. First, the

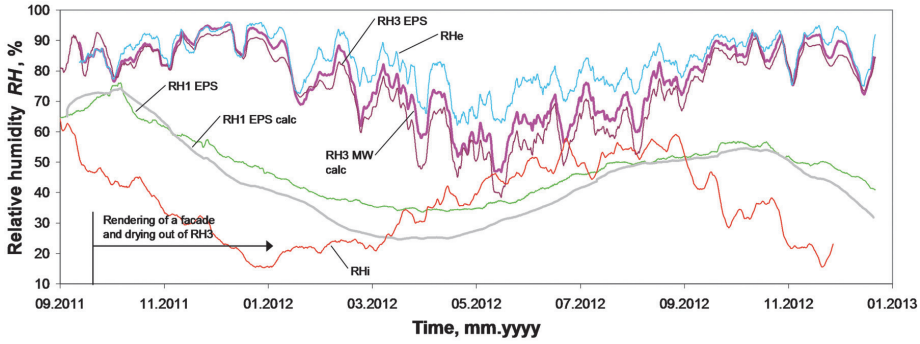

Figure 17 Measured and calculated RH in the wall additionally insulated with EPS.

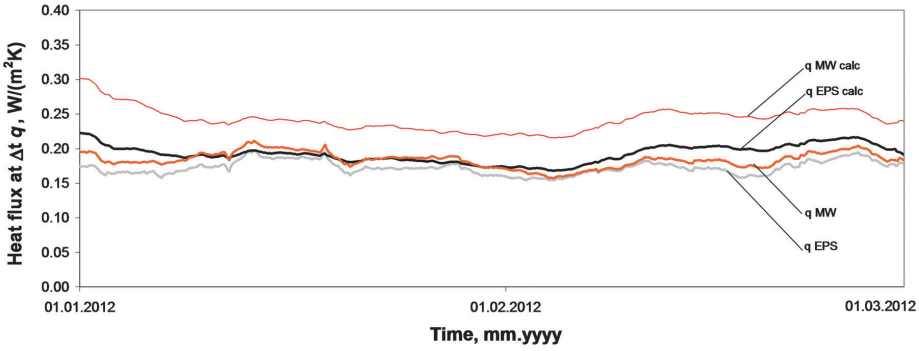

Figure 18 Measured and calculated thermal transmittances in the wall additionally insulated with EPS and MW. Lines represent weekly average values.

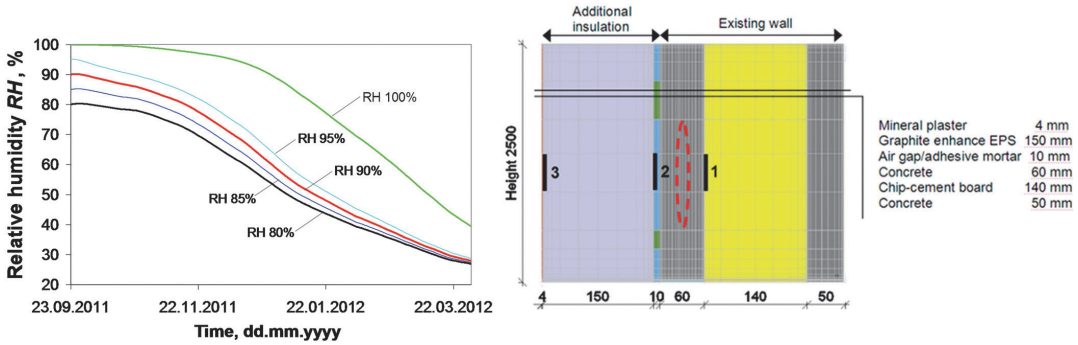

Figure 19 *Moisture drying out time from the external layer of concrete between measuring points 1 and 2 (right) with different initial moisture.*

exhaust fan was set to minimum speed soon after the installation due to energy saving, lower sound level, and better thermal comfort. Also, building fabric became more airtight with new windows and additional insulation that decreased infiltration. The indoor moisture excess 2–3 g/m^3 after the renovation indicates average indoor humidity load level. This means that moisture production/living density had been relatively low.

There was a problem with low floor temperatures on the first floor. The floor was not insulated from the bottom side (cellar's ceiling) because of lack of finance, low height of cellar, and impracticability of workmanship (pipes, lighting, cables, etc. are attached to the cellar's ceiling).

Thermal Bridges

During typical low-budget energy renovation, only old wooden windows are replaced and previously replaced windows remain in the same location. Since the thickness of additional insulation into walls is typically 150–200mm, windows become located 200–270 mm inside the surface of the façade instead of 50–70mm originally. This is a problem because of esthetics and architecture, reduced day lighting, energy efficiency, and mainly thermal bridges around the windows. Negative impact is greater in the case of small and narrow windows. Generally, some insulation is recommended to be placed at window's jamb, but in practice this is complicated and often only 5–20mm is achievable. If the temperature factor f_{Rsi} does not change much, then the linear thermal transmittance Ψ is very sensitive to the jamb's insulation. A remarkable impact of a window's position in the wall and sensitivity on the jamb's insulation has been also found by Hens and Carmeliet (2002). Heat loss through thermal bridges around the windows compared to the rest of a wall is often at a similar scale. In the future, moving of all the windows towards outside is advisable. Also, most of the windows installed about 10 years ago can be replaced again since selective covering was not yet common then and remarkable development of windows has taken place during last years.

Another thermal bridge that remained after the renovation is the external wall/balcony junction. It could be eliminated by insulating a balcony slab from the bottom and top. Technical condition of concrete balconies and awning is sometimes problematic and steel elements, including reinforcement mesh, is sometimes corroded. Since after additional insulation the original 1 m width of a balcony becomes only about 0.8 m, removal of all existing balconies should be considered. New, durable, and wider balconies containing minor thermal bridges would be a sustainable investment.

Hygrothermal Performance of ETICS on a Concrete Element

One of the main goal of this study was to analyse hygrothermal performance of an external wall insulated additionally with mineral wool and expanded polystyrene ETICS. Initial simulation results considering only diffusion showed remarkable mismatch during the first heating season. Although the adhesive mortar/air gap was sealed with PU foam at the basement wall and roof, there was probably some air leakage. Air leakage between the insulation and original wall (measurement point 2) is possible because of rubble bulk covered with particles of different sizes. This in contact with adhesive mortar did not assure totally airtight connection. The air pressure difference created by stack effect enabled some air movement along the wall. Calculations show that a narrow 0.5–1 mm opening below and above the wall is able to transport more moisture than by diffusion. Cracks with such a small width could originate from shrinkage of monolitization concrete connecting pre-fabricated elements or those could be in the elements produced from three layers. Considerable impact of air gaps in the ETICS has been also found by Olson and Taylor (2009) and Sedlbauer and Krus

(2002). In Sedlbauer and Krus (2002), a drying out time of up to 8 years is stated.

The impact of air convection between the additional thermal insulation and original wall is small enough not to appear in the results of thermal transmittance of the wall in practice, see Figure 18. Small impact of air convection to thermal transmittance is also found by Hens and Carmeliet (2002) where 2 mm air gap increased thermal transmittance 12% at ETICS on masonry. Higher calculated thermal transmittance might be caused by air leakage through MW insulation. Slightly higher thermal transmittance in case of MW can be explained with lower thermal conductivity of EPS, having declared value λ_D = 0.032 W/(m·K) compared to λ_D = 0.038 W/(m·K) in the case of MW. The addition of 150 mm of additional EPS/MW insulation contributes more than 2/3 to the total thermal resistance of the wall.

Measurements and calculations showed that moisture in the analysed wall dried out in half of the heating season (see Figure 11 and Figure 19), approximately 3–4 months. If dried only by diffusion, it would have taken about a year for most of the moisture and the rest of it would have dried out during the second year. Slow drying out by diffusion from ETICS on masonry is also declared by Hens and Carmeliet (2002). In the analyzed case with convection totally wet, an external layer would have dried out from most of the moisture also within 3–4 months but in that case, large moisture flux through the wall and possible condensation behind the plaster would be a threat. In that case there would probably be some drying out toward indoors as found in work made by Hens and Carmeliet (2002).

Different aspects of hygrothermal performance of ETICS have been studied for decades. There should be separate viewpoint between ETICS on concrete/masonry and wooden structures. Although it has been found to be a functioning solution in principle (Karagiozis and Kumaran 1997; Holm and Künzel 1999; Kvande 2008; Künzel, H.M. and Zirkelbach, D. 2008) it is very sensitive to driving-rain-caused water leakage from cracks in finishing layer (Bomberg et al. 1997; Krus et al. 2008). Already, 1% of driving rain leakage can be crucial (Künzel 1998). Performance of ETICS has also been studied by Balocco at al. (2008). Solid computational analyses are done by Vares et al. (2012) and Desjarlais (2001). Literature review is conducted by Cheple and Huelman (2000).

According to Zwayer (1995), performance of ETICS walls depends on the design and materials choice, connections between plaster and other materials in joints, workmanship, technology, and quality. In the cold climate of Finland, Pakkala (2011) has found poor frost resistance of ETICS to be a problem and testing methods and criteria according to ETAG 004 worked out in central Europe might not be proper.

Tested walls had also minor driving rain loads since it was sheltered by a neighboring higher building and because of other factors of the surrounding environment. Performance of ETICS walls under high driving rain loads and in the case of higher buildings must be handled as another field of research that was not the aim of this paper.

Also, durability and factors impacting it in addition to climate loads (content and type of plaster, vapour permeability, water uptake coefficient, adhesion, cracking, frost resistance, etc.) is a field of the future research. During maintenance of ETICS, one should also consider a possible layer of painting that might be added later.

General Success of Current Energy-Renovation Pilot Project

The main progress of the current energy renovation pilot project was its better design and workmanship quality. It must be noticed that since it was a pilot project, workmanship under strict supervision was probably somewhat better than usual. From now on, similar renovations can be started with existing know-how about success and problems. In addition to lower heating bills, renovation should lead also to better durability, longer service life of structures, and better indoor climate and aesthetics. These all have also a positive impact on the value of real estate. One should also move on towards the next more progressive steps by modernizing older housing stock.

Similar low-cost renovation described in this paper is wide-spread in Estonia and in neighboring countries today. Often renovation is conducted in many stages without a holistic approach. Main renovation solutions employed are typical: additional external insulation and changing of old wooden windows. Together with the change of membrane waterproofing, an additional thermal insulation is added to the roof. The renovation of balconies and awnings depends on damages.

Overall success of this example project can acquire satisfactory evaluation avowals. A novel solution in this pilot project was holistic approach and an air heat pump for heat recovery of the new mechanical ventilation. Attitudes of inhabitants to the renovation varied both before and after renovation. In the current pilot project, people were somewhat more tolerant since approximately half of the whole investment came from sponsors and subsidizers. Still, there were complaints about designed solutions, execution of workmanship, and some unfamiliar changes.

CONCLUSIONS

This case-study analysis studied measured and calculated hygrothermal performance of a mineral wool (MW) and graphite enhanced expanded polystyrene (EPS) external thermal insulation composite systems (ETICS/EIFS). Also, indoor climate, air leakage rate and thermal bridges were measured before and after the low-budget energy renovation of an existing concrete large panel elements apartment building.

Indoor climate measurements showed no major changes in moisture excess, mostly because mechanical ventilation airflows were decreased by the operator. Overheating that existed before was avoided after the renovation with a new adjusted heating system. Airtightness of the building fabric improved only in apartments where old leaky windows were

replaced. Additional external insulation solves the serious problem of thermal bridges, except at external wall/window junction if windows remain at their original position and also at external wall/balcony and external wall/foundation wall junction. Therefore, windows should be attached to the external side of the existing façade.

Measured hygrothermal performance of both walls was good and correlation existed with the calculated temperature, vapour pressure, and RH distributions. Built-in moisture of the whole wall (measuring spots 1 and 2 on both sides of the external layer of concrete) dried out during the first heating season, achieving RH values below 50%. Moisture in thin plastering (measuring spot 3 between insulation and plaster) dried out within few days but stayed quite high, especially in the case of mineral wool, being over 90%. It means that the content and properties of the external finishing plaster must be carefully designed to achieve low enough vapour permeability and low water uptake. This becomes even more crucial at a greater vapour flow due to material with higher vapour permeability instead of concrete. Average measured thermal transmittance U during the winter was 0.17 W/(m^2·K) in the case of graphite enhanced EPS and 0.19 W/(m^{2}K) for mineral wool. This is close to the expected value calculated from a producer's data and allows us to make positive conclusions about thermal performance. Hygric performance was also satisfactory and moisture dried out during the first heating season. Measurements and calculations showed that there had been some convection of moist air in the wall. A drying out process by diffusion only would have been much slower.

Short term hygrothermal performance of ETICS is normal when proper design and workmanship is performed, in particular, related to joints. Additional insulation lowers the RH inside the existing wall that stops the corrosion process and frost damages. Long term performance and durability of ETICS in cold climate and under driving rain loads needs to be further investigated with special attention to content and properties of render, frost resistance, cracking, staining, maintenance, and repainting.

ACKNOWLEDGMENTS

The research has been conducted as part of the IUT1–15 project "Nearly-zero energy solutions and their implementation on deep renovation of buildings."

REFERENCES

Balaras, C.A., Droutsa, K., Dascalaki, E., Kontoyiannidis, S. 2005. Deterioration of European apartment buildings. *Energy and Buildings*, 37 (5), pp. 515–527.

Balocco, C. / Grazzini, G. / Cavalera, A. Transient analysis of an external building cladding, *Energy and Buildings*, 40 (7), p.1273–1277, Jan 2008.

Bomberg, M. / Lstiburek, J. / Nabhan, F. Long-Term, Hygrothermal Performance of Exterior Insulation and Finish Systems (EIFS), *Journal of Building Physics*, 20 (3), p.227–248, Jan 1997.

Cheple, M. and Huelman, P. (2000). Literature Review of Exterior Insulation Finish Systems and Stucco Finishes, Report MNDC/RP B80-0130, University of Minnesota.

Desjarlais, A.O., Karagiozis, A.N., and Aoki-Kramer, M. (2001): Wall Moisture Problems in Seattle. Buildings VIII proceedings, ASHRAE, 8p.

Dol, K.; Haffner, M. 2010. Housing Statistics in the European Union 2010. OTB Research Institute for the Built Environment, Delft University of Technology.

Dall'O', G., Galante, A., Pasetti, G. A methodology for evaluating the potential energy savings of retrofitting residential building stocks. *Sustainable Cities and Society.* 4-1, October 2012, Pages 12–21.

Economidou, M., Atanasiu, B., Despret, C., Maio, J., Nolte, I., and Rapf, O. (2011). European buildings under the microscope: A country-by-country review of the energy performance of European buildings. Buildings Performance Institute. Europe 2011.

EN ISO 10211 *Thermal bridges in building construction - Heat flows and surface temperatures - Detailed calculations*. Part 1:2000 and Part 2:2001.

EN ISO 13788 *Hygrothermal performance of building components and building elements - Internal surface temperature to avoid critical surface humidity and interstitial condensation - Calculation methods.*

EN 13187 *Thermal performance of buildings - Qualitative detection of thermal irregularities in building envelopes - Infrared method.*

EN 13829 *Thermal performance of buildings - Determination of air permeability of buildings - Fan pressurization method.*

Hagentoft, C. E. 2010. Importance of a correct overall performance assessment – Probability assessment of performance and cost. Large scale national implementation plans for building airtightness assessment: a must for 2020. We should start now to be ready in 2020. June 14–15, 2010 Brussels, Belgium.

Hens, H. and J. Carmeliet, (2002), Performance prediction for masonry walls with EIFS using calculation procedures and laboratory testing, *Journal of Thermal Envelope and Building Science*, 25(03).

Holm, A. and Künzel, H.M, (1999), Combined effect of temperature and humidity of the deterioration process of insulation materials in ETICS, Building Physics in the Nordic Country, August, Gothenburg.

Ilomets, S.; Kalamees, T.; Agasild, T.; Õiger, K.; Raado, L. M. (2011). Durability of concrete and brick facades of apartment buildings built between 1960–90 in Estonia. In proceedings: XII DBMC International Conference on Durability of Building Materials and Components, Portugal, Porto, 2011, 1171–1178.

Holopainen, R., Tuomaala, P. (2011) Effect of energy renovation on thermal sensation and comfort during heating season. 9th Nordic Symposium on Building Physics - NSB 2011 p. 1069–1076.

Kalamees T; Õiger K; Kõiv T. A., et al. 2009. Technical condition and service life of Estonian apartment buildings, built with prefabricated concrete elements. Tallinn University of Technology (in Estonian).

Kalamees, T., 2006. Hygrothermal Criteria for Design and Simulation of Buildings. Doctoral theses, Tallinn University of Technology, Tallinn: TTU Press.

Karagiozis, A. and Kumaran, K. (1997). Drying Potential of EIFS Walls: Innovative Vapor Control Strategies. STP 1339, American Society for Testing and Materials (ASTM), West Conshohocken.

Krus, M., Hofbauer, W. and Lengsfeld, K. Microbial Growth on ETICS as a Result of the New Building Technology? Building Physics Symposium. Leuven, Belgium 2008-10-29 - 2008-10-31.

Kvande, B. Bergheim Einar Thue, Jan Vincent. Durability of external thermal insulation composite systems (ETICS) with rendering. Building Physics Symposium Leuven, Belgium 2008.

Künzel, H.M.: Drying of Masonry with Exterior Insulation. Proceedings of the Fifth International Masonry Conference. British Masonry Society, No. 8, Stoke-on-Trent 1998, pp 245–250.

Künzel, H.M.; Zirkelbach, D. Influence of rain water leakage on the hygrothermal performance of exterior insulation systems. In Rode, C.; Technical University of Denmark -DTU-, Lyngby: 8th Nordic Symposium on Building Physics in the Nordic Countries 2008. Proceedings. Vol.1: Copenhagen, June 16–18, 2008 Lyngby, 2008 (DTU Byg Report 189).

Nemry, F., Uihlein, A., Colodel, C.M., Wetzel, C., Braune, A., Wittstock, B., Hasan, I., Kreißig, J., Gallon, N., Niemeier, S., Frech, Y. Options to reduce the environmental impacts of residential buildings in the European Union-Potential and costs. Energy and Buildings Volume 42, Issue 7, July 2010, 976–984.

Nicolai, A. 2008. Modeling and Numerical Simulation of Salt Transport and Phase Transitions in Unsaturated Porous Building Materials, Dissertation, Syracuse University.

Olson P.E., E.K., Taylor, J.A. 2009. Retrofitting barrier exterior insulation and finish system: Methodology and performance assessment. ASTM Special Technical Publication 1493 STP, pp. 229–237

Sedlbauer, K. and Krus, M., (2002), Information and Technology Transfer from IBP: Mold Growth on ETICS (EIFS) as a Result of "Bad Workmanship"?, *Journal of Thermal Envelope and Building Science*, vol. 26, no. 2, pp. 117–121.

Silva, P.C.P., Almeida, M., Bragança, L., Mesquita, V. Development of prefabricated retrofit module towards nearly zero energy buildings. *Energy and Buildings*, Volume 56, January 2013, 115–125.

Uihlein, A., Eder, P. Policy options towards an energy efficient residential building stock in the EU-27. 2010. *Energy and Buildings* 42 (6), pp. 791–798

Vares Sirje, Pulakka Sakari, Toratti Tomi, Fulop Ludovic, Hradil Petr, Vesikari Erkki, et al. 2012. Sustainable refurbishment of exterior walls and building facades. Final report, Part B – General refurbishment concepts. VTT TECHNOLOGY 33. ISBN 978-951-38-7849-8, ISSN 2242-122X. VTT. Espoo Finland. 244 p. + App. 30 p.

PUBLICATION V

Ilomets, S., Kalamees, T., Lahdensivu, J. Validation of the method to evaluate the corrosion propagation stage by hygrothermal simulation. In: Proceedings of Central Europe towards Sustainable Building 2016; Innovations for Sustainable Future, 22−24.06.2016, Prague

VALIDATION OF THE METHOD TO EVALUATE THE CORROSION PROPAGATION STAGE BY HYGROTHERMAL SIMULATION

Simo ILOMETS[a], Targo KALAMEES[b], Jukka LAHDENSIVU[c]

[a] *Tallinn University of Technology, Ehitajate tee 5, Tallinn 19086, Estonia, simo.ilomets@ttu.ee*
[b] *Tallinn University of Technology, Ehitajate tee 5, Tallinn 19086, Estonia, targo.kalamees@ttu.ee*
[c] *Tampere University of Technology, P.O. Box 600 FI-33101 Tampere, Finland, jukka.lahdensivu@tut.fi*

Abstract

Evaluating the propagation period for reinforcement corrosion in concrete facades is an important but complex task which contains a high level of uncertainty. Corrosion current intensity during the propagation period have been measured in a large number of studies and there is a general consensus in regard to factors affecting carbonation induced corrosion. Hence, a proper evaluation of hygrothermal conditions in concrete facade becomes crucial.

In this study a method to calculate the corrosion propagation period was validated based upon a field survey of prefabricated concrete facades in large-panel apartment buildings. The method combines existing corrosion propagation models and the Delphin dynamic hygrothermal simulation tool, and takes into consideration material properties, carbonation depth, concrete cover depth, indoor and outdoor climate loads. With the proposed method, propagation consists of a time that is required for a concrete cover to begin cracking and a further expansion of the crack to open to 0.3 mm in width.

As a result, the method is validated via the correlation between measured and calculated propagation periods across a range of twenty years. The sensitivity of the results are also studied. The method allows for an evaluation to be carried out on degradation, residual service life, and the need for the renovation of reinforced concrete facades.

Keywords: *corrosion model, corrosion propagation, concrete damage, service life, hygrothermal simulation*

1 Introduction

The durability of concrete facades that were put up in the 1960s and 1970s has become a very relevant field of research, since degradation mechanisms – carbonation induced corrosion and frost damage – have become very evident.

Detecting a correlation between actual deterioration and climate loads is a highly complicated task thanks to a large number of uncertainties such as, for example, material properties (depending on moisture conditions), local climate loads on the building site, and the complexity of deterioration phenomena.

Hygrothermal simulation tools have a wide field of application when it comes to modelling heat, air and moisture transfer. Since the hygric conditions in concrete are mainly responsible for corrosion intensity via resistivity, applying dynamic simulation tools becomes highly useful.

The proposed method is attempting to fill in a gap that is related to the evaluation of carbonation induced corrosion. The aim of the paper is to validate the method by comparing the calculated corrosion propagation rates against the results of a field survey.

An illustration of a research problem and a description of a wall that has been studied, with indoor and outdoor climate loads affecting its performance, is shown in **Fig. 1.**

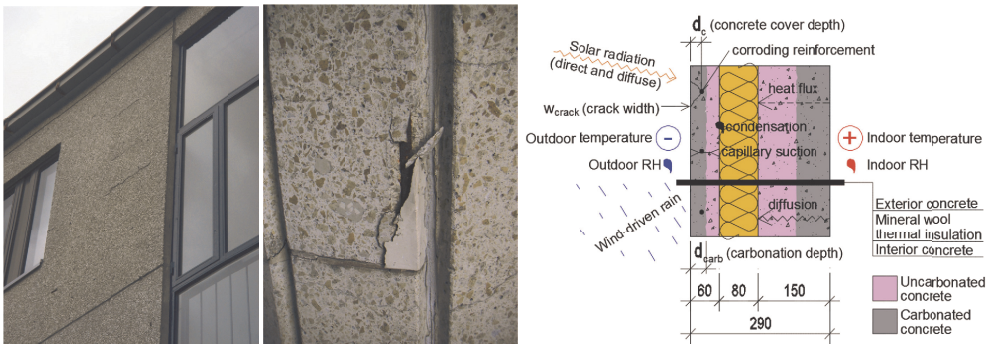

Fig. 1 *Illustration of a research problem (left and middle) and cross-section of a studied wall (right). Reinforcement corrosion takes place in exterior concrete if the carbonation depth d_{carb}>cover depth d_c.*

2 Corrosion model

2.1 Background and theory

Corrosion of concrete reinforcement can be divided into two main stages: initiation and propagation, Otieno (2011). During the initiation stage, carbonation (i.e. the penetration of CO_2 from ambient air into the concrete by diffusion) in concrete reaches the depth of the embedded steel and breaks down the passive film that surrounds the reinforcement (the onslaught of a grey tinge in **Fig. 1**, right, leading to the neutralisation of the concrete's pH). The propagation stage covers the actual deterioration of the steel and the concrete cover.

Corrosion current during propagation is an electrochemical process that comprises steel as a connector of anode and cathode, and pore water as an electrolyte. Electrical resistivity is related primarily to relative humidity (RH) in concrete, since resistivity/conductivity depends on the volume of water molecules in the pores. There is a thicker layer of water molecules on the pore walls at higher RH, causing higher conductivity i.e. lower resistivity.

Corrosion current during the propagation stage depends on the following: the electrical resistivity of concrete (depending on concrete RH), temperature, oxygen availability, and the pH of the pore solution.

A correlation between corrosion rate and resistivity has been found for carbonated concrete by Bouteiller et al. (2012), but this is controlled by resistivity up to certain critical RH ~90-95%, Yu et al. (2014). Above this figure, corrosion of steel is under the control of the cathodic reaction (oxygen diffusion) and the corrosion rate decreases due to a shortage of oxygen – see **Fig. 2**, left.

Higher temperatures accelerate corrosion since there is more intensive electrochemical reaction that is caused by electrons that are moving faster. Broomfield (1997) has estimated the change in corrosion current at between five and ten times with a 10°C temperature drop.

The critical depth for steel corrosion (a cross-section loss) which causes cracks, chipping, and spalling of the concrete covering is 15-40 μm, Broomfield (1997), 15-50 μm,

Alonso (1998), 54 μm on average (Köliö et al. 2015), and up to 100 μm. Critical depth depends on cover thickness and a lower value of 15 μm represents a small cover depth while the upper part at 100 μm is rather typical of a large cover depth.

Empirical or experimental models to calculate the corrosion and service life of a structure have been developed, most of them reviewed by Ahmad (2003) and Jamali (2013). Since the corrosion mechanism depends on many factors, calculation results are never accurate and tend to be valid only for the conditions in which they were developed.

Rouchier et al. (2013) found that cracking affects the hygrothermal performance of the façade. There is a porous zone at the reinforcement/concrete intersection, but expansion of corrosion products creates internal stress that itself causes cracks in the concrete cover, Šavija et al. (2013). After the formation of the initial crack (w=0.05 mm, see **Fig. 2**, middle), propagation accelerates locally due to increased penetration of wind-driven-rain (WDR). For the crack width to become visible, a range of 0.1-0.3 mm is needed, but this depends on a large number of factors – surface characteristics, surface covering, the distance of the observer, lighting conditions, etc. Limit criterion proposed by Khan et al. (2014), for a crack width w_{max}=0.3 mm was chosen in this study in order to evaluate the service life.

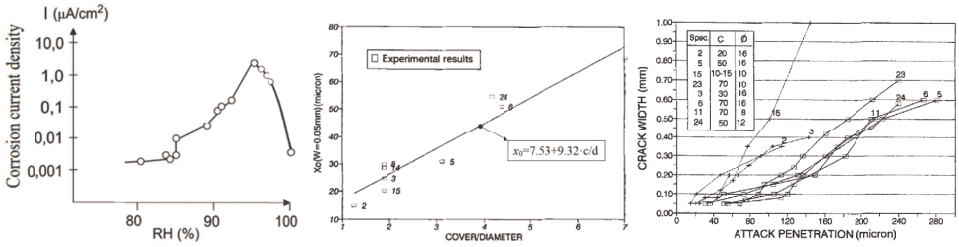

Fig. 2 *On the left, corrosion current depending on the RH of concrete (valid for a temperature of +5°C), based on Tuutti (1982). In the middle, the ratio of the reinforcement's cover depth/diameter causing the first crack (w=0.05 mm) and further crack evolution (w=0.3 mm, right) Alonso (1998).*

2.2 Corrosion calculation

The process that covered the calculated propagation period $t_{p,c}$ was carried out by observing the following steps:

- Hourly values for temperature and RH were calculated inside the external concrete at the depth of the reinforcement d_c (**Fig. 1**, right) by using a dynamic hygrothermal simulation tool (a description of the buildings and a simulation tool follows in a later chapter);
- Hourly values for corrosion current I_{cor} were calculated from the RH according to Tuutti (1982) in **Fig. 2**, left (MS Excel post-processing);
- Hourly values for corrosion current I_{cor} were corrected with the temperature (by 7.5 times with a 10 °C temperature change by reference to a 5 °C baseline);
- A cross-section loss of the reinforcement was calculated according to Faraday's Law (Eq. 1), from El Maaddawy (2007):

$$M_{loss} = \frac{M \cdot I_{corr} \cdot t}{z \cdot F} \tag{1}$$

where: M_{loss} is the mass of steel dissolved at the anode during the overall time t, kg/m^2; M is the molecular weight of corroding steel (M=55.8 g/mol); I_{corr} is the corrosion current, A/m^2; t is the corrosion duration, s; z is the valence of corroding metal, i.e. the

number of electrons involved in the electrochemical reaction (z=2 for steel); F is Faraday's constant, F=96487 A·s/mol.

- A cross-section loss x_0 that relates to the first visible crack (w=0.05 mm) depends on cover depth c, mm and diameter of the reinforcement d, mm, being calculated (see **Fig. 2**, middle): x_0=7.53+9.32·c/d. The uniform corrosion of a cylinder-shaped reinforcement and the density of the steel ρ=7.85 g/cm^3 is assumed.
- Further attack penetration for the crack's opening, from 0.05 mm up to 0.3 mm (Δ0.25mm crack width corresponds to Δ80 μm attack penetration) is independent of cover/diameter ratio from **Fig. 2**, right. Alonso (1998) models were chosen since those showed the best performance in a solid comparison carried out by Jamali et al. (2013).

Finnish prefabricated multi-storey concrete-element dwellings from a low-rise district of Helsinki called Siltamäki were used in the study. The district was built up between 1967-1971 and a field survey was carried out in 2007. By this point, the age of the buildings covered by the field survey was between 36-40 years. The buildings have an external wall that comprises three layers – 150 mm of internal concrete, 80 mm of mineral wool, and 60 mm of external concrete – see **Fig. 1**, right, and Lahdensivu (2012).

The profound dynamic hygrothermal simulation tool, Delphin 5.8.1, was used for the hygrothermal calculations. The software has been validated by Scheffler (2008) and Sontag et al. (2013) – see more information in Nicolai (2008) and in the user manual. Delphin has also been validated in a study in which the calculated results for hygrothermal performance were compared to the results from the field measurements in Ilomets and Kalamees (2013).

Façades facing in various directions – south, west, etc – were selected according to the real-life situation of the building, and temperature and RH values during the propagation period were calculated in the outer layer of the concrete.

WDR loads for the vertical façade, depending on wind speed, wind direction, and rain intensity, were calculated by the user according to the standard rain model contained within the Delphin software. This approach lead to an average catch ratio of η~0.2 which was representative of the lower part of the façade, i.e. the first floor for a building that had the dimensions of 100·10·20 m^3 in Blocken et al. (2013). The WDR load was doubled (η~0.4) for the second floor and quadrupled (η~0.8) for the third floor.

Delphin`s default material data and functions were mostly used in a study, although some of the hygrothermal properties of the concrete specimen were measured in the laboratory. Thermal conductivity was at λ=1.35 W/(m·K), specific heat capacity at c_e=900 J/(kg·K) and water uptake coefficient at A_w=0.016 kg/(m$^2\sqrt{s}$) – see also **Tab. 1**.

The hourly outdoor climate readings (temperature, RH, wind direction and velocity, rain intensity, and diffuse and direct solar radiation) as measured by the Finnish Meteorological Institute during the propagation period t_p from Helsinki was used.

An indoor air temperature of +22 °C (with an outdoor temperature of <+10 °C) and moisture excess Δv=+2 g/m^3 (with an outdoor temperature of <+5 °C) was used in calculations based on Vinha et al. (2009).

3 Model validation

Only uniform corrosion (which are rather typical of carbonation induced corrosion) are being considered. The concrete is assumed to be solid, at first without any cracks and not deformable. The corrosion process is assumed to be carbonation induced, i.e. the content of chlorides should be below 0.03% according to Lahdensivu (2012). A principled scheme for

a service life from the time of construction t_0 until the point at which a failure occurs t_f is described in **Fig. 3,** left.

The validation process was carried out by concerning the real (measured) data:

- Data about real-time failures as cracks or spalling in a concrete façade was collected from the field survey reports (time of the field survey t_{survey}, time of construction t_0);
- Measurements of carbonation depth d_{carb} and concrete cover depth d_c were carried out in the laboratory directly after the field survey, whereby $d_{carb}>d_c$;
- Vesikari (1986) carbonation coef. k, mm/√years was calculated for each specimen from the age of a building t_a and carbonation depth d_{carb}, mm: $k=d_{carb}/\sqrt{t_a}$. In addition to the exponent of a time 0.5, whilst values of 0.4 and 0.3 were also examined.
- The initiation period t_i, years was calculated back from the concrete cover depth d_c, mm and carbonation coefficient k, mm/√years: $t_i=d_c^2/k^2$. If lower values for the exponent of a time instead of the value of 0.5 were examined, the equation resulted in $t_i=d_c^{2.5}/k^{2.5}$ and $t_i=d_c^{3.3(3)}/k^{3.3(3)}$ respectively;
- Finally, real-time propagation period $t_{p,r}$, was calculated: $t_{p,r}=(t_f-t_0)-t_i$
  where: $t_{p,r}$ is the real-time propagation period, t_f is the failure time (the same as for survey time t_{survey}), t_0 is construction time, and t_i is initiation period, all in years.

A typical carbonation curve can be seen in **Fig. 3**, left during initiation t_i and the curve also continues during propagation t_p (the black dotted line). The real-time propagation period $t_{p,r}$ is the period between the end of initiation t_i and the determined failure time t_f or the field survey time t_{survey}.

Field survey time t_{survey} and failure time t_f are taken to be the same in calculations since the exact failure time is unknown but it probably did not occur much before the field survey.

3.1 Validation results

The results of calculated propagation periods $t_{p,c}$ and real propagation periods $t_{p,r}$ used in the validation process are presented in **Fig. 3**, right. Each five points represents one degradation case from one façade. It took several rounds of combining various WDR loads, carbonation coefficients, and crack width limits to achieve the satisfactory final result that has been presented here. Average calculated propagation periods of $t_{p,c}$=20.4 years compared to an average real-time propagation period of $t_{p,r}$=19.8 years. A notable deviation can be seen but results of this form of validation can never have an ideal match due to the stochastic nature of degradation and the large number of variables that can affect the result.

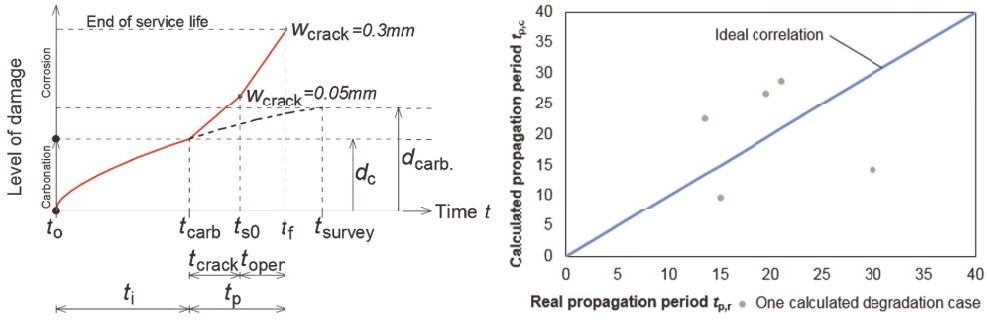

Fig. 3 *Principled scheme of service life, comprising of initiation (t_i) and propagation (t_p) periods (left) and results as a comparison of real-time and calculated propagation periods (right)*

A sensitivity analysis of material properties was carried out in order to detect its impact on the calculated propagation periods. The results are presented in **Table 1**.

Tab. 1 *The impact of changed material properties on calculated propagation periods*

Material property	**Open porosity* Θ, m^3/m^3**		**Water uptake coef.** A_w, $kg/(m^2\sqrt{s})$**		**Water vapor diffusion resistance factor μ, -**	
	Base value	Base+st.dev	Base value	Base+st.dev	Base value	Base+st.dev
	0.1686	0.1933	0.016	0.024	41	62
	Calculated propagation period $t_{p,c}$, years					
	16.1	16.3	16.1	27.4	16.1	15.9

*Effective saturation and capillary saturation content were scaled proportionally with porosity
**Liquid water conductivity k_l was scaled in accordance to changed water uptake coefficient A_w

As can be seen, an increase in the water uptake coefficient substantially prolongs the propagation period, meaning a lower RH inside the concrete. The reason for this is the faster moisture drying out process for an RH value that is close to 100% (liquid moisture flux) dominating over the higher water uptake of the surface.

4 Discussion

4.1 The sensitivity of a corrosion model

Alternative exponents of time in addition to n=0.5 as used in calculating the carbonation coefficient k was studied. Values of $0.2<n<0.5$ could be justified when it came to the cyclic wetting and drying nature of the concrete facade according to Köliö et al. (2016), also $n<0.5$ as cracks due to shrinkage and frost attack were present in the facade. An impact of changing the exponent n is relevant and it tends to be linear when it comes to corrosion propagation.

The limiting state criterion for the crack width (w=0.3 mm as used in this study) upon which the propagation period depends has a notable impact. The latter width of 0.1-1 mm may be discussed but its further opening after the initial emergence should be included by all means in order to achieve a more accurate prediction.

A small change in temperature coefficient of 7.5 times per 10 °C has no relevant impact.

4.2 Uncertainties to consider

Using the hygrothermal simulation tool includes many crucial aspects:

- Moisture penetration via cracks. It has been taken into account by increasing the corrosion current by a factor of two after the expected time of cracking. Although the correct quantity of the latter phenomenon is unknown, it is still to be considered;
- Material data – its variability, cost, and long-lasting measurement procedure, especially in a over-capillary range. The material functions used are based on so-called normal concrete that is measured in TU Dresden. The design of a concrete mixture (involving the class of concrete, cement type, the amount of cement, w/c ratio, and the type and grain size of aggregate) is similar, and the main material properties of the specimen (see **Table 1**) as measured in laboratory approximate as well;
- Material properties of the ~0.04 mm thick porous zone at the reinforcement/concrete interface as described by Chernin (2011) is evaluated not to have substantial impact due to large thermal conductivity and liquid water conductivity of corrosion products;

- Local WDR load to upper corners in urban environment (possible to evaluate by applying Computational Fluid Dynamics). WDR loads applied confluent the catch ratios by Blocken et al. (2013), taking into consideration a zone of the façade from which the specimen was taken. None of the specimens originated from the upper corner of a building which had an extreme WDR load;
- The impact of the WDR calculation method (either weighed with wind velocity or not) and its time frequency. The WDR load on facade depended on the wind velocity, wind direction, and horizontal rain with a one hour step being calculated by the user meaning weighed WDR. The calculated WDR load was compared to climate data that was typical to the region in order to ensure the catch ratios being fully trustworthy;
- Calculation principles and simplifications in the simulation tool.

5 Conclusions

The proposed method was validated based upon field measurements. The method combines existing corrosion propagation models and the dynamic hygrothermal simulation tool.

As a result, measured and calculated corrosion propagation periods were confluent by using 0.3 as an exponent of time during carbonation and by taking a crack width of 0.3 mm as a criterion. Faraday's corrosion model performs well and the concrete cover/reinforcement ratio should be included in the initial crack model. A sensitivity analysis detected that the corrosion propagation period is highly dependent upon WDR loads and the liquid water conductivity of a material.

The method proposed in the study demonstrates an ability to evaluate the corrosion propagation period by using existing professional know-how and the dynamic hygrothermal simulation tool. This ability has a wide field of application when it comes to evaluating degradation, service life, and the need for the renovation of reinforced concrete facades.

Acknowledgement

This research was supported by the Estonian Centre of Excellence in Zero Energy and Resource Efficient Smart Buildings and Districts, ZEBE, grant TK146, funded by the European Regional Development Fund, and by the Estonian Research Council, with Institutional research funding grant IUT1−15.

References

[1] AHMAD, S. (2003). Reinforcement corrosion in concrete structures, its monitoring and service life prediction – a review. *Cement & Concrete Composites* 25, 459-471.

[2] ALONSO, C., ANDRADE, C., RODRIGUEZ, J., DIEZ, J.M. 1998. Factors controlling cracking of concrete affected by reinforcement corrosion. *Materials and Structures*. Vol. 31. Pp. 435-441.

[3] BLOCKEN B, DEROME D, CARMELIET, J 2013. Rainwater runoff from building facades: A review. *Building and Environment* 60 p. 339-361

[4] BOUTEILLER, V., CHERRIER J-F., L'HOSTIS V., REBOLLEDO, N., ANDRADE C., MARIE-VICTOIRE, E. Influence of humidity and temperature on the corrosion of reinforced concrete prisms, *European J. of Environmental and Civil Engineering*, 16:3-4 (2012), 471-480.

[5] BROOMFIELD, J. P. 1997. Corrosion of steel in concrete – understanding, investigation and repair. London. E&FN Spon, 240 p.

[6] CHERNIN, L., VAL, D.V. Prediction of corrosion-induced cover cracking in reinforced concrete structures. *Constructions and Building Materials* 25 (2011) 1854-1869.

[7] ILOMETS. S., KALAMEES, T. Case-study analysis on hygrothermal performance of ETICS on concrete wall after low-budget energy-renovation. In: Proceedings of *XII Int. Conference on Performance of Exterior Envelopes of Whole Buildings*: Florida, USA, December 1-5, 2013.

[8] JAMALI, A., ANGST, U., ADAY, B., ELSENR B. Modeling of corrosion-induced concrete cover cracking: A critical analysis. *Construction and Building Materials* 42 (2013) 225-237.

[9] KHAN, I., FRANCOIS, R., CASTEL, A. Prediction of reinforcement corrosion using corrosion induced cracks width in corroded reinforcement concrete beams. *Cement and Concrete Research* 56 (2014) 84-86.

[10] KÖLIÖ, A., HONKANEN, M., LAHDENSIVU, J., VIPPOLA, M., PENTTI, M. Corrosion products of carbonation induced corrosion in existing reinforced concrete facades. *Cement and Concrete Research* 78 (2015) 200-207.

[11] KÖLIÖ, A., NIEMELÄ, P.J., LAHDENSIVU, J. Evaluation of a carbonation model for existing concrete facades and balconies by consecutive field measurements. *Cement and Concrete Composites* 65 (2016) 29-40.

[12] LAHDENSIVU, J. Durability properties and actual deterioration of Finnish concrete facades and balconies. PhD thesis, publication 1028. *Tampere University of Technology*. 2012.

[13] NICOLAI, A. Modeling and Numerical Simulation of Salt Transport and Phase Transitions in Unsaturated Porous Building Materials. Dissertation. *Syracuse University*. 2008.

[14] OTIENO, M., BEUSHAUSEN, H., ALEXANDER, M. Modelling corrosion propagation in reinforced concrete structures – A critical review. *Cement & Concrete Composites* 33 (2011). Pp. 240–245.

[15] ROUCHIER, S., WOLOSZYN, M., FORAY, G., ROUX, J-J. Influence of concrete fracture on the rain infiltration and thermal performance of building façade. *International Journal of Heat and Mass Transfer* 61 (2013) 340-352.

[16] SCHEFFLER, G.A. Validation of hygrothermal material modelling under consideration of the hysteresis of moisture storage. PhD thesis. *Dresden University of Technology*. 2008.

[17] SONTAG, L., Nicolai, A., VOGELSANG, S. Validierung der Solverimplementierung des hygrothermischen Simulationsprogramms Delphin 2013 (in deutch). www.qucosa.de/fileadmin/data/qucosa/documents/12896/DelphinValidierung.pdf (28.09.2015)

[18] ŠAVIJA, B., LUKOVIC, M., PACHETO, J., SCHLANGEN, E. Cracking of the concrete cover due to reinforcement corrosion: A two-dimensional model study. *Construction and Building Materials* 44 (2013) 626-638.

[19] TUUTTI, K. Corrosion of steel in concrete. Stockholm. *Swedish Cement and Concrete Research Institute*. CBI Research 4:82. 304 p. 1982.

[20] VESIKARI, E. Betonirakenteiden käyttöikä. *VTT tutkimuksia 417* (in finnish). 1986.

[21] VINHA, J., KORPI, M., KALAMEES, T., JOKISALO, J., ESKOLA, L., PALONEN, J., KURNITSKI, J., AHO, H., SALMINEN, M., SALMINEN, K., KATO, M. Asuinrakennusten ilmanpitävyys, siseilmasto ja energiatalous. Research report 140. *Tampere University of Technology, Department of Civil Engineering* (in finnish). 2009.

[22] YU, B., YANG, L., WU, M., BING, L. Practical model for predicting corrosion rate of steel reinforcement. *Construction and Building Materials* 54 (2014) 385-401.

PUBLICATION VI

Ilomets, S., Kalamees, T., Lahdensivu, J., Klõšeiko, P. Impact of ETICS on corrosion propagation of concrete facade. In: SBE16 Tallinn and Helsinki Conference. Build Green and Renovate Deep 5–7 October 2016, Tallinn and Helsinki / Energy Procedia 96 (2016) 67–76

Available online at www.sciencedirect.com

ScienceDirect

Energy Procedia 96 (2016) 67 – 76

Energy Procedia

SBE16 Tallinn and Helsinki Conference; Build Green and Renovate Deep, 5-7 October 2016, Tallinn and Helsinki

Impact of ETICS on corrosion propagation of concrete facade

Simo Ilomets[a*], Targo Kalamees[a], Jukka Lahdensivu[b], Paul Klõšeiko[a]

[a]*Tallinn University of Technology, Ehitajate tee 5, Tallinn 19086, Estonia*
[b]*Tampere University of Technology, P.O. Box 600 FI-33101 Tampere, Finland*

Abstract

The durability of reinforced concrete facades is an important field of research as the majority of dwellings in Northern and Eastern Europe were constructed 30–50 years ago. Recent condition assessments of the façades have indicated damage related to carbonation induced corrosion. Moreover, the problem might escalate since the future climate scenarios predict a significant increase of CO_2 in ambient air being a driving force for carbonation.

Assessment of residual service life of concrete facades is a complex phenomenon with a high level of uncertainty. A validated method used in this study combines dynamic hygrothermal simulation tool Delphin and existing corrosion models. Corrosion propagation consists of the time needed to concrete cover cracking and further expansion of a crack up to a width of 0.3 mm as a limit criterion. Additional exterior thermal insulation (mostly ETICS) is applied to existing dwellings as a renovation scenario in order to decrease the heat loss, improve thermal comfort and prevent the degradation mechanism e.g. carbonation induced corrosion. Hence, reinforcement corrosion before and after installing ETICS with mineral wool, EPS or PIR has to be evaluated. Impact of boundary conditions, e.g. wind-driven rain in addition to material properties, and built-in moisture was included.

The results indicate that corrosion propagation after carbonation has reached the reinforcement, is three to six years depending on the ratio of concrete cover depth against the reinforcement diameter. While applying ETICS, corrosion accelerates for a short period of time up to one year. Temperature inside the wall rises above +10 °C throughout the year, meaning no more freeze-thaw damage. Corrosion of reinforcement in carbonated concrete after applying ETICS is so slow, that no cracking will develop. Drying out moisture or vapour diffusion from indoor air is not able to propagate corrosion of reinforcement in carbonated concrete.

Peer-review under responsibility of the organizing committee of the SBE16 Tallinn and Helsinki Conference.

Keywords: Corrosion propagation; ETICS; concrete façade; crack width; Delphin; wind-driven rain

* Corresponding author. Tel.: +372-620-2402.
E-mail address: simo.ilomets@ttu.ee

Peer-review under responsibility of the organizing committee of the SBE16 Tallinn and Helsinki Conference.
doi:10.1016/j.egypro.2016.09.101

Nomenclature

d_c	concrete cover depth, mm
d_{carb}	carbonation depth, mm
d	diameter of reinforcement, mm
F	Faraday's constant, F=96487 A·s/mol
I_{corr}	corrosion current, A/m^2
J_{WDR}	wind-driven rain intensity to the vertical facade, l/(m^2·h)
M_{loss}	mass of steel dissolved at the anode during the overall duration t, kg/m^2
M	molecular weight of corroding steel (M=55.8 g/mol)
η	catch ratio of wind-driven rain, -
ρ	density of steel, g/cm^3
τ	corrosion duration, s
w_{crack}	crack width, mm
x_0	attack penetration or the radius loss of reinforcement, mm
z	valence of corroding metal, i.e. the number of electrons involved in the el.chemical reaction (z=2 for steel)

1. Introduction

The majority of dwellings in Northern and Eastern Europe were constructed in the 1960-s, 1970-s, and 1980-s during the industrialisation period. A significant amount of these dwellings in Estonia are constructed by reinforced concrete (RC) large-panels. Recent condition assessments of the façades have indicated the natural degradation mechanisms as carbonation induced corrosion and freeze-thaw damage [1]. In addition to degradation to due the time, problems appeared as a result of poor real estate maintenance and a lack of regular condition investigation leading to the growing need for renovation. Reliable renovation scenarios need to be developed to prolong the service life of RC facades.

In terms of the longer perspective and sustainability, tendencies of future climate scenarios should also be taken into account. For example the concentration of CO_2 in ambient air as a driving force for carbonation could rise up to 840 ppm by the year 2100 [2]. Future climate scenarios proposed for Southern Finland are also applicable for Estonia - rise in temperature, higher relative humidity (RH) and more precipitation, higher wind velocity and less solar radiation [3] are all worsening the situation in terms of corrosion. Also, extreme weather will be more likely.

Detecting a correlation between actual deterioration and climate loads is a highly complicated task because of many uncertainties, e.g. material properties (depending on moisture conditions), local climate loads at the building site and complexity of deterioration phenomenon. Regardless of this, durability properties of concrete and actual deterioration depending on climate loads has been studied in detail based on a field survey. Wind-driven rain (WDR) is involved in most of the main degradation mechanisms, like corrosion of reinforcement and freeze-thaw damage [4]. It has been estimated that the amount of WDR will increase by approx. 20% by 2100 in Southern Finland. At the same time the main wind directions remain from South-East to South-West [5].

Hygrothermal conditions for corrosion in concrete depend heavily on WDR that must be considered in addition to the convection and diffusion of moisture [6] [7]. Impact of WDR can be divided into two large fields of research [8] – impinging WDR intensity (before raindrop impact) and response of a building wall (at and after raindrop impact). The first part must also consider averaging the technique and time step of WDR data. The second part analysed in the paper gives a solid overview of research conducted and progress related to the subject and points out the shortage – development, validation and implementation of WDR into hygrothermal models. In addition to experimental measurement in situ and in laboratories, (semi)-empirical, analytical and numerical methods also have a perspective to become a valuable tool in order to quantify WDR loads on building façade [6] [8]. A solid overview and comparison of two semi-empirical models and computational fluid dynamics (CFD) model is made by Choi [9] and extended by

Blocken and Carmeliet [10]. Variability of the wind velocity and horizontal rain intensity in time should be preserved where feasible, while applying WDR as boundary conditions for heat, air and moisture transfer modelling [11].

Hygrothermal simulation tools have a wide field of applications in modelling heat, air and moisture transfer in a building envelope. Main bottlenecks related to the use of hygrothermal simulation tools are the reliability of input data, calculation principles and simplifications. Even if reliable output data has been calculated, the application of this data in order to model the degradation phenomenon is limited as calibrated degradation models do not yet exist. Implementation of finite-element hygrothermal simulation in order to analyse the impact of cracking has been described by Rouchier [12]. This advanced research analysed the durability of porous material with and without cracking by taking WDR and hygrothermal conditions into account.

Computational simulations to assess the damage and service life of structures are already in use for corrosion [13], degradation of wood [14], and growth of mould [15], [16], [17].

The main aim of the paper was to evaluate the corrosion propagation in RC facades and answer the following questions:

- What is the time of corrosion propagation of RC façade in various boundary conditions?
- What is the critical moisture content for the exterior layer of RC before installing ETICS to prevent corrosion propagation and moisture damage during the latter drying out?

These questions are crucial to answer in order to evaluate the service life of RC facades after carbonation has reached the embedded steel.

2. Methods

2.1. Corrosion propagation model

Corrosion of RC can be divided into two main phases: initiation and the propagation [18], [19], [20], [21]. During initiation carbonation of concrete reaches the depth of embedded steel and breaks down the passive film surrounding the reinforcement. The propagation phase covers the actual deterioration of reinforcement and concrete cover. The main assumption in this paper is that in the beginning of the calculation, carbonation depth has just reached the reinforcement. The concrete is assumed to be solid, without cracks and not deformable at first. The corrosion process is assumed to be carbonation induced (i.e. content of chlorides <0.03 wt% [4].

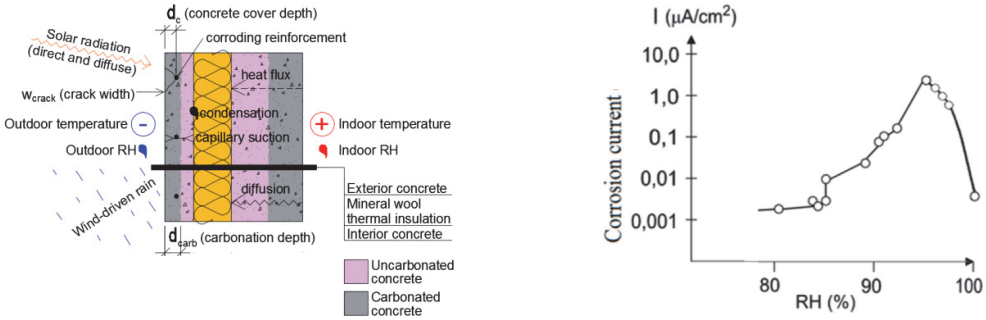

Fig. 1. Introduction of the research problem as a cross-section of a studied wall (left) and corrosion current depending on the RH of concrete (valid for a temperature of +5°C), based on [18] (right).

Corrosion model used in the study is the same as that which is described thoroughly and compared with field measurements in [22]. The research problem itself is introduced in Fig. 1, left. In the propagation phase, carbonation induced corrosion current primarily depends on RH as shown in Fig. 1, right and secondly on the temperature inside the concrete.

Electrical resistivity is related to RH in concrete, since resistivity/conductivity depends on the amount of water molecules in the pores. There is a thicker layer of water molecules on pore walls at high RH causing smaller electrical resistivity. Appearance of a first crack and its expansion up to a limit criterion is shown in Fig. 2.

Higher temperatures accelerate corrosion as there are more intensive electrochemical (anodic and cathodic) reactions caused by electrons that are moving faster. In [22] and in this study as well, a change of corrosion current 5-10 times with a 10°C temperature based on [24], is used.

Corrosion propagation was calculated according to the following steps:

- Hourly values for temperature and RH were calculated inside the exterior concrete at different depths of the reinforcement (d_c=10–15 mm, d_c=15–20 mm and d_c=20–25 mm, see Fig. 1, left) by using a dynamic hygrothermal simulation tool (a description of the buildings and a simulation tool follows in a later chapter);
- Hourly values for corrosion current I_{cor} were calculated from the RH according to [18] in Fig. 2, right (MS Excel post-processing);
- Hourly values for corrosion current I_{cor} were corrected with the temperature (by 7.5 times with a 10 °C temperature change reference to a 5 °C baseline);
- A cross-section loss of the reinforcement was calculated according to Faraday's Law (Eq. 1), from [25].
-

$$M_{loss} = \frac{M \cdot I_{cor} \cdot \tau}{z \cdot F} \quad (1)$$

where M_{loss} is the mass of steel dissolved at the anode during the overall time τ, kg/m^2; M is the molecular weight of corroding steel (M = 55.8 g/mol); I_{cor} is the corrosion current, A/m^2; τ is the corrosion duration, s; z is the valence of corroding metal, i.e. the number of electrons involved in the electrochemical reaction (z = 2 for steel); F is Faraday's constant, F = 96487 A·s/mol;

- A cross-section loss x_0 that relates to the first visible crack (w=0.05 mm) depends on the cover depth c, mm and diameter of the reinforcement d, mm being calculated (see Fig. 2, left): x_0=7.53+9.32·d_c/d. The uniform corrosion of a cylinder-shaped reinforcement and the density of the steel ρ=7.85 g/cm^3 is assumed.

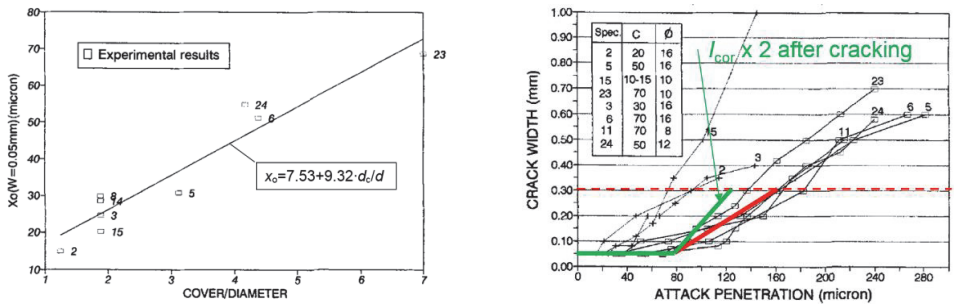

Fig. 2. In the left, the ratio of the reinforcement's cover depth against diameter causing the first crack (crack width at the y axis w=0.05 mm) and further crack evolution (w=0.3 mm, right) [23].

Further attack penetration for the crack's opening, from 0.05 mm up to 0.3 mm (Δ0.25 mm crack width corresponds to Δ80 μm attack penetration) is independent of the cover/diameter ratio from Fig. 2, right. Corrosion current is assumed to double (Δ0.25 mm crack width corresponds to Δ40 μm attack penetration) after the formation of the first crack caused by increased WDR penetration as well as the dependence of the crack opening on the corrosion current as stated in [23]. Cracks wider than 0.3 mm lead to escalating degradation as well as aesthetic problems.

2.2. Calculations

The studied wall of a typical five story apartment building composing of two layers of RC and thermal insulation in between is shown in Fig. 3. Dynamic hygrothermal simulation tool Delphin was applied for calculation conformity in two earlier studies, in which the hygrothermal simulation model was developed and validated [26], and validation of a corrosion propagation model [22].

Indoor hygrothermal loads based on measured data in Estonia by [27] was used. Indoor air temperature level was stable at +22 °C during the heating season. Two moisture excess levels Δv=3 g/m^3 as a typical average and 5 g/m^3 being a critical value representative for the occupancy level ~25 m^2/person was used.

Outdoor climate conditions with an hourly resolution shown in Fig. 1, left, was measured by the Estonian Weather Service during 2006–2012 (and 1970–1976 for the comparison). Direct solar radiation was ignored since the wall might shaded by the neighbouring buildings or trees. The vertical wall was chosen to have South-West orientation having the most severe WDR loads [28]. Rainfall to the vertical façade was calculated by the user according to the standard rain model of Delphin, considering rain intensity, wind direction, and wind velocity. This approach with an average catch ratio η~0.2 represents a typical load for the centre of a façade in an urban environment and is well consistent with η~0.5 at wind velocity 10 m/s given in [10]. A critical WDR level at the centre of the unobstructed façade was achieved via the corrections according to [29], ending up with a catch ratio η~0.43. A critical WDR level at the top edge of a low rise building was doubled (η~0.86), as proposed in [10]. One percent of WDR load [30] was assumed to penetrate through the ETICS on the exterior surface of the original RC facade.

Several calculation cases were set in order to cover the variability of factors affecting the wall`s performance (base case is marked in **bold**):

- Calculation period (climate): 1970-1976/**2006-2012**
- Initial moisture content of exterior layer of RC: w_0=**90**/110 kg/m^3
- Wind-driven rain load: η~**0.43**/0.86
- Indoor moisture excess: Δv=**3**/5 g/m^3
- Water vapour diffusion resistance of exterior RC: μ=**19**/41
- Three different materials for additional thermal insulation: **EPS**, mineral wool, polyisocyanurate (PIR)

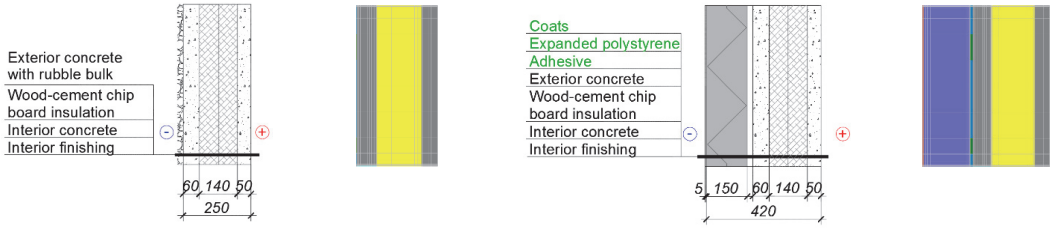

Fig. 3. Cross-section of original RC wall (left) and its simulation model from the software Delphin (2nd from the left). Cross-section of the wall with the installed ETICS (2nd from the right) and the same as a Delphin model (right).

Table 1. Material properties used in calculations.

	Concrete	Wood-cement chip-board	Adhesive mortar	EPS	MW	PIR	Exterior rendering
Bulk density ρ, kg/m^3	2320	500	700	35	75	35	1270
Porosity θ, m^3/m^3	0.14	0.93	0.73	0.94	0.92	0.91	0.50
Specific heat capacity c, J/(kg·K)	850	1470	945	1500	840	1500	960
Thermal conductivity λ, W/(m·K)	1.5	0.12	0.19	0.035	0.038	0.027	1.0
Vapour diffusion resistance factor μ, -	19/41	3.8	15	15	2	225	10
Liquid water conductivity k, kg/(m·s·Pa)	$4.4\cdot10^{-11}$	$16\cdot10^{-9}$	$3.2\cdot10^{-9}$	0	0	$8\cdot10^{-6}$	$0.27\cdot10^{-6}$
Air permeability K_g, s	$1\cdot10^{-6}$	$7\cdot10^{-3}$	$1\cdot10^{-5}$	$1\cdot10^{-6}$	$1\cdot10^{-2}$	0	$1\cdot10^{-6}$
Initial moisture w_0, kg/m^3 / RH, %	90-110/98.2-99.8	27 / 60	200 / 100	0.6 / 60	3.1 / 60	~0 / 60	300

Material properties used in the calculation are given in Table 1. Material properties originate from the software`s database and were corrected in the case of concrete according to data measured in Tampere University of Technology in Finland. In addition to the latter fixed values, Delphin`s default functions of material properties depending on the hygric environment, was included.

3. Results

Presentation of the results is derived from the research questions set up in the introduction. Hence, the temperature, RH, and corrosion current in the exterior layer of RC during the propagation period is presented, see Fig. 4. As expected, the temperature inside the RC after applying ETICS is relatively stable and does not drop below +10 °C even in winter. Hence, no more freeze-thaw cycles in RC will appear.

A notable delay of approximately ten days between the WDR hitting the façade and an increase of RH/corrosion current at 20–25 mm (as a typical cover depth) from the concrete`s surface was observed. RH in the beginning of the calculation inside the exterior RC is close to 100% for the original wall as well as for the ETICS wall, see Fig. 4, left. In the case of the original, uncovered wall, RH drops in spring within each year but rises up to close to 100% due to WDR in summer and autumn. In the case of ETICS, the majority of the initial moisture in RC dries out during the first year and the rest during the second year). Fig. 4, right, indicates that summer periods characteristic of severe WDR cause the majority of the corrosion propagation.

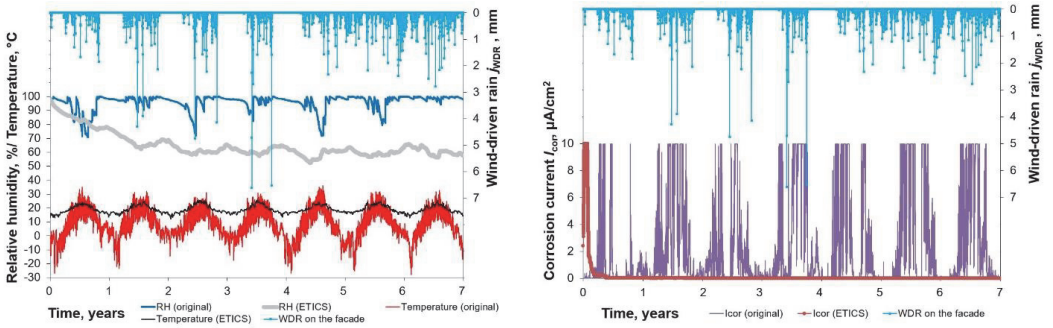

Fig. 4. Temperature and RH inside the exterior layer of RC (left) at a depth of 20–25 mm from the façade surface. Corrosion current of an original wall against after applying ETICS (right).

Corrosion current (shown in Fig. 4, right) was summarised for the total corrosion current, see Fig. 5 and Fig. 6. This enables us to evaluate whether the total corrosion propagation causes cracking of RC or not.

One of the main results of the paper is the residual service life for an original RC wall of three to six years (see Fig. 5) if using a failure criterion crack width w=0.3 mm, as in the paper where the method was validated in. Latter residual service life is valid for a façade, where carbonation depth has just reached the reinforcement and a building facing the South-West is not sheltered from WDR. Variations between the corrosion current at a different depth from the surface (10–15 mm; 15–20 mm; 20–25 mm) are rather small whereas a higher and more stable RH level deeper inside the concrete leads to faster corrosion. The key factor to define the residual service life is the ratio of concrete cover depth d_c against reinforcement diameter d that the initiation of the crack depends on. In the case of a small cover depth, say 10 mm, or thick reinforcement, say Ø8 mm, cover depth d_c diameter d ratio is only 2–3, meaning a residual service life of 3–4 years.

Installation of ETICS (another, lower group of results in Fig. 5 and Fig. 6) increases the corrosion propagation during a short period of time while the moisture dries out. Corrosion at the start of drying out is most intensive with a material having the highest vapour diffusion resistance (PIR, μ=225). In this case, the total corrosion current increases linearly for about half a year, followed by slower growth for about a year. Levels of total corrosion have similar behaviour in the case of high initial moisture content of concrete (w_0=110 kg/m^3), reaching much higher levels compared to the ETICS base case (defined in the last section of methods). From the criterion of corrosion propagation (crack width w=0.3 mm), all three thermal insulation materials used for ETICS are fair. Still, the durability of ETICS, especially in the case of mineral wool, has to be further analysed in terms of large moisture flux originating from the concrete while drying out. If one would use ETICS with PUR insulation or initial moisture content w=110 kg/m^3, it would cause failure in the case of cover depth/diameter ratio d_c/d<4 and taking the crack initiation (w=0.05 mm) as the criterion. Since only one parameter was changed at the time to study its effect, using PIR insulation in combination with high initial moisture content might lead to failure and therefore, should be avoided.

Small deviation of the results concerning different climatic years, WDR load, material properties, and indoor moisture excess in Fig. 6 increase the reliability of the calculated residual service lives. An increase of WDR load (η=0.86) indicates a somewhat surprising result – the total corrosion current during certain periods (e.g. fourth year) decreases. The reason for such phenomenon can be derived from Fig. 1, right, and Fig. 4, left, where the dependency of corrosion current on RH, and RH of concrete, respectively, is presented. An increase of WDR causes too high levels of RH in terms of corrosion current, being >≈97%. Climatic years chosen (1970–1976 vs 2006–2013) have a detectable impact on the results. In any case, the statement for the residual service life being three to six years is evident. An increase of moisture excess (Δv=5 g/m^3) accelerates the corrosion a little as expected.

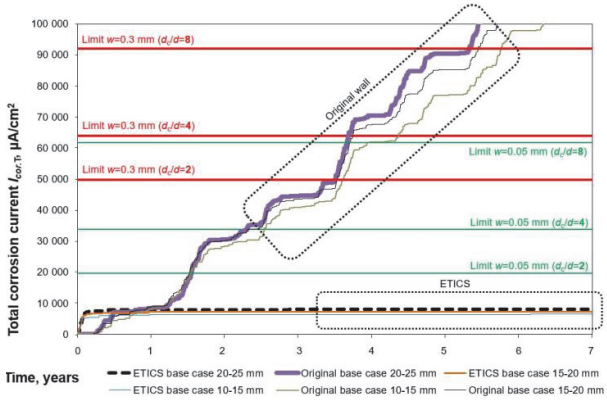

Fig. 5. Total corrosion current at different depths from the surface without ETICS (original wall) and after applying ETICS. Horizontal lines stand for the limit criteria for different ratios of concrete cover depth d_c against reinforcement diameter d.

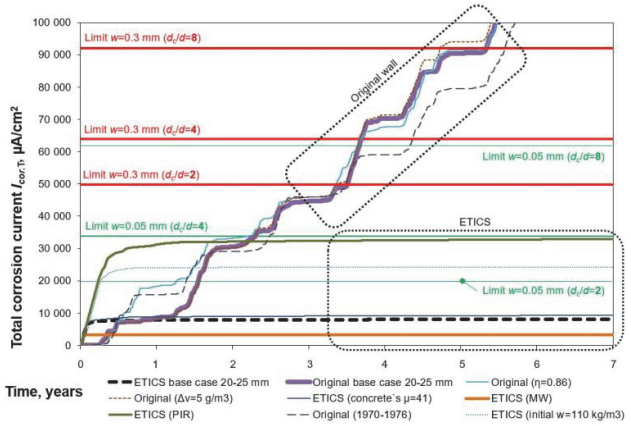

Fig. 6. Total corrosion current of different calculation cases against the limit criteria and the impact of applying ETICS at a 20–25 mm cover depth. Each calculation case represents one deviation from the base case – changed parameter named in the parentheses.

4. Discussion

According to the studies carried out, the propagation time of reinforcement corrosion after the carbonation depth has reached the reinforcement takes only three to six years for the crack to appear. Three years stand for a small cover depth/diameter ratio (e.g. $d_c/d<2$) while six years stand for a typical cover depth in combination with a thin, say Ø 3 mm reinforcement ($d_c/d>8$). A limit criterion for the crack width w=0.3 mm was used for defining the residual service life conformity with the study in which the method was validated in [22]. Other criterion can be discussed but an increase of corrosion propagation after the appearance of the first crack w=0.05 mm is evident. This is to say that the initiation period, i.e. time until CO_2 penetrates into RC and the carbonation front reaches the reinforcement, is crucial for the service life of RC façades. Studies [1] have shown that the average measured carbonation depth of exterior concrete of Estonian RC facades is typically 10−40 mm and up to 40−70mm in maximum cases. Since the carbonation depth could exceed concrete cover depth, RC facades should be protected against future corrosion.

Different climate periods (1970–1976 vs 2006–2012) were studied in order to determine the impact on the results. In the long term, the earlier period (1970–1976) ends up with lower levels of corrosion, although, it has more intense rainfall (537 vs 506 mm as annual average). The explanation for this is larger WDR loads leading to RH being too high (initial moisture content of concrete is high already). Another reason is the time resolution of climate data that is automatically saved with an hourly interval since 2006. In earlier times, data was collected manually with a three or six hour interval. For the hourly resolution used in our study, data had to be converted first. As stated in [31], as short resolution as possible (maximum an hour or ten minutes, if available) should be used, since averaging the data might cause significant inaccuracy. Evenly distributed WDR penetrates into the façade much more as saturated water film and run-off emerges later.

5. Conclusions

Corrosion propagation time of unprotected concrete facade exposed to WDR loads is approximately three to six years after the carbonation depth has reached the reinforcement. The exact duration depends mostly on the outdoor climate, hygrothermal properties of concrete, but also on the ratio of concrete cover depth against the reinforcement diameter. The most intense time of the year in terms of corrosion for the original RC facade is summer, characterised by a high level of rainfall and outdoor temperature.

The results also show that the ETICS with all the studied thermal insulation materials do not increase the reinforcement corrosion in long term. Corrosion of reinforcement in carbonated concrete after applying ETICS rises for less than a year but becomes low later on, and therefore, no cracking will occur. Therefore, ETICS as a renovation scenario is acceptable in terms of corrosion propagation. Drying out moisture or vapour diffusion from indoor air is not able to propagate the corrosion of reinforcement in carbonated concrete if it has not started yet before installing ETICS. Temperature of exterior layer of old concrete facade after applying ETICS remains above +10 °C throughout the year, meaning no more freeze-thaw damage. High initial moisture content of concrete (w_0>90 kg/m^3) in combination with high water vapour resistance of the additional exterior thermal insulation (e.g. μ=225) might cause corrosion induced cracking and is therefore advised to avoid.

Acknowledgements

This research was supported by the Estonian Centre of Excellence in Zero Energy and Resource Efficient Smart Buildings and Districts, ZEBE, grant TK146 funded by the European Regional Development Fund, VFP692 "Development and advanced prefabrication of innovative, multifunctional building envelope elements for MOdular REtrofitting and CONNECTions (7.11.2014–6.11.2018)" and by the Estonian Research Council, with Institutional research funding grant IUT1−15.

References

[1] Ilomets S, Kalamees T, Agasild T, Õiger K, Raado L. Durability of concrete and brick facades of apartment buildings built between 1960-90 in Estonia. In: Freitas VP, Corvacho H, Lacasse M, editors. 12th Int. Conf. Durab. Build. Mater. Components, vol. III, Porto. Portugal 12-15 April: FEUP Faculdade de Engenharia da Universidade do Porto; 2011, p. 1171–8.
[2] IPCC. Climate Change 2014. Synthesis report. 2014.
[3] Ruosteenoja K, Räisänen J, Jylhä K, Mäkelä H, Lehtonen I, Simola H, et al. Maailmanlaajuisiin CMIP3-melleihin perustuvia arvioita Suomen tulevasta ilmastosta. 2013.
[4] Lahdensivu J. Durability Properties and Actual Deterioration of Finnish Concrete Facades and Balconies. Doctoral thesis. Publication 1028. Tampere University of Technology, 2012.
[5] Pakkala TA, Köliö A, Lahdensivu J, Kiviste M. Durability demands related to frost attack for Finnish concrete buildings in changing climate. Build Environ 2014;82:27–41. doi:10.1016/j.buildenv.2014.07.028.
[6] Blocken B, Carmeliet J. A review of wind-driven rain research in building science 2004;92:1079–130.
[7] Cornick S, Dalgliesh WA. Adapting rain data for hygrothermal models. Build Environ 2009;44:987–96. doi:10.1016/j.buildenv.2008.07.002.
[8] Blocken B, Derome D, Carmeliet J. Rainwater runoff from building facades : A review. Build Environ 2013;60:339–61. doi:10.1016/j.buildenv.2012.10.008.
[9] Choi ECC. Determination of wind-driven-rain intensity on building faces. J Wind Eng Ind Aerodyn 1994;51:55–69. doi:10.1016/0167-6105(94)90077-9.
[10] Blocken B, Carmeliet J. Overview of three state-of-the-art wind-driven rain assessment models and comparison based on model theory. Build Environ 2010;45:691–703. doi:10.1016/j.buildenv.2009.08.007.
[11] Janssen H, Blocken B, Roels S, Carmeliet J. Wind-driven rain as a boundary condition for HAM simulations: analysis of simplified modelling 2007:1–24.
[12] Rouchier S, Woloszyn M, Foray G, Roux J. International Journal of Heat and Mass Transfer Influence of concrete fracture on the rain infiltration and thermal performance of building facades. Int J Heat Mass Transf 2013;61:340–52. doi:10.1016/j.ijheatmasstransfer.2013.02.013.
[13] Zelinka SL, Derome D, Glass S V. Combining hygrothermal and corrosion models to predict corrosion of metal fasteners embedded in wood. Build Environ 2011;46:2060–8. doi:10.1016/j.buildenv.2011.04.017.
[14] Nofal M, Kumaran K. Biological damage function models for durability assessments of wood and wood-based products in building envelopes. Eur J Wood Wood Prod 2011:619–31. doi:10.1007/s00107-010-0508-9.
[15] Hukka A, Viitanen H. A mathematical model of mould growth on wooden material. Wood Sci Technol 33 475±485 1999. http://citeseerx.ist.psu.edu/viewdoc/download?doi=10.1.1.555.745&rep=rep1&type=pdf (accessed May 10, 2016).
[16] Sedlbauer K. Prediction of Mould Growth by Hygrothermal Calculation. J Build Phys 2002;25:321–36. doi:10.1177/007542420202500409 3.

[17] Moon HJ, Augenbroe G. Empowerment of decision-makers in mould remediation Empowerment of decision-makers in mould remediation 2008:37–41.
[18] Tuutti K. Corrosion of steel in concrete. Stockholm. Swedish Cement and Concrete Research Institute. CBI Research 4:82. 304 P.: 1982.
[19] Liu Y. Modeling the Time-to-Corrosion Cracking of the Cover Concrete in Chloride Contaminated Reinforced Concrete Structures. State University, 1996.
[20] Li CQ. Reliability Based Service Life Prediction of Corrosion Affected Concrete Structures 2004:1570–8.
[21] Otieno MB, Beushausen HD, Alexander MG. Modelling corrosion propagation in reinforced concrete structures – A critical review. Cem Concr Compos 2011;33:240–5. doi:10.1016/j.cemconcomp.2010.11.002.
[22] Ilomets S, Kalamees T, Lahdensivu J. Validation of the method to evaluate the corrosion propagation stage by hygrothermal simulation. Cent. Eur. Towar. Sustain. Build. 2016, Prague: 2016.
[23] Alonso C, Andradel C, Diez JM. Factors controlling cracking of concrete affected by reinforcement corrosion. Mater Struct 1998;31:435–41.
[24] Broomfield JP. Corrosion in reinforced concrete. London: 243e24; 1997.
[25] El Maaddawy T, Soudki K. A model for prediction of time from corrosion initiation to corrosion cracking. Cem Concr Compos 2007;29:168–75. doi:10.1016/j.cemconcomp.2006.11.004.
[26] Ilomets S, Kalamees T. Case-study analysis on hygrothermal performance of ETICS on concrete wall after low-budget energy-renovation. Proc. XII Int. Conf. Perform. Exter. Envel. Whole Build. Florida, USA, December 1-5, 2013., ASHRAE; 2013.
[27] Ilomets S, Kalamees T. Indoor hygrothermal loads for the deterministic and stochastic design of the building envelope of dwellings in cold climates. J Build Phys 2016;Submitted.
[28] Pihelo P, Lelumees M, Kalamees T. Potential of Moisture Dry-out from Concrete Wall in Estonian Climate. Int. RILEM Conf. Mater. Syst. Struct. Civ. Eng. Conf. Segm. Moisture Mater. Struct. 22-24 August 2016, Tech. Univ. Denmark, Lyngby, Denmark, 2016.
[29] EN ISO 15927-3. Hygrothermal performance of buildings - Calculation and presentation of climatic data - Part 3: Calculation of a driving rain index for vertical surface from hourly wind and rain data. Brussels, Belgium: 2009.
[30] ASHRAE 160P. Criteria for Moisture Control Design Analysis in Buildings. Atlanta GA: 2009.
[31] Blocken B, Carmeliet J. Guidelines for the required time resolution of meteorological input data for wind-driven rain calculations on buildings 2008;96:621–39. doi:10.1016/j.jweia.2008.02.008.

DISSERTATIONS DEFENDED AT TALLINN UNIVERSITY OF TECHNOLOGY ON *CIVIL ENGINEERING*

1. **Heino Mölder**. Cycle of Investigations to Improve the Efficiency and Reliability of Activated Sludge Process in Sewage Treatment Plants. 1992.

2. **Stellian Grabko**. Structure and Properties of Oil-Shale Portland Cement Concrete. 1993.

3. **Kent Arvidsson**. Analysis of Interacting Systems of Shear Walls, Coupled Shear Walls and Frames in Multi-Storey Buildings. 1996.

4. **Andrus Aavik**. Methodical Basis for the Evaluation of Pavement Structural Strength in Estonian Pavement Management System (EPMS). 2003.

5. **Priit Vilba**. Unstiffened Welded Thin-Walled Metal Girder under Uniform Loading. 2003.

6. **Irene Lill.** Evaluation of Labour Management Strategies in Construction. 2004.

7. **Juhan Idnurm**. Discrete Analysis of Cable-Supported Bridges. 2004.

8. **Arvo Iital**. Monitoring of Surface Water Quality in Small Agricultural Watersheds. Methodology and Optimization of monitoring Network. 2005.

9. **Liis Sipelgas**. Application of Satellite Data for Monitoring the Marine Environment. 2006.

10. **Ott Koppel**. Infrastruktuuri arvestus vertikaalselt integreeritud raudtee-ettevõtja korral: hinnakujunduse aspekt (Eesti peamise raudtee-ettevõtja näitel). 2006.

11. **Targo Kalamees**. Hygrothermal Criteria for Design and Simulation of Buildings. 2006.

12. **Raido Puust**. Probabilistic Leak Detection in Pipe Networks Using the SCEM-UA Algorithm. 2007.

13. **Sergei Zub**. Combined Treatment of Sulfate-Rich Molasses Wastewater from Yeast Industry. Technology Optimization. 2007.

14. **Alvina Reihan**. Analysis of Long-Term River Runoff Trends and Climate Change Impact on Water Resources in Estonia. 2008.

15. **Ain Valdmann**. On the Coastal Zone Management of the City of Tallinn under Natural and Anthropogenic Pressure. 2008.

16. **Ira Didenkulova**. Long Wave Dynamics in the Coastal Zone. 2008.

17. **Alvar Toode**. DHW Consumption, Consumption Profiles and Their Influence on Dimensioning of a District Heating Network. 2008.

18. **Annely Kuu**. Biological Diversity of Agricultural Soils in Estonia. 2008.

19. **Andres Tolli**. Hiina konteinerveod läbi Eesti Venemaale ja Hiinasse tagasisaadetavate tühjade konteinerite arvu vähendamise võimalused. 2008.

20. **Heiki Onton**. Investigation of the Causes of Deterioration of Old Reinforced Concrete Constructions and Possibilities of Their Restoration. 2008.

21. **Harri Moora**. Life Cycle Assessment as a Decision Support Tool for System optimisation – the Case of Waste Management in Estonia. 2009.

22. **Andres Kask**. Lithohydrodynamic Processes in the Tallinn Bay Area. 2009.

23. **Loreta Kelpšaitė**. Changing Properties of Wind Waves and Vessel Wakes on the Eastern Coast of the Baltic Sea. 2009.

24. **Dmitry Kurennoy.** Analysis of the Properties of Fast Ferry Wakes in the Context of Coastal Management. 2009.

25. **Egon Kivi**. Structural Behavior of Cable-Stayed Suspension Bridge Structure. 2009.

26. **Madis Ratassepp**. Wave Scattering at Discontinuities in Plates and Pipes. 2010.

27. **Tiia Pedusaar**. Management of Lake Ülemiste, a Drinking Water Reservoir. 2010.

28. **Karin Pachel**. Water Resources, Sustainable Use and Integrated Management in Estonia. 2010.

29. **Andrus Räämet**. Spatio-Temporal Variability of the Baltic Sea Wave Fields. 2010.

30. **Alar Just**. Structural Fire Design of Timber Frame Assemblies Insulated by Glass Wool and Covered by Gypsum Plasterboards. 2010.

31. **Toomas Liiv**. Experimental Analysis of Boundary Layer Dynamics in Plunging Breaking Wave. 2011.

32. **Martti Kiisa**. Discrete Analysis of Single-Pylon Suspension Bridges. 2011.

33. **Ivar Annus**. Development of Accelerating Pipe Flow Starting from Rest. 2011.

34. **Emlyn D. Q. Witt**. Risk Transfer and Construction Project Delivery Efficiency – Implications for Public Private Partnerships. 2012.

35. **Oxana Kurkina**. Nonlinear Dynamics of Internal Gravity Waves in Shallow Seas. 2012.

36. **Allan Hani**. Investigation of Energy Efficiency in Buildings and HVAC Systems. 2012.

37. **Tiina Hain**. Characteristics of Portland Cements for Sulfate and Weather Resistant Concrete. 2012.

38. **Dmitri Loginov**. Autonomous Design Systems (ADS) in HVAC Field. Synergetics-Based Approach. 2012.

39. **Kati Kõrbe Kaare**. Performance Measurement for the Road Network: Conceptual Approach and Technologies for Estonia. 2013.

40. **Viktoria Voronova**. Assessment of Environmental Impacts of Landfilling and Alternatives for Management of Municipal Solid Waste. 2013.

41. **Joonas Vaabel**. Hydraulic Power Capacity of Water Supply Systems. 2013.

42. **Inga Zaitseva-Pärnaste**. Wave Climate and its Decadal Changes in the Baltic Sea Derived from Visual Observations. 2013.

43. **Bert Viikmäe**. Optimising Fairways in the Gulf of Finland Using Patterns of Surface Currents. 2014.

44. **Raili Niine**. Population Equivalence Based Discharge Criteria of Wastewater Treatment Plants in Estonia. 2014.

45. **Marika Eik**. Orientation of Short Steel Fibers in Cocrete. Measuring and Modelling. 2014.

46. **Maija Viška**. Sediment Transport Patterns Along the Eastern Coasts of the Baltic Sea. 2014.

47. **Jana Põldnurk**. Integrated Economic and Environmental Impact Assessment and Optimisation of the Municipal Waste Management Model in Rural Area by Case of Harju County Municipalities in Estonia. 2014.

48. **Nicole Delpeche-Ellmann**. Circulation Patterns in the Gulf of Finland Applied to Environmental Management of Marine Protected Areas. 2014.

49. **Andrea Giudici**. Quantification of Spontaneous Current-Induced Patch Formation in the Marine Surface Layer. 2015.

50. **Tiina Nuuter**. Comparison of Housing Market Sustainability in European Countries Based on Multiple Criteria Assessment. 2015.

51. **Erkki Seinre**. Quantification of Environmental and Economic Impacts in Building Sustainability Assessment. 2015.

52. **Artem Rodin**. Propagation and Run-up of Nonlinear Solitary Surface Waves in Shallow Seas and Coastal Areas. 2015.

53. **Kaspar Lasn**. Evaluation of Stiffness and Damage of Laminar Composites. 2015.

54. **Margus Koor**. Water Distribution System Modelling and Pumping Optimization Based on Real Network of Tallinn. 2015.

55. **Mikk Maivel**. Heating System Efficiency Aspects in Low-Energy Residential Buildings. 2015.

56. **Kalle Kuusk**. Integrated Cost-Optimal Renovation of Apartment Buildings toward Nearly Zero-Energy Buildings. 2015.

57. **Endrik Arumägi**. Renovation of Historic Wooden Apartment Buildings. 2015.

58. **Tarvo Niine**. New Approach to Logistics Education with Emphasis to Engineering Competences. 2015.

59. **Martin Thalfeldt**. Total Economy of Energy-Efficient Office Building Facades in a Cold Climate. 2016.

60. **Aare Kuusik**. Intensifying Landfill Wastewater and Biodegradable Waste Treatment in Estonia. 2016.

61. **Mart Hiob**. The Shifting Paradigm of Spatial Planning in Estonia: The Rise of Neighbourhood Participation and Conservation of Built-up Areas through the Detailed Case Study of Supilinn, a Historic Suburb of Tartu City, Estonia. 2016.

62. **Martin Heinvee**. The Rapid Prediction of Grounding Behavior of Double Bottom Tankers. 2016.

63. **Bharat Maharjan**. Stormwater Quantity and Quality of Large Urban Catchment in Tallinn. 2016.

64. **Nele Nutt**. The Restoration of Nationally Protected Estonian Manor Parks in the Light of the Florence Charter. 2017.